DISSERTATION

MENISCAL ROOT TEARS AND REPAIRS

Submitted by

Brett Daniel Steineman

Graduate Degree Program in Bioengineering

In partial fulfillment of the requirements

For the Degree of Doctor of Philosophy

Colorado State University

Fort Collins, Colorado

Summer 2018

Doctoral Committee:

Advisor: Tammy L. Haut Donahue

Robert F. LaPrade
Laurie R. Goodrich
Paul R. Heyliger

ABSTRACT

MENISCAL ROOT TEARS AND REPAIRS

Meniscal root tears are defined as radial tears of the meniscal insertions and lead to an inability for the menisci to transmit compressive loads into circumferential hoop stresses. These are common among the posterior meniscal insertions due to acute or chronic conditions. Anterior root tears have also been shown to occur from iatrogenic injury during anterior cruciate ligament reconstructions; however, the relationship between anterior insertions and the anterior cruciate ligament are understudied. Root tears of the posterior insertions lead to measurable osteoarthritis within a year if left untreated. Despite this, changes to tissue characteristics due to anterior root tears are unknown. If untreated anterior roots result in tissue degeneration, then it is important for both anterior and posterior root tears to be repaired to prevent, or at least delay, the onset of osteoarthritis.

Meniscal root repair techniques have been developed to prevent joint degeneration following meniscal root tears; however, clinical studies of root repairs show that meniscal extrusion and joint degeneration are not completely prevented. This limited repair success may be due to inaccurate placement of repairs during surgery or from repair loosening postoperatively as early as during rehabilitation. The goals of this work are to better understand anterior root tears and to investigate potential causes for insufficient meniscal root repairs. Thus, the aims are to:

1) Quantify the overlap between the anterior cruciate ligament and the anterolateral meniscal insertion in the coronal and sagittal planes.
2) Assess early *in vivo* degeneration after untreated anterior meniscal root tears.

3) Determine the extent of repair loosening and recovery due to short-term rehabilitation.
4) Develop finite element knee models to determine the effect of repair placement and loosening on knee mechanics.

The completion of this project will improve clinical practice and basic scientific knowledge of current issues facing meniscal root tears and repairs.

ACKNOWLEDGEMENTS

I would like to first thank my outstanding advisor, Dr. Tammy Haut Donahue, who took a great risk by inviting me into her lab despite initially rejecting an interview with me and only granting a phone interview after I won over her current graduate students. At the time, I did not realize how little I deserved to be a part of your lab. You have been a better mentor than I could have imagined – providing me with unique collaborative opportunities, allowing me the freedom to utilize my creativity and ingenuity, and pushing me beyond the point that anyone has every pushed me professionally. I owe a significant portion of my future success to you, your lab, and the opportunities you provided.

I would also like to thank my committee member, Dr. Robert LaPrade, and many others at The Steadman Clinic and Steadman Philippon Research Institute for welcoming me into the clinical realm and providing me invaluable feedback and advice over the years. I would also like to acknowledge my other committee members, Dr. Laurie Goodrich and Dr. Paul Heyliger, for their commitment to this project and who both played significant roles in my research and professional development.

Another acknowledgement I would like to make goes to my brothers, friends, family members, high school instructors, undergraduate professors, and anyone else who made a large or small impact on my life to help me reach this point.

Finally, I would like to thank God for His infinite love and mercy, along with the internal desire and skills necessary to help people with their physical conditions.

DEDICATION

To my parents for their unwavering support of me and my professional pursuits. Thank you for your personal sacrifices made throughout your lives in order for my brothers and I to have everything we needed to pursue our dreams. Additionally, thank you for your exemplary work ethic, mercy, and selflessness towards others that has shaped me to be the man I am today and has been a model to continually work towards.

TABLE OF CONTENTS

CHAPTER 1:

INTRODUCTION

1.1 Menisci Anatomy and Physiology

Menisci are crescent-shaped, fibrocartilaginous wedges between the femoral and tibial condyles that are important for proper knee function.[14,44] The medial meniscus is located between the medial femoral and medial tibial condyles where the meniscus covers about 50% of the medial articular cartilage surface of the tibia.[7,16] Much of the midportion of the meniscus body attaches to the deep part of the medial collateral ligament as part of the joint capsule with meniscofemoral and meniscotibial components.[34] These connections prevent the medial menisci from being as mobile as the lateral meniscus during flexion and extension.[17] The lateral meniscus is located between the lateral femoral and lateral tibial condyles and covers approximately 60% of the articular cartilage surface of the lateral tibia.[7,16] A ligamentous connection between the anterior roots of the medial and lateral meniscus may be present called the anterior intermeniscal, or transverse, ligament.[39] Near the posterior root of the lateral meniscus, the meniscus body may also attach to the fibula and femur.[20,38]

The menisci are primarily composed of water, with about 20-25% collagen and 5% non-collagenous proteins such as proteoglycans and elastin.[4] With the large composition of interstitial fluid, the menisci are considered viscoelastic materials.[9,23] The viscoelasticity of meniscal tissue allows the accommodation of a wide range of compressive loads at different strain rates to prevent traumatic damage to the menisci and the underlying articular cartilage.[9] The collagen is formed as fiber bundles within the bulk of menisci and is oriented in the circumferential direction.[42] The orientation of collagen facilitates the transmission of compressive loads away from the articular

cartilage and into circumferential hoop stresses.[5,42] The size, shape, and mobility of menisci also helps to increase the congruency within the tibiofemoral joint which is important for efficient transmission tibiofemoral loads.[5,14,44,45,47]

1.2 Meniscal Insertion Anatomy and Physiology

The meniscal insertions, also referred to as meniscal attachments or entheses, are the main ligamentous structures that secure the menisci to the tibial plateau.[22,25,28] In humans, both medial and lateral menisci primarily attach to the tibial plateau by anterior and posterior insertions. The anterior root of the medial meniscus typically inserts near the anterior slope of the tibial plateau.[25,28] The posterior root of the medial meniscus typically inserts posterior from the medial tibial eminence apex and anteromedial from the tibial insertion of the posterior cruciate ligament.[22,25] The anterior insertion of the lateral meniscus has an intricate relationship with the anterior cruciate ligament. A portion of the anterolateral meniscal insertion inserts underneath the anterior cruciate ligament leading to a risk of damage during reconstruction;[25,28,48] however, the details of this relationship are unknown in the coronal and sagittal planes. The posterior portion of the lateral meniscus is where it begins to attach to the femur and fibula, but the main attachment is with the tibial plateau.[20,25,38] The posterior insertion of the lateral meniscus typically inserts within the intercondylar region posteromedial from the lateral tibial eminence apex and anterior from the posterior cruciate ligament.[22,25]

The meniscal insertions consist mostly of collagen that is a continuation from the meniscal body.[36] Although studies suggest that meniscal insertions may be subjected to compressive loads at times, their primary functions are to secure menisci to the tibial plateau and withstand tensile loads during load transmission of the menisci.[19,46] The meniscal insertions transition from ligament

structures to uncalcified fibrocartilage, calcified fibrocartilage, then subchondral bone to reduce stress concentrations from tibiofemoral loading.[6] Their integrity is important to maintain proper meniscal function.[3]

1.3 Meniscal Root Tears

In general, meniscal root tears are defined as partial or complete tears of the meniscal insertions from the tibial plateau.[30] These tears are a subset of meniscus injuries that disrupt the collagen fibers of the meniscal insertions resulting in an inability to transmit tibiofemoral loads. This inability to transmit tibiofemoral compression into circumferential hoop stresses results in loading patterns on the articular cartilage surface similar to total meniscectomies.[3] Biomechanical studies have reported significantly decreased tibiofemoral contact area and increased peak contact pressure resulting from both posteromedial and posterolateral meniscal root tears.[3,32,40] Additionally, previous studies demonstrate that meniscal root tears, which correspond to greater than 3 mm of extrusion from the tibial plateau and altered loading, are associated with the progression of joint degeneration.[3,35] Most studies have previously evaluated posterior meniscal root tears, as they are more common, but there is less information on anterior meniscal root tears and what happens to knee tissues when left untreated. This is important to understand as iatrogenic injury occurs from anterior cruciate ligament reconstruction to both anterior insertions.[31,48] Untreated meniscal root tears are becoming increasingly recognized to progressively increase meniscal extrusion and worsening arthritis within a year;[26,27] therefore, proper treatment is essential to prevent or at least delay the onset of joint degeneration.

1.4 Meniscal Root Repairs

In the past, partial or total meniscectomies have generally been the treatment of choice for meniscal tears; however, the amount of meniscus removed during the meniscectomy is correlated with progression of osteoarthritis.[21] Therefore, meniscal root repairs techniques have been developed to restore proper meniscal function.[1,2,10,13] Arthroscopic surgical repairs of these injuries are more desirable because they significantly improve clinical and radiologic outcomes when compared to meniscectomies.[12] For all repairs, sutures are arthroscopically passed through the injured meniscal root.[24,37,41] Some of these techniques have been developed using a suture anchor to secure the sutured meniscal root to the tibial plateau.[10,13] Additionally, other techniques have been developed to instead pass the sutures through transtibial tunnels and securely fasten them to the tibial diaphysis periphery.[1,2] The transtibial tunnel technique is the more common technique as it is less technically challenging and creates a tunnel to help promote repair healing to the tibial plateau.[1,2]

Repairs often result in better patient-reported outcomes, improved activity levels, and slower progression of osteoarthritis in comparison to meniscectomies;[49] however, meniscal root repairs still face challenges that limit their efficacy. Cadaveric studies demonstrate that cartilage contact mechanics are nearly restored to the intact condition after repair;[3,32,40] however, repairs do not always reduce meniscal extrusion or prevent joint degeneration.[11,12,15] One potential explanation for limited success is that these repairs are technically challenging and can result in misplacement of repairs 3 to 5 mm away from the anatomic center of the injured meniscal insertion.[18] An experimental study demonstrated that nonanatomic meniscal root repairs were unable to restore tibiofemoral contact mechanics; however, only one extreme location away from

anatomic was assessed.[29] Therefore, the necessary repair accuracy to properly restore knee mechanics is currently unknown.

Another explanation for limited success of repairs is that cyclic loading causes repairs to loosen from their intended location. Previous studies evaluating repair displacement have only been loaded for 1,000 cycles, which may not adequately challenge the repair.[8,33] Additionally, none of these studies have allowed the repairs to recover to determine if this displacement is a result of permanent loosening or due to the inherent viscoelastic nature of the meniscus. If a portion of the displacement is unrecoverable, repairs are at risk for loosening into a less-restorative position. Therefore, the extent of repair displacement and potential recoverability of repairs should be evaluated. Once the extent of repair displacement is better understood, there is still a lack of information about how this displacement or unrecoverable loosening affects knee mechanics and the efficacy of repairs. This is because previous studies evaluating repair displacement are destructive to the meniscus; therefore, they are unable to measure changes in knee mechanics.[8,33] A previous biomechanical experiment confirmed that cartilage deformation after meniscal root repairs increases compared to the intact condition from compression.[43] These results are limited to only deformation of cartilage at a single location; however, this study shows that repair loosening may have a significant effect on knee mechanics and needs to be studied further.

1.5 Specific Aims

The following specific aims will investigate current issues facing meniscal root tears and repairs to improve basic scientific knowledge and clinical practice. With limited information on anterior meniscal root tears and repairs, the initial work will assess early outcomes of untreated tears and establish an *in vivo* model. Further microscopic analysis between the anterolateral

meniscal insertion and the anterior cruciate ligament will be conducted to improve clinical understanding of the overlapping relationship to help prevent iatrogenic injury during anterior cruciate ligament reconstructions. There are also still general challenges facing repairs of each meniscal root that the posteromedial meniscal root repair will specifically be used to address. A finite element approach will be used to assess changes in knee mechanics for repair tunnel placement around the anatomic center of the meniscal insertion. This will help to understand the dependence of tunnel accuracy for posteromedial meniscal root repairs to restore knee mechanics. The extent of repair loosening will also be assessed by loading repairs to a greater number of cycles than has previously been evaluated and to determine if repairs recover with rest. Repair loosening will also be assessed using a finite element approach to determine how knee mechanics change as meniscal root repairs loosen due to rehabilitative loading.

Specific Aim 1: Quantify the microstructural overlap between the anterior cruciate ligament and the anterolateral meniscal insertion in the coronal and sagittal plane. It is hypothesized that a significant portion of the anterior cruciate ligament would overlap the anterolateral meniscal insertion in both the coronal and sagittal planes. **Approach 1:** Cadaveric human knees will be dissected to isolate the insertions of the anterior cruciate ligament and anterolateral meniscus. Specimens will then be sectioned into either coronal or sagittal sections and prepped for scanning electron microscopy. After confirming fiber directions of the insertions in each section plane, the percentage of the anterior cruciate ligament that overlaps with the anterolateral meniscal insertion instead of inserting into bone will be calculated.

Specific Aim 2: Evaluate early *in vivo* degeneration after untreated anterior meniscal root tears. It is hypothesized that if anterior meniscal root tears of either the medial or lateral menisci are left untreated after injury, early degenerative changes will occur within major tissues of the knee. **Approach 2:** Anterolateral and anteromedial meniscal root tears will be created in one knee of adult Flemish Giant rabbits. The contralateral limbs will be used as unoperated controls. After the animals are euthanized 8 weeks postoperatively, synovial fluid will be aspirated from the joint then tissue samples of menisci and tibial articular cartilage will be collected. The amount and type of inflammatory cells present in the synovial fluid, the compressive material properties of the menisci and tibial articular cartilage, the subchondral bone morphology of the tibial plateau, the coverage and content of glycosaminoglycans of menisci and tibial articular cartilage, the total content of intact DNA, and the relative gene expression of matrix-degrading enzymes will be measured after the anterior meniscal root tears to assess early joint degeneration.

Specific Aim 3: Determine the extent of loosening due to short-term rehabilitation following transtibial pull-out meniscal root repairs. It is hypothesized that a significant amount of displacement due to early rehabilitative loading is unrecoverable. Additionally, it was hypothesized that single- and double-tunnel repairs would not be significantly different for repair displacement and recoverability measurements. **Approach 3:** Transtibial pull-out repairs will be performed on the posteromedial meniscal root of ovine cadaveric knees. The repairs will be loaded in tension to simulate typical rehabilitative loading, allowed to recover, and then loaded in tension for another session of rehabilitative loading. The amount of displacement after cycles of interest and the amount of displacement recovered after rest will be assessed and compared for single- and double-tunnel repair techniques.

Specific Aim 4: Develop a sample population of finite element knee models to assess current challenges of meniscal root repair, including tunnel placement and repair loosening. To address these challenges, Specific Aim 4 will be divided into two sub-aims.

Sub-Aim 4A: Determine how accurate surgeons need to be with repair placement to restore intact knee mechanics relating to the injured meniscus and tibial articular cartilage. It is hypothesized that further posterior placement, both medially and laterally, for a posteromedial meniscal root tear would decrease the ability for the meniscus to transmit tibiofemoral loads and increase the loading on the articular cartilage. Additionally, it was hypothesized that further anterior placement, both medially and laterally, would best restore meniscal load transmission and cartilage contact mechanics. **Approach 4A:** The unrecoverable repair loosening calculated in Specific Aim 3 will be implemented into the three finite element knee models. Knee mechanics of the tibial articular cartilage, medial menisci, and anteromedial meniscal insertions will be assessed with tibiofemoral compression to simulate rehabilitation and return-to-activity loading at different flexion angles. Anatomic repairs and nonanatomic repairs around the anatomic center of the injured meniscal insertion will be evaluated for these changes in knee mechanics with respect to the intact condition.

Sub-Aim 4B: Determine the effect of loosening on cartilage contact and meniscus mechanics for anatomic and nonanatomic repairs. It is hypothesized that loosened anatomic repairs will result in significant changes to cartilage contact or meniscus mechanics with respect to the intact condition. Additionally, it is hypothesized that none of the nonanatomic repairs will completely restore knee mechanics, but nonanatomic repairs placed further anterior will be the most restorative. Based on the findings of Specific Aim 3, the finite element knee models developed in Sub-Aim 4A will be

used to simulate compression with loosened meniscal root repairs. **Approach 4B:** The unrecoverable repair loosening calculated in Specific Aim 3 will be implemented into the three finite element knee models. Knee mechanics of the tibial articular cartilage, medial menisci, and anteromedial meniscal insertions will be assessed with tibiofemoral compression to simulate rehabilitation and return-to-activity loading at different flexion angles. Loosened anatomic repairs and loosened nonanatomic repairs will be evaluated for these changes in knee mechanics with respect to the intact condition.

REFERENCES

[1] Ahn JH, Wang JH, Lim HC, Bae JH, Park JS, Yoo JC, Shyam AK. Double transosseous pull out suture technique for transection of posterior horn of medial meniscus. *Arch Orthop Trauma Surg*. 2009; 129(3): 387-392.

[2] Ahn JH, Wang JH, Yoo JC, Noh HK, Park JH. A pull out suture for transection of the posterior horn of the medial meniscus: using a posterior trans-septal portal. *Knee Surg Sports Traumatol Arthrosc*. 2007; 15(12): 1510-1513.

[3] Allaire R, Muriuki M, Gilbertson L, Harner CD. Biomechanical consequences of a tear of the posterior root of the medial meniscus: similar to total meniscectomy. *J Bone Joint Surg Am*. 2008; 90(9) 1922-1931.

[4] Allen AA, Caldwell GL, Fu FH. Anatomy and biomechanics of the meniscus. *Oper Tech Orthop*. 1995; 5(1); 2-9.

[5] Aspden RM, Yarker YE, Hukins DW. Collagen orientations in the meniscus of the knee joint. *J Anat*. 1985; 140(3): 371-380.

[6] Benjamin M, Evans EJ, Rao RD, Findlay JA, Pemberton DJ. Quantitative differences in the histology of the attachment zones of the meniscal horns in the knee joint of man. *J Anat*. 1991; 177: 127-134.

[7] Bloecker K, Guermazi A, Wirth W, Benichou O, Kwoh CK, Hunter DJ, Englund M, Resch H, Eckstein F. Tibial coverage, meniscus position, size and damage in knees discordant for joint space narrowing – data from the Osteoarthritis Initiative. *Osteoarthritis Cartilage*. 2013; 21(3): 419-427.

[8] Cerminara AJ, LaPrade CM, Smith SD, Ellman MB, Wijdicks CA, LaPrade RF. Biomechanical evaluation of a transtibial pull-out meniscal root repair: challenging the bungee effect. *Am J Sports Med*. 2014; 42(12): 2988-2995.

[9] Chia HN, Hull ML. Compressive moduli of the human medial meniscus in the axial and radial directions at equilibrium and at a physiological strain rate. *J Orthop Res*. 2008; 26(7): 951-956.

[10] Choi NH, Son KM, Victoroff BN. Arthroscopic all-inside repair for a tear of posterior root of the medial meniscus: a technical note. *Knee Surg Sports Traumatol Arthrosc*. 2008; 16(9): 891-893.

[11] Chung KS, Ha JK, Ra RJ, Kim JG. A meta-analysis of clinical and radiographic outcomes of posterior horn medial meniscus root repairs. *Knee Surg Sports Traumatol Arthrosc*. 2016; 24(5): 1455-1468.

[12] Chung KS, Ha JK, Yeom CH, Ra HJ, Jang HS, Choi SH, Kim JG. Comparison of clinical and radiologic results between partial meniscectomy and refixation of medial meniscus posterior root tears: a minimum 5-year follow-up. *Arthroscopy*. 2015; 31(10): 1941-1950.

[13] Engelsohn E, Umans H, DiFelice GS. Marginal fractures of the medial tibial plateau: possible association with medial meniscal root tear. *Skeletal Radiol*. 2007; 36(1): 73-76.

[14] Fairbank TJ. Knee joint changes after meniscectomy. *J Bone Joint Surg Br*. 1948; 30B0(4): 664-670.

[15] Feucht MJ, Kühle J, Bode G, Mehl J, Schmal H, Südkamp NP, Niemeyer P. Arthroscopic transtibial pullout repair for posterior medial meniscus root tears: A systematic review of

clinical, radiographic, and second-look arthroscopic results. *Arthroscopy*. 2015; 31(9): 1808-1816.
[16] Fox AJ, Wanivenhaus F, Burge AJ, Warren RF, Rodeo SA. The human meniscus: a review of anatomy, function, injury, and advances in treatment. *Clin Anat*. 2015; 28(2): 269-287.
[17] Fukubayashi T, Kurosawa H. The contact area and pressure distribution pattern of the knee: a study of normal and osteoarthrotic knee joints. *Acta Orthop Scand*. 1980; 51(6): 871-879.
[18] Furumatsu T, Kodama Y, Fujii M, Tanaka T, Hino T, Kamatsuki Y, Yamada K, Miyazawa S, Ozaki T. A new aiming guide can create the tibial tunnel at favorable position in transtibial pullout repair for the medial meniscus posterior root tear. *Orthop Traumatol Surg Res*. 2017; 103(3): 367-371.
[19] Gao J, Oqvist G, Messner K. The attachments of the rabbit medial meniscus. A morphological investigation using image analysis and immunohistochemistry. *J Anat*. 1994; 185(Pt 3): 663.
[20] Gupte CM, Bull AM, Amis AA. A review of the function and biomechanics of the meniscofemoral ligaments. *Arthroscopy*. 2003; 19(2): 161-171.
[21] Hede A, Larsen E, Sandberg H. The long term outcome of open total and partial meniscectomy related to the quantity and site of the meniscus removed. *Int Orthop*. 1992; 16(2): 122-125.
[22] Johannsen AM, Civitarese DM, Padalecki JR, Goldsmith MT, Wijdicks CA, LaPrade RF. Qualitative and quantitative anatomic analysis of the posterior root attachments of the medial and lateral menisci. *Am J Sports Med*. 2012; 40(10): 2342-2347.
[23] Joshi MD, Suh JK, Marui T, Woo SL. Interspecies variation of compressive biomechanical properties of the meniscus. *J Biomed Mater Res*. 1995; 29(7): 823-828.
[24] Kim YM, Rhee KJ, Lee JK, Hwang DS, Yang JY, Kim SJ. Arthroscopic pullout repair of a complete radial tear of the tibial attachment site of the medial meniscus posterior horn. *Arthroscopy*. 2006; 22(7): 795.e1-795.e4.
[25] Koenig JH, Ranawat AS, Umans HR, DiFelice GS. Meniscal root tears: diagnosis and treatment. *Arthroscopy*. 2009; 25(9): 1025-1032.
[26] Krych AJ, Johnson NR, Mohan R, Hevesi M, Stuart MJ, Littrell LA, Collins MS. Arthritis progression on serial MRIs following diagnosis of medial meniscal posterior horn root tear. *J Knee Surg*. 2017 [Epub Ahead of Print] PMID: 28950387.
[27] Krych AJ, Reardon PJ, Johnson NR, Mohan R, Peter L, Levy BA, Stuart MJ. Non-operative management of medial meniscus posterior horn root tears is associated with worsening arthritis and poor clinical outcome at 5-year follow-up. *Knee Surg Sports Traumatol Arthrosc*. 2017; 25(2): 383-389.
[28] LaPrade CM, Ellman MB, Rasmussen MT, James EW, Wijdicks CA, Engebretsen L, LaPrade RF. Anatomy of the anterior root attachments of the medial and lateral menisci: a quantitative analysis. *Am J Sports Med*. 2014; 42(10): 2386-2392.
[29] LaPrade CM, Foad A, Smith SD, Turnbull TL, Dornan GJ, Engebretsen L, Wijdicks CA, LaPrade RF. Biomechanical consequences of a nonanatomic posterior medial meniscal root repair. *Am J Sports Med*. 2015; 43(4): 912-920.
[30] LaPrade CM, James EW, Cram TR, Feagin JA, Engebretsen L, LaPrade RF. Meniscal root tears: a classification system based on tear morphology. *Am J Sports Med*. 2014; 43(2): 363-369.
[31] LaPrade CM, James EW, Engebretsen L, LaPrade RF. Anterior medial meniscal root avulsions due to malposition of the tibial tunnel during anterior cruciate ligament

reconstruction: two case reports. *Knee Surg Sports Traumatol Arthrosc*. 2014; 22(5): 1119-1123.

[32] LaPrade CM, Jansson KS, Dornan G, Smith SD, Wijdicks CA, LaPrade RF. Altered tibiofemoral contact mechanics due to lateral meniscus posterior horn root avulsions and radial tears can be restored with in situ pull-out suture repairs. *J Bone Joint Surg Am*. 2014; 96(6): 471-479.

[33] LaPrade CM, LaPrade MD, Turnbull TL, Wijdicks CA, LaPrade RF. Biomechanical evaluation of the transtibial pull-out technique for posterior medial meniscal root repairs using 1 and 2 transtibial bone tunnels. *Am J Sports Med*. 2015; 43(4): 899-904.

[34] LaPrade RF, Ly TV, Wentorf FA, Engebretsen AH, Johansen S, Engebretsen L. The anatomy of the medial part of the knee. *J Bone Joint Surg*. 2007; 89(9): 2000-2010.

[35] Lerer DB, Umans HR, Hu MX, Jones MH. The role of meniscal root pathology and radial meniscal tear in medial meniscal extrusion. *Skeletal Radiol*. 2004; 33(10): 569-574.

[36] Messner K, Gao J. The menisci of the knee joint. Anatomical and functional characteristics, and a rationale for clinical treatment. *J Anat*. 1998; 193(2): 161-178.

[37] Moon HK, Koh YG, Kim YC, Park YS, Jo SB, Kwon SK. Prognostic factors of arthroscopic pull-out repair for a posterior root tear of the medial meniscus. *Am J Sports Med*. 2012; 40(5): 1138-1143.

[38] Natsis K, Paraskevas G, Anastasopoulos N, Papamitsou T, Sioga A. Meniscofibular ligament: morphology and functional significance of a relatively unknown anatomical structure. *Anat Res Int*. 2012: 2012:214784.

[39] Nelson EW, LaPrade RF. The anterior intermeniscal ligament of the knee: an anatomic study. *Am J Sports Med*. 2000; 28(1): 74-76.

[40] Padalecki JR, Jansson KS, Smith SD, Dornan GJ, Pierce CM, Wijdicks CA, LaPrade RF. Biomechanical consequences of a complete radial tear adjacent to the medial meniscus posterior root attachment site: in situ pull-out repair restores derangement of joint mechanics. *Am J Sports Med*. 2014; 42(3): 699-707.

[41] Park YS, Moon HK, Koh YG, Kim YC, Sim DS, Jo SB, Kwon SK. Arthroscopic pullout repair of posterior root tear of the medial meniscus: the anterior approach using medial collateral ligament pie-crusting release. *Knee Surg Sports Traumatol Arthrosc*. 2011; 19(8): 1334-1336

[42] Peterson W, Tillmann B. Collagenous fibril texture of the human knee joint menisci. *Anat Embryol (Berl).* 1998; 197(4): 317-324.

[43] Röpke EF, Kopf S, Drange S, Becker R, Lohmann CH, Starke C. Biomechanical evaluation of meniscal root repair: a porcine study. *Knee Surg Sports Traumatol Arthrosc*. 2015; 23(1): 45-50.

[44] Seedhom BB, Dowson D, Wright V. Functions of the menisci: a preliminary study. *Ann Rheum Dis*. 1974; 33(1): 111.

[45] Vedi V, Williams A, Tennant SJ, Spouse E, Hunt DM, Gedroyc WMW. Meniscal movement: An in vivo study using dynamic MRI. *J Bone Joint Surg (Br)*. 1999; 81(1): 37-41.

[46] Villegas DF, Hansen TA, Liu DF, Haut Donahue TL. A quantitative study of the microstructure and biochemistry of the medial meniscal horn attachments. *Ann Biomed Eng*. 2008; 26(1): 123-131.

[47] Walker PS, Erkman MJ. The role of the menisci in force transmission across the knee. *Clin Orthop Relat Res*. 1975; 109: 184-192.

[48] Watson JN, Wilson KJ, LaPrade CM, Kennedy NI, Campbell KJ, Hutchinson MR, Wijdicks CA, LaPrade RF. Iatrogenic injury of the anterior meniscal root attachments following anterior cruciate ligament reconstruction tunnel reaming. *Knee Surg Sports Traumatol Arthrosc*. 2015; 23(8): 2360-2366.

[49] Xu C, Zhao J. A meta-analysis comparing meniscal repair with meniscectomy in the treatment of meniscal tears: the more meniscus, the better outcome? *Knee Surg Sports Traumatol Arthrosc*. 2015; 23(1): 164-170.

CHAPTER 2:

OVERLAP BETWEEN ANTERIOR CRUCIATE LIGAMENT AND ANTEROLATERAL MENISCAL ROOT INSERTIONS: A SCANNING ELECTRON MICROSCOPY STUDY†

2.1 Introduction

Over the past decade, there has been an increasing emphasis on anatomic anterior cruciate ligament (ACL) reconstruction to best restore knee kinematics after an ACL tear. Although studies have shown that the position,[20] size,[15] and shape[11] of the ACL insertion site are variable, anatomic single- and double-bundle ACL reconstructions have both shown improved outcomes, especially when performed using an individualized technique.[13] However, recent investigations of anatomic ACL reconstruction have highlighted concern over iatrogenic injuries of anterior meniscal root insertions caused by reaming of tibial bone tunnels, specifically the anterolateral meniscal root (ALMR) insertion.[17,22]

While many studies have investigated the significance of the ACL and potential reconstruction techniques,[1,5,12,14,25] the complex relationship between the tibial ACL and the lateral meniscus has become a recent area of focus.[6,9,16-19,22] The ALMR insertion has been described to attach underneath the lateral portion of the ACL insertion with a disorganized fiber network connecting the 2 insertions.[9,18] An investigation of ACL reconstruction tunnel reaming demonstrated that iatro-genic injuries of the ALMR insertion area occurred in two-thirds of sample groups and that the average area of injuries was at least 25% of the original ALMR insertion area,

---

†This chapter has been accepted as a Research Paper in the American Journal of Sports Medicine (Volume 45, Issue 2, 2017). All content has been adapted with permission from SAGE Publishing.

likely because of this intricate relationship.[22] More importantly, damage to the ALMR insertion caused by tunnel reaming was found to significantly decrease its ultimate failureload.[17] Although variability in tibial ACL tunnel placement has been reported to be relatively consistent between surgeons, with 90% of tibial tunnels within applied literature-based guidelines, these studies of iatrogenic injuries suggest that even well-placed anatomic tunnels may disrupt the ALMR insertion.[23] Because the lateral meniscus has been reported to be an important secondary stabilizer of the knee, particularly during pivot-shift loading,[19] the demonstrated risk of iatrogenic injuries to the ALMR insertion during ACL reconstruction may pose a threat to overall knee integrity after this procedure.

While these studies begin to describe the complex relation-ship and the risk of ACL reconstruction on the ALMR insertion, further investigation of how the 2 insertions interact is necessary to understand and define the 3-dimensional relationship between these 2 structures. To further understand the quantitative anatomy of the insertion relationship, LaPrade et al.[16] reported that, on average, 41% of the ACL insertion area and 63% of the ALMR insertion area overlapped with one another. Microscopic studies of the tibial insertion site have been previously conducted to investigate quantities of fibrocartilaginous zones to relate biomechanical properties of the insertion[2,3,7,8]; however, the authors are unaware of any study that has microscopically evaluated the fibrocartilaginous insertion of the tibial insertion with respect to the ALMR insertion, particularly in the sagittal and coronal planes.

Therefore, the purpose of this study was to investigate the microstructural relationship between the tibial ACL and ALMR insertions using scanning electron microscopy (SEM) in the coronal and sagittal planes. It was hypothesized that a significant portion of the ACL would overlap the ALMR insertion in both the coronal and sagittal planes.

2.2 Methods

2.2.1 Specimen Preparation

Institutional review board approval was obtained for this study (Colorado State University 14-5240H). A total of 10 fresh-frozen human cadaveric knees from 5 male and 5 female specimens were used with a mean age of 52.7 years (range, 33-63 years) and mean body mass index of 22.4 kg/m^2 (range, 15-34 kg/m^2), and knees that displayed macroscopic degenerative changes or evidence of trauma, such as osteoarthritis, meniscal tears, or ligament injuries, were excluded. Specimens were dissected to remove all soft tissues around the knee, including the collateral ligaments and the posterior cruciate ligament. Care was taken to isolate and preserve the entire ACL and ALMR insertions throughout dissection. The midsubstance of the ACL was then transected to separate the femoral and tibial insertions. Once separated, the proximal tibias were transected 20 mm from the articular cartilage surface using an oscillating saw. A bone saw was then used to remove the excess tibial plateau and create a 30 × 30 × 20–mm rectangular block encompassing the tibial ACL and ALMR insertions (Figure 2.1).

Samples were prepared for SEM similar to previously presented methods.[21,24] Briefly, the samples were placed in fixative (2.5% glutaraldehyde) for 48 hours at room temperature. The samples were then submerged in 10% formic acid to decalcify at room temperature. After decalcification, the samples were immersed in a 1% tannic acid solution buffered with 0.05 M cacodylate (pH 7.2) for 4 hours and then rinsed in distilled water for 24 hours. Samples were then dehydrated in ascending concentrations of ethanol (30%, 50%, 70%, 80%, 90%, and 100%) for 10 minutes each and cut into 2-mm sections. The number of sections ranged from 5 to 7 sections per specimen. Samples from 5 specimens were cut into coronal sections with the ALMR insertion fibers running approximately parallel to the section plane, and samples from the remaining 5

specimens were cut into sagittal sections with the ACL fibers running approximately parallel to the section plane. Once sectioned, the samples were placed in ascending concentrations of hexamethyldisilazane for 10 minutes each. The samples were then dried and stored in a vacuum desiccator.

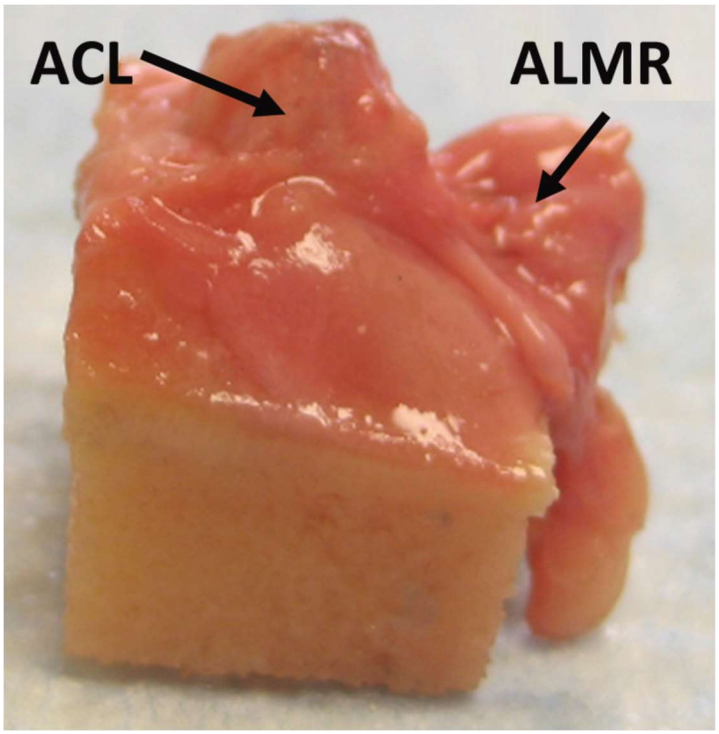

Figure 2.1 – Sample photograph of the rectangular bone block cut to include the tibial anterior cruciate ligament (ACL) and anterolateral meniscal root (ALMR) insertions.

2.2.2 Imaging

Samples were mounted onto a stub with conductive double-sided tape and copper tape with the surface of interest facing up toward the electron beam. The samples were then coated with 10 nm gold and scanned with a scanning electron microscope (JEOL USA Inc.) in the secondary electron emission mode with an accelerating voltage of 15 kV.

To evaluate the relationship between the tibial ACL insertion and the ALMR insertion in the coronal plane, a section from each specimen was taken from the middle of the ALMR insertion

to image. A section from each specimen used for viewing the sagittal plane was taken closer to the lateral side of the ACL insertion to incorporate the ALMR insertion. Section locations were chosen to evaluate the maximum overlap of the ACL and ALMR insertions. Each section was assessed at high magnification (up to 1500×) to view individual insertion fibers. SEM allowed real-time imaging of sections with the availability to maneuver around the sections at high magnifications; thus, these high-resolution images were used to identify the entirety of both insertions and observe where they overlap. The 4-phase fibers of the tibial ACL insertion were evaluated with respect to the ALMR insertion fibers. Fibrocartilaginous entheses have been previously described as 4 distinct zones: zone 1 consists of dense, fibrous connective tissue; zone 2 consists of uncalcified fibrocartilage; zone 3 consists of calcified fibrocartilage; and zone 4 consists of subchondral bone.[2,4,24] Approximately 15 to 20 lower magnification (15×) images were then taken using the built-in SEM camera across the entirety of each sample and stitched together for quantitative analysis of the insertion relationship using ImageJ software (National Institutes of Health).

2.2.3 Data Analysis

The percentage of the tibial ACL insertion that overlapped with the ALMR insertion instead of inserting into subchondral bone was determined in each plane to further understand the relationship between the 2 insertions. For each sample, the length of the ACL insertion that visibly inserted into subchondral bone was initially determined by measuring the boundary between the ligament-bone interface of the 2-phase insertion fibers and tidemark of the 4-phase insertion fibers described in previous literature.[2,4,24] The length of the ACL insertion that overlapped with the ALMR insertion was determined using the high-magnification images. The percentage of the ACL insertion that overlapped with the ALMR insertion fibers instead of inserting into subchondral

bone was then calculated for each sample. Measurements were taken by 2 raters from the stitched SEM images using ImageJ software.

A 2-sample, equal-variance Student *t* test was performed on the percentages of insertion interaction between the coronal and sagittal sections. Statistical significance was determined to be present for $p < 0.05$. Additionally, interrater intraclass correlation coefficients (ICCs) were calculated to test the reliability of measurements between the 2 raters. Measurements were also taken again after 2 weeks to calculate the intrarater ICCs and determine the reliability between measurements repeated by a single rater.

2.3 Results

2.3.1 Macroscopic Appearance

The ACL tibial insertion had a fan-like appearance macroscopically and was located posteromedial to the ALMR insertion. In all 10 specimens, the ALMR inserted underneath the lateral portion of the ACL. The relationship of the ACL tibial insertion and the ALMR insertion was visible upon forming the coronal and sagittal sections. On the coronal sections, the ALMR insertion fibers clearly coursed under the lateral portion of the tibial ACL insertion. On the sagittal sections, the ALMR insertion fibers were visible inferior to the ACL insertion fibers on sections from the lateral portion of the ACL tibial insertion but were not visible or present on sections from the central or medial portion.

2.3.2 Microscopic Appearance

The tibial ACL insertion displayed an intimate relationship with the ALMR insertion as both structures transitioned into bone in both the sagittal and coronal sections. The ALMR

insertion fibers were distinguished from the ACL fibers in the SEM images by the difference in orientation at high magnification. Initially, at low magnification, each section was viewed, and the region of overlap in the coronal (Figure 2.2) and sagittal (Figure 2.3) planes was identified to investigate further at higher magnification. With increasing magnification, the individual fibers became more easily distinguishable, and the orientations of individual fibers of the ACL and ALMR insertions were identified. For all coronal sections, the ACL insertion fibers appeared to run vertically in and out of the image (Figure 2.4A). The ALMR insertion fibers ran in a diagonal orientation along the plane of view as they approached the bone interface (Figure 2.4B). For all sagittal sections, the appearance of the fibers in SEM images was reversed. The ACL insertion fibers ran diagonally along the plane of view, while the ALMR insertion fibers appeared to run vertically in and out of the image (Figure 2.5). Once the separate insertions were identified, the overlap was mapped across each image (Figure 2.3). Additionally, 4-phase fibers of the tibial ACL were found medially adjacent to the ALMR insertion in the coronal plane (Figure 2.2). The 4-phase insertion fibers of the ACL were not clearly visible or not present in the sagittal sections imaged.

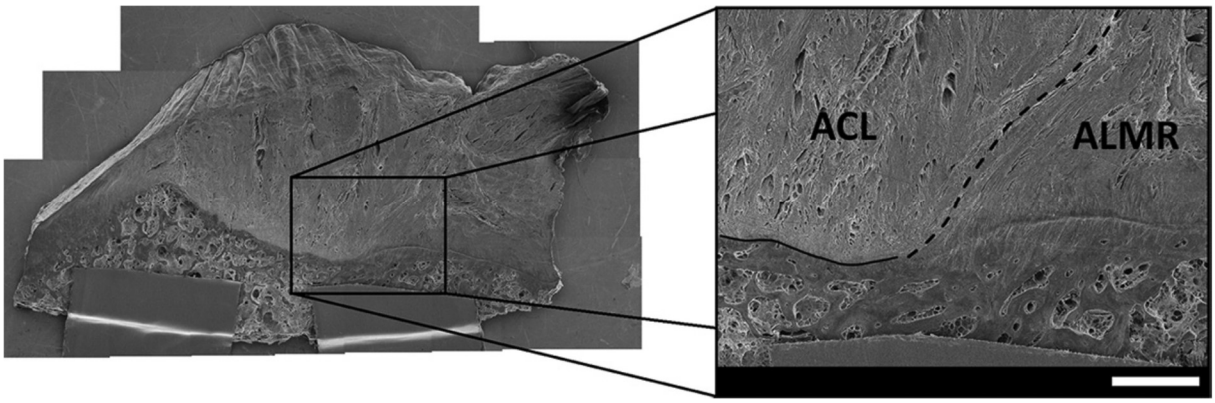

Figure 2.2 – Scanning electron microscopy image of the intricate relationship between the 2 insertions in the coronal plane. Note the 4-phase insertion fibers of the anterior cruciate ligament (ACL) with the tidemark (solid line) separating the uncalcified fibrocartilage layer from the calcified fibrocartilage layer directly adjacent to the anterolateral meniscal root (ALMR) insertion.

The dashed line represents the interaction between the ACL and ALMR. (Close-up image: 15×; working distance = 25 mm; scale bar = 1 mm).

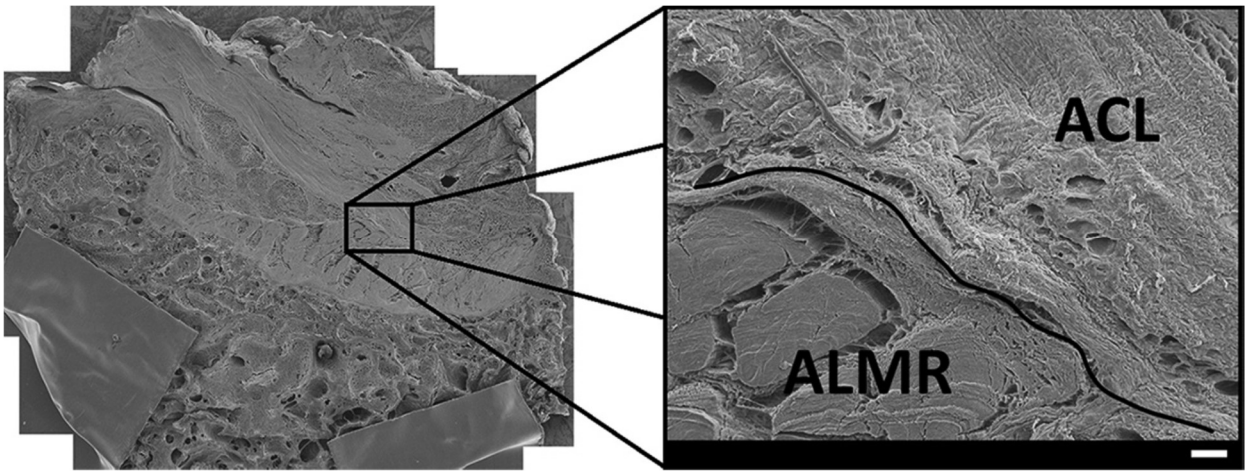

Figure 2.3 – Scanning electron microscopy image of the intricate relationship between the 2 insertions in the sagittal plane. The solid line represents where the anterior cruciate ligament (ACL) insertion overlaps the anterolateral meniscal root (ALMR) insertion within the plane of view. 153; working distance = 25 mm. (Close-up image: 75×; working distance = 10 mm; scale bar = 100 μm).

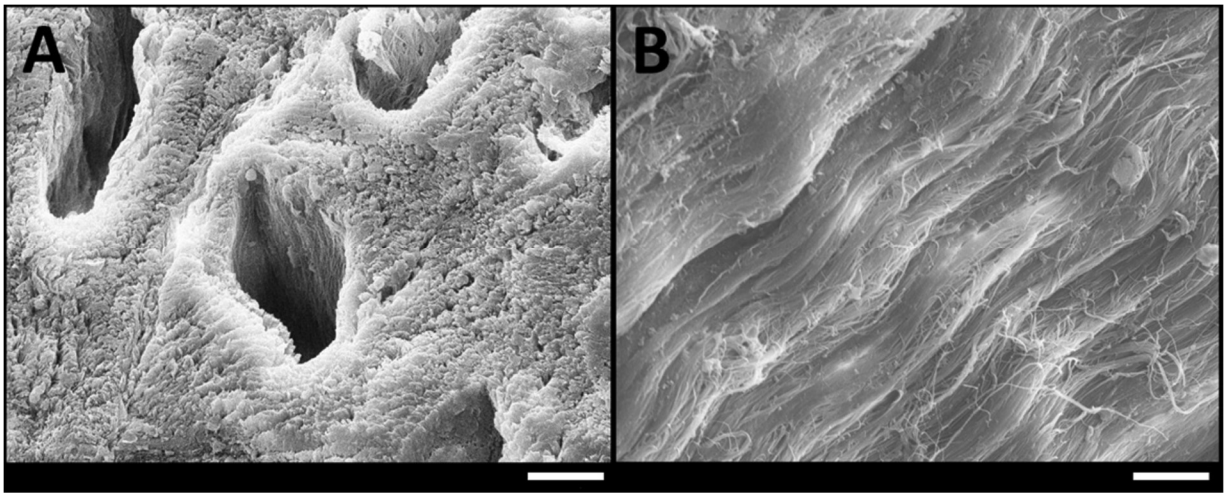

Figure 2.4 – Scanning electron microscopy images of the (A) tibial anterior cruciate ligament (ACL) insertion fibers and the (B) anterolateral meniscal root (ALMR) insertion fibers taken of a coronal section. Note that the ACL fibers appear to run vertically in and out of the image while the ALMR fibers run along the image plane. 1500×; working distance = 10 mm; scale bars = 10 μm.

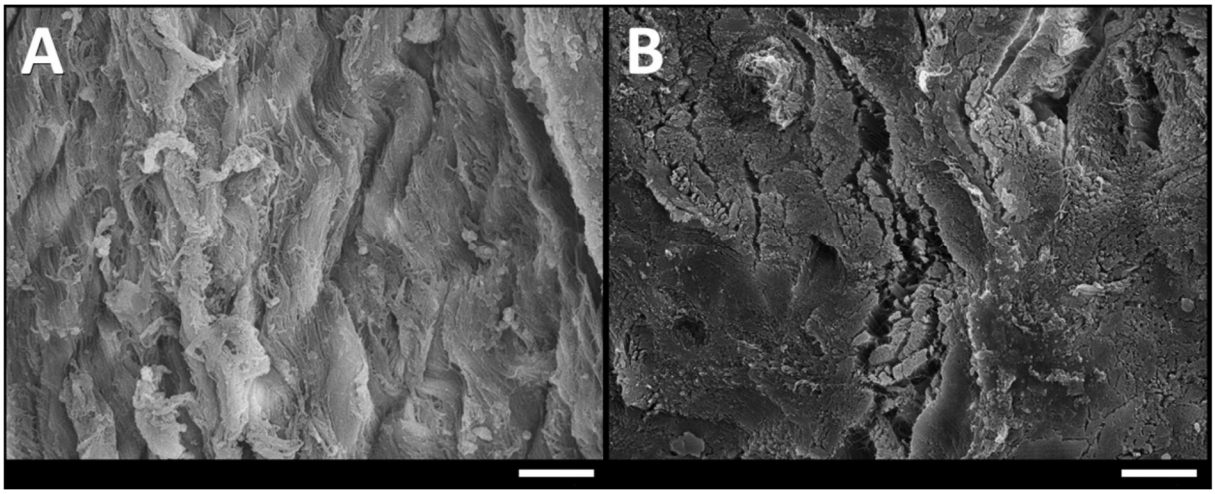

Figure 2.5 – Scanning electron microscopy images of the (A) tibial anterior cruciate ligament (ACL) insertion fibers and the (B) anterolateral meniscal root (ALMR) insertion fibers taken of a sagittal section. Note that the ACL fibers appear to run along the image plane while the ALMR fibers run vertically in and out of the image. 1500×; working distance = 10 mm; scale bars = 10 μm.

After the insertions of the tibial ACL and ALMR were identified, the percentage of the ACL insertion overlapping the ALMR insertion was calculated for each section in both planes. The combined interrater ICC was 0.81 for all measurement values, with interrater ICCs of 0.78 and 0.84 for measurements of coronal and sagittal sections, respectively. The intrarater ICC was 0.98 for all measurements, with intrarater ICCs of 0.98 and 0.95 for measurements of coronal and sagittal sections, respectively. For the coronal sections, the tibial ACL insertion overlapped the ALMR insertion with a mean percentage of 41.0% ± 8.9% (Table 2.1). The mean length of the measured overlap between the 2 insertions in the coronal plane was 6.5 ± 1.9 mm, while the mean length of the measured interaction between the ACL insertion and subchondral bone was 9.2 ± 1.4 mm (Table 2.1). For the sagittal sections, the tibial ACL insertion overlapped the ALMR insertion with a mean percentage of 53.9% ± 4.3% (Table 2.2). The mean length of the measured overlap between the 2 insertions in the sagittal plane was 9.5 ± 2.0 mm, while the mean length of the measured interaction between the ACL insertion and subchondral bone was 8.3 ± 2.8 mm (Table

2.2). The percentage of insertion overlap in the sagittal plane was significantly higher than in the coronal plane (p = .02).

Table 1. Average measurement values between two raters for each specimen used to calculate the overlap of the ACL and ALMR insertions within the coronal plane with the mean and 95% confidence intervals of the five specimens together.

Coronal Sections (Superior-Inferior and Medial-Lateral Plane)

	ACL-ALMR [mm]	ACL-Bone [mm]	ACL-ALMR Overlap [%]
Specimen 1	8.2	9.0	47.7
Specimen 2	3.6	10.3	25.9
Specimen 3	7.5	10.9	40.8
Specimen 4	7.4	8.4	46.8
Specimen 5	5.7	7.3	43.8
Mean [95% CI]	6.5 [4.2, 8.8]	9.2 [7.4, 11.0]	41.0 [30.0, 52.0]

Table 2.2 – Average measurement values between two raters for each specimen used to calculate the overlap of the ACL and ALMR insertions within the sagittal plane with the mean and 95% confidence intervals of the five specimens together.

Sagittal Sections (Superior-Inferior and Anterior-Posterior Plane)

	ACL-ALMR [mm]	ACL-Bone [mm]	ACL-ALMR Overlap [%]
Specimen 6	8.3	8.0	51.0
Specimen 7	7.7	6.5	54.2
Specimen 8	8.0	5.2	60.6
Specimen 9	11.1	9.4	54.1
Specimen 10	12.2	12.5	49.4
Mean [95% CI]	9.5 [6.9, 12.0]	8.3 [4.8, 11.8]	53.9 [48.6, 59.2]

2.4 Discussion

The purpose of this study was to microscopically investigate and quantify the overlap between the tibial ACL and ALMR insertions using SEM in the coronal and sagittal planes. The results of the investigation support our hypothesis that a significant portion of the tibial ACL insertion overlaps the ALMR insertion in both the coronal and sagittal planes. Our investigation showed that, on average, 41.0% of the ACL insertion overlaps the ALMR insertion in the coronal

plane and 53.9% in the sagittal plane. Although only a single section was viewed for each specimen, the imaged sections were selected to represent the maximum overlap of the tibial ACL insertion in the 2 planes of interest. Previously, a measurement of ACL-ALMR overlap in the transverse plane, described as insertion areas on the tibial plateau, was conducted.[16] That study measured the entire area of both the tibial ACL and ALMR insertions on the tibial plateau using a coordinate measuring device and demonstrated that an average of 41% of the ACL insertion area overlapped the ALMR insertion. The present study supplements previous knowledge of the overlap by providing information of the additional 2 anatomic planes. In com-bination, the 2 studies show that the tibial ACL overlaps the ALMR insertion by at least 40%, on average, in all 3 anatomic planes with the greatest overlap found in the sagittal plane.

The additional information regarding the anterior horn of the lateral meniscus and its intimate relationship with the tibial ACL insertion may have important clinical implications. Although there are no case reports of ALMR avulsions due to bone tunnel drilling, previous studies have demonstrated a clinical risk of iatrogenic injuries to the ALMR insertion.[17,22] Most notably, anatomically placed tibial tunnels for ACL reconstruction have been reported to lead to damage of a significant portion of the ALMR insertion area and to significantly decrease the insertion failureload.[17] This study utilized an 11 mm–diameter reamer, which is larger than the 9 mm–diameter reamer commonly used during hamstring ACL reconstruction techniques; however, an 11 mm–diameter reamer is often used for bone-tendon-bone grafts and reconstructions in young and active populations. Therefore, the previous study may not represent the results of all ACL reconstruction procedures, but it does represent a larger diameter reamer used in some ACL reconstructions. Additionally, this study reported that all failures of the ALMR insertion were caused by bony avulsions. The authors also mentioned that the bony avulsions in their study were

not necessarily consistent clinically, so the bony avulsion failures may have been an intrinsic result of their testing procedure. Although this study did not demonstrate complete tears from the tibial plateau as failures, it did find that failure was caused by ALMR insertion disruption by tunnel reaming.

Another study utilized a 10 mm–diameter reamer to create anatomically placed tibial tunnels using a tibial aiming device set at 2 different angles of 40°and 60°.[22] That study reported iatrogenic damage to 29% and 26% of the ALMR insertion area for the 40°and 60° groups, respectively. This study utilized a 10 mm–diameter reamer, which as previously stated is larger than the9 mm–diameter reamer used for some ACL reconstructions; however, a 10 mm–diameter reamer is in the range of common clinically used reamers. Additionally, this study demonstrated significant anterior translation of the reamed tunnel center from the native ACL insertion area. Although this translation may have contributed to an increase in iatrogenic injuries to the ALMR insertion, the authors utilized a precise measurement technique to determine appropriate tunnel locations. Because the cadaveric joints were open and the femur removed, the tunnel site was accurately located. Therefore, the authors believed that this translation might be an intrinsic risk for reaming the tibial tunnels during ACL reconstruction. The significance of the amount of ALMR insertion damage caused by tunnel reaming has not yet been quantified; however, these studies have demonstrated the clinical risk of iatrogenic injuries to the ALMR insertion involved with even properly placed tibial tunnels.

The results from the present study supplement previous knowledge of insertion overlap and the risk of iatrogenic injuries. Primarily, this study was the first to quantify the ACL insertion overlap of the ALMR insertion in the coronal and sagittal planes. Overlap of the insertion a reason the tibial plateau has been previously reported; how-ever, the results of this study demonstrate

significant overlap of the insertions superior to the insertion sites on the tibial plateau as well. The results of the present study in addition to the iatrogenic injury studies may suggest that the angle of the guide contributes to the amount of ALMR insertion fibers that are disrupted. Although these studies have used the insertion area as an outcome variable, the guide angle may cause damage to the further superior fibers of the insertion even if the insertion area is not disrupted because of this significant overlap in the coronal and sagittal planes. Again, the clinically significant amount of disruption in the ALMR insertion, whether of the insertion area or the insertion fibers superior to the tibial plateau surface, has yet to be defined. Future studies should be conducted to determine how much damage to the ALMR insertion is acceptable to properly restore ACL function without increasing the risk for tears of the ALMR.

Additionally, 4-phase insertion fibers consisting of dense, fibrous connective tissue; uncalcified fibrocartilage; calcified fibrocartilage; and subchondral bone zones were identified in the ACL insertion medially adjacent to ALMR insertion fibers in the central coronal plane.[2,24] The 4-phase insertion fibers were not present or identifiable in images where the ACL overlapped the ALMR insertion in the sagittal plane because these sections were taken from the furthest lateral side of the ACL and these superficial portions are frequently more fibrous.[4] While it has been believed that a main goal during ACL reconstruction should be to place a tunnel within the center of the 4-phase insertion fibers, described as the most structurally important insertion fibers,[10] this study found that 4-phase insertion fibers of the tibial ACL were found medial to the overlap with the ALMR. This intricate relationship and overlap theoretically complicate the placement of a tibial tunnel for ACL reconstruction. These structurally important fibers that insert adjacent to the ALMR insertion need to be accounted for during ACL reconstruction. The risk of iatrogenic injuries to the ALMR fibers has previously been discussed; however, the clinically significant

amount of ALMR insertion disruption has yet to be defined. Therefore, further investigation of the tibial ACL4-phase insertion fibers with respect to the location of the ALMR insertion fibers is warranted to determine how much damage to the ALMR insertion is clinically acceptable during ACL reconstruction.

We also recognize that this study has limitations. The analysis was limited to 10 total specimens. Although the shape of the insertions varied among specimens, overlap between the tibial ACL and ALMR insertions was present in all 10 specimens. Additionally, the shape of the tibial insertion site has been shown to vary among 3 common patterns, and this study did not identify the shapes of the insertion sites for the specimens.[11] How the tibial insertion site pattern affects the overlap of the ALMR insertion is unknown; therefore, the tibial insertion pattern may have caused variability in the overlap measured. The overlapping relationship with respect to the different tibial insertion sites should be investigated to further understand this relationship and how it affects ACL reconstruction.

2.5 Conclusion

This study demonstrated significant overlap of the ALMR insertion by the tibial ACL insertion in the coronal and sagittal planes and supplements a previous study's evaluation of the overlapping relationship insertion areas. As the ACL inserted into tibial subchondral bone, the lateral portion of the ACL overlapped the ALMR insertion in both the coronal and sagittal planes, on average, by 41.0% and 53.9%, respectively. Previous studies showing iatrogenic damage to the ALMR insertion and the results of this study illustrate the intricacy of this relationship, and further studies should determine what amount of ALMR insertion disruption is acceptable for a clinically successful ACL reconstruction procedure.

REFERENCES

[1] Arnoczky SP. Anatomy of the anterior cruciate ligament. *Clin Orthop Relat Res*. 1983; 172: 19-25.

[2] Beaulieu ML, Carey GE, Schlecht SH, et al. Quantitative comparison of the microscopic anatomy of the human ACL femoral and tibial entheses. *J Orthop Res*. 2015; 33(12): 1811-1817.

[3] Benjamin M, Evans EJ, Rao RD, et al. Quantitative differences in the histology of the attachment zones of the meniscal horns in the knee joint of man. *J Anat*. 1991; 177: 127-134.

[4] Benjamin M, Kumai T, Milz S, et al. The skeletal attachment of tendons-tendon ‘‘entheses.’’ *Comp Biochem Physiol A Mol Integr Physiol*. 2002; 133(4): 931-945.

[5] Edwards A, Bull AM, Amis AA. The attachments of the anteromedial and posterolateral fibre bundles of the anterior cruciate ligament, part 1: tibial attachment. *Knee Surg Sports Traumatol Arthrosc*. 2007; 15(12): 1414-1421.

[6] Ellman MB, LaPrade CM, Smith SD, et al. Structural properties of the meniscal roots. *Am J Sports Med*. 2014; 42(8): 1881-1887.

[7] Evans EJ, Benjamin M, Pemberton DJ. Fibrocartilage in the attachment zones of the quadriceps tendon and patellar ligament of man. *J Anat*. 1990; 171: 155-162.

[8] Evans EJ, Benjamin M, Pemberton DJ. Variations in the amount of calcified tissue at the attachments of the quadriceps tendon and patellar ligament in man. *J Anat*. 1991; 174: 145-151.

[9] Furumatsu T, Kodama Y, Maehara A, et al. The anterior cruciate ligament-lateral meniscus complex: a histological study. *Connect Tissue Res*. 2016; 57(2): 91-98.

[10] Gao J, Messner K. Quantitative comparison of soft tissue-bone interface at chondral ligament insertions in the rabbit knee joint. *J Anat*. 1996; 188(Pt 2): 367-373.

[11] Guenther D, Irarrázaval S, Nishizawa Y, et al. Variation in the shape of the tibial insertion site of the anterior cruciate ligament: classification is required. *Knee Surg Sports Traumatol Arthrosc*. 2017; 25(8): 2428-2432.

[12] Harner CD, Baek GH, Vogrin TM, Carlin GJ, Kashiwaguchi S, Woo SL. Quantitative analysis of human cruciate ligament insertions. *Arthroscopy*. 1999; 15(7): 741-749.

[13] Hussein M, van Eck CF, Cretnik A, et al. Individualized anterior cruciate ligament surgery: a prospective study comparing anatomic single-and double-bundle reconstruction. *Am J Sports Med*. 2012; 40(8): 1781-1788.

[14] Kopf S, Musahl V, Tashman S, Szczodry M, Shen W, Fu FH. A systematic review of the femoral origin and tibial insertion morphology of the ACL. *Knee Surg Sports Traumatol Arthrosc.* 2009; 17(3): 213-219.

[15] Kopf S, Pombo MW, Szczodry M, et al. Size variability of the human anterior cruciate ligament insertion sites. *Am J Sports Med*. 2011; 39(1): 108-113.

[16] LaPrade CM, Ellman MB, Rasmussen MT, et al. Anatomy of the anterior root attachments of the medial and lateral menisci: a quantitative analysis. *Am J Sports Med*. 2014; 42(10): 2386-2392.

[17] LaPrade CM, Smith SD, Rasmussen MT, et al. Consequences of tibial tunnel reaming on the meniscal roots during cruciate ligament reconstruction in a cadaveric model, part 1: the anterior cruciate ligament. *Am J Sports Med*. 2015; 43(1): 200-206.
[18] Seibold R, Shuhmacher P, Fernandez F, et al. Flat midsubstance of the anterior cruciate ligament with tibial ‘‘C’’-shaped insertion site. *Knee Surg Sports Traumatol Arthrosc*. 2015; 23(11): 3136-3142.
[19] Shybut TB, Vega CE, Haddad J, et al. Effect of lateral meniscal root tear on the stability of the anterior cruciate ligament-deficient knee. *Am J Sports Med*. 2015; 43(4): 905-911.
[20] Takahashi M, Doi M, Abe M, et al. Anatomical study of the femoral and tibial insertions of the anteromedial and posterolateral bundles of human anterior cruciate ligament. *Am J Sports Med*. 2006; 34(5): 787-792.
[21] Villegas DF, Haut Donahue TL. Collagen morphology in human meniscal attachments: a SEM study. *Connect Tissue Res*. 2010; 51(5): 327-336.
[22] Watson JN, Wilson KJ, LaPrade CM, et al. Iatrogenic injury of the anterior meniscal root attachments following anterior cruciate ligament reconstruction tunnel reaming. *Knee Surg Sports Traumatol Arthrosc*. 2014; 23(8): 2360-2366.
[23] Wolf BR, Ramme AJ, Wright RW, et al. Variability in ACL tunnel placement: observational clinical study of surgeon ACL tunnel variability. *Am J Sports Med*. 2013; 41(6): 1265-1273.
[24] Zhao L, Thambyah A, Broom ND. A multi-scale structural study of the porcine anterior cruciate ligament tibial enthesis. *J Anat*. 2014; 224(6): 624-633.
[25] Ziegler CG, Pietrini SD, Westerhaus BD, et al. Arthroscopically pertinent landmarks for tunnel positioning in single-bundle and double-bundle anterior cruciate ligament reconstructions. *Am J Sports Med*. 2011; 39(4): 743-752.

CHAPTER 3:

EARLY OSTEOARTHRITIS AFTER UNTREATED ANTERIOR MENISCAL ROOT TEARS: AN *IN VIVO* ANIMAL STUDY†

3.1 Introduction

Menisci are crescent-shaped, fibrocartilaginous wedges that play an important role in complex knee mechanics and func-tion.[3,39] The menisci are primarily responsible for distributing loads through the tibiofemoral joint, joint stabilization, and congruency.[1,20,27,30,49,55] The circumferential collagen fibers in the meniscus body continue into the anterior and posterior root insertional ligaments that attach to the tibialplateau.[5,7,18,22,45] Continuity of the circumferential fibers between the meniscus body and its insertions enables proper fixation into bone and facilitates the distribution of axial tibiofemoral stresses to circumferential hoop stresses.[13,5]

Meniscal root tears (MRTs) are complete radial tears or avulsion injuries of the meniscal root insertions from the tibial plateau and are a subset of injuries that cause the meniscus to inadequately distribute loads and protect the underlying articular cartilage.[26,32,48] Untreated MRTs are becoming increasingly recognized to induce articular cartilage degradation over time[2,24]; therefore, proper understanding of injury and progression of degeneration is essential.

Previously, studies on meniscal release, or destabilization of the medial meniscus (DMM), have been used to induce and analyze degeneration of knee joint tissues in murine, lapine, canine, and ovine models over time.[10,11,21-23,29,36] These models all demonstrate measurable degeneration within the knee joint tissues. Despite the wide use of these models for osteoarthritis research,

---

†This chapter has been accepted as a Research Paper in the Orthopaedic Journal of Sports Medicine (Volume 5, Issue 4, 2017). All content has been adapted with permission from SAGE Publishing.

however, the authors are not aware of any, studies assessing the degeneration of several tissues within the knee joint after release of the anterior insertions for both the lateral and medial menisci. Cadavers have also been used to investigate MRTs; however, these studies primarily focus on changes in knee biomechanics to the posteromedial and posterolateral meniscal insertions.[2,6,34]

Although tears of the anterior meniscal root insertions may be less common than posterior tears, a recent study reported that iatrogenic injury occurs at the anterior insertions of the lateral and medial menisci while reaming tibial tunnels for anterior cruciate ligament (ACL) reconstruction.[56] Currently, literature on anterior MRTs is limited to reports of case studies and anatomic analysis of the relationship between the ACL and anterior meniscal root inser-tions.[15,31,33,40,54] Since the anterior meniscal insertions are susceptible to damage during ACL reconstructions, increasing the risk for MRTs, it is important to understand how these injuries affect the joint tissues. Additionally, since clinical samples of articular cartilage and menisci are usually salvaged from advanced stages of osteoarthritis after total knee reconstructions, animal models are commonly used to experimentally induce injury and assess early degeneration.

Therefore, the purpose of this study was to measure characteristics of early degeneration in the rabbit knee after untreated anterior MRTs for major sites of earliest discernible joint involvement seen in osteoarthritis.[38] The amount and type of inflammatory cells present in the synovial fluid, the compressive material properties of the menisci and tibial articular cartilage, the subchondral bone morphology of the tibial plateau, the coverage and content of glycosaminoglycans (GAGs) of menisci and tibial articular cartilage, the total content of intact DNA, and the relative gene expression of matrix-degrading enzymes were measured after anterolateral MRTs (ALMRTs) and anteromedial MRTs (AMMRTs). It was hypothesized that if

anterior MRTs of either the medial or lateral menisci were left untreated after injury, early osteoarthritic change would occur within the joint tissues.

3.2 Methods

Institutional Animal Care and Use Committee (IACUC) approval was obtained prior to performing the study. Nine skeletally mature Flemish Giant rabbits (5.2 ± 0.2 kg) were housed in individual cages and given 3 weeks to acclimate to the housing facility. During housing, animals were monitored daily for health status, and no adverse events were observed. Before surgery, the animals were given 0.2 mg/kg butorphanol, 0.05 mg acepromazine, and 0.005 mg glycopyrrolate and then anesthetized with 5% isoflurane. A small-joint arthroscope was used to confirm the absence of preexisting arthritis or meniscal injury. Under arthroscopic visualization, a scalpel was used to create ALMRTs in 1 knee joint of 5 rabbits and AMMRTs were created in the remaining 4. After sectioning with a scalpel, the meniscal roots were probed to verify they were completely sectioned off their root attachments. A top view of the dissected proximal tibia with the menisci intact is presented for visualization of the rabbit knee anatomy in Figure 3.1. To minimize the effects of subjective bias, the animals were randomly assigned to an MRT group and surgeries were alternated between left and right limbs. The contralateral knees were left intact with no sham incision and used as nonoperative controls. The animals were monitored postoperatively and returned to normal activity in individual cages before euthanasia 8 weeks post-surgery.

Figure 3.1 – A dissected, proximal tibia with menisci intact for visualization of the rabbit knee anatomy from a left, control limb.

3.2.1 Cytologic Joint Evaluation

Immediately after euthanasia, 1.5 mL of sterile saline was injected into both injured and control knee joints just medial to the patellar tendon. The knee was flexed and extended 3 to 5 times, and diluted synovial fluid was re-aspirated from the joint using the initial delivery syringe by a veterinary technician. The volume acquired from each joint was recorded to determine whether joint effusion was present. After collection, approximately 20mL of joint fluid was placed onto a microscope slide and spread using a separate slide to make a standard "push smear" for cytologic evaluation. Duplicate smears for each joint were blinded and viewed by a board-certified veterinary clinical pathologist. Joint fluid was then subjectively interpreted and objectively scored for overall cellularity, individual cell types observed, evidence of synovial hyperplasia, and presence of osteoclasts (Table 3.1).

Table 3.1 – Objective scoring scheme to grade cytologic findings present in synovial fluid smears.[a]

Cytology Score Grading Scheme				
Measure	Score			
	0	1	2	3
Number of cells observed	Normal	Mild increase	Moderate increase	Marked increase
Cell types observed	>95% large mononuclear cells present	>95% large mononuclear cells present, but activated cells seen	Mixed inflammation	Neutrophilic inflammation
Synovial hyperplasia (Aggregates of spindle-shaped fibroblasts)	Absent	Present		
Osteoclast (Evidence for bone remodeling)	Absent	Present		

[a]This system, which allows increments from 0 to 8, provides an interpretation of inflammation, synovial hyperplasia, and bone remodeling that may occur in a joint.

3.2.2 Mechanical Testing

Indentation-relaxation testing was performed on menisci and tibial cartilage similar to previous studies within 12 hours of sacrifice and dissection.[16,17,35,52] The menisci and proximal tibias were wrapped separately in gauze, saturated with 1× phosphate-buffered saline, and stored at 4°C until ready to test. All tissues were hydrated in a 1× phosphate-buffered saline bath at room temperature during testing. Prior to mechanical testing, the menisci were each transected into anterior and posterior halves. Indentation-relaxation tests were then conducted in the middle of each anterior and posterior meniscus half (Figure 3.2). A spherical, steel indenter with a 1.59 mm diameter was used to indent to a depth of 0.2 mm at 0.2 mm/s for all samples and held for 900 s to reach equilibrium.

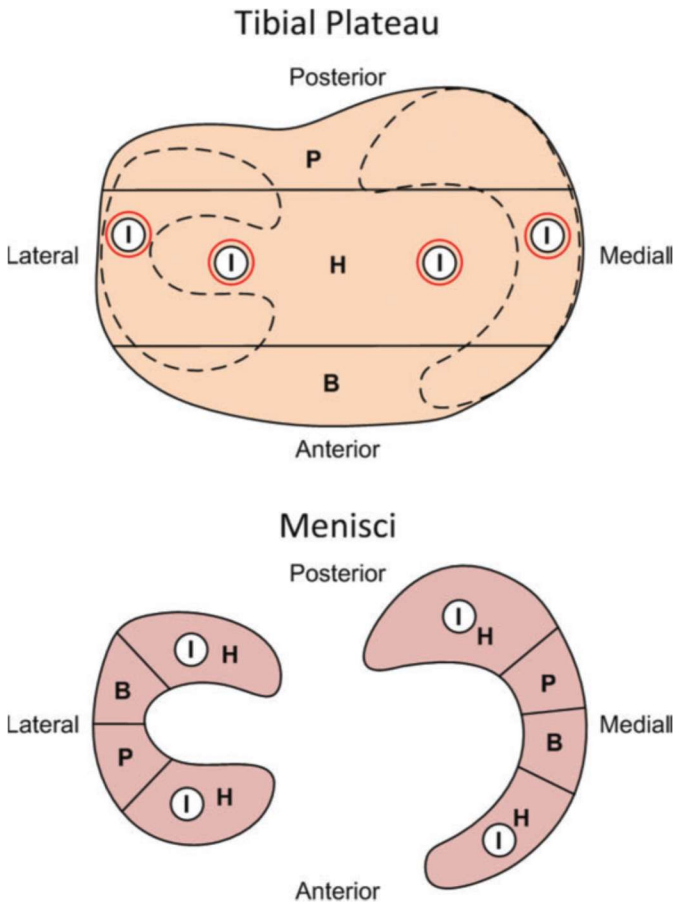

Figure 3.2 – Tissue locations allocated for different analyses on the menisci and tibial plateaus including: indentation relaxation (I), histology (H), biochemical assays (B), and quantitative reverse transcription polymerase chain reaction (qRT-PCR) (P).

Indentation-relaxation tests were conducted at 4 locations on the articular cartilage of the tibial plateau to account for locations normally covered and uncovered by the menisci, similar to a previous study (Figure 3.2).[16] Thickness measurements of the articular cartilage indentation sites were estimated by inserting a needle at a location adjacent to each indentation site and observing when the force changed due to contact with calcified cartilage, similar to previous studies.[16,46] The distance between the initial force due to the needle first contacting the cartilage surface and the force peak observed when the needle displaced through the articular cartilage and contacted the calcified cartilage was used as the thickness measurement. The spherical indenter was then pressed

into the cartilage to a depth of 20% of its estimated thickness at 20% strain/s and held for 180 seconds to reach equilibrium. After a 1200-second rest time, the indenter was replaced with the needle and the actual thickness of the articular cartilage at the indentation site was determined.[16] Hertzian contact was assumed between the tissue (elastic half-space) and the steel, spherical indenter (rigid sphere), similar to previous studies.[16,17,35,46] The instantaneous and equilibrium elastic moduli were then calculated to determine the compressive elasticity immediately after compression before interstitial fluid dissipated and again once fluid dissipation reached equilibrium, respectively. Poisson ratios for menisci and articular cartilage in rabbits have been esti-matedinpreviousstudies.[16,17,46,52] Based on these studies, the Poisson ratio was assigned to be 0.01 for menisci and 0.3 for the articular cartilage. The elastic modulus and Poisson ratio of the indenter were 210 GPa and 0.3, respectively.[16,17]

After mechanical testing, all tissue was divided and stored separately for additional analysis (Figure 3.2). Menisci were sectioned to store anterior and posterior samples in 10% formalin to fix the tissue for histological analysis. The central portions of each menisci were cut to store half in RNAlater RNA Stabilization Reagent (QIAGEN) to immediately stabilize tissue RNA for gene expression analysis and the rest in Allprotect Tissue Reagent (QIAGEN) to stabilize DNA, RNA, and protein in tissue samples for quantitative biochemical assays. Cylindrical, full-depth samples of the articular cartilage using a 5-mm biopsy punch were taken from the anterior and posterior locations of the tibial plateau, with half of the tissue stored in RNAlater and the rest stored in Allprotect. The remainder of the proximal tibias were fixed in 10% formalin. All samples in RNAlater and Allprotect were refrigerated for 24 hours to allow the reagents to penetrate the tissues and then stored at –80°C until analyzed.

3.2.3 Bone Morphology Analysis

Proximal tibias were scanned via a micro–computed tomography machine (Scanco Medical AG) to evaluate subchondral bone changes.[44] Briefly, 4 spatially distributed, cylindrical volumes of interest (VOIs) were identified foreach tibia based on anatomical markers and corresponding with the mechanical indentation testing sites of the articular cartilage (Figure 3.2). Trabecular VOIs had a diameter of 2.2 mm and height of 3.7 mm and were taken immediately under the subchondral bone plate to analyze the trabeculae within the subarticular spongiosa.[37] Subchondral bone plate VOIs had a diameter of 2.2 mm with varying heights because of anatomic differences. The following variables were measured within the analyzed VOIs: trabecular material bone mineral density, trabecular bone volume fraction, trabecular number, trabecular thickness, trabecular spacing, subchondral bone mineral density, and subchondral bone volume fraction.

3.2.4 Histological Analysis

Fixed menisci were embedded in optimum cutting temperature medium (Pelco), flash frozen using liquid nitrogen, and sectioned into 6-mm slices. The fixed proximal tibias were decalcified with 10% formic acid and cut to evaluate central, coronal sections of the tibial plateaus (Figure 3.2). The tibial plateaus were then embedded in paraffin and sectioned into6-mm slices. All sections were stained using hematoxylin, safranin-O, and fast green before being imaged using a light microscope (Olympus) and camera setup (QImaging).[47]

Imaged meniscal and tibial articular cartilage sections were analyzed similarly to previous studies.[16,17,43] Briefly, the meniscal sections were analyzed quantitatively by measuring the percentage of red-stained GAG covering the entire meniscal section using Image J software (National Institutes of Health) with the FIJI package. The GAG stain intensity of the menisci was

then blindly evaluated by 4 individuals using a previously used grading scale: no staining = 0, slight staining = 1, moderate staining = 2, and strong staining = 3. Articular cartilage and subchondral bone sections were graded histologically using a modified Mankin scale in 3 categories (Table 3.2).[16] Qualitative grades of the menisci and articular cartilage for each specimen and region were averaged across all graders.

Table 3.2 – Modified Mankin grading scale used to assess histological staining of the tibial articular cartilage.

Measure	Score						
	0	1	2	3	4	5	6
GAG Staining	Uniform	Loss of staining in superficial zone < 50% of length of plateau	Loss of staining in superficial zone > 50% of length of plateau	Loss of staining in upper 2/3 < 50% of length of plateau	Loss of staining in upper > 50% of length of plateau	Loss of staining in full depth of cartilage < 50% of length of plateau	Loss of staining in full depth of cartilage > 50% of length of plateau
Fissures	Absent	Surface fibrillation < 50% of length of plateau	Surface fibrillation > 50% of length of plateau	1-2 midzone fissures	3-5 midzone fissures	Full depth fissures or 5+ midzone fissures	Large segments of cartilage eroded with full depth fissures
Tidemark Integrity	Normal	Disrupted					

3.2.5 Biochemical Analysis

The menisci and articular cartilage samples stored in Allprotect Tissue Reagent were used to assess the biochemical con-tent between the anterior MRT groups and controls. Samples were removed from the –80°C freezer, thawed, and all immediately digested with 200mL of papain (125mg/mL) in 0.1 M sodium acetate, 5 mM L-cysteine–HCl, 0.05 mM ethylenediamine tetra-acetic acid, pH 6 (Sigma-Aldrich) constantly agitated at 60°C for 18 hours. DNA content of each sample was quantified using a PicoGreen double-stranded DNA quantification kit (Molecular Probes). Proteoglycan content was estimated by quantifying the amount of sulfated GAGs using a dimethylmethylene blue assay with a shark chondroitin sulfate standard.[14] Each constituent was normalized to the tissue wet weight and the GAG was normalized to the DNA content for analysis.

3.2.6 Quantitative Reverse Transcription Polymerase Chain Reaction

Tissue samples stored in RNAlater were used to assess the relative gene expression of various proteins between the anterior MRT and control groups using quantitative reverse transcription polymerase chain reaction (qRT-PCR). Expressions of known catabolic proteins within articular cartilage and meniscal tissue, matrix metalloproteinase (MMP)-1, MMP-9, MMP-13, and aggrecanase-2 (ADAM-TS5), were targeted for gene analysis similar to previous studies.[8,9,19,53] Furthermore, tissue inhibitor of metalloproteinase-1 (TIMP-1) was assessed to measure the expression of catabolic protein inhibition within the tissues.[8,9] Thawed menisci and articular cartilage samples were pulverized and homogenized in Trizol (Invitrogen) on ice using a tissue homogenizer to extract RNA. Homogenized samples were then allowed to incubate at room temperature for 20 minutes in Trizol followed by centrifugation at 12,000*g* for 12 minutes at 4°C. Supernatants were transferred to a new microcentrifuge tube, mixed with 200mL of chloroform, incubated at room temperature for 3 minutes, and then centrifuged at 12,000*g* for 15 minutes at 4°C. The upper aqueous phase was transferred to a new microcentrifuge tube and mixed with 500mL of isopropanol. Samples were incubated at room temperature for 10 minutes followed by centrifugation at 12,000*g* for 10 minutes at 4°C to pellet the RNA. The RNA fraction was rinsed with 70% ethanol and resuspended with RNase-free water (QIAGEN). qRT-PCR was then carried out through a single-step process using an iTaq Universal SYBR Green One-Step kit (Bio-Rad Laboratories) as per manufacturer's instructions with the primers listed in Table 3.3 (Integrated DNA Technologies). To determine relative expression of the target genes, 5 ng of RNA were used per sample and assessed in duplicate. Quantification cycle (Cq) values were determined, and duplicates were averaged for the targeted genes of interest and the reference gene, glyceraldehyde

3-phosphate dehydrogenase (GAPDH). Expression values were presented relative to GAPDH, and each gene was adjusted using the respective PCR amplification efficiencies.

Table 3.3 – Specific primer sequences, product sizes, and references for targeted genes and reference gene for the qRT-PCR analysis.

Gene of Interest	Primer Direction	Primer Sequence	Product Size (bp)	Reference Sequence
MMP-1	Forward	5'-CCA AAG TCT CCA AGG GTC AA-3'	83	NM_001171139.1
	Reverse	5'-CTG TCC TTC AGG TCC ATC AAA-3'		
MMP-9	Forward	5'-TGC GAG TTT CCG TTC ATC TT-3'	117	NM_001082203.1
	Reverse	5'-GTA GAG CTT GTC CTT GTC GTA G-3'		
MMP-13	Forward	5'-GGG ATT CCC AAG AGA GGT TAA-3'	100	NM_001082037.1
	Reverse	5'-TCA TAG CTC CAG ACT TGG TTT C-3'		
TIMP-1	Forward	5'-ACT CCC ACA AAT CCC AGA A-3'	98	NM_001082232.2
	Reverse	5'-GGA ACC ACG AAA CTG CAA-3'		
ADAMS-T5	Forward	5'-GTC ATC CAT CCT CAC CAG TAT C-3'	116	AF317415
	Reverse	5'-TCG TGG TAC ATC TAG CAA ACA G-3'		
GAPDH	Forward	5'-GGT CGG AGT GAA CGG ATT T-3'	114	NM_001082253.1
	Reverse	5'-TGT AGT GGA GGT CAA TGA ATG G-3'		

[a]ADAM-TS5, aggrecanase-2; GAPDH, glyceraldehyde 3-phosphate dehydrogenase; MMP, matrix metalloproteinase; qRT-PCR, quantitative reverse transcription polymerase chain reaction; TIMP-1, tissue inhibitor of metalloproteinase-1.

3.2.7 Statistical Analysis

Synovial fluid volumes were confirmed for Gaussian distribution by the D'Agostino-Pearson omnibus normality test; therefore, paired *t* tests were used to determine differences between knees with anterior MRTs and control knees. Objective scorings of synovial fluid and histological staining were not normally distributed; thus, data were analyzed using the Wilcoxon matched-pairs signed rank test. The remainder of analysis methods utilized 2-sample, equal variance Student *t* tests to determine differences between the anterior MRT groups and controls. An a priori power analysis established that with 9 total specimens, our study was powered to detect differences with power of ≥80% for all statistical tests except the objective scoring. The study was powered to detect differences with power of ≥70% for the objective scoring of the synovial fluid and histological staining. Significant differences were set at $p < 0.05$ for all tests performed.

3.3 Results

After surgery, the rabbits favored the contralateral limb for the initial 1 to 2 days but showed no further signs of gait irregularity prior to euthanasia. All meniscal insertions were inspected during dissection and remained free-floating. Little to no macroscopic differences of the menisci and articular cartilage were observed between the injured and control knees during dissection. Inflammation of the synovial membrane surrounding the knee was observed for all anterior MRT knees when compared with the contralateral macroscopically.

3.3.1 Cytology Evaluation

A significant increase ($p = 0.001$) in synovial fluid volume was aspirated from the joints with surgically induced MRTs, suggesting an effusive process was present. Synovial fluid volume aspirated from the control and injured knees was 297 ± 112 and 1050 ± 125mL, respectively. Compared with control knees, injured knees demonstrated a significantly higher ($p = 0.004$) objective cytology score. Cytology scores were interpreted from the synovial fluid of each joint using the scoring scheme in Table 3.1, and medians with interquartile ranges were calculated between groups. The cytology score was 0 with an interquartile range of (0, 0) and 3 with an interquartile range of (2, 3) for control and injured knees, respectively. Synovial fluid from control knees did not demonstrate cytologic abnormalities. Joint fluid collected from injured knees, however, had mild to moderate increases in activated large mononuclear cells interpreted as nonsuppurative inflammation. Neither synovial hyperplasia nor osteoclasts were observed.

3.3.2 Mechanics

Indentation-relaxation testing of the menisci resulted in decreases of both the instantaneous and equilibrium elastic moduli in the injured limbs compared with control limbs. The instantaneous (p = 0.01) and equilibrium (p = 0.02) elastic moduli of the anteromedial region significantly decreased when comparing the AMMRT group with the control group (Figure 3.3). Similarly, the instantaneous elastic modulus of the anterolateral region in the ALMRT group significantly decreased when compared with the control group (p = 0.009) (Figure 3.3A). Although not significant, the mean equilibrium elastic modulus decreased for both the anterior and posterior regions of the lateral meniscus after the ALMRT (Figure 3.3B). In the analysis of the tibial articular cartilage, significant changes were not present in either the instantaneous or equilibrium elastic moduli for either MRT group when compared with the control group (Figure 3.4).

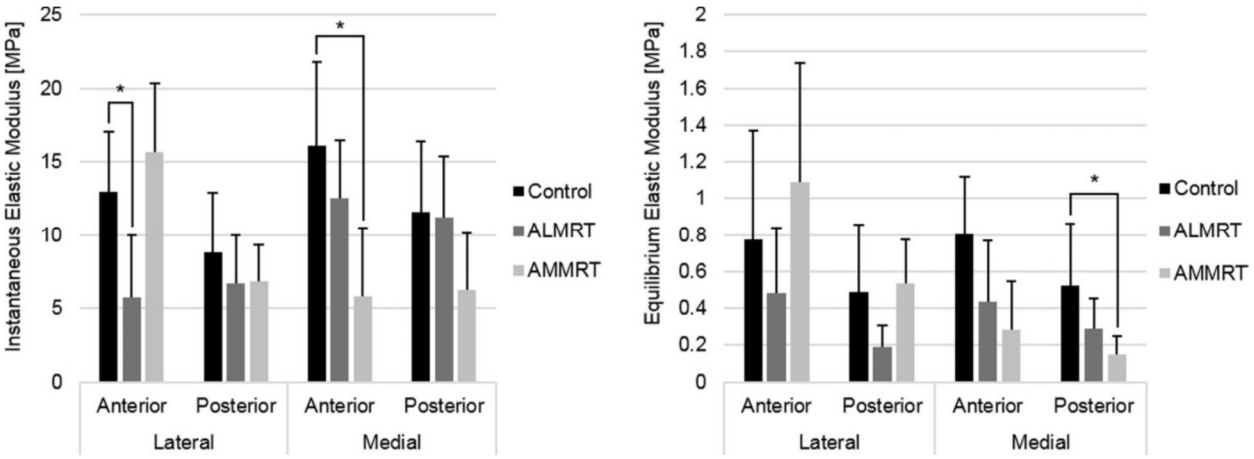

Figure 3.3 – Instantaneous and equilibrium elastic moduli of meniscus regions (mean with standard deviation). *Statistically significant (p < 0.05). ALMRT, anterolateral meniscal root tear; AMMRT, anteromedial meniscal root tear.

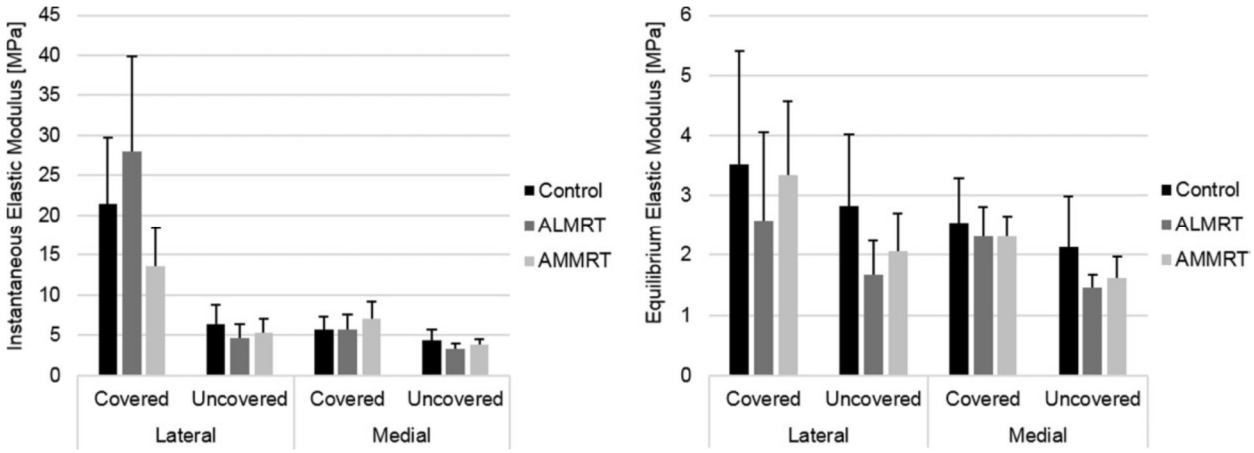

Figure 3.4 – Instantaneous and equilibrium elastic moduli of tibial articular cartilage regions (mean with standard deviation). *Statistically significant ($p < 0.05$). ALMRT, anterolateral meniscal root tear; AMMRT, anteromedial meniscal root tear.

3.3.3 Bone Morphology

Significant decreases in subchondral bone integrity were present after anterior MRTs, primarily within the trabecular structure of the subarticular spongiosa region (Table 3.4). When an anterior MRT was left untreated, the region uncovered by the menisci within the hemijoint opposite the MRT demonstrated a significant decrease in the mean number of trabeculae and a significant increase in the average spacing between trabeculae. For example, the number of trabeculae decreased and spacing between trabeculae increased for the lateral uncovered region after the AMMRT. Additionally, the mean thickness of the trabeculae significantly decreased in the medial covered region after the AMMRT ($p = 0.04$). No significant changes were seen in trabecular thickness for any regions after ALMRT. There were no significant changes within the trabecular or subchondral bone volume fraction for all regions when compared between MRT groups and controls. Similarly, there were also no significant changes to the mineral content within the trabecular or subchondral bone plate tissue in any regions. Volume-rendering examples for the

trabecular and subchondral bone VOIs in control and both anterior MRT limbs are shown in Figure 3.5.

Table 3.4 – Subchondral bone morphology measurement variables (mean with standard deviation) for MRT and control groups.

			Trabecular Thickness [mm]	Trabecular Spacing [mm]	Trabecular Number [1/mm]	Trabecular Bone Volume Fraction [mm^3/mm^3]	Trabecular Bone Mineral Density [mg HA/mm^3]	Subchondral Bone Volume Fraction [mm^3/mm^3]	Subchondral Bone Mineral Density [mg HA/mm^3]
Control	Lateral	Covered	0.24 (0.03)	0.33 (0.06)	2.88 (0.49)	0.56 (0.07)	873 (22)	0.92 (0.07)	905 (14)
		Uncovered	0.24 (0.04)	0.50 (0.14)	2.15 (0.50)	0.41 (0.04)	889 (26)	0.90 (0.06)	952 (13)
	Medial	Covered	0.28 (0.04)	0.52 (0.12)	2.10 (0.44)	0.46 (0.09)	865 (26)	0.91 (0.04)	897 (29)
		Uncovered	0.25 (0.06)	0.68 (0.22)	1.67 (0.51)	0.34 (0.12)	871 (34)	0.89 (0.08)	934 (25)
ALMRT	Lateral	Covered	0.26 (0.05)	0.34 (0.07)	2.65 (0.32)	0.57 (0.08)	884 (18)	0.95 (0.02)	920 (9)
		Uncovered	0.29 (0.06)	0.43 (0.04)	2.28 (0.15)	0.47 (0.05)	920 (26)	0.96 (0.01)	957 (4)
	Medial	Covered	0.29 (0.05)	0.57 (0.11)	1.94 (0.25)	0.44 (0.08)	885 (26)	0.92 (0.04)	926 (15)
		Uncovered	0.27 (0.06)	**0.96 (0.11)***	**1.15 (0.09)***	0.27 (0.05)	902 (27)	0.91 (0.04)	946 (25)
AMMRT	Lateral	Covered	0.26 (0.03)	0.56 (0.32)	2.14 (0.78)	0.50 (0.11)	868 (17)	0.95 (0.03)	901 (20)
		Uncovered	0.21 (0.03)	**0.78 (0.32)***	**1.48 (0.48)***	0.32 (0.12)	871 (21)	0.87 (0.04)	938 (11)
	Medial	Covered	0.23 (0.03)	0.39 (0.32)	2.50 (0.24)	0.50 (0.05)	868 (18)	0.93 (0.03)	910 (32)
		Uncovered	0.22 (0.02)	0.74 (0.25)	1.50 (0.43)	0.31 (0.11)	871 (24)	0.85 (0.07)	913 (30)

[a]Values are presented as mean (SD). Values in boldface indicate statistical significance ($p < 0.05$ when compared with the control group). ALMRT, anterolateral meniscal root tear; AMMRT, anteromedial meniscal root tear; HA, hydroxyapatite.

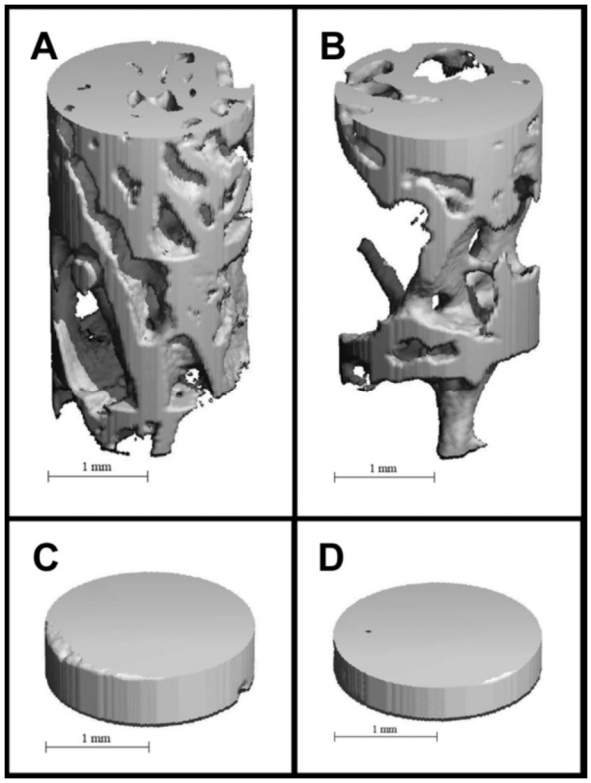

Figure 3.5 – Volume renderings of trabecular and subchondral bone volumes of interest (VOIs) in control and anterior meniscal root tear limbs. Examples are provided for trabecular bone VOI from (A) the lateral uncovered region in the control limb, (B) trabecular bone VOI from the lateral uncovered region in the anteromedial meniscal root tear limb, (C) subchondral bone VOI from the medial uncovered region in the control limb, and (D) subchondral bone VOI from the medial uncovered region in the anterolateral meniscal root tear limb.

3.3.4 Histology

There was a positive correlation between the quantitative percentages of meniscal GAG coverage and the qualitative GAG stain intensity scores ($R^2 = 0.84$). A significant decrease was found in the mean percentage of GAG coverage in the PM region of the meniscus after the AMMRT ($p = 0.04$) (Figure 3.6). Similar results were obtained from GAG stain intensity grading, where the only significant decrease in GAG was in the PM region after the AMMRT ($p = 0.01$) (Table 3.5). Additionally, although not significant, average GAG decreased in the anterior regions after the transection of that meniscal root, with a greater decrease in the anteromedial region after

the AMMRT. Examples of GAG staining in meniscal regions for control, AMMRT, and ALMRT limbs are shown in Figure 3.7.

Table 3.5 – Histological results of meniscal GAG stain intensity for meniscal root tear and control groups.[a]

			GAG Stain Intensity (0 – 3)
Control	Lateral	Covered	2 [2,3]
		Uncovered	2 [2,3]
	Medial	Covered	2 [1.25,3]
		Uncovered	2 [1,2]
ALMRT	Lateral	Covered	1.5 [1,2.75]
		Uncovered	2 [1,3]
	Medial	Covered	3 [2,3]
		Uncovered	1 [0.25,1]
AMMRT	Lateral	Covered	2 [1,3]
		Uncovered	2 [1,2]
	Medial	Covered	0 [0,2.25]
		Uncovered	**0 [0,0.75]**

[a]Values are presented as median (interquartile range). Values in boldface indicate statistical significance ($p < 0.05$, when compared with the control group). ALMRT, anterolateral meniscal root tear; AMMRT, anteromedial meniscal root tear; GAG, glycosaminoglycan.

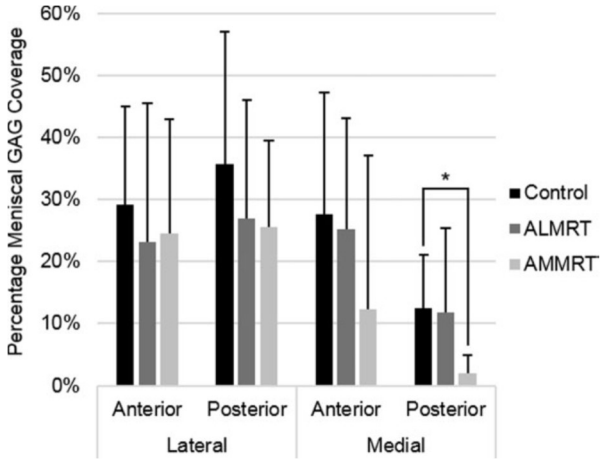

Figure 3.6 – Histological staining results of meniscal glycosaminoglycan (GAG) coverage (mean with standard deviation). *Statistically significant ($p < 0.05$). ALMRT, anterolateral meniscal root tear; AMMRT, anteromedial meniscal root tear.

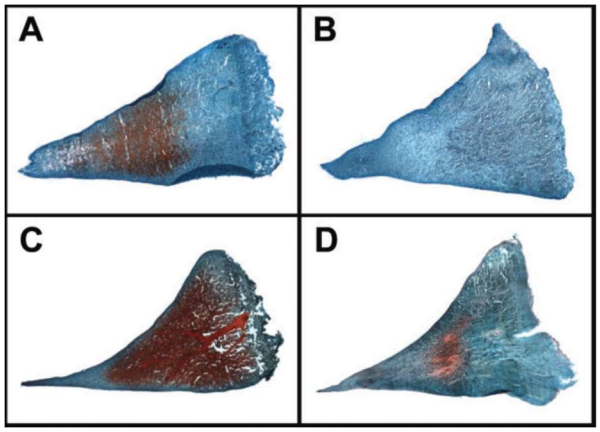

Figure 3.7 – Glycosaminoglycan staining in anterior meniscal regions for control and both anterior meniscal root tear limbs. Examples provided are (A) the posterior region of the medial meniscus in a control limb, (B) the posterior region of the medial meniscus in an anteromedial meniscal root tear limb, (C) the anterior region of the lateral meniscus in a control limb, and (D) the anterior region of the lateral meniscus in an anterolateral meniscal root tear limb.

Qualitative Mankin scores suggest little to no change in the tibial articular cartilage after untreated anterior MRTs (Table 3.6). There were no significant changes to the scores for GAG stain intensity or fissures within the articular cartilage, and tidemark integrity appeared unchanged when the MRTs were left untreated for 8 weeks. Examples of GAG staining in tibial articular cartilage for control and anterior MRT limbs are shown in Figure 3.8.

Table 3.6 – Average Mankin scores for tibial articular cartilage analysis (median with interquartile range) for MRT and control groups.

		GAG Stain Intensity (0 - 6)	Fissures (0 - 6)	Tidemark Integrity (0 - 1)
Control	Lateral	1 [0,1]	0.75 [0.25,1]	0.25 [0,0.25]
	Medial	0.63 [0.44,1]	1.5 [0.44,2.56]	0 [0,0.25]
ALMRT	Lateral	0.75 [0.75,1]	0 [0,0.5]	0.25 [0,0.75]
	Medial	0.75 [0.75,0.75]	1.5 [0.25,2.75]	0 [0,0.25]
AMMRT	Lateral	1.13 [1,1.31]	0.25 [0,0.63]	0.25 [0.19,0.31]
	Medial	1 [1,1.38]	3.25 [2.56,3.63]	0 [0,0.06]

[a]Values are presented as median (interquartile range). ALMRT, anterolateral meniscal root tear; AMMRT, anteromedial meniscal root tear; GAG, glycosaminoglycan.

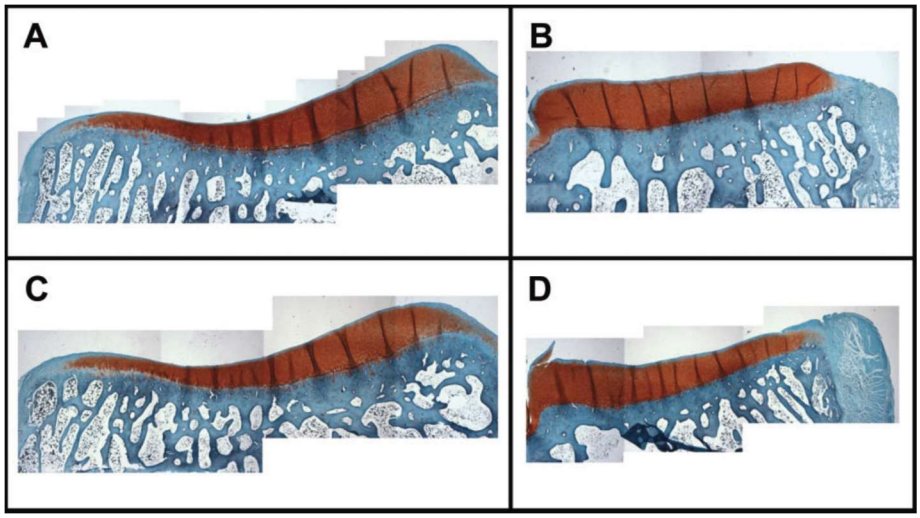

Figure 3.8 – Examples of glycosaminoglycan staining in the tibial articular cartilage for a control limb in the (A) lateral and (B) medial hemijoint as well as an anterolateral meniscal root tear limb in the (C) lateral and (D) medial hemijoint.

3.3.5 Biochemical Content

There were no significant changes to the meniscus regions in total DNA content normalized to wet weight or total GAG content when normalized to wet weight or DNA content (Figure 3.9). There were also no significant changes in the total DNA content or GAG content observed in the tibial articular cartilage when comparing the MRT groups to the control group.

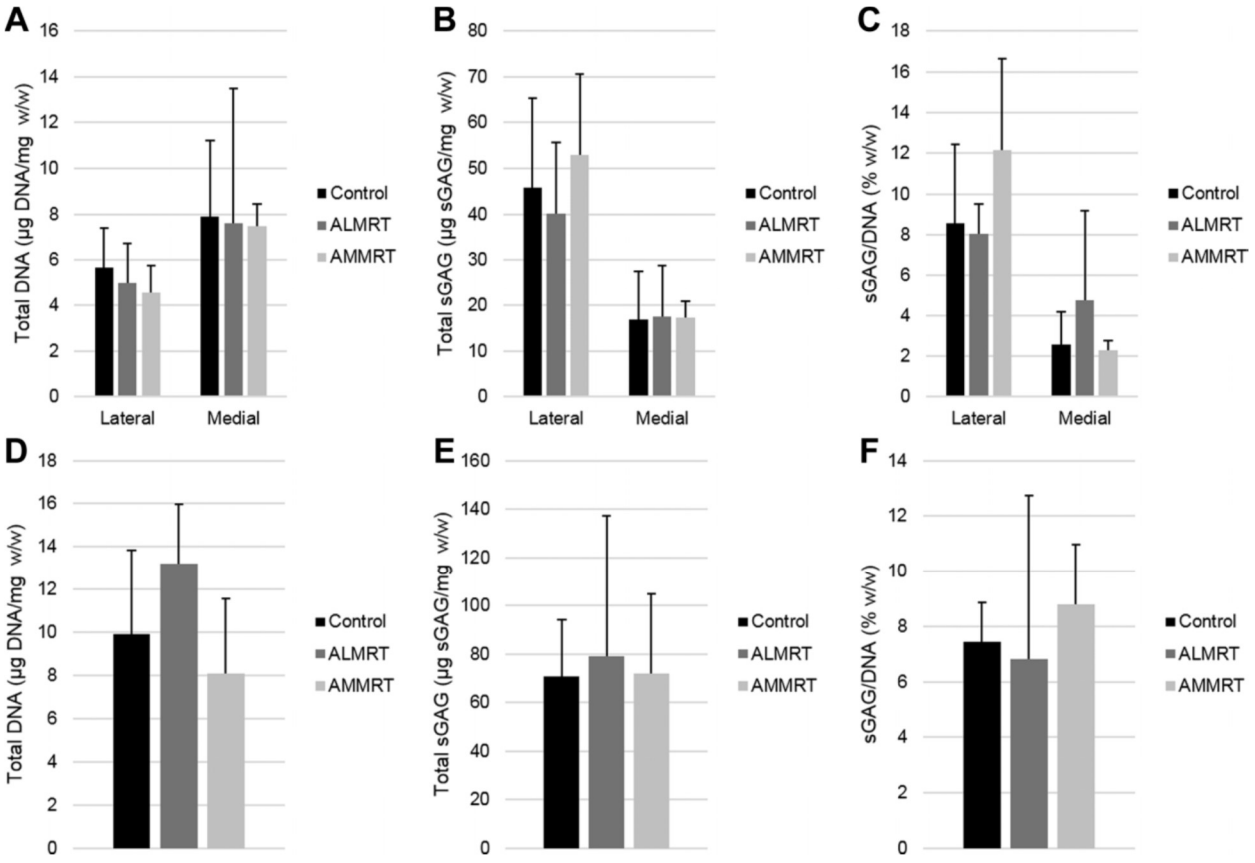

Figure 3.9 – Total DNA content with respect to wet weight, total glycosaminoglycan (GAG) content with regard to wet weight, and total GAG with regard to total DNA content for menisci (A, B, and C, respectively) and tibial articular cartilage (D, E, and F, respectively). ALMRT, anterolateral meniscal root tear; AMMRT, anteromedial meniscal root tear.

3.3.6 Gene Expression

There were no significant differences between the ALMRT and AMMRT meniscus sample groups for any of the targeted genes; they were therefore pooled for comparison with the controls. The results were evaluated to determine relative gene expression changes that occurred after an anterior MRT, regardless of whether the injury was induced in the medial or lateral compartment. For the menisci, the comparison was made between the menisci of the control knees, the menisci in the injured joint that were left intact, and the menisci that were surgically cut to induce an

anterior MRT. Since articular cartilage was taken from both compartments for each knee, the control limbs were compared with the limbs with an induced anterior MRT.

Menisci with surgically-induced, anterior MRTs showed significant increases in the gene expressions of MMP-1 ($p = 0.03$), MMP-9 ($p = 0.03$), and MMP-13 ($p < 0.001$) when compared with the control meniscal tissue (Figure 3.10). Additionally, the relative gene expression of MMP-13 was significantly higher in the menisci with the anterior MRT than the menisci within the same joint that were left intact ($p = 0.01$). There were no significant changes between any of the menisci groups for TIMP-1 and ADAM-TS5 gene expressions. There were also no significant changes in all targeted gene expressions between the tibial articular cartilage of the control knees and the knees with induced anterior MRTs (Figure 3.11).

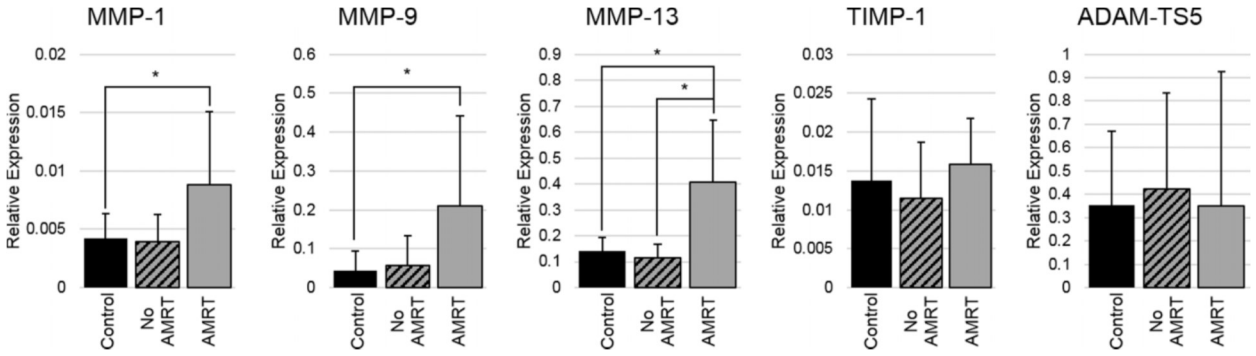

Figure 3.10 – Relative gene expressions for meniscus samples (mean with standard deviation). Anterior meniscal root tears (AMRT) of medial and lateral insertions were pooled for gene expression analysis. *Statistically significant ($p < 0.05$). ADAM-TS5, aggrecanase-2; MMP, matrix metalloproteinase; TIMP-1, tissue inhibitor of metalloproteinase-1.

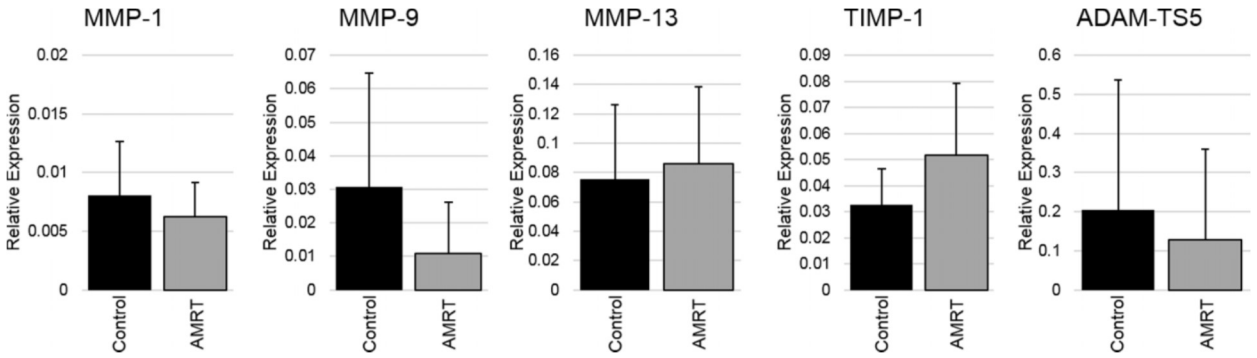

Figure 3.11 – Relative gene expressions for tibial articular cartilage samples (mean with standard deviation). Anterior meniscal root tears (AMRT) of medial and lateral insertions were pooled for gene expression analysis. *Statistically significant ($p < 0.05$). ADAM-TS5, aggrecanase-2; MMP, matrix metalloproteinase; TIMP-1, tissue inhibitor of metalloproteinase-1.

3.4 Discussion

The results of this study demonstrate that knees with surgically induced anterior MRTs left untreated begin to display early degenerative change, particularly within the synovial fluid, menisci, and tibial subchondral bone. The cytologic evaluation of joint inflammation between knees with anterior MRTs and the unoperated control knees suggest these injuries produce an effusive process in the joint with increases in activated large mononuclear cells. Collectively, these findings are consistent with chronic joint inflammation, suggesting early signs of synovitis possibly contributing to the pathogenesis of osteoarthritis.[51]

Instantaneous elastic moduli comparisons for the menisci demonstrated significant decreases to the anterior meniscal regions that experience the MRT. This suggests that untreated anterior MRTs decrease the ability for the anterior regions of the injured meniscus to immediately resist compressive loads. Although there have been no previous studies evaluating changes of internal stresses and strains of menisci after MRTs, the separation of the meniscal insertion from the tibial plateau prevents proper load distribution, which may change the mechanical environment the meniscal tissue is exposed to. We theorize that this lack of proper fixation and change in

mechanical environment of the region near the torn insertion induces a response to change the structure of the meniscal tissue. Additionally, the equilibrium elastic modulus significantly decreased for the AM meniscal region after AMMRT. These changes may also suggest that decreases in material properties of the menisci are more severe for the medial meniscus after anterior MRTs than the lateral meniscus. This unequal response to anterior MRTs and a greater disturbance in medial meniscal integrity may be a result of the presence of the popliteus tendon helping prevent extrusion and greater meniscal coverage of the lateral tibial condyle. Calculated elastic moduli values from control samples corresponded well with previous studies using a similar testing procedure analyzing menisci from Giant Flemish rabbits under posttraumatic osteoarthritis conditions.[16,17] These studies evaluated meniscal material properties after traumatic impact or surgical injury and showed decreases to both moduli of the lateral and medial menisci when compared with the control groups. Compared with the present study, the equilibrium elastic modulus of the meniscus after an anterior MRT was similar to the menisci after traumatic impact or combined transection of the ACL and menisci. Instantaneous elastic moduli for the menisci after anterior MRTs remained slightly higher compared with menisci in these studies, which may be due to the shorter time period of 8 weeks compared with 12 weeks.

Significant decreases in GAG coverage and stain intensity were found within the PM meniscus region after AMMRT. These results along with the mechanical analysis suggest that both anterior and posterior regions of the meniscus may be negatively affected by untreated anterior MRTs. In a previous study, GAG content measured after release of only the anteromedial meniscal insertion in rabbits demonstrated moderate changes in the subjectively graded scores after 8 weeks.[4] However, the subjective scores in this study were analyzed and presented using means and standard deviations even though the Mankin grading scheme is ordinal and may have detected

significance when there may not have been any. In other studies, observing significant decreases in meniscal GAG content has been difficult. A previous study evaluating GAG content after surgically inducing bucket-handle tears in a canine model showed that GAG content only significantly decreased after 48 weeks.[41] Another study, however, showed significant decreases in GAG content in most meniscal regions after traumatic impact in a lapine model after only 12weeks.[16] These studies suggest that perhaps if MRTs were evaluated after traumatically occurring or left untreated for longer, a greater decrease in meniscal GAG may be apparent. The changes seen in GAG content may also only be temporal as the tissue compensates; therefore, further analysis of the menisci after these injuries over a longer period with multiple time points should be investigated.

There were no significant changes in the compressive elastic moduli or histological parameters of the tibial articular cartilage. The changes in contact mechanics after anterior MRTs are unknown; however, posteromedial MRTs in humans have demonstrated loading conditions similar to total meniscectomies, which are known to lead to degenerative articular cartilage.[2] Previous animal studies have demonstrated osteoarthritic change within 3 months of meniscectomy.[25] Since the loading conditions after anterior MRTs are unknown, perhaps the anterior MRTs are less severe and may need to be left untreated longer to see results similar to previous meniscectomy animal studies. Changes to the subchondral bone morphology were present within the hemijoint that did not experience the anterior MRT. These decreases in the subchondral bone integrity may be due to the shift in load distribution along the tibial plateau since the injured meniscus is unable to properly distribute the load. While the biomechanical loading of rabbit knees has not been elucidated, a previous study in human knees evaluating posteromedial MRTs demonstrated these injuries increased lateral translations of the tibia.[2] Perhaps this shifting

causes abnormal loading patterns, and the trabecular morphology changes are a result of tibial regions that are being loaded much differently than normal. Additionally, another study evaluating the bone baseline trabecular integrity, an indication of number, spacing, and cross-connectivity of trabeculae, suggested these changes may be an early indicator of osteoarthritis progression.[28] These findings suggest that anterior MRTs in 1 hemijoint may induce early degenerative change in the form of decreased subchondral bone integrity in the uninjured hemijoint. Relative gene expressions for catabolic proteins significantly increased in the menisci with an anterior MRT when compared with both the intact menisci and the menisci of control knees. Three of the targeted catabolic genes significantly increased when compared with the control menisci; however, only 1 of those genes significantly increased compared with the intact menisci. This may suggest that there are increases within both the injured and intact menisci of a joint with an anterior MRT, with a greater increase in the catabolic gene expression in the injured menisci. Additionally, there was no difference in TIMP-1 expression between any of the evaluated groups. This may suggest that the tissue is not compensating for the increase in MMP expression with inhibitory proteins. These results may help explain the significant decreases in the compressive material properties of the menisci. With an increase in catabolic proteins degrading the collagen matrix and no change in inhibitory proteins, a disruption in this balance may occur and contribute to tissue breakdown causing a subsequent change in material properties.[12] Other MMPs or additional catabolic gene expressions may also have been upregulated; however, the tested genes were limited to a few that were anticipated to change after the surgery and within the timeframe of the study. Finally, the lack of gene expression changes within the articular cartilage suggests there are no early pathological changes after these injuries occurring after 8 weeks.

There are limitations of this study that should be considered when reviewing the presented results. The controls used in this study were nonoperative controls; thus, the influence of inflammation on these results is unknown. Despite this, the inflammatory responses present in the synovial fluid after 8 weeks are likely due to the MRTs since inflammatory responses are typically cleared away from an open wound after approximately 2 weeks.[57] In the gene expression analysis, for example, the MMP gene expressions measured in the menisci left intact within the operated knee were not significantly different from the unoperated control, while the surgically cut meniscus expression was upregulated. Thus, the effect of inflammation was predicted to be little or negligible. Another limitation is that only 1 time point of 8 weeks was studied. Multiple time points with longer time periods would allow the tracking of osteoarthritis progression and may reveal changes within the articular cartilage. This study was a short, proof-of-concept study to evaluate results from different analysis methods following untreated MRTs of both the lateral and medial menisci before progressing toward a longer, refined study. The purpose of evaluating changes at 8 weeks in this study was to determine whether the anterior destabilization performed arthroscopically was able to produce measurable, degenerative changes, and a previous study demonstrated this as an appropriate period to detect degradation within rabbit knees.[42] Since the present study was able to produce measurable changes, future studies evaluating longer time periods or different repair techniques may confidently produce additional results. Also, the small animal model may not be as useful as a larger animal model for interpreting results for the human knee. Previous studies have utilized similar small animal models and they provide useful information to build on in future studies while keeping the cost low.[4,29] Additionally, using the contralateral knees as controls may have skewed results due to altered weight-bearing; however,

animal gait returned to normal a couple days after surgery, so the impact on the results was likely minimal.

3.5 Conclusion

This study demonstrated that early degenerative changes occur within the synovial fluid, menisci, and tibial subchondral bone after MRTs while the tibial articular cartilage appeared mostly unaffected at 8 weeks. The results suggest that changes occur to meniscal tissue prior to the tibial articular cartilage after anterior MRTs. Decreases in the material properties and GAG, and the increasing imbalance of MMP expressions relative to TIMP-1 within the menisci after 8 weeks, suggest that these injuries are capable of diminishing the integrity of the menisci. As this was a single, early time point study, further investigation of longer time points into the progression of these changes in the menisci and the onset of articular cartilage changes after these injuries are warranted. Also, this study showed that anterior destabilization of the meniscus arthroscopically without creating a posterior arthrotomy leads to measurable degenerative changes and may be useful for future in vivo studies of MRTs to expand on the presented results. Clinically, it is important to understand the progression of degenerative changes within the joint tissues after anterior MRTs to properly approach repairs. Therefore, the results of this study provide promising direction for further analysis of these injuries left untreated for longer time points and for establishing a model to evaluate *in vivo* repairs in future studies.

REFERENCES

[1] Ahmed AM, Burke DL. In-vitro measurement of static pressure distribution in synovial joints—part I: tibial surface of the knee. *J Biomech Eng*. 1983; 105: 216-225.

[2] Allaire R, Muriuki M, Gilbertson L, Harner CD. Biomechanical consequences of a tear of the posterior root of the medial meniscus. J Bone Joint Surg Am. 2008; 90: 1922-1931.

[3] Allen AA, Caldwell GL, Fu FH. Anatomy and biomechanics of the meniscus. *Oper Tech Orthop*. 1995; 5: 2-9.

[4] Arunakul M, Tochigi Y, Goetz JE, et al. Replication of chronic abnormal cartilage loading by medial meniscus destabilization for modeling osteoarthritis in the rabbit knee in vivo. *J Orthop Res*. 2013; 31: 1555-1560.

[5] Aspden RM, Yarker YE, Hukins DW. Collagen orientations in the meniscus of the knee joint. *J Anat*. 1985; 140(pt. 3): 371-380.

[6] Baratz ME, Fu FH, Mengato R. Meniscal tears: the effect of meniscectomy and of repair on intra-articular contact areas and stress in the human knee. A preliminary report. *Am J Sports Med*. 1986; 14: 270-275.

[7] Benjamin M, Evans EJ, Rao RD, Findlay JA, Pemberton DJ. Quantitative differences in the histology of the attachment zones of the meniscal horns in the knee joint of man. *J Anat*. 1991; 177: 127-134.

[8] Bluteau G, Conrozier T, Mathieu P, Vignon E, Herbage D, Mallein-Gerin F. Matrix metalloproteinase-1, -3, -13 and aggrecanase-1 and-2 are differentially expressed in experimental osteoarthritis. *Biochim Biophys Acta*. 2001; 1526: 147-158.

[9] Bluteau G, Gouttenoire J, Conrozier T, et al. Differential gene expression analysis in a rabbit model of osteoarthritis induced by anterior cruciate ligament (ACL) section. *Biorheology*. 2002; 39: 247-258.

[10] Brophy RH, Martinez M, Borrelli J, Silva MJ. Effect of combined traumatic impact and radial transection of medial meniscus on knee articular cartilage in a rabbit in vivo model. *Arthroscopy*. 2012; 28: 1490-1496.

[11] Cake MA, Read RA, Corfield G, et al. Comparison of gait and pathology outcomes of three meniscal procedures for induction of knee osteoarthritis in sheep. *Osteoarthritis Cartilage*. 2013; 21: 226-236.

[12] Dean DD, Martel-Pelletier J, Pelletier J-P, Howell DS, Woessner JF Jr. Evidence for metalloproteinase inhibitor imbalance in human osteoarthritic cartilage. *J Clin Invest*. 1989; 84: 678-685.

[13] Fairbank TJ. Knee joint changes after meniscectomy. *J Bone Joint Surg Br*. 1948; 30B: 664-670.

[14] Farndale RW, Buttle DJ, Barrett AJ. Improved quantitation and discrimination of sulphated glycosaminoglycans by use of dimethyl-methylene blue. *Biochim Biophys Acta*. 1986; 883: 173-177.

[15] Feucht MJ, Minzlaff P, Saier T, Lenich A, Imhoff AB, Hinterwimmer S. Avulsion of the anterior medial meniscus root: case report and surgical technique. *Knee Surg Sports Traumatol Arthrosc*. 2015; 23: 146-151.

[16] Fischenich KM, Button KD, Coatney GA, et al. Chronic changes in the articular cartilage and meniscus following traumatic impact to the lapine knee. *J Biomech*. 2014; 48: 246-253.
[17] Fischenich KM, Coatney GA, Haverkamp JH, et al. Evaluation of meniscal mechanics and proteoglycan content in a modified anterior cruciate ligament transection model. *J Biomech Eng*. 2014; 136: 1-8.
[18] Fithian DC, Kelly MA, Mow VC. Material properties and structure-function relationships in the menisci. *Clin Orthop Relat Res*. 1990; 252: 19-31.
[19] Freemont AJ, Hampson V, Tilman R, Goupille P, Taiwo Y, Hoyland JA. Gene expression of matrix metalloproteinases 1, 3, and 9 by chondrocytes in osteoarthritic human knee articular cartilage is zone and grade specific. *Ann Rheum Dis*. 1997; 56: 542-549.
[20] Fukubayashi T, Kurosawa H. The contact area and pressure distribution pattern of the knee. A study of normal and osteoarthrotic knee joints. *Acta Orthop Scand*. 1980; 51: 871-879.
[21] Gao J, Messner K. Natural healing of anterior and posterior attachments of the rabbit meniscus. *Clin Orthop Relat Res*. 1996; 328: 276-284.
[22] Gao J, Oqvist G, Messner K. The attachments of the rabbit medial meniscus. A morphological investigation using image analysis and immunohistochemistry. *J Anat*. 1994; 185(pt 3): 663-667.
[23] Glasson SS, Blanchet TJ, Morris EA. The surgical destabilization of the medial meniscus (DMM) model of osteoarthritis in the 129/SvEv mouse. *Osteoarthritis Cartilage*. 2007; 15: 1061-1069.
[24] Han SB, Shetty GM, Lee DH, et al. Unfavorable results of partial meniscectomy for complete posterior medial meniscus root tear with early osteoarthritis: a 5- to 8-year follow-up study. *Arthroscopy*. 2010; 26: 1326-1332.
[25] Hede A, Svalastoga E, Reimann I. Articular cartilage changes following meniscal lesions. Repair and meniscectomy studied in the rabbit knee. *Acta Orthop Scand*. 1991; 62: 319-322.
[26] Hunter DJ, Zhang YQ, Niu JB, et al. The association of meniscal pathologic changes with cartilage loss in symptomatic knee osteoarthritis. *Arthritis Rheum*. 2006; 54: 795-801.
[27] Kettelkamp DB, Jacobs AW. Tibiofemoral contact area—determination and implications. *J Bone Joint Surg Am*. 1972; 54: 349-356.
[28] Kraus VB, Feng S, Wang S, et al. Subchondral bone trabecular integrity predicts and changes concurrently with radiographic and magnetic resonance imaging–determined knee osteoarthritis progression. *Arthritis Rheum*. 2013; 65: 1812-1821.
[29] Kuroki K, Cook CR, Cook JL. Subchondral bone changes in three different canine models of osteoarthritis. *Osteoarthritis Cartilage*. 2011; 19: 1142-1149.
[30] Kurosawa H, Fukubayashi T, Nakajima H. Load-bearing mode of the knee joint: physical behavior of the knee joint with or without menisci. *Clin Orthop Relat Res*. 1980; 149: 283-290.
[31] LaPrade CM, Ellman MB, Rasmussen MT, et al. Anatomy of the anterior root attachments of the medial and lateral menisci: a quantitative analysis. *Am J Sports Med*. 2014; 42: 2386-2392.
[32] LaPrade CM, James EW, Cram TR, Feagin JA, Engebretsen L, LaPrade RF. Meniscal root tears: a classification system based on tear morphology. *Am J Sports Med*. 2015; 43: 363-369.

[33] LaPrade CM, James EW, Engebretsen L, LaPrade RF. Anterior medial meniscal root avulsions due to malposition of the tibial tunnel during anterior cruciate ligament reconstruction: two case reports. *Knee Surg Sports Traumatol Arthrosc*. 2014; 22: 1119-1123.
[34] LaPrade CM, Jansson KS, Dornan G, Smith SD, Wijdicks CA, LaPrade RF. Altered tibiofemoral contact mechanics due to pull-out suture repairs. *J Bone Joint Surg Am*. 2014; 96: 471-479.
[35] Li G, Moses JM, Papannagari R, Pathare NP, DeFrate LE, Gill TJ. Anterior cruciate ligament deficiency alters the in vivo motion of the tibiofemoral cartilage contact points in both the anteroposterior and mediolateral directions. *J Bone Joint Surg Am*. 2006; 88: 1826-1834.
[36] Luther JK, Cook CR, Cook JL. Meniscal release in cruciate ligament intact stifles causes lameness and medial compartment cartilage pathology in dogs 12 weeks postoperatively. *Vet Surg*. 2009; 38: 520-529.
[37] Madry H, van Dijk CN, Mueller-Gerbl M. The basic science of the subchondral bone. *Knee Surg Sports Traumatol Arthrosc*. 2010; 18: 419-433.
[38] McGonagle D, Tan AL, Carey J, Benjamin M. The anatomical basis for a novel classification of osteoarthritis and allied disorders. *J Anat*. 2010; 216: 279-291.
[39] Messner K, Gao J. The menisci of the knee joint. Anatomical and functional characteristics, and a rationale for clinical treatment. *J Anat*. 1998; 193: 161-178.
[40] Navarro-Holgado P, Cuevas-Pérez A, Aguayo-Galeote MA, Carpintero-Benítez P. Anterior medial meniscus detachment and anterior cruciate ligament tear. *Knee Surg Sports Traumatol Arthrosc*. 2007; 15: 587-590.
[41] Nishida M, Higuchi H, Kobayashi Y, Takagishi K. Histological and biochemical changes of experimental meniscus tear in the dog knee. *J Orthop Sci*. 2005; 10: 406-413.
[42] Papaioannou N, Krallis N, Triantafillopoulos I, Khaldi L, Dontas I, Lyritis G. Optimal timing of research after anterior cruciate ligament resection in rabbits. *Contemp Top Lab Anim Sci*. 2004; 43(6): 22-27.
[43] Pauli C, Grogan SP, Patil S, et al. Macroscopic and histopathologic analysis of human knee menisci in aging and osteoarthritis. *Osteoarthritis Cartilage*. 2011; 19: 1132-1141.
[44] Pauly HM, Larson BE, Coatney GA, et al. Assessment of cortical and trabecular bone changes in two models of post-traumatic osteoarthritis. *J Orthop Res*. 2015; 33: 1835-1845.
[45] Petersen W, Tillmann B. Collagenous fibril texture of the human knee joint menisci. *Anat Embryol (Berl)*. 1998; 197: 317-324.
[46] Roemhildt ML, Coughlin KM, Peura GD, Fleming BC, Beynnon BD. Material properties of articular cartilage in the rabbit tibial plateau. *J Biomech*. 2006; 39: 2331-2337.
[47] Rosenberg L. Chemical basis for the histological rise of safranin O in the study of articular cartilage. *J Bone Joint Surg Am*. 1971; 53: 69-82.
[48] Sharma L, Eckstein F, Song J, et al. Relationship of meniscal damage, meniscal extrusion, malalignment, and joint laxity to subsequent cartilage loss in osteoarthritic knees. *Arthritis Rheum*. 2008; 58: 1716-1726.
[49] Shoemaker SC, Markolf KL. The role of the meniscus in the anterior-posterior stability of the loaded anterior cruciate–deficient knee. Effects of partial versus total excision. *J Bone Joint Surg Am*. 1986; 68: 71-79.

[50] Shrive NG, O'Connor JJ, Goodfellow JW. Load-bearing in the knee joint. *Clin Orthop Relat Res*. 1978; 131: 279-287.
[51] Smith MD, Triantafillou S, Parker A, Youssef PP, Coleman M. Synovial membrane inflammation and cytokine production in patients with early osteoarthritis. *J Rheumatol*. 1997; 24: 365-371.
[52] Sweigart MA, Zhu CF, Burt DM, et al. Intraspecies and interspecies comparison of the compressive properties of the medial meniscus. *Ann Biomed Eng*. 2004; 32: 1569-1579.
[53] Tortorella MD, Malfait AM, Deccico C, Arner E. The role of ADAM-TS4 (aggrecanase-1) and ADAM-TS5 (aggrecanase-2) in a model of cartilage degradation. *Osteoarthritis Cartilage*. 2001; 9: 539-552.
[54] Toy JO, Feeley BT, Gulotta LV, Warren RF. Arthroscopic avulsion repair of a pediatric ACL with an anomalous primary insertion into the lateral meniscus. *HSS J*. 2011; 7: 190-193.
[55] Walker PS, Erkman MJ. The role of the menisci in force transmission across the knee. *Clin Orthop Relat Res*. 1975; 109: 184-192.
[56] Watson JN, Wilson KJ, LaPrade CM, et al. Iatrogenic injury of the anterior meniscal root attachments following anterior cruciate ligament reconstruction tunnel reaming. *Knee Surg Sports Traumatol Arthrosc.* 2014; 23: 2360-2366.
[57] Witte MB, Barbul A. General principles of wound healing. *Surg Clin North Am*. 1997; 77: 509-528.

CHAPTER 4:

LOOSENING OF TRANSTIBIAL PULL-OUT MENISCAL ROOT REPAIRS DUE TO SIMULATED REHABILITATION IS UNRECOVERABLE: A BIOMECHANICAL STUDY

4.1 Introduction

Untreated meniscal root tears are becoming increasingly recognized with progressive increases in meniscal extrusion and articular cartilage degeneration detectable within a year.[15] Therefore, surgical treatment is essential to reduce the risk of developing osteoarthritis following meniscal root tears. Repairs of meniscal root tears are becoming more desirable than performing meniscectomies because they significantly improve clinical and radiologic outcomes while reducing cost.[8,13]

Previous *ex vivo* biomechanical experiments have reported that anatomic, transtibial pull-out meniscal root repairs nearly restore intact contact mechanics immediately after repair.[1,16,17,22] Despite this, postoperative follow-up studies show meniscal extrusion was only restored in 56% of patients and progression of osteoarthritis was not always prevented.[7,10] A potential reason for limited success of repairs may be due to significant displacement in meniscal root repairs demonstrated to occur in biomechanical studies that simulate rehabilitative loading.[4,18] Although these studies demonstrate that displacement accumulates with loading of repairs, they are unable to distinguish whether this displacement is due to viscoelastic creep of the meniscal root or due to permanent, unrecoverable loosening of the repair. Displacement due to tissue viscoelasticity would be recoverable and result in small changes in the intra-specimen repeatability of tests with

appropriate rest.[21] If these repairs are unable to recover to the initial state of repair, then these nearly-restorative repairs may loosen into a less-restorative position *in vivo*.

In previous second-look arthroscopy studies of meniscal root repairs, little to no healing has been demonstrated to occur in some patients with earliest follow-up around a year postoperatively.[6,25] Previous studies evaluating repair displacement have only loaded repairs for 1,000 cycles as they assume some healing occurs prior to partial-weight bearing in rehabilitation.[4,18] Therefore, 1,000 loading cycles does not represent cases of meniscal root repairs that may occur *in vivo*. In addition, the authors are unaware of any study that has assessed the quantity and quality of healing that occurs postoperatively for meniscal root repairs around the time of partial weight-bearing, typically beginning around 6 weeks.[2] Since some cases of partial or no healing have been observed and the progress of healing near rehabilitative loading is unknown, the extent of repair displacement needs to be examined further.

The purpose of this study was to determine if meniscal root repairs recover from the resultant displacement of rehabilitative loading. It was hypothesized that a significant amount of displacement due to rehabilitative loading is unrecoverable loosening of repairs. Although previous studies demonstrate that single- and double-tunnel repairs mechanically respond similarly, both repairs were also performed and compared to assess for differences in recoverability of displacement.[18] It was hypothesized that single- and double-tunnel repairs would not be significantly different in repair displacement or in recovery from this displacement.

4.2 Methods

4.2.1 Specimen Preparation

Sixteen cadaveric knees from adult ovine were collected from the Colorado State University Veterinary Teaching Hospital that had been euthanized for unrelated purposes. Animals were approximately 3 years old and weighed between 65–90 kg. Knees were dissected free of all extra-articular skin, muscle, and soft tissue. The anterior and posterior cruciate ligaments, medial and fibular collateral ligaments, and lateral meniscal insertions were sharply transected to expose the tibial plateau with only the medial menisci intact. The tibiae were then cut at mid-diaphysis to remove the distal portion and potted in a two-part urethane casting resin (Smooth Cast 321, Smooth-on, Easton, PA).

4.2.2 Repair Technique

Knees were randomly distributed between the single- and double-tunnel transtibial pull-out repair groups, with eight specimens per group. All tears and repairs were performed by an experienced orthopaedic surgeon (RFL). Initially, the posteromedial meniscal root insertion was cut with a scalpel at the interface with the tibial plateau and the insertion area was marked with a surgical pen to identify anatomic placement. For the single-tunnel group, a 4.5 mm diameter transtibial tunnel was created using a guide pin and reamer (Smith & Nephew, Andover, MD) in the middle of the posterior medial meniscal root attachment. Two No. 2 nonabsorbable sutures (Ultrabraid, Smith & Nephew, Andover, MD) were passed between 5-7 mm medial within the meniscal root.[14] The two-simple-suture technique was performed for all repairs as this technique demonstrates the lowest technical difficulty and resists displacement from cyclic loading better than other techniques assessed.[19] In addition, this technique is the one that most current published

studies have utilized.[20] The sutures were placed into a looped nitinol wire, pulled through the tunnel, manually tensioned to reduce the menisci to the native position, and firmly tied to a 4 mm by 12 mm surgical fixation button (Endobutton, Smith & Nephew, Andover MD) over the anteromedial tibia using a surgeon's knot followed by 5 half hitches on alternating posts over the fixation button.

For the double-tunnel group, the first transtibial tunnel was drilled in the same manner as the single-tunnel group with a diameter of 3 mm. A second transtibial tunnel was then drilled using a calibrated offset guide to position the second tunnel parallel and 3 mm posterior to the initial tunnel and to ensure no tunnel convergence. In addition, the passing cannulas were left in place until the sutures were pulled down the tunnels. The sutures in the anterior portion of the meniscal root were then shuttled through the anatomic transtibial bone tunnel, while the sutures from the posterior portion of the meniscal root were pulled through the posterior transtibial bone tunnel. The sutures were then both tied to a 4 mm by 12 mm surgical fixation button over the anteromedial surface of the tibia using a surgeon's knot. Once repairs were complete, the limbs were frozen at -20º C until testing.

4.2.3 Biomechanical Testing

Limbs were individually thawed for experimental testing. The anteromedial meniscal insertion was transected with a scalpel so that the meniscus was only attached to the tibia posteriorly by the meniscal root repair. The anterior portion of the meniscus was then rigidly clamped 1 cm from the sutures in line with the circumferential collagen fibers and marked with a surgical pen at the boundary of the clamp to confirm no slippage occurred during the experiment. The clamp was then fastened to the actuator of a servo-hydraulic, material testing machine (Bionic

Model 370.02 MTS Corp., Eden Prairie, MN). The potted diaphysis was fastened to a custom fixture allowing the tibia to be positioned with the transtibial tunnel(s) in the axial direction of the actuator (Figure 4.1).

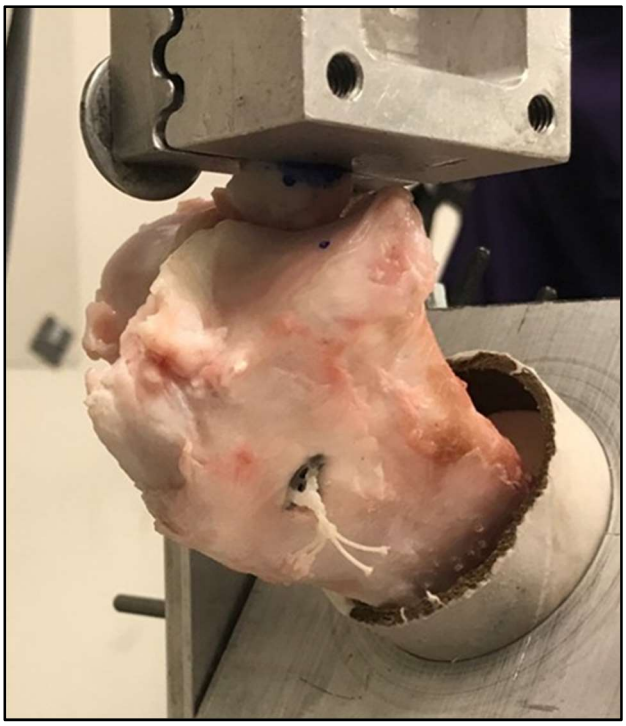

Figure 4.1 – Experimental testing setup. The potted limbs were secured to allow the tibiae to be positioned with the transtibial tunnel(s) in the axial direction of the actuator. The repaired menisci were clamped with the circumferential fibers in line with the actuator.

Both single- and double-tunnel repairs were subjected to the same cyclic loading procedure. The repaired attachments were first tensioned for 10 cycles from 1 N to 10 N at 0.1 Hz to precondition and minimize creep within the repair. After preconditioning, the menisci were cyclically tensioned for 10,000 cycles from 10 to 30 N at 0.5 Hz. This loading protocol has been used by previous studies to simulate tension that the posteromedial meniscal root may experience under neutral rotation, a range of motion from 30° to 60°, and 500 N of tibiofemoral load, representing the range of motion and partial weight-bearing seen in a typical, postoperative rehabilitation regimen after meniscal root repair.[4,18,27] Repairs were then returned to their original,

unloaded position and allowed to recover for 30 minutes. Good intra-specimen repeatability for tension testing of ligament has been demonstrated with at least 30 minutes rest; thus, this period was presumed to allow the meniscal root sufficient time for reasonable recovery.[21] After rest, the repairs underwent another loading session of preconditioning for 10 cycles from 1 N to 10 N at 0.1 Hz and then tensioned for an additional 1,000 cycles from 10 N to 30 N at 0.5 Hz to assess repair recoverability after rest.

Repair displacement was measured at the peak displacement for each cycle as tension reached 30 N. The displacement of single- and double-tunnel repairs at 1, 100, 500, 1,000, 5,000, and 10,000 cycle(s) were recorded for comparison between groups. Displacement was measured at the testing machine actuator as done in previous studies evaluating meniscal displacement.[4,18] The difference in displacement between the first loading cycle and the first loading cycle after rest was calculated to evaluate whether repairs recovered to their original position or if the simulated rehabilitative loading caused unrecoverable loosening within repairs. Recoverability was also evaluated by determining if repairs returned to the displacement of the final loading cycle after rest and additional loading. The difference in displacement between cycle 10,000 and cycle 1,000 after the period of rest was calculated to assess this recovery.

4.2.4 Statistical Analysis

Using previous literature results, a sample size calculation was performed for the present experiment. The standard deviation for the sample size calculation was assumed to be 0.6 mm, which was taken as an approximate value from a previous study.[18] Assuming a significance level, α, of 0.05 and requiring 80% power, group sample sizes of 8 were sufficiently powered to detect a 0.9 mm difference for comparisons between the single- and double-tunnel repairs.

Mann-Whitney U tests were performed to compare the single- and double-tunnel repairs for the repair displacement at cycles of interest and for recoverability outcomes. A paired samples *t* test was performed for comparison of the difference in displacement between the first loading cycles and the first loading cycles after rest to determine if loosening occurred and was significantly different from 0. The Wilcoxon signed-rank test was performed for comparison of repair displacement at cycle 10,000 to the displacement at cycle 1,000 after rest to determine if the repairs returned to their peak displacement within 1,000 additional cycles after rest. Effect size with bias-corrected Hedges' *g* and its 95% confidence intervals (CIs) were calculated to interpret the practical importance of paired comparisons.[12] Hedges' *g* effect size was used instead of the Cohen's *d* effect size to account for the small sample size, giving a more conservative interpretation of the effect size. The Hedges' *g* may be interpreted similarly to the Cohen's *d*, where $g = 0.2$ for a small effect, $g = 0.5$ for a moderate effect, and $g \geq 0.8$ for a large effect. A small effect would suggest a trivial difference between tested means and a large effect would suggest an important difference.

4.3 Results

Repair displacements at cycles of interest were not significantly different between single- and double-tunnel techniques ($p > 0.3$ for all comparisons); therefore, the results were pooled (Tables 1 & 2). Recoverability outcomes between single- and double-tunnel repairs were also not significantly different; therefore, they were also pooled. The difference in displacement between the first loading cycle and the first loading cycle after rest was 1.59 ± 0.69 mm for repair groups pooled and was significantly different from 0 ($p < 0.001$) (Figure 4.2A). The Hedges' *g* effect size was calculated to be 2.1 with 95% CIs = [1.2, 3.1]. The measured difference in displacement

between the first cycle and first cycle after rest was 1.65 ± 0.51 mm and 1.54 ± 0.86 mm for single- and double-tunnel repairs, respectively (p = 0.38). When single- and double-tunnel data was pooled, the difference in displacement between cycle 10,000 and cycle 1,000 after rest was 0.04 ± 0.04 mm and was significantly different from 0 (p = 0.004) (Figure 4.2B). The Hedges' g effect size was calculated as 0.04 with 95% CIs = [0.01, 0.07]. The difference in displacement between cycle 10,000 and cycle 1,000 after rest was 0.05 ± 0.05 mm and 0.04 ± 0.03 mm for single- and double-tunnel repairs, respectively (p = 0.29).

Table 4.1 – Cyclic displacement of single- and double-tunnel techniques and with data pooled.[a]

	Displacement [mm]					
Group	1 Cycle	100 Cycles	500 Cycles	1,000 Cycles	5,000 Cycles	10,000 Cycles
Single	2.20 ± 0.33	2.98 ± 0.47	3.36 ± 0.61	3.73 ± 0.62	4.33 ± 0.77	4.55 ± 0.83
Double	2.25 ± 0.57	2.86 ± 0.70	3.30 ± 0.81	3.52 ± 0.88	4.11 ± 1.09	4.38 ± 1.11
Pooled	2.22 ± 0.45	2.92 ± 0.58	3.33 ± 0.69	3.63 ± 0.74	4.22 ± 0.92	4.47 ± 1.00

[a]Data reported as mean ± standard deviation. No significant differences were noted between the single- and double-tunnel groups.

Table 4.2 – Cyclic displacement of single- and double-tunnel techniques after rest and with data pooled.[a]

	Displacement [mm]	
Group	1 Cycle After Rest	1,000 Cycles After Rest
Single	3.86 ± 0.77	4.51 ± 0.85
Double	3.78 ± 1.11	4.39 ± 1.25
Pooled	3.82 ± 0.92	4.45 ± 1.04

[a]Data reported as mean ± standard deviation. No significant differences were noted between the single- and double-tunnel groups.

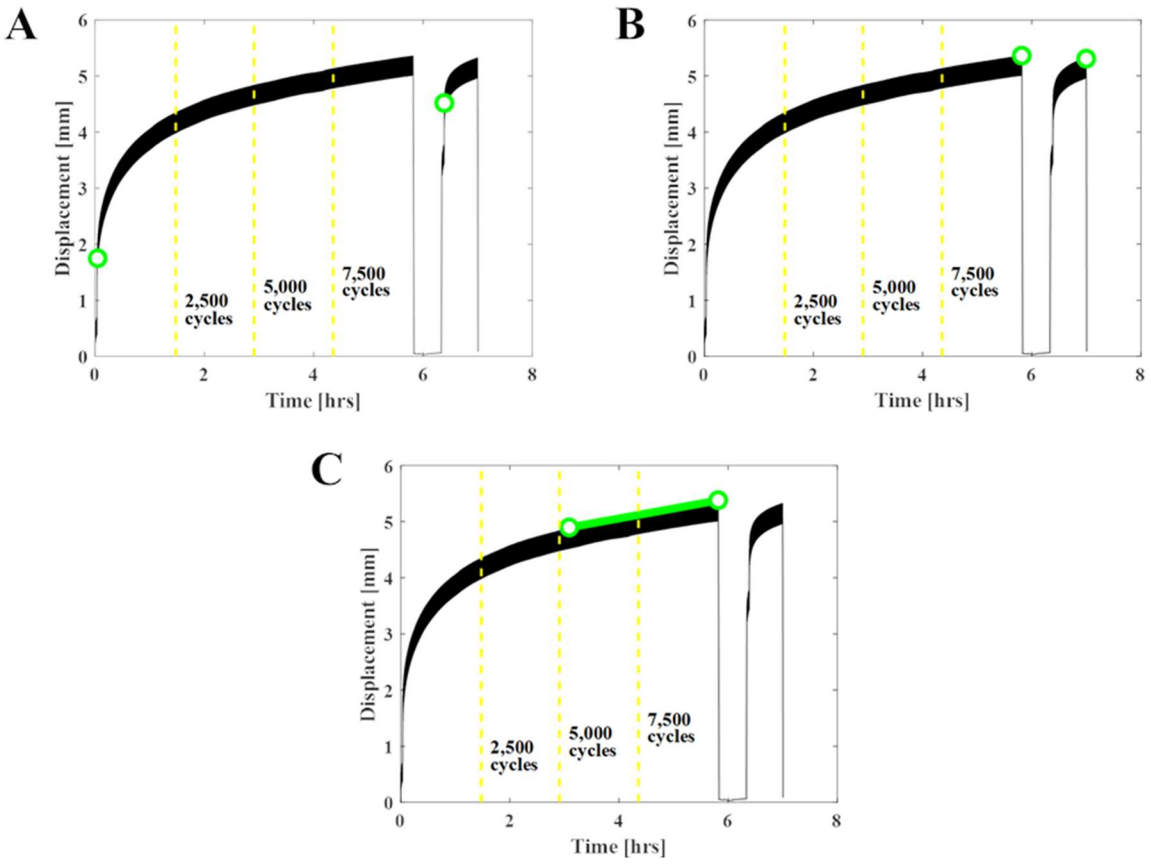

Figure 4.2 – Example of sample cyclic test data (black) and highlighted in green is (A) the displacement of the first cycle and the first cycle after rest, (B) the displacement of cycle 10,000 and cycle 1,000 after rest, and (C) the steady-state creep rate of repairs. Dotted yellow lines indicate intervals of 2,500 cycles.

Repairs did not appear to reach an equilibrium displacement within 10,000 cycles. Instead, the repair displacement gradually increased with cycle time. The cycle peaks were fit to a linear regression model to identify the point within 10,000 cycles that creep began to increase linearly with RMSE less than or equal to 0.01 (Figure 4.2C). The median and interquartile range at which steady-state creep began was cycle 4,531 [3,752, 5,253]. The steady-state creep rate was calculated as an increase of 0.05 ± 0.02 mm per additional 1,000 cycles once the repair reached the point of linear progression.

The suture-meniscus interfaces of repairs were also inspected macroscopically after the testing procedure. Elongation of the holes created through the meniscal root by the sutures was macroscopically visible in both single- and double-tunnel repairs (Figure 4.3). This elongation was permanent damage caused by sutures gradually cutting through the meniscal root during the loading procedure.

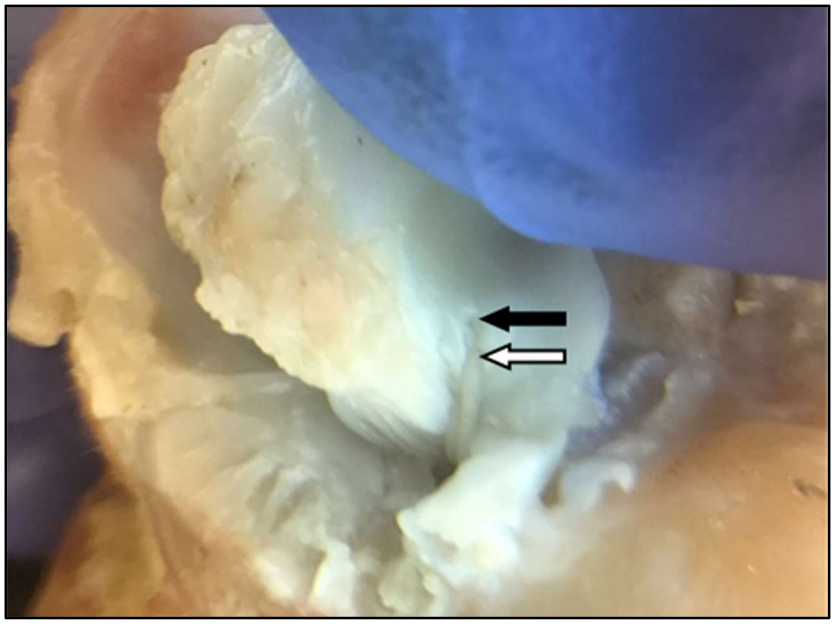

Figure 4.3 – Macroscopic elongation of suture holes in the meniscal root from the original position of the sutures (black arrow) to the final position (white arrow) was present in both single- and double-tunnel repairs after the loading procedure.

4.4 Discussion

In this study, the major finding was that transtibial pull-out meniscal root repairs demonstrated a significant amount of unrecoverable loosening due to simulated rehabilitative loading. The large effect size calculated from this measurement indicates that 10,000 cycles of simulated rehabilitation and rest had a substantial impact on root repair loosening. This result implies that patient repairs are susceptible to loosening from their intended position early within their rehabilitation. A previous experimental study demonstrated that an intact, anteromedial

meniscal insertion loosened by 3 mm medially affects the transmission of tibiofemoral loads.[26] Therefore, this unrecoverable loosening indicates that repairs become less restorative from rehabilitative loading. The typical rehabilitation protocol for meniscal root repairs allows partial weight-bearing around 6 weeks postoperatively.[2] The healing progress of root repairs around the 6-week period is unknown, but second-look arthroscopy studies have demonstrated that incomplete or no healing is still present beyond rehabilitation.[6,25] Therefore, unrecoverable loosening of meniscal root repairs may help to explain the inability to reduce extrusion and reported healing of the meniscus in an extruded position *in vivo*.[6,10,25]

Another finding of this study was that displacement in repairs continued to linearly increase with additional loading instead of reaching an equilibrium. The mean increase of 0.05 mm per additional 1,000 cycles was noted; however, the goal was to minimize the displacement and prevent as much loosening as possible. There was an average increase in displacement of 0.25 mm over the final 5,000 cycles of this study. Also, the present study only assessed these repairs up to 11,000 total loading cycles. After 10,000 cycles, the unrecoverable loosening was 1.59 mm which is less than the 3 mm of displacement demonstrated to significantly reduce the efficiency of menisci to transmit axial loads into hoop stresses.[26] Despite this, Starke et al. evaluated this 3 mm of displacement with the meniscal insertion still intact and did not assess meniscal root repair function with this displacement. Strength of the intact, native meniscal insertions has been demonstrated to not be restored with repairs.[9] Therefore, a weaker fixation of the meniscus and loosening of 1.59 mm in the repair may result in similarly poor load transmission. Additionally, repairs may exceed the 3 mm of displacement with more loading cycles or higher loads and this is especially a concern if healing does not occur early in rehabilitation.

The displacement of repairs at cycle 10,000 and at cycle 1,000 after rest were significantly different; however, the Hedges' *g* effect size was low. The low effect size indicates that rest of the root repair contributed little to the recovery of repair displacement. Thus, patients with meniscal root repairs that loosen from rehabilitative loading cannot hope to recover the intended position of the repaired meniscus with rest. The present study only assessed repairs with 30 minutes of rest before another loading session. It is possible that 30 minutes was not sufficient for repairs to recover; however, previous studies have demonstrated minimal change in the intra-specimen repeatability of viscoelastic soft tissues in tension with 30 minutes of rest.[21] Additionally, visible damage of sutures pulling through the meniscal root suggests that rest time is not the main concern. Instead, suture cut-out with loading causes concern for repair loosening and should be addressed in future studies.

When compared to previous repair displacement studies, the present study supports the conclusion that single- and double-tunnel repairs mechanically respond similarly in tension. A few studies have assessed the two-simple-suture technique with either single- or double-tunnel repairs.[4,18] Each of these studies have only assessed repairs up to 1,000 cycles, but they reported comparable displacement values with respect to the present study. Based on reported means and standard deviations, there were no significant differences between displacement of either technique at 500 or 1000 cycles. Conversely, the repair displacement at the earlier cycles of 1 and 100 were significantly different. The difference between displacement in this study and other repair displacement studies at early cycles may be explained by the loading rate used to transition between preconditioning and full loading cycles. The strain rate dependence of meniscal tissue could cause different repair displacements at initial cycles when transitioned using the 0.1 Hz of preconditioning or the 0.5 Hz of the full loading cycles. Since the displacement of this study with

respect to other studies are similar for the higher cycles, this likely had minimal effect on results of the initial loading cycles of repairs.

The results of this study may also be beneficial for refining the current root repair surgical technique. In this study, the two-simple-suture method with traditional sutures was used and significant unrecoverable loosening of repairs occurred. During comparisons of different repair techniques at 1,000 cycles, the two-simple-suture method demonstrated low displacement with respect to other techniques.[9] Other studies have demonstrated that a three-simple-suture technique or different configurations of the modified Mason-Allen technique are potential candidates for reducing repair displacement.[3,10,11] Although some of these are perceived as more technically challenging, these suture techniques may help to prevent unrecoverable loosening of repairs and the gradual damage that occurs with further loading. Furthermore, a previous study compared traditional sutures to suture tape and found no significant differences within 1,000 cycles, however it is unknown whether the suture tape helps to prevent loosening and suture cut-out with further loading.

This study is clinically relevant because the results demonstrate there is a potential for early and unrecoverable loosening of meniscal root repairs until healing occurs. Thus, it is essential that guided rehabilitation protocols be followed in the first few weeks postoperatively to ensure that healing of the root repair occurs prior to loosening of the repair sutures due to repetitive knee motion. Since healing of meniscal root repairs is not well understood, it is unknown whether the amount of healing present at early rehabilitation will be able to mitigate the amount of loosening that occurs from repetitive loading. Therefore, further evaluation of healing progress and quality around 6 weeks when partial weight-bearing typically occurs would help to determine if augmentation of healing or conservative rehabilitation are necessary. Until healing progress is

better understood, a slower incorporation of partial and full weight-bearing may be beneficial for patients. Other studies have confirmed that meniscal root repairs, independent of suture technique, are not able to restore the full strength of the native meniscal root.[9] This fact emphasizes the importance of healing to the success of meniscal root repairs. Thus, slower incorporation of weight-bearing should be recommended until healing occurs.

Postoperative studies demonstrate that incomplete healing or no healing may occur even if these are a small percentage of cases;[6,25] thus, the response of repairs without healing is warranted. Another potentially useful assessment of repairs would investigate intermittent loading where rest occurs between shorter loading sessions. This would simulate a more physiologic loading scenario as patients will rarely load their repairs 10,000 times during rehabilitation without rest. The present study also only assessed loosening of the two-simple-suture technique. Prior to this study, the concept of unrecoverable loosening from repairs was unknown. Now that unrecoverable loosening has been demonstrated to occur with this technique, other suture techniques and types should be evaluated to determine if all repairs result in significant unrecoverable loosening or maybe the increased difficulty of other repairs is worth a potential decrease in loosening. This study was also limited with the use of ovine menisci instead of human menisci; however, ovine menisci are structurally and mechanically similar to human menisci so the differences due to this are anticipated to be minimal.[5,24]

4.5 Conclusion

This study demonstrated that a significant amount of unrecoverable loosening occurs with transtibial pull-out meniscal root repairs from rehabilitative loading. Root repairs also gradually displaced with continued loading instead of reaching an equilibrium displacement. Conservative

rehabilitation may be important to prevent loosening of repairs to a less-restorative position before healing occurs. The current focus postoperatively of these repairs should be to ensure proper healing occurs before partial weight-bearing is allowed.

REFERENCES

[1] Allaire R, Muriuki M, Gilbertson L, Harner CD. Biomechanical consequences of a tear of the posterior root of the medial meniscus. Similar to total meniscectomy. *J Bone Joint Surg Am*. 2008; 90(9): 1922-1931.

[2] Bhatia S, LaPrade CM, Ellman MB, LaPrade RF. Meniscal root tears: significance, diagnosis, and treatment. *Am J Sports Med*. 2014; 42(12): 3016-3030.

[3] Camarda L, Pitarresi G, Lauria M, Fazzari F, D'Arienzo M. Three single loops enhance the biomechanical behavior of the transtibial pull-out technique for posterior meniscal root repair. *Arch Orthop Trauma Surg*. 2017; 137(9): 1301-1306.

[4] Cerminara AJ, LaPrade CM, Smith SD, Ellman MB, Wijdicks CA, LaPrade RF. Biomechanical evaluation of a transtibial pull-out meniscal root repair: challenging the bungee effect. *Am J Sports Med*. 2014; 42(12): 2988-2995.

[5] Chevrier A, Nelea M, Hurtig MB, Hoemann CD, Buschmann MD. Meniscus structure in human, sheep, and rabbit for animal models of meniscus repair. *J Orthop Res*. 2009; 27(9): 1197-1203.

[6] Cho JH, Song JG. Second-look arthroscopic assessment and clinical results of modified pull-out suture for posterior root tear of the medial meniscus. *Knee Surg Relat Res*. 2014; 26(2): 106-113.

[7] Chung KS, Ha JK, Ra HJ, Kim JG. A meta-analysis of clinical and radiographic outcomes of posterior horn medial meniscus root repairs. *Knee Surg Sports Traumatol Arthrosc*. 2016; 24(5): 1455-1468.

[8] Faucett SC, Geisler BP, Chahla J, et al. Meniscus root repair vs meniscectomy or nonoperative management to prevent knee osteoarthritis after medial meniscus root tears: clinical and economic effectiveness. *Am J Sports Med*. 2018 [Epub Ahead of Print] PMID: 29517925.

[9] Feucht MJ, Grande E, Brunhuber J, Burgkart R, Imhoff AB, Braun S. Biomechanical evaluation of different suture techniques for arthroscopic transtibial pull-out repair of posterior medial meniscus root tears. *Am J Sports Med*. 2013; 41(12): 2784-2790.

[10] Feucht MJ, Kühle J, Bode G, et al. Arthroscopic transtibial pullout repair for posterior medial meniscus root tears: A systematic review of clinical, radiographic, and second-look arthroscopic results. *Arthroscopy*. 2015; 31(9): 1808-1816.

[11] Fujii M, Furumatsu T, Xue H, et al. Tensile strength of the pullout repair technique for the medial meniscus posterior root tear: a porcine study. *Int Orthop*. 2017; 41(10): 2113-2118.

[12] Hedges LV, Olkin I. Statistical methods for meta-analysis. New York, NY: Academic Press, Inc; 1985.

[13] Kim SB, Ha JK, Lee SW, et al. Medial meniscus root tear refixation: comparison of clinical, radiologic, and arthroscopic findings with medial meniscectomy. *Arthroscopy*. 2011; 27(3): 346-354.

[14] Kim YM, Joo YB, Noh CK, Park IY. The optimal suture site for the repair of posterior horn root tears: biomechanical evaluation of pullout strength in porcine menisci. *Knee Surg Relat Res*. 2016; 28(2): 147-152.

[15] Krych AJ, Johnson NR, Mohan R, et al. Arthritis progression on serial MRIs following diagnosis of medial meniscal posterior horn root tear. *J Knee Surg*. 2017 [Epub Ahead of Print] PMID: 28950387.
[16] LaPrade CM, Foad A, Smith SD, et al. Biomechanical consequences of a nonanatomic posterior medial meniscal root repair. *Am J Sports Med*. 2015; 43(4): 912-920.
[17] LaPrade CM, Jansson KS, Dornan G, Smith SD, Wijdicks CA, LaPrade RF. Altered tibiofemoral contact mechanics due to lateral meniscus posterior horn root avulsions and radial tears can be restored with in situ pull-out suture repairs. *J Bone Joint Surg Am*. 2014; 96(6): 471-479.
[18] LaPrade CM, LaPrade MD, Turnbull TL, Wijdicks CA, LaPrade RF. Biomechanical evaluation of the transtibial pull-out technique for posterior medial meniscal root repairs using 1 and 2 transtibial bone tunnels. *Am J Sports Med*. 2015; 43(4): 899-904.
[19] LaPrade RF, LaPrade CM, Ellman MB, Turnbull TL, Cerminara AJ, Wijdicks CA. Cyclic displacement after meniscal root repair fixation: a human biomechanical evaluation. *Am J Sports Med*. 2015; 43(4): 892-898.
[20] LaPrade RF, Matheny M, Moulton SG, James EW, Dean CS. Posterior meniscal root repairs: outcomes of an anatomic transtibial pull-out technique. *Am J Sports Med*. 2017; 45(4): 884-891.
[21] Öhman C, Baleani M, Viceconti M. Repeatability of experimental procedures to determine mechanical behavior of ligaments. *Acta Bioeng Biomech*. 2009; 11(1): 19-23.
[22] Padalecki JR, Jansson KS, Smith SD, et al. Biomechanical consequences of a complete radial tear adjacent to the medial meniscus posterior root attachment site: in situ pull-out repair restores derangement of joint mechanics. *Am J Sports Med*. 2014; 42(3): 699-707.
[23] Perez-Blanca A, Prado Nóvoa M, Lombardo Torre M, Espejo-Reina A, Ezquerro Juanco F, Espejo-Baena A. The role of suture cutout in the failure of meniscal root repair during the early post-operative period: a biomechanical study. *Int Orthop*. 2018 [Epub Ahead of Print] PMID: 29396804.
[24] Sandmann GH, Adamczyk C, Garcia EG, et al. Biomechanical comparison of menisci from different species and artificial constructs. BMC Musculoskelet Disord. 2013; 14(1): 324.
[25] Seo HS, Lee SC, Jung KA. Second-look arthroscopic findings after repairs of posterior root tears of the medial meniscus. *Am J Sports Med*. 2011; 39(1): 99-107.
[26] Stärke C, Kopf S, Gröbel KH, Becker R. The effect of a nonanatomic repair of the meniscal horn attachment on meniscal tension: a biomechanical study. *Arthroscopy*. 2010; 26(3): 358-365.
[27] Stärke C, Kopf S, Lippisch R, Lohmann CH, Becker R. Tensile forces on repaired medial meniscal root tears. *Arthroscopy*. 2013; 29(2): 205-212.

CHAPTER 5:

NONANATOMIC PLACEMENT OF POSTEROMEDIAL MENISCAL ROOT REPAIRS: A FINITE ELEMENT STUDY

5.1 Introduction

Meniscal root tears, when left untreated, lead to progressive meniscal extrusion, worsening arthritis, poor clinical outcomes, and often results in knee arthroplasty.[36,37] To prevent progressive extrusion and degeneration from these tears, meniscal root repairs have been developed to restore meniscal function.[3,4,15,19] All-side techniques have been developed where sutures are passed through the injured meniscal root and secured to the tibial plateau using a suture anchor.[15,19] Similarly, transtibial pull-out techniques pass sutures through the injured root; however, the sutures are instead passed through a transtibial tunnel and securely fastened to the tibial diaphysis periphery.[3,4]

With both techniques, the sutures passed through the meniscal root help to restore meniscal function.[33] Previous biomechanical experiments have demonstrated that anatomic repair of an injured meniscal root with either of these techniques nearly restores contact mechanics to intact.[39,47] Despite this, other studies show that the progression of meniscal extrusion and joint degeneration are not always prevented postoperatively.[24] A potential cause of limited repair success clinically may be repair misplacement during surgery. Previous studies have also shown that nonanatomic positioning of the meniscus is detrimental to resultant knee mechanics.[39,54] The cadaveric study evaluating nonanatomic placement of repairs showed that a repair placed 5 mm posteromedial along the edge of the medial side of the tibial articular cartilage resulted in significant decreases to contact area and increased peak contact pressures.[39] This study elucidated

that placement of repairs is important to properly restore contact mechanics; however, the accuracy of repair placement necessary to restore mechanics to normal is still unknown. A postoperative assessment of transtibial tunnel placement using either a multi-use guide or a root repair-specific guide demonstrated that the root repair-specific guide created tunnels significantly closer to anatomic; however, both guides still resulted in an average placement of tunnels around 3 to 5 mm away from anatomic.[26] Therefore, suture placement may often be misplaced in a nonanatomic position instead of anatomically.

Cadaveric studies are primarily used to assess knee mechanics following meniscal root tears and repairs.[5,39,47] Although useful information has been gathered in these studies, they are incomplete because of the financial and ethical burden associated with cadaveric studies. For example, the assessment of nonanatomic repairs on knee mechanics was only assessed in an extreme, nonanatomic location 5 mm posteromedial along the line of articular cartilage instead of at multiple locations around the anatomic center of the meniscal insertion since it would require a large quantity of specimens.[39] To avoid these limitations, a finite element approach may be useful to further evaluate nonanatomic placement of meniscal root repairs.

Therefore, the purpose of this study was to develop and utilize a sample population of finite element knee models to determine how accurate surgeons need to be with repair placement to restore intact knee mechanics relating to the injured meniscus and tibial articular cartilage. It was hypothesized that further posterior placement, both medially and laterally, for a posteromedial meniscal root tear would decrease the ability for the meniscus to transmit tibiofemoral loads and increase the loading on the articular cartilage. Additionally, it was hypothesized that further anterior placement, both medially and laterally, would best restore meniscal load transmission and cartilage contact mechanics.

5.2 Methods

5.2.1 Specimens

Two finite element tibiofemoral models were created from image datasets available through the OpenKnee(s) project.[7,11,21,22] The imaged cadaveric knee specimens used for model development included a right knee (male, age 71) and left knee (female, age 25) with no reported signs of osteoarthritis. A third knee model was created from an additional open-source dataset where subject information was not collected.[20,44] All knee specimens were imaged at full extension, also denoted as 0° of knee flexion.

5.2.2 Model Development

Image datasets were imported into open-source segmentation software (Seg3D, University of Utah, Salt Lake City, Utah) to isolate tissue components. The tibial articular cartilage, femoral articular cartilage, and the medial and lateral menisci including their insertions into the tibial plateau were isolated using a semi-automated threshold of each component in the datasets. Surface definitions of the component segmentations were then imported into the commercial meshing software, TrueGrid (XYZ Scientific Applications Inc., Livermore, CA). TrueGrid was used to generate linear, hexahedral meshes and projected to the geometry of each segmented component.

5.2.3 Material Properties

Tissue material properties for all three models were taken from previously validated, finite element knee models for tibiofemoral compression.[12,32] Bone of the distal femur and proximal tibia were treated as rigid. Each meniscal insertion site was represented by an insertion plane approximating the curvature of the anatomical insertion of the meniscus with the tibial plateau.

Modeling bone as rigid has been shown to have minimal effect on contact solutions in a previously validated model assessing quasi-static tibiofemoral compression.[31]

Tibial and femoral articular cartilage were modeled as homogeneous, linearly elastic, isotropic materials with properties taken from previous studies.[12,32] The modulus and Poisson's ratio were 15 MPa and 0.475, respectively, to maintain the nearly incompressible behavior of the articular cartilage under short loading times.

The medial and lateral meniscus bodies were modeled as homogeneous, linearly elastic, transversely isotropic materials with properties taken from previous studies.[12,25,32,53,56,57] The modulus and Poisson's ratio in the collagen fiber direction of the menisci were 150 MPa and 0.3, respectively. In the plane perpendicular to the collagen fibers, the modulus and Poisson's ratio were 20 MPa and 0.2, respectively. Additionally, the shear modulus in the plane perpendicular to the collagen fibers was 57.3 MPa. Viscoelastic time dependence of the menisci was not considered due to the quasi-static model analysis.[6,18,52]

Ligaments were represented as two or more tension-only, nonlinear spring elements within the models. A piecewise function was used to represent the force-strain relationship of individual ligament bundles, similar to previous studies.[9,10,32,28,58] The piecewise function, $f(\epsilon)$, approximates the tensile force due to the strain in the ligament bundle (Eq. 1). This force-strain approximation is nonlinear for low strains and linear for strains higher than $2\epsilon_l$, where ϵ_l is assumed to be 0.03.[58]

$$f(\epsilon) = k(\epsilon - \epsilon_l) \quad \text{if} \quad \epsilon \geq 2\epsilon_l$$

$$f(\epsilon) = 0.25k(\epsilon^2/\epsilon_l) \quad \text{if} \quad 0 < \epsilon < 2\epsilon_l$$

$$f(\epsilon) = 0 \quad \text{if} \quad \epsilon \leq 0, \tag{1}$$

where k is a stiffness parameter characteristic of each ligament bundle (Table 5.1), and ϵ is the ligament bundle strain. The ligament strain is defined with respect to the zero-load length of the ligament bundle (Eq. 2).

$$\epsilon = (L - L_0)/L_0, \tag{2}$$

where L is the length of the ligament bundle in the model, and L_0 is the zero-load length of the ligament bundle.

The zero-load lengths of each ligament bundle were calculated from their reference lengths in full extension and initial strains from literature (Eq. 3).[10,58] Since the knee specimen were imaged in full extension, the reference lengths of each ligament bundle were determined from the MR images.

$$L_0 = L_r/(\epsilon_r + 1), \tag{3}$$

where L_r is the reference length of the ligament bundle at full extension, and ϵ_r is the initial strain in the ligament bundle at full extension.

Table 5.1 – Stiffness values for the tibiofemoral ligament bundles modeled.

Ligament Bundle	Stiffness parameter (N)
ACL – anteromedial	6200
ACL – posterolateral	3400
PCL – anterolateral	12500
PCL – posteromedial	1500
LCL – anterior	2000
LCL – middle	2000
LCL – posterior	2000
MCL – anterior superficial	2500
MCL – middle superficial	2600
MCL – posterior superficial	2700
MCL – anterior deep	1500
MCL – posterior deep	1500

In each model, the anterior cruciate ligament (ACL) was represented by anteromedial and posterolateral bundles.[17] The posterior cruciate ligament (PCL) was represented by anterolateral and posteromedial bundles.[46] The medial collateral ligament (MCL) was represented by anterior, middle, and posterior bundles for the superficial MCL and by anterior and posterior bundles for the deep MCL.[29,42,43] The lateral collateral ligament (LCL), was represented by anterior, middle, and posterior bundles.[49] Ligament insertions into bone were identified from the MR images.[38] The transverse ligament was represented by superior and inferior bundles, and the ligament stiffness was taken from a previous optimization study.[32] The insertions of the transverse ligaments were determined to be at the interface of the anterior root of the lateral and medial menisci with their anterior insertions.[38]

Experimental studies characterizing tensile properties of the meniscal insertions have demonstrated that the modulus along the fiber direction is not significantly different than the meniscus body.[2,30] Material characterization of meniscal insertions in the transverse direction demonstrated that the material properties significantly change in a short distance from insertion to bone through the fibrocartilaginous zones, with a modulus of approximately 10 MPa.[1] Therefore, in the present study, the meniscal insertions were modeled as homogenous, linearly elastic, transversely isotropic materials. The modulus in the collagen fiber direction, Poisson's ratio in the fiber direction, and shear modulus were identical to the menisci. In the plane perpendicular to the collagen fibers, the modulus and Poisson's ratio were 10 MPa and 0.2, respectively.

5.2.4 Finite Element Analysis

The general-purpose finite element code, ABAQUS (Dassault Systèmes Simulia Corp., Johnston, RI), was used to approximate contact solutions for a quasi-static analysis using the

implicit solver. Hard, frictionless contact was modeled for the six contact-surface pairs in each model. For simulation of contact pairs, meniscal insertion surfaces were grouped with the meniscal bodies in case they contacted the femoral or tibial cartilage. Therefore, the six contact surface pairs modeled were between the femoral cartilage and the meniscus body/insertions, the tibial cartilage and the meniscus body/insertions, and the femoral cartilage and the tibial cartilage for both the lateral and medial hemijoints.

5.2.5 Loading Conditions

Tibiofemoral loading simulations for all models were designed to assess two separate conditions. The first type of loading was intended to simulate tibiofemoral loading during rehabilitation following meniscal root repairs.[8,13,55] This included a tibiofemoral load of 500 N with knee flexion within the range of 30° to 60°, the standard range of motion and toe-touch weight-bearing protocols typical of 6-week postoperative rehabilitation following meniscal root repairs. Simulation of the rehabilitative loading was also conducted at 0° of knee flexion. The second type of loading was intended to simulate the tibiofemoral loading of full weight-bearing, typically achieved 2 months after repair.[8] This included a tibiofemoral load of 1,000 N and was also simulated at 0°, 30°, and 60° of knee flexion. This resulted in six loading scenarios for each model that were then assessed in the intact, posteromedial meniscal root tear, and various posteromedial root repair conditions.

5.2.6 Joint Kinematics

Specimen-specific joint kinematics for two knee specimens were available through the OpenKnee(s) project and used to approximate knee flexion.[22] A combination of a six degree-of-

freedom robot and motion tracking system were used to record position data of the tibiofemoral joints undergoing passive flexion from 0° to 90° with a 50 N compressive load. The anatomical knee joint coordinate system was determined using a previously defined method from literature.[27] This included finding the transepicondylar axis of the femur by identifying the medial and lateral epicondyles, then calculating the centroid of the mid-diaphysis to define the long axis of the femur. Since the tibiofemoral joint is not a perfect hinge joint, the six degree-of-freedom robot and motion tracking system were then used to optimize the femoral coordinate system to minimize resulting translations and rotations when flexing the joint. The tibial coordinate system was found in a similar way by identifying the most medial point on the tibial plateau, most lateral point on the tibial plateau, and calculating the centroid of the mid-diaphysis. See the joint mechanics protocol at the OpenKnee(s) project website for additional details of the experimental procedure.[22]

For the finite element knee models, the MR images were used to identify the medial epicondyle, lateral condyle, and the centroid of the mid-diaphysis to define the femoral coordinate systems. With the femoral coordinate system defined, the femoral articular cartilage was adjusted in the knee models based on the resultant kinematic data of the optimized passive flexion at 30° and 60°. This provided an approximation of the tibiofemoral joint orientation to assess mechanics at different flexion angles. The tibial coordinate systems were similarly defined using the MR image datasets. Joint kinematic data from the eight available knee specimens through the OpenKnee(s) project were averaged and used to approximate tibiofemoral joint flexion for the third model. This provided two models with specimen-specific joint kinematics and one model as a general case using average joint kinematics from a sample population.

5.2.7 Boundary Conditions

Simulations began with tibiofemoral compression of each knee model in the intact condition for the six loading scenarios. The interface of femoral cartilage with bone was initially preloaded until the femoral cartilage contacted the menisci/tibial cartilage with all other translations and rotations fixed. After preloading, a specified compressive load of interest was applied to the distal femur with the flexion angle fixed, all other rotations free, and all translations free. This allowed the femoral cartilage to adjust from the experimentally determined orientation at 50 N of compression from the joint kinematic data into the optimum orientation resulting from compression at the specified load (500 or 1000 N) and ligament stiffness for the intact condition.

5.2.8 Root Repairs

Representation of posteromedial meniscal root repairs began with the partial deletion of mesh elements from the posteromedial meniscal insertion. The mesh was split into two halves and the half inserting into the tibial plateau was removed. The two-simple-suture method for meniscal root repairs was represented within the models because of this configuration's ability to resist displacement in comparison to other suture techniques.[8,23] Sutures were represented within the model as tension-only spring elements. With the two-simple-suture configuration, two sutures are passed through the meniscus. [34,45,50] Both sutures are passed through the posteromedial meniscal root 5 mm from the root tear with one suture passed through the midportion of the meniscus root and the second sutures passed through the exterior portion of the red-red region.[34,45,50] This results in four individual suture braids passed through the transtibial tunnel; therefore, the spring elements within the model represented four times the stiffness of an individual suture braid. The stiffness of

the meniscus-suture interface using the two-simple-suture method has been reported to be 45 N/mm, which was implemented into the model for the repair stiffness.[51]

5.2.9 Tunnel Placement

The anatomic center of the posteromedial meniscal insertion was determined by calculating the centroid of the insertion mesh surface that interfaces with bone. To best assess different transtibial tunnel placements, anatomic coordinates were modified to account for the slope of the meniscal insertion plane on the tibial plateau. The anterior-posterior axis was defined by connecting the most anterior point of the meniscal insertion site and the most posterior point. The medial-lateral axis was defined as being perpendicular to the anterior-posterior axis. Both axes were also defined to be coplanar with the meniscal insertion plane previously defined.

In modeling repairs, the meniscus was left in place to simulate reduction to its native position which is recommended for meniscal root repairs.[4,40] The ends of the suture elements that were not attached to the meniscus body were fixed to the anatomic center of the meniscal insertion to simulate an anatomic meniscal root repair. To simulate nonanatomic repairs, the suture elements were fixed to points away from the anatomic center. Positions assessed in the present study included locations 1 mm anterior, posterior, medial, lateral, anteromedial, anterolateral, posteromedial, and posterolateral from the anatomic center using the modified anatomic directions. Simulated repairs were also assessed at locations 2 mm around the anatomic center, and 3 mm around the center. This resulted in assessment of 25 different repair locations including the anatomic repairs and the array of locations around the anatomic center for each scenario.

5.2.10 Mesh Convergence

A mesh convergence study was conducted to ensure the mesh density was appropriate for all tissue components of the three models. The convergence study was conducted with one knee model in the intact condition. The average element volume varied to create a range of knee models that ranged from coarse to fine. The root-mean-square-error, RMSE, was used to determine percent change in outcomes when comparing meshes with different mesh densities. The knee model was determined to have an appropriate mesh density when outcome variables of interest changed by less than 5% when compared to a more refined mesh. The average volume for the appropriate mesh density was then used to mesh the other two finite element knee models.

5.3.11 Monte Carlo Simulation

A Monte Carlo simulation was performed to produce a distribution of possible outcomes when material properties ranged from all values previously measured experimentally and implemented into the three knee meshes. MATLAB (MathWorks, Naticks, MA) was used to randomly generate possible material property scenarios with assumed normal distributions for all moduli and Poisson's ratios. The ranges of material properties were taken from previous literature and listed in Table 5.2. Simulations were compared for the three intact knee models at 60° flexion and a 1,000 N compressive load. A pilot analysis of one knee model demonstrated that 50 simulations were sufficient for outcome variable means and standard deviations to change by less than 5% when compared to a different set of 50 simulations. Therefore, 100 simulations were sufficient to represent a consistent distribution of outcomes for a single knee model. Material properties were then generated to produce outcome distributions for the second and third models. This resulted in 300 simulations representing three different knee geometries with 100 different

combinations of possible tissue material properties. Cumulative distribution functions were created for all outcome variables to identify the probability range that the three knee models represented.

Table 5.2 – Approximate means and standard deviations from literature used to generate material properties distributions in Monte Carlo simulation. For transversely isotropic material characterization: $_L$ = longitudinal; $_T$ = transverse.

Cartilage[48,52]	E [MPa]	10 (4)
	ν	0.42 (0.04)
Meniscus Body[14,25,32,53,56]	E_L [MPa]	100 (35)
	E_T [MPa]	20 (5)
	ν_L	0.2 (0.04)
	ν_T	0.2 (0.04)
Meniscal Insertion[2,30,32]	E_L [MPa]	180 (100)
	E_T [MPa]	5 (2.5)
	ν_L	0.2 (0.04)
	ν_T	0.2 (0.04)

5.3.12 Outcome Variables

The mean hoop stress, represented by the mean Cauchy stress, along the collagen fiber direction was measured at the midbody of the medial meniscus and at the midbody of the anteromedial meniscal insertion. To assess tibiofemoral contact mechanics, the mean and peak contact pressures on the medial surface of the tibial articular cartilage were recorded. The total contact area and the cartilage-cartilage contact on the medial surface of the tibial plateau were evaluated, as well as the total contact area of the medial meniscus with the tibial and femoral cartilage surfaces. Meniscal extrusion was measured as the distance between the outer edge of the medial meniscus and the medial edge of the tibial articular cartilage in the medial-lateral direction of the tibial coordinate system. Extrusion was measured at three locations on the medial meniscus – the anterior root, meniscus midbody, and posterior root. Repair tension of nonanatomic repairs was also compared to anatomic repairs to determine how nonanatomic placement alters tension.

5.3.13 Statistical Analysis

Differences in outcomes between repairs and the intact conditions are presented as percent changes. Paired-samples *t* tests were performed to determine if percent changes were significantly different than zero. The Benjamini-Hochberg correction method was performed to adjust the familywise error rate to ensure the significance level, α, was 0.05. In accordance with de Winter, statistical comparisons of paired data with $N = 3$ is sufficiently powered (> 80%) if there is a strong within-pairs correlation ($r \geq 0.8$) and a large effect size (Cohen's $d \geq 2$).[16] Therefore, significant results were only reported if $r \geq 0.8$ and Cohen's $d \geq 2$.

5.3 Results

5.3.1 Mesh Convergence

The convergence analysis demonstrated that the finite element solution converged for a mesh with an average element volume of 0.88 mm^3. The other two knee models were then discretized to have a similar element volume. The average element volumes of the other two models were 0.55 and 0.30 mm^3. The average element count for the models was approximately 32,000 elements.

5.3.2 Monte Carlo Simulation

On average, the three knee models were able to represent 39% of the 300 simulations for all outcomes. Mean hoop stress in the meniscus midbody was bound at probabilities of 0.34 and 0.84, for a predicted outcome probability of 50% (Figure 5.1). Total contact area on medial meniscus surface was bound at probabilities of 0.1 and 0.24, for a predicted outcome probability of 14%. Mean hoop stress in the anteromedial meniscal insertion was bound at probabilities of 0.3

and 0.82, for a predicted outcome probability of 52%. Mean contact pressure was bound at probabilities of 0.75 and 0.99, for a predicted outcome probability of 24%. Peak contact pressure was bound at probabilities of 0.6 and 0.95, for a predicted outcome probability of 35%. Total contact area on the medial surface of the tibial plateau was bound at probabilities of 0.03 and 0.49, for a predicted outcome probability of 46%. The cartilage-cartilage contact area was bound at probabilities of 0.13 and 0.62, for a predicted outcome probability of 49%.

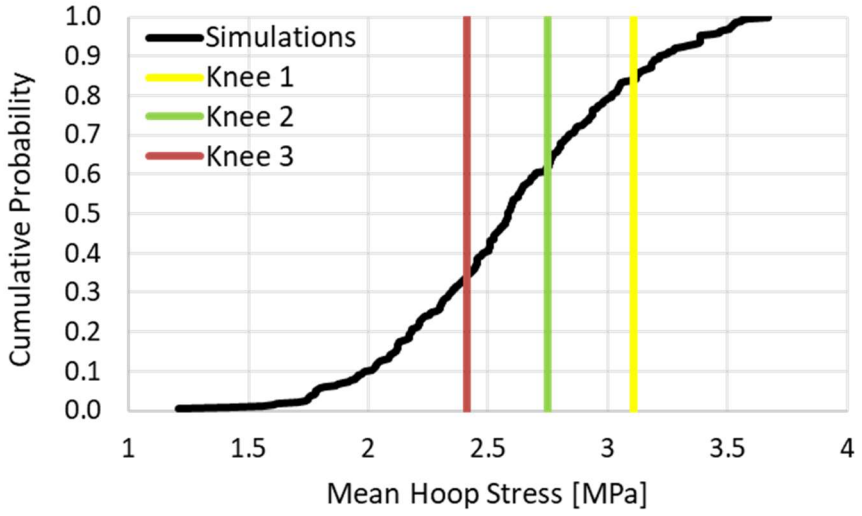

Figure 5.1 – Example of cumulative density functions calculated from Monte Carlo simulations. Mean hoop stress of the medial meniscus midbody is shown to be bound at a probability of 0.34 by knee 3 (red line) and at 0.84 by knee 1 (yellow line), for a predicted outcome probability of 50%.

5.3.3 Medial Meniscus Hoop Stress

The mean hoop stress measured at the midbody of the medial meniscus decreased for anatomic and all nonanatomic repairs with respect to intact (Figure 5.2). Meniscal hoop stress at 60° flexion and a 1,000 N load significantly decreased when placed 3 and 5 mm posterior (p = 0.006; p = 0.002), 5 mm posterolateral (p = 0.004), and 5 mm posteromedial (p = 0.007). The meniscal hoop stress changed similarly at 30° flexion with a 1,000 N, where there were significant

decreases when repairs were placed further posterior from the anatomic center (Appendix A.1). There were no significant decreases at 30° or 60° flexion with a 500 N load (Appendix A.2). At 0° flexion, anatomic and all nonanatomic repairs significantly decreased with a 1,000 N load. All repairs except for the 5 mm anterior repair significantly decreased the mean hoop stress in the midbody of the medial meniscus for 0° flexion with a 500 N load.

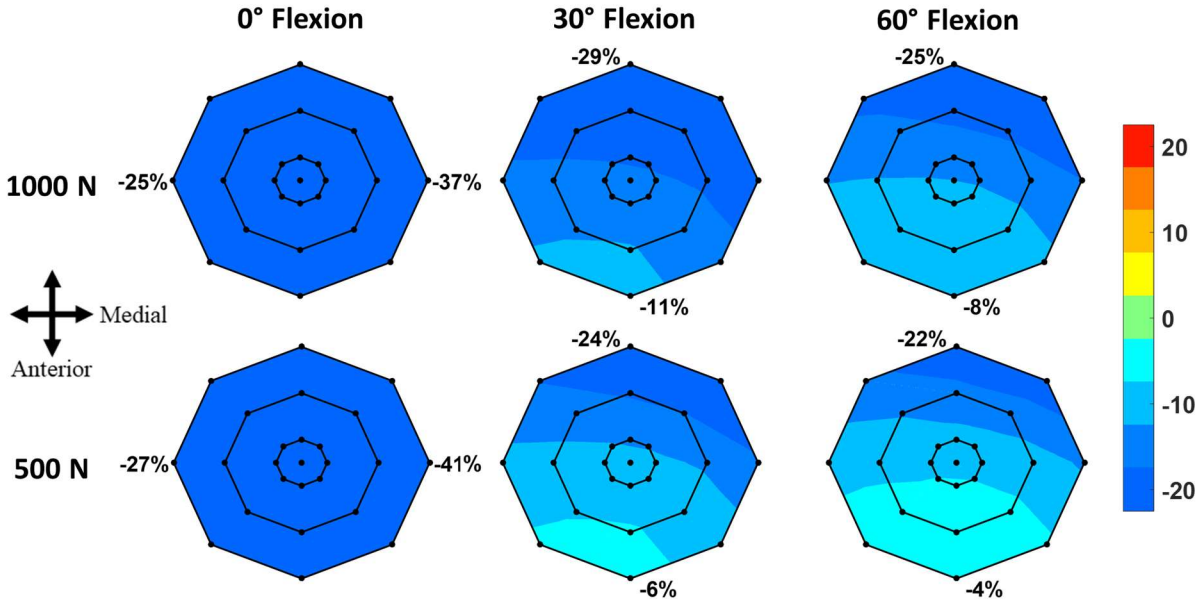

Figure 5.2 – Percent changes to the mean hoop stress of the medial meniscus with respect to intact for anatomic and nonanatomic repairs.

Mean hoop stress within the anteromedial meniscal insertion were similar to changes within the meniscus midbody (Appendix A.3). Repairs placed 5 mm posterior resulted in the largest decreases to meniscal hoop stress, while repairs placed 5 mm anterior best restored hoop stresses to intact values (Figure 5.3). There were no significant changes to the meniscal hoop stress with respect to intact at any of the flexion angles with a 500 N load (Appendix A.4).

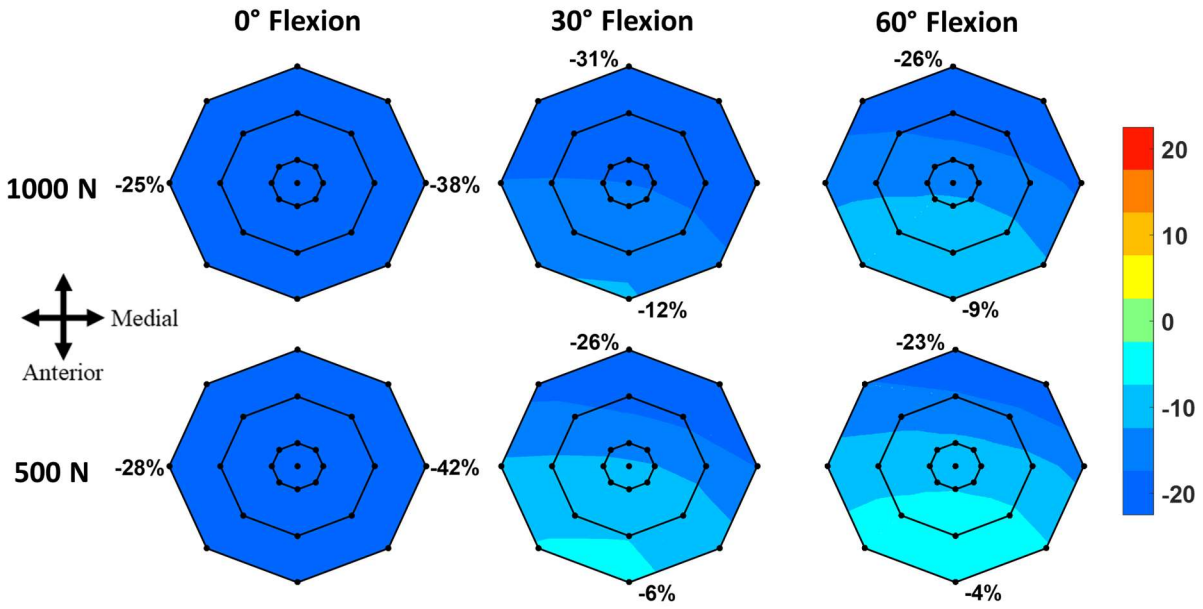

Figure 5.3 – Percent changes to mean hoop stress of the anteromedial meniscal insertion with respect to intact for anatomic and nonanatomic repairs.

5.3.4 Tibial Cartilage Contact Pressures

Mean contact pressure significantly decreased for the anatomic repair and all nonanatomic repairs with respect to intact at 30° flexion only (Appendix A.5 and A.6). There were no significant differences for either the 1,000 N or the 500 N load at 0° flexion and 60° flexion. Despite the lack of statistical significance, the percent decrease in mean contact pressure at 60° flexion was similar to the knees at 30° flexion. The greatest decrease in mean contact pressure for all flexion angles occurred when repairs were placed further posterior (Figure 5.4). Repairs placed 5 mm anterior or 5 mm anteromedial were the best at restoring mean contact pressure to normal on the medial surface of the tibial articular cartilage. At 0° flexion, the mean contact pressure is nearly restored on average for all anatomic and nonanatomic repairs.

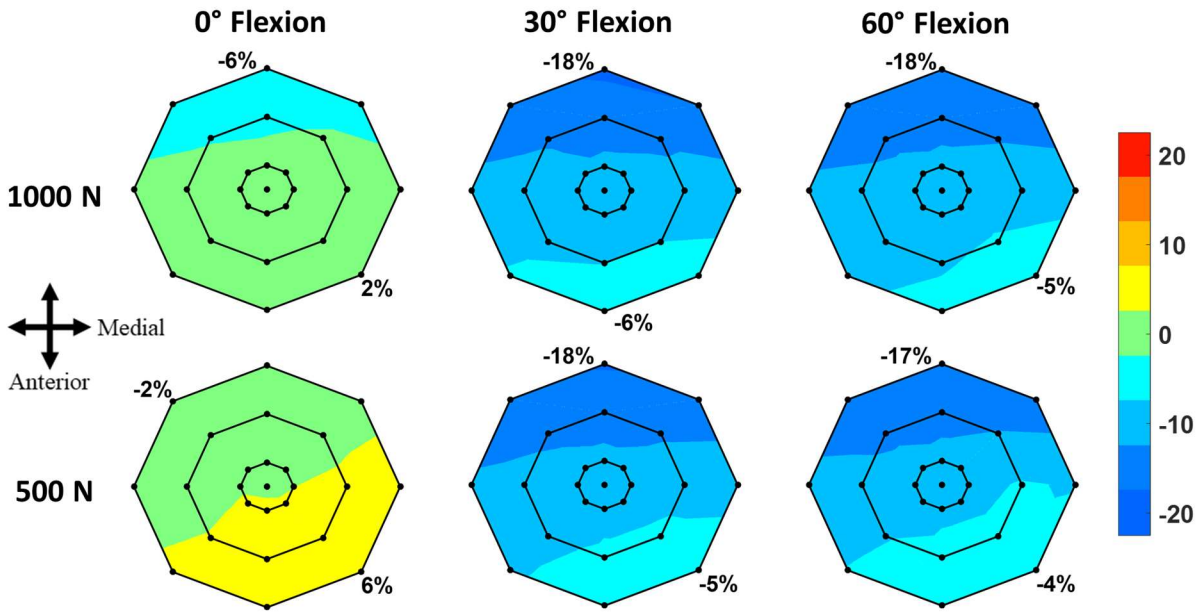

Figure 5.4 – Percent changes to mean contact pressure with respect to intact on medial surface of tibial articular cartilage for anatomic and nonanatomic repairs.

The peak contact pressure on the medial surface of the tibial plateau did not significantly change for anatomic or any nonanatomic repairs at either loading condition (Appendix A.7 and A.8). Even though the results were not significant, all repairs assessed resulted in a mean increase to the peak contact pressure (Figure 5.5). Repairs placed further posterior from the anatomic center resulted in larger increases to the peak contact pressure. For both loading conditions at 30° flexion, the average changes in peak contact pressure were much greater than at 0° or 60° flexion.

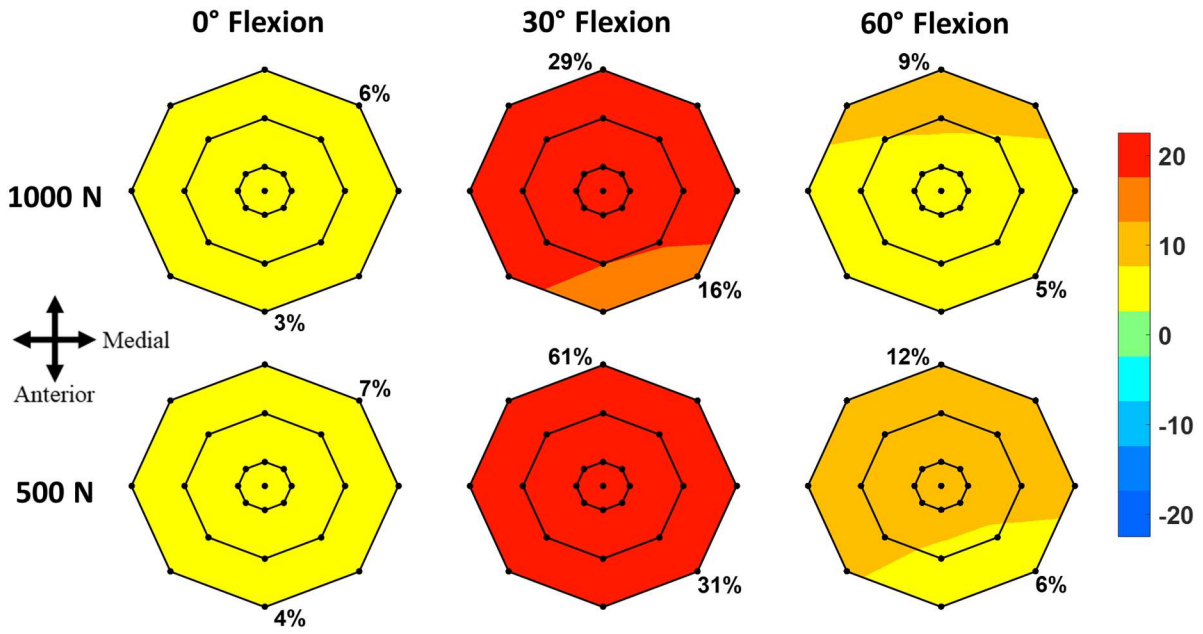

Figure 5.5 – Percent changes to peak contact pressure with respect to intact on medial surface of tibial articular cartilage for anatomic and nonanatomic repairs.

5.3.5 Cartilage and Meniscus Contact Areas

Anatomic and all nonanatomic repairs resulted in no significant changes to the total contact area on the medial surface of the tibial plateau at 30° and 60° flexion (Appendix A.9 and A.10). The largest percent decrease in contact area was -7% ± 2% from the 5 mm posterolateral repair at 30° flexion and 1,000 N load, and the largest increase was 4% ± 8% from the 5 mm medial repair at 30° and 60° flexion with a 500 N load (Figure 5.6). On average, repairs nearly restored the total contact area at flexion angles of 30° and 60°. However, at 0° flexion, the average contact area decreased by at least 11% for anatomic and nonanatomic repairs (Figure 5.6). The only significant decreases were with a 1,000 N load at 0° flexion for all repairs other than the repairs placed 3 mm anterior, 5 mm anterior, 3 mm anteromedial, and 5 mm anteromedial. Therefore, repairs placed more posteriorly or more laterally resulted in a significant decrease in total contact area ($p < 0.04$).

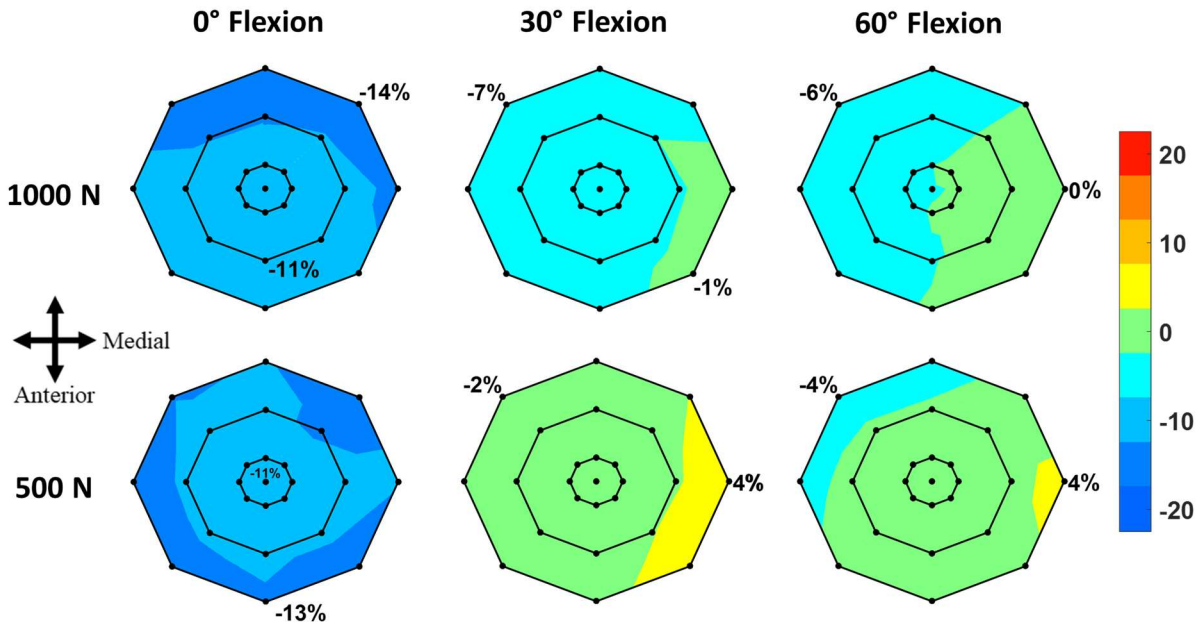

Figure 5.6 – Percent changes of the total contact area on the medial surface of tibial articular cartilage for anatomic and nonanatomic repairs with respect to the intact condition.

Although the total contact area resulted in few significant changes from intact, the cartilage-cartilage contact area significantly increased for anatomic and many nonanatomic repairs at most of the assessed loading conditions (Figure 5.7). At 60° flexion, there was a significant increase in the amount of cartilage-cartilage contact for all repairs with a 1,000 N load except for repairs placed 5 mm medial (p = 0.051) (Appendix A.11). The maximum increase in cartilage-cartilage contact at 60° flexion was 22% ± 5% (p = 0.01) at 5 mm posterolateral and 27% ± 5% (p = 0.01) at 5 mm posterior with 1,000 N and 500 N loads, respectively. At 30° flexion, the percent changes from intact were larger on average than at 60° flexion with increases of 46% ± 10% (p = 0.02) and 74% ± 27% (p = 0.04) for repairs 5 mm posterior to anatomic with 1,000 N and 500 N, respectively. The large standard deviations of results for repairs at 30° flexion prevented any significant changes with the 500 N load (Appendix A.12). Anatomic and all nonanatomic repairs

except the repairs 5 mm anterior and 5 mm anteromedial resulted in significant increases in cartilage-cartilage contact area at 0° flexion for both the 1,000 N and 500 N loads ($p < 0.04$).

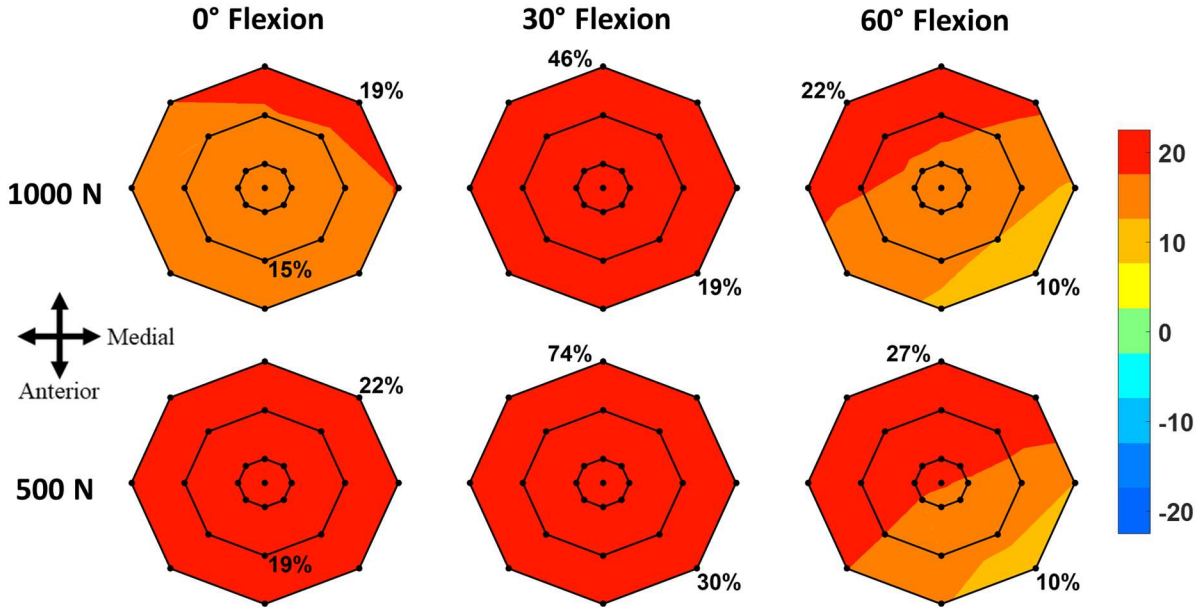

Figure 5.7 – Percent changes of the cartilage-cartilage contact area on the medial surface of tibial articular cartilage for anatomic and nonanatomic repairs with respect to the intact condition.

The total area of contact with the medial meniscus from the tibial and femoral cartilage significantly decreased for all repairs at 30° and 60° flexion (Appendix A.13 and A.14). The largest decreases to the meniscal congruency within the joint resulted from repairs 5 mm posterior for both loads at these flexion angles ($p < 0.04$). Repairs placed 5 mm anteromedial were the most restorative; however, they still resulted in a significant decrease to meniscal congruency (Figure 5.8). At 0° flexion, total contact area on the medial meniscus surface decreased for all repairs but none were significant except the repair 5 mm posterior with a 500 N load.

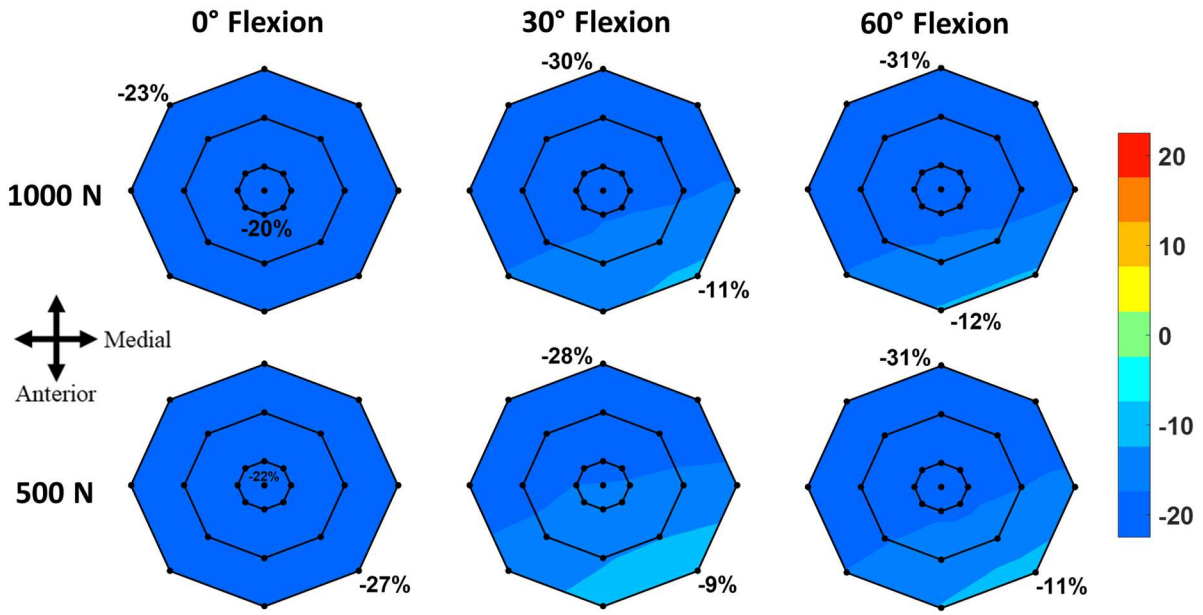

Figure 5.8 – Percent changes to total contact area of the medial meniscus with respect to intact for anatomic and nonanatomic repairs.

5.3.6 Meniscal Extrusion

Extrusion of the meniscus measured at the anterior root and midbody of the medial meniscus did not result in any significant changes, with mean extrusion less than 0.1 mm. For repairs of the posteromedial meniscal root tear, most extrusion resulted from the posterior root of the medial meniscus. Anatomic repairs at all flexion angles ranged from around 0.2-0.6 mm of extrusion following tibiofemoral compression of 1,000 N and 500 N (Figure 5.9). Meniscal extrusion with anatomic repairs significantly increased at 60° flexion with a 1,000 N load (p = 0.02) and a 500 N load (p = 0.02) and did not significantly change at lower flexion angles. The greatest increase in meniscal extrusion at 60° flexion resulted from a 5 mm posterior repair with 1.1 ± 0.2 mm (p = 0.009), and the 5 mm anterior repair best restored the meniscus extrusion with 0.4 ± 0.2 mm (p = 0.11) (Figure 5.9). There were no significant changes to extrusion at 30° flexion, but extrusion followed a similar trend to results at 60° flexion where repairs placed further

posterior resulted in more extrusion and anterior repairs reduced extrusion (Appendix A.15 and A.16). At 0° flexion, anatomic and all nonanatomic repairs did not significantly change and were all near the same mean value of 0.4 mm and 0.2 mm from the 1,000 N and 500 N loads, respectively.

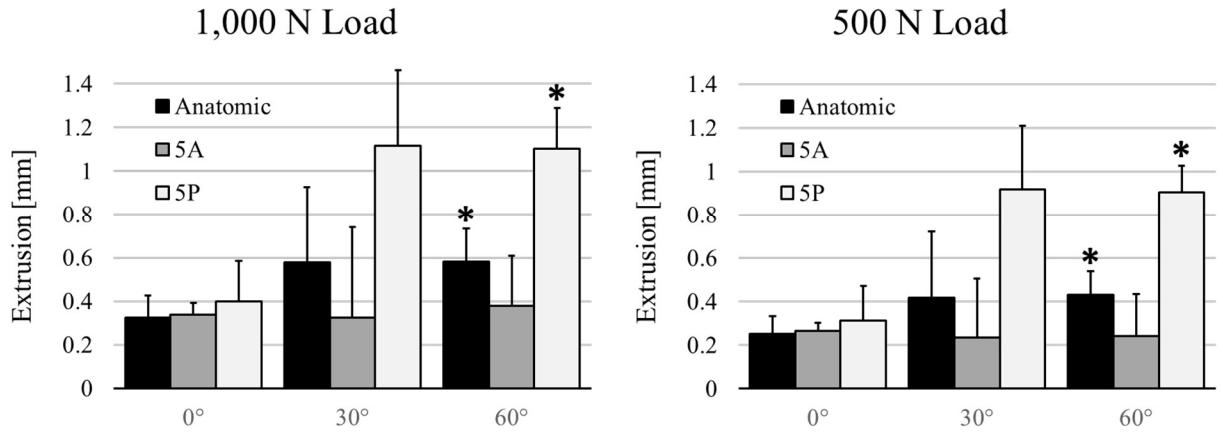

Figure 5.9 – Increases in meniscal extrusion measured at the posterior portion of the medial meniscus. * denotes statistical significance of increases greater than zero. 5A = 5 mm anterior repair; 5P = 5 mm posterior repair

5.3.7 Repair Tension

Repair tension did not significantly change for nonanatomic repairs with respect to anatomic repairs at any flexion angle or tibiofemoral load assessed (Appendix A.17 and A.18). Despite this, the repair tension increased when repairs were placed further anterior or medial and decreased when repairs were placed further posterior or lateral at 30° and 60° flexion (Figure 5.10). At these flexion angles, there were average increases of at least 16% when repairs were placed 5 mm anteromedial and average decreases of at least 10% when repairs were placed 5 mm posterior and 5 mm posterolateral. At 0° flexion, the nonanatomic repairs were all within 3% of the anatomic repair tension.

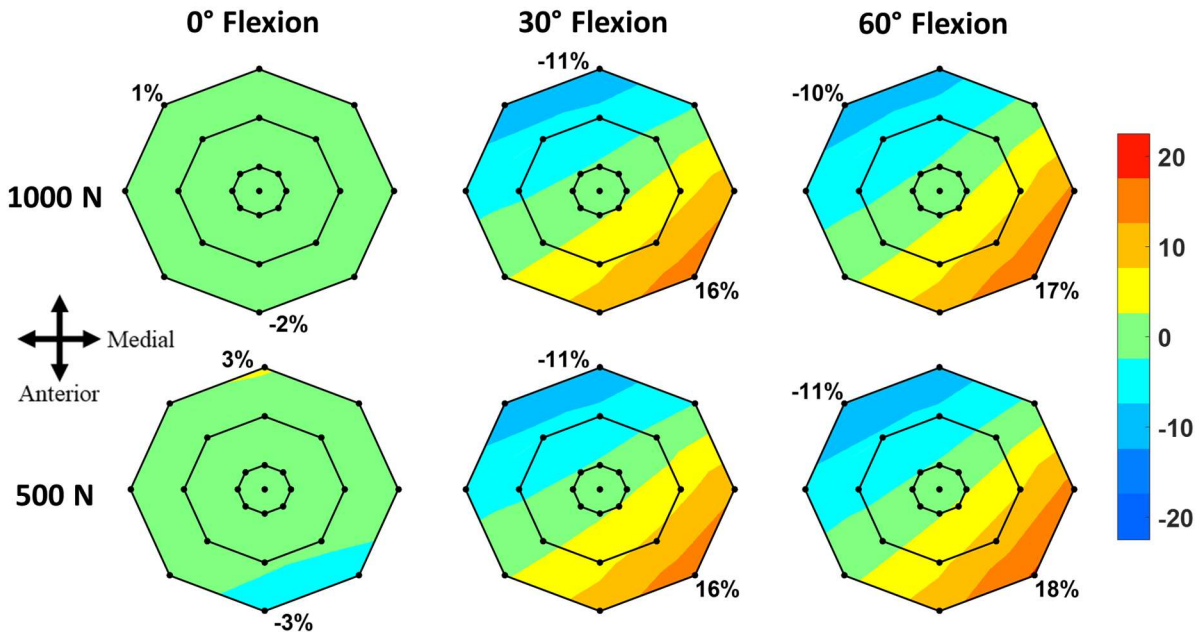

Figure 5.10 – Percent changes to nonanatomic root repair tension with respect to anatomic root repairs.

5.4 Discussion

This study demonstrated that suture placement plays an important role in creating meniscal root repairs to restore knee mechanics. In general, repairs placed further anterior were better at restoring knee mechanics to normal while posteriorly placed repairs resulted in the greatest changes to cartilage and meniscus mechanics. Anatomic repairs were able to nearly restore the total contact area and contact pressures, as has been demonstrated in previous studies; however, the present study revealed that anatomic repairs do not completely restore other important changes to the tibiofemoral joint that have not been previously evaluated.

A major finding of the present study was that anatomic repairs were unable to completely restore meniscal hoop stresses to normal for all loading conditions. This means that the clinical standard of meniscal root repairs was unable to restore the ability for menisci to transmit transtibial loads into hoop stresses, resulting in more load through the articular cartilage. Additionally, the

mean hoop stress within the menisci significantly decreased for repairs placed further posterior and resulted in large decreases for all other nonanatomic repair placement. Anterior repairs were the best at restoring load transmission through the menisci; however, they were still unable to completely restore meniscal hoop stresses. This result is important because it demonstrates the insufficient mechanical properties of current meniscal root repairs, which has also been noted in previous studies.[35,51] No previous study has directly compared tension in the intact meniscus to tension in the meniscal root repair with identical loads; however, some studies have compared their mechanical characteristics. Kopf et al. demonstrated that suture repairs were unable to replicate the ultimate tensile strength of intact meniscal insertions.[35] Rosslenbroich et al. demonstrated that the stiffness of the native meniscal insertion was not significantly different than the two-simple-suture technique; however, the suture repair on average was less stiff.[51] In the present study, there were only statistical significant decreases in the meniscal hoop stress for repairs placed further posterior with respect to the anatomic center. These repairs are not positioned well enough to restore hoop stresses. The results of the anatomic and anteriorly placed repairs agree with the results of Rosslenbroich et al. because these repairs were not significantly different than anatomic repairs but did not completely restore hoop stresses because the repairs are slightly less stiff than the native meniscal insertion.[51]

The changes to contact area on the medial surface of the tibial plateau demonstrates how information previously gathered about root repairs may be misleading. In the present study, anatomic repairs were shown to nearly restore the total contact area at all flexion angles and both loads assessed. In previous cadaveric studies, anatomic repairs have also been shown to restore the total contact area on the tibial plateau;[5,39,47] however, these studies were unable to distinguish between cartilage-meniscus contact or cartilage-cartilage contact. Using finite element analysis,

the present study was able to measure cartilage-meniscus contact and cartilage-cartilage contact separately. Even though meniscal root repairs have been shown to nearly restore total contact area within the joint in the present study and in previous experimental studies, there is a significant increase in the contact area between the femoral and tibial articular cartilage for most repairs assessed. This is further explained when considering the total contact area measured on the surface of the medial meniscus. The total contact of the medial meniscus with the femoral and tibial cartilage significantly decreased for anatomic and nearly all nonanatomic repairs. These results suggest that current root repairs may cause the menisci to be less congruent with the tibia and femur. This decrease in congruency then leads to the increase in cartilage-cartilage contact to compensate for the meniscus. This is important because the restoration of total contact area may mislead clinicians into thinking that loads are also being properly distributed between the meniscus and cartilage, when the present study demonstrates that the articular cartilage is being overloaded due to the meniscal repair.

On average, all repairs resulted in an increase in extrusion from the joint with respect to the native meniscus. Anatomic repairs ranged from 0.2-0.6 mm of extrusion that occurred purely from creation of the repair. While there was only a significant increase with an anatomic repair at 60° flexion, this data still suggests that anatomic repairs are unable to eliminate extrusion entirely. Additionally, repairs placed 5 mm posterior from the anatomic center of the meniscal insertion resulted in a significant increase of around 1 mm of extrusion. Repairs placed further anterior were able to reduce the amount of meniscal extrusion below 0.5 mm. These results demonstrate that suture placement is important to prevent unnecessary extrusion from occurring, and demonstrate how a small variance in placement can create significant extrusion. A previous study showed that ACL guides or root repair-specific guides for creating transtibial tunnels may be misplaced away

from the anatomic center by approximately 3 to 5 mm.[26] , whereby making patients susceptible to meniscal extrusion due to misplacement of repairs. Previous follow-up studies have shown that meniscal extrusion may increase postoperatively;[24] therefore, it is important to minimize extrusion due to the surgical procedure to not encourage even greater extrusion.

Large increases in peak contact pressure occurred for all repairs at 30° of flexion. Additionally, the results suggest that repairs placed further posterior result in greater increases of the peak contact pressure on the tibial cartilage surface. Previous studies have demonstrated that peak contact pressure significantly increase with meniscal root tears.[5,39,47] which could cause changes in meniscal congruency whereby rendering the menisci less able to protect the underlying cartilage in the long-term. Mean contact pressure also did not significantly change for most conditions assessed, except at 30° of flexion. For the other two flexion angles assessed, there was again not a large enough effect due to repair placement to detect a statistical difference with only three samples. Repairs placed 5 mm anterior and 5 mm anteromedial were the best at restoring the mean contact pressure to normal, while repairs placed posteriorly 5 mm away from anatomic resulted in the greatest decreases in mean contact pressure. These results suggest that anteriorly placed repairs are best at restoring contact pressures to normal. Previous experimental studies have demonstrated that mean contact pressure increases with meniscal root repairs.[5,39,47] When repairs were created in the present study, the pressure within any location on the medial tibial cartilage mostly decreased while the pressure in a small area increased. The calculation of mean contact pressure within the finite element models accounted for the entire tibial surface, whereas pressure sensor used experimentally are limited to a predefined area on the plateau surface. This may explain the decrease in mean contact pressure within the models instead of the increase demonstrated in cadaveric experiments.

At higher degrees of flexion, repairs placed further anterior and medial increased the repair tension and repairs placed further posterior and lateral decreased the repair tension with respect to the anatomic repair. These results suggest that repairs placed further anterior and medial increase the risk for suture cut-out through the meniscal root or potential failure of the repair. The ultimate failure load of repairs has been shown to be much lower than the native meniscal insertion.[35] By increasing the tension seen in repairs due to placement, the repairs may reach the ultimate failure load from lower tibiofemoral loads than with repairs placed further posterior. Additionally, loosening of repairs has been demonstrated to occur because of suture cut-out from repetitive loads simulating rehabilitation as seen in Chapter 4. An increase in repair tension would ultimately result to a progression of meniscal extrusion postoperatively, which has been demonstrated to occur clinically.[24]

Repairs placed further anterior were the best at restoring all outcomes of cartilage contact and meniscus mechanics to the intact condition. These results together suggest that anterior placement of repairs helps to restore knee mechanics; however, conservative rehabilitation should be recommended to prevent suture cut-out or repair failure due to the resultant increase in repair tension. A previous biomechanical experiment has evaluated changes in tension when the intact meniscal insertion was placed 3 mm medial and 3 mm lateral. Starke et al. demonstrated that medial placement of the intact meniscal insertion resulted in a decrease in tension because the meniscus ring became wider, and lateral placement resulted in an increase in tension.[54] In the present study, medial placement of sutures in meniscal root repairs resulted in an increase in tension and lateral placement resulted in a decrease in tension. This apparent disagreement may be explained by the difference between placement of the intact meniscal insertion or the meniscal root repair sutures. When the intact meniscal insertion is moved medially 3 mm, for example, the body

of the meniscus is also moved medially resulting in a wider meniscal ring. When the repair sutures were moved medially 3 mm in the present study, the medial meniscus remained in its native position as recommended for root repairs.[8] Therefore, repairs placed medially did not widen the meniscal ring. Instead, they shortened the length of sutures and limited the mobility of the meniscus during compress, resulting in increased tension.

This study is not without some limitations that should be considered when interpreting the results. Because of the small number of finite element models used to assess repair placement (N = 3), this study is unable to completely distinguish all significant changes that may occur with different placement for certain. Despite this, the results presented were sufficient to detect significance for large changes that occur with different placement of meniscal root repairs and provide a better idea of how knee mechanics change with respect to position. The critical p-values were adjusted using a Benjamini-Hochberg correction for the 25 repair positions at each flexion angle and load to mitigate the risk of reporting a false positive result of significance. Additionally, this study does not consider any effects that may change results due to healing, or any negative effects that may occur with repair loosening. Therefore, the results of this study only consider effects due to misplacement of root repairs. Suture placement in the present study is also idealized with respect to clinical root repairs. When sutures are passed through tunnels, or secured to a bone screw, at the anatomic center of the injured meniscal insertion clinically, the sutures may not exactly be in the most anatomic position. For example, the diameter of tunnels used for transtibial pull-out root repairs may range from 2.4 mm to 4.5 mm in diameter.[26,41] Therefore, if the center of the created tunnel matches the anatomic center of the meniscal insertion, the sutures will be pulled further away from the center with a larger tunnel during joint loading. For suture anchor repairs, the sutures will be secured to the edge of the bone screw diameter resulting a similar position of

the sutures away from the true anatomic center. Therefore, the anatomic placement in this study may not be directly compared to an anatomic repair created clinically and should be considered when interpreting the results.

5.5 Conclusion

The results of this study suggest that placement is important for successful meniscal root repairs and demonstrates that anterior misplacement of repairs best restored cartilage and meniscus mechanics. Conservative rehabilitation is recommended for patients to help mitigate the risk of suture cut-out or repair failure since anterior repairs increased tension. Additionally, surgeons should take care not to place repairs posteriorly as this placement resulted in the significant changes to knee mechanics and significant extrusion to occur. Anatomic and most nonanatomic repairs resulted in significant increases in the cartilage-cartilage contact and significant decreases in meniscal hoop stress indicating that the mechanical properties of repairs need to be improved to better restore load transmission through the meniscus and away from the articular cartilage. Future work should also focus on improving the accuracy of repair placement, because the results demonstrated that small misplacement of current repairs results in significant alterations to cartilage and meniscus mechanics.

REFERENCES

[1] Abraham AC, Haut Donahue TL. From meniscus to bone: a quantitative evaluation of structure and function of the human meniscal attachments. *Acta Biomater*. 2013; 9(5): 6322-6329.

[2] Abraham AC, Moyer JT, Villegas DF, Odegard GM, Haut Donahue TL. Hyperelastic properties of human meniscal attachments. *J Biomech*. 2011; 44(3): 413-418.

[3] Ahn JH, Wang JH, Lim HC, Bae JH, Park JS, Yoo JC, Shyam AK. Double transosseous pull out suture technique for transection of posterior horn of medial meniscus. *Arch Orthop Trauma Surg*. 2009; 129(3): 387-392.

[4] Ahn JH, Wang JH, Yoo JC, Noh HK, Park JH. A pull out suture for transection of the posterior horn of the medial meniscus: using a posterior trans-septal portal. *Knee Surg Sports Traumatol Arthrosc*. 2007; 15(12): 1510-1513.

[5] Allaire R, Muriuki M, Gilbertson L, Harner CD. Biomechanical consequences of a tear of the posterior root of the medial meniscus: similar to total meniscectomy. *J Bone Joint Surg Am*. 2008; 90(9) 1922-1931.

[6] Armstrong CG, Lai WM, Mow VC. An analysis of the unconfined compression of articular cartilage. *J Biomech Eng*. 1984. 106(2): 165-173.

[7] Bennetts CJ, Chokhandre S, Donnola SB, Flask CA, Bonner TF, Colbrunn RW, Erdemir A. Open Knee(s): magnetic resonance imaging for specimen-specific next generation knee models. Paper presented at: *SB3C2015, Summer Biomechanics, Bioengineering and Biotransport Conference;* June 17-20, 2015; Snowbird Resort, Utah.

[8] Bhatia S, LaPrade CM, Ellman MB, LaPrade RF. Meniscal root tears: significance, diagnosis, and treatment. *Am J Sports Med*. 2014; 42(12): 3016-3030.

[9] Blankevoort L, Huiskes R. Ligament-bone interaction in a three-dimensional model of the knee. *J Biomech Eng*. 1991; 113(3): 263-269.

[10] Blankevoort L, Kuiper JH, Huiskes R, Grootenboer HJ. Articular contact in a three-dimensional model of the knee. *J Biomech*. 1991; 24(11): 1019-1031.

[11] Bonner TF, Colbrunn RW, Chokhandre S, Bennetts C, Erdemir A. Open Knee(s): comprehensive tibiofemoral joint testing for specimen-specific next generation knee models Paper presented at: *SB3C2015, Summer Biomechanics, Bioengineering, and Biotransport Conference*; June 17-20, 2015; Snowbird Resort, Utah.

[12] Carey RE, Zheng L, Aiyangar AK, Harner CD, Zhang X. Subject-specific finite element modeling of the tibiofemoral joint based on CT, magnetic resonance imaging and dynamic stereo-radiography data *in vivo*. *J Biomech Eng*. 2014; 136(4): 041004-0410048.

[13] Cerminara AJ, LaPrade CM, Smith SD, Ellman MB, Wijdicks CA, LaPrade RF. Biomechanical evaluation of a transtibial pull-out meniscal root repair: challenging the bungee effect. *Am J Sports Med*. 2014; 42(12): 2988-2995.

[14] Chia HN, Hull ML. Compressive moduli of the human medial meniscus in the axial and radial directions at equilibrium and at a physiological strain rate. *J Orthop Res*. 2008; 26(7): 951-956.

[15] Choi NH, Son KM, Victoroff BN. Arthroscopic all-inside repair for a tear of posterior root of the medial meniscus: a technical note. *Knee Surg Sports Traumatol Arthrosc*. 2008; 16(9): 891-893.

[16] de Winter JCF. Using the Student's t-test with extremely small sample sizes. *Pract Assess Res Eval*. 2013; 18(10): 1-12.
[17] Duthon VB, Barea C, Abrassart S, Fasel JH, Fritschy D, Ménétrey J. Anatomy of the anterior cruciate ligament. *Knee Surg Sports Traumatol Arthrosc*. 2006; 14(3): 204-213.
[18] Eberhardt AW, Keer LM, Lewis JL, Vithoontien V. An analytical model of joint contact. *J Biomech Eng*. 1990; 112(4): 407-413.
[19] Engelsohn E, Umans H, DiFelice GS. Marginal fractures of the medial tibial plateau: possible association with medial meniscal root tear. *Skeletal Radiol*. 2007; 36(1): 73-76.
[20] Epperson K, Sawyer AM, Lustig M, Alley M, Uecker M, Virtue P, Lai P, Vasanawala S. Creation of fully sampled MR data repository for compressed sensing of the knee. Paper presented at: *2013 Meeting Proceedings of the Section for Magnetic Resonance Technologists*; April 20-26, 2013; Salt Lake City, Utah.
[21] Erdemir A, Bennetts C, Bonner T, Chokhandre S, Colbrunn R. Open Knee(s): founding data for next generation knee models. Paper presented at: *BMES/FDA Frontiers in Medical Devices Conference: Innovations in Modeling and Simulation*; May 18-20, 2015; Washington, DC.
[22] Erdemir A. Open knee(s): virtual biomechanical representations of the knee joint https://simtk.org/projects/openknee. Updated: April 26, 2017. Accessed: October 21, 2017.
[23] Feucht MJ, Grande E, Brunhuber J, Burgkart R, Imhoff AB, Braun S. Biomechanical evaluation of different suture techniques for arthroscopic transtibial pull-out repair of posterior medial meniscus root tears. *Am J Sports Med*. 2013; 41(12): 2784-2790.
[24] Feucht MJ, Kühle J, Bode G, Mehl J, Schmal H, Südkamp NP, Niemeyer P. Arthroscopic transtibial pullout repair for posterior medial meniscus root tears: A systematic review of clinical, radiographic, and second-look arthroscopic results. *Arthroscopy*. 2015; 31(9): 1808-1816.
[25] Fithian DC, Kelly MA, Mow VC. Material properties and structure-function relationships in the menisci. *Clin Orthop Relat Res*. 1990; 252: 19-31.
[26] Furumatsu T, Kodama Y, Fujii M, Tanaka T, Hino T, Kamatsuki Y, Yamada K, Miyazawa S, Ozaki T. A new aiming guide can create the tibial tunnel at favorable position in transtibial pullout repair for the medial meniscus posterior root tear. *Orthop Traumatol Surg Res*. 2017; 103(3): 367-371.
[27] Grood ES, Suntay WJ. A joint coordinate system for the clinical description of three-dimensional motions: application to the knee. *J Biomech Eng*. 1983; 105(2): 136-144.
[28] Guess TM, Razu S, Jahandar H, Stylianou A. Predicted loading on the menisci during gait: the effect of horn laxity. *J Biomech*. 2015; 48(8): 1490-1498.
[29] Hartshorn T, Otarodifard K, White EA, Hatch III GF. Radiographic landmarks for locating the femoral origin of the superficial medial collateral ligament. *Am J Sports Med*. 2013; 41(11): 2527-2532.
[30] Hauch KN, Villegas DF, Haut Donahue TL. Geometry, time-dependent and failure properties of human meniscal attachments. *J Biomech*. 2010; 43(3): 463-468.
[31] Haut Donahue TL, Hull ML, Rashid MM, Jacobs CR. A finite element model of the human knee joint for the study of tibio-femoral contact. *J Biomech Eng*. 2002; 124(3): 273-280.
[32] Haut Donahue TL, Hull ML, Rashid MM, Jacobs CR. How the stiffness of meniscal attachments and meniscal material properties affect tibio-femoral contact pressure computed using a validated finite element model of the human knee joint. *J Biomech*. 2003; 36(1): 19-34.

[33] Kim JH Chung JH, Lee DH, Lee YS, Kim JR, Ryu KJ. Arthroscopic suture anchor repair versus pullout suture repair in posterior root tear of the medial meniscus: a prospective comparison study. *Arthroscopy*. 2011; 27(12): 1644-1653.
[34] Kim YM, Rhee KJ, Lee JK, Hwang DS, Yang JY, Kim SJ. Arthroscopic pullout repair of a complete radial tear of the tibial attachment site of the medial meniscus posterior horn. *Arthroscopy*. 2006; 22(7): 795.e1-795.e4.
[35] Kopf S, Colvin AC, Muriuki M, Zhang X, Harner CD. Meniscal root suturing techniques: implications for root fixation. *Am J Sports Med*. 2011; 39(10): 2141-2146.
[36] Krych AJ, Johnson NR, Mohan R, Hevesi M, Stuart MJ, Littrell LA, Collins MS. Arthritis progression on serial MRIs following diagnosis of medial meniscal posterior horn root tear. *J Knee Surg*. 2017 [Epub Ahead of Print] PMID: 28950387.
[37] Krych AJ, Reardon PJ, Johnson NR, Mohan R, Peter L, Levy BA, Stuart MJ. Non-operative management of medial meniscus posterior horn root tears is associated with worsening arthritis and poor clinical outcome at 5-year follow-up. *Knee Surg Sports Traumatol Arthrosc*. 2017; 25(2): 383-389.
[38] LaPrade CM, Ellman MB, Rasmussen MT, James EW, Wijdicks CA, Engebretsen L, LaPrade RF. Anatomy of the anterior root attachments of the medial and lateral menisci: a quantitative analysis. *Am J Sports Med*. 2014; 42(10): 2386-2392.
[39] LaPrade CM, Foad A, Smith SD, Turnbull TL, Dornan GJ, Engebretsen L, Wijdicks CA, LaPrade RF. Biomechanical consequences of a nonanatomic posterior medial meniscal root repair. *Am J Sports Med*. 2015; 43(4): 912-920.
[40] LaPrade CM, James EW, Engebretsen L, LaPrade RF. Anterior medial meniscal root avulsions due to malposition of the tibial tunnel during anterior cruciate ligament reconstruction: two case reports. *Knee Surg Sports Traumatol Arthrosc*. 2014; 22(5): 1119-1123.
[41] LaPrade CM, LaPrade MD, Turnbull TL, Wijdicks CA, LaPrade RF. Biomechanical evaluation of the transtibial pull-out technique for posterior medial meniscal root repairs using 1 and 2 transtibial bone tunnels. *Am J Sports Med*. 2015; 43(4): 899-904.
[42] Liu F, Gadikota HR, Kozanek M, Hosseini A, Yue B, Gill TJ, Rubash HE, Li G. *In vivo* length patterns of the medial collateral ligament during the stance phase of gait. *Knee Surg Sports Traumatol Arthrosc*. 2011; 19(5): 719-727.
[43] Liu F, Yue B, Gadikota HR, Kozanek M, Liu W, Gill TJ, Rubash HE, Li G. Morphology of the medial collateral ligament of the knee. *J Orthop Surg Res*. 2010; 5(1): 69.
[44] Lustig M, Vasanawala S. MRI Datasets for Compressed Sensing. http://mridata.org. Accessed: October 21, 2017.
[45] Moon HK, Koh YG, Kim YC, Park YS, Jo SB, Kwon SK. Prognostic factors of arthroscopic pull-out repair for a posterior root tear of the medial meniscus. *Am J Sports Med*. 2012; 40(5): 1138-1143.
[46] Osti M, Tschann P, Künzel KH, Benedetto KP. Anatomic characteristics and radiographic references of the anterolateral and posteromedial bundles of the posterior cruciate ligament. *Am J Sports Med*. 2012; 40(7): 1558-1563.
[47] Padalecki JR, Jansson KS, Smith SD, Dornan GJ, Pierce CM, Wijdicks CA, LaPrade RF. Biomechanical consequences of a complete radial tear adjacent to the medial meniscus posterior root attachment site: in situ pull-out repair restores derangement of joint mechanics. *Am J Sports Med*. 2014; 42(3): 699-707.

[48] Park S, Hung CT, Ateshian GA. Mechanical response of bovine articular cartilage under dynamic unconfined compression loading at physiological stress levels. *Osteoarthritis Cartilage*. 2004; 12(1): 65-73.
[49] Park SE, DeFrate LE, Suggs JF, Gill TJ, Rubash HE, Li G. The change in length of the medial and lateral collateral ligaments during *in vivo* knee flexion. *Knee*. 2005; 12(5): 377-382.
[50] Park YS, Moon HK, Koh YG, Kim YC, Sim DS, Jo SB, Kwon SK. Arthroscopic pullout repair of posterior root tear of the medial meniscus: the anterior approach using medial collateral ligament pie-crusting release. *Knee Surg Sports Traumatol Arthrosc*. 2011; 19(8): 1334-1336.
[51] Rosslenbroich SB, Borgmann J, Herbort M, Raschke MJ, Peterson W, Zantop T. Root tear of the meniscus: biomechanical evaluation of an arthroscopic refixation technique. *Arch Orthop Trauma Surg*. 2013. 133(1): 111-115.
[52] Shepherd DE, Seedhom BB. The 'instantaneous' compressive modulus of human articular cartilage in joints of the lower limb. *Rheumatology (Oxford)*. 1999; 38(2) 124-132.
[53] Skaggs DL, Warden WH, Mow VC. Radial tie fibers influence the tensile properties of the bovine medial meniscus. *J Orthop Res*. 1994; 12(2): 176-185.
[54] Stärke C, Kopf S, Gröbel KH, Becker R. The effect of a nonanatomic repair of the meniscal horn attachment on meniscal tension: a biomechanical study. *Arthroscopy*. 2010; 26(3): 358-365.
[55] Stärke C, Kopf S, Lippisch R, Lohmann CH, Becker R. Tensile forces on repaired medial meniscal root tears. *Arthroscopy*. 2013; 29(2): 205-212.
[56] Tissakht M, Ahmed AM. Tensile stress-strain characteristics of the human meniscal material. *J Biomech*. 1995; 28(4): 411-422.
[57] Whipple R, Wirth CR, Mow VC. Mechanical properties of the meniscus. *ASME Advances in Bioengineering*. 1984; 32-33.
[58] Wismans J, Veldpaus F, Janssen J. Huson A, Struben P. A three-dimensional mathematical model of the knee joint. *J Biomech*. 1980; 13(8): 677-685.

CHAPTER 6:

LOOSENING OF POSTEROMEDIAL MENISCAL ROOT REPAIRS SIGNIFICANTLY ALTERS KNEE MECHANICS: A FINITE ELEMENT STUDY

6.1 Introduction

Meniscal root tears are harmful to knee health as they result in loading patterns similar to total meniscectomies, leading to progressive meniscal extrusion and worsening arthritis.[5,29,30] Therefore, meniscal root repair techniques have been developed to restore knee mechanics and prevent degeneration from these tears.[3,4] Cadaveric biomechanical studies have concluded that meniscal root repairs nearly restore cartilage contact mechanics;[5,31,36] however, these studies are evaluating their function immediately after repairs were created. Follow-up clinical studies demonstrate that meniscal extrusion is still present postoperatively and that cartilage degeneration is not always prevented.[20,27,28,35] These studies suggest that something may prevent meniscal root repairs from being as effective as they are shown to be when initially created.

A possible explanation for this change in repair function over time is repair loosening. Previous biomechanical studies have demonstrated that displacement progressively increases in meniscal root repairs with further cyclic loading.[13,32,42] Also, the most recent of these studies demonstrated that repairs do not completely recover from this cyclic loading.[42] This suggests that repair displacement may not only be a result of the viscoelastic nature of meniscal tissue, it may also be due to permanent displacement resulting from cyclic loading whereby the initial position of the meniscus during repair is not retained.

Although these studies have demonstrated that displacement occurs and that a portion of this displacement is unrecoverable loosening of repairs, prior studies have not evaluated how the

resultant loosening affects knee mechanics because such experimental procedures are destructive to the menisci.[13,32,42] Therefore, little is known about how repair loosening alters overall knee joint behavior. One experimental study in porcine limbs has shown that cartilage deformation after meniscal root repairs increases compared to the intact condition after only 50 cycles of compression.[37] This study suggests that repair loosening may have a significant effect on knee mechanics, but the information is limited to deformation of cartilage at a single location. Repair misplacement has also been demonstrated to occur clinically and to significantly affect knee mechanics;[22,43] thus, the effect of loosening with anatomic and nonanatomic placement needs to be better understood.

The purpose of this study was to determine the effect of loosening on cartilage contact and meniscus mechanics for anatomic and nonanatomic repairs. It is hypothesized that loosened anatomic repairs will result in significant changes to cartilage contact or meniscus mechanics with respect to the intact condition. Additionally, it is hypothesized that none of the nonanatomic repairs will completely restore knee mechanics, but nonanatomic repairs placed further anterior will be the most restorative.

6.2 Methods

6.2.1 Model Simulations

Three finite element knee models were created as previously described in Chapter 5 and used to evaluate changes to cartilage and meniscus mechanics with loosened meniscal root repairs. Briefly, the models were generated from open-source image datasets and all knee specimens were imaged at 0° flexion.[7,11,17,18,19,34,43] An open-source segmentation software was used to isolate tibiofemoral articular cartilage and menisci, and commercial meshing software was used to

generate hexahedral meshes for all tissues components. A mesh convergence study was performed to determine appropriate mesh density and Monte Carlo simulations demonstrated that the three models represented 39% of possible material property variations.[43]

Material properties were taken from previously validated, finite element knee models for tibiofemoral compression.[12,26] The interface of bone with articular cartilage and the meniscal insertions were modeled as rigid as this has a minimal effect on contact solutions when evaluating quasi-static tibiofemoral compression.[25] Articular cartilage was modeled as homogenous, linearly elastic, isotropic materials with a modulus of 15 MPa and Poisson's ratio of 0.475 to maintain the nearly incompressible behavior during short loading times.[6,16,39] The body of the menisci were modeled as homogeneous, linearly elastic, transversely isotropic materials.[12,21,26,40,44,45] In the collagen fiber direction of the menisci, the modulus was defined as 150 MPa and Poisson's ratio as 0.3. In the transverse plane, the elastic modulus was defined as 20 MPa, Poisson's ratio as 0.2, and shear modulus as 57.3 MPa. The time dependence due to viscoelasticity of menisci was not considered with the quasi-static analysis. Meniscal insertions were modeled similarly to the meniscal bodies, with the exception that the in-plane elastic modulus was 10 MPa.[1,2,24] Ligaments were modeled as tension-only, nonlinear spring elements with their stiffness dependent upon initial strains at full extension and the reference length of ligament bundles identified in the image datasets.[9,10,23,26,43,46]

The general-purpose finite element code, ABAQUS (Dassault Systèmes Simulia Corp., Johnston, RI), was used to approximate contact solutions for a quasi-static analysis using the implicit solver. Hard, frictionless contact was modeled for the six contact-surface pairs in each model, which included contact of femoral cartilage with the meniscus body/insertions, tibial

cartilage with the meniscus body/insertions, and femoral cartilage with tibial cartilage for both the lateral and medial hemijoints.

Simulations of tibiofemoral compression were designed to assess rehabilitation and return-to-activity loading.[8,13,41] Rehabilitative loading consisted of a 500 N compressive load with knee flexion at 0°, 30°, and 60° flexion. This was used to represent standard range of motion and toe-touch weight-bearing protocols typical of 6-week postoperative rehabilitation following meniscal root repairs. Return-to-activity loading consisted of a 1,000 N compressive load with knee flexion at 0°, 30°, and 60° flexion. Simulations of these six loading scenarios were evaluated in the intact condition and compared to various loosened posteromedial root repairs. Specimen-specific joint kinematics were implemented for two models and average joint kinematics from a sample population were implemented into the third model as a general case to simulate the different angles of knee flexion.[19,43]

Loosened repairs require a greater change in displacement to reach a target tensile load.[42] To simulate this within the finite element knee models, repair loosening was represented as a decrease in suture element stiffness. Equation 1 was used to calculate the loosened stiffness of repairs, k_l .

$$k_l = \frac{F}{(\Delta x + \Delta x_l)} \tag{1}$$

where F is the total tensile force of the suture elements during simulation of joint compression, Δx is the change in length of the suture elements during simulation of joint compression, and Δx_l is the change in length of repairs due to repair loosening. The tension and change in length of the sutures represent the variables of the first cycle of compression when no repair loosening has occurred, and these values were taken from each previous repair simulations without loosening.[42] Loosening was represented by the average change in repair length experimentally determined after

10,000 loading cycles and 30 minutes of rest, where Δx_l = 1.59 mm.[42] This represents the amount of repair displacement that does not recover after rest. The value for the loosened repair stiffness was individually calculated for each condition to incorporate the appropriate tension seen by the various repairs in all conditions.

The finite element knee models were previously developed to assess nonanatomic repairs around the anatomic center of the meniscal insertion;[43] therefore, only anatomic and nonanatomic placement of repairs with the incorporation of loosening were evaluated in this study. Anatomic coordinates were modified to account for the slope of the posteromedial meniscal insertion. The anatomic center was calculated as the centroid of the posteromedial meniscal insertion area. The anterior-posterior axis was defined by connecting the most anterior point of the meniscal insertion site and the most posterior point and the medial-lateral axis was perpendicular to the anterior-posterior axis. Along the modified anatomic coordinates, repair positions assessed included locations anterior, posterior, medial, lateral, anteromedial, anterolateral, posteromedial, and posterolateral from the anatomic center by 1 mm, 3 mm, and 5 mm.

6.2.2 Outcome Variables

The mean hoop stress, defined as the mean Cauchy stress, was measured at the midbody of the medial meniscus and the midportion of the anteromedial meniscal insertion in the direction of the collagen fiber orientation. Total contact area, cartilage-cartilage contact area, and peak contact pressure on the medial surface of the tibial articular cartilage were recorded to assess cartilage contact mechanics. The total contact area of the tibial and femoral cartilage surfaces with the medial meniscus was also measured to assess congruency within the joint. Meniscal extrusion was measured as the distance between the outer edge of the medial meniscus and the medial edge

of the tibial articular cartilage in the medial-lateral direction of the tibia. Extrusion was measured at three locations on the medial meniscus – the anterior root, the central portion of the meniscus, and posterior root.

6.2.3 Statistical Analysis

Differences between loosened repairs and intact are presented as percent changes. Paired-samples *t* tests were performed to determine if percent changes were significantly different than zero. The Benjamini-Hochberg correction method was performed to adjust the familywise error rate to ensure the significance level, α, was 0.05. Statistical comparisons of paired data with N = 3 has been shown to be sufficiently powered (> 80%) if there is a strong within-pairs correlation ($r \geq 0.8$) and a large effect size (Cohen's $d \geq 2$).[15] Therefore, significant results were only reported if $r \geq 0.8$ and Cohen's $d \geq 2$.

6.3 Results

6.3.1 Medial Meniscus Hoop Stress

With all loading scenarios, the mean hoop stress of the medial meniscus midbody significantly decreased for anatomic and all nonanatomic repairs with respect to intact ($p < 0.02$ for all repairs). At 0° flexion, all loosened repairs resulted in decreases greater than 50% for meniscal hoop stress (Appendix B.1 and B.2). Anterior placement of loosened repairs resulted in less pronounced changes at 30° and 60° flexion (Figure 6.1) The minimum decrease in meniscal hoop stress was 25% ± 5% for a loosened 5 mm anterior repair with the knee at 60° flexion and a 500 N compressive load.

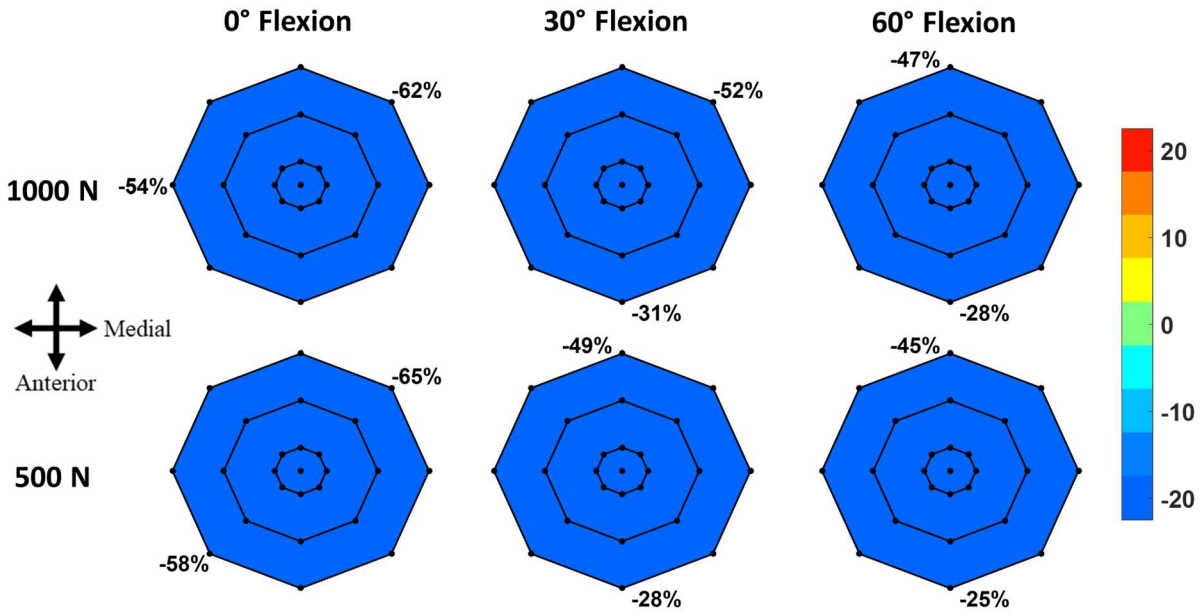

Figure 6.1 – Percent changes to the mean hoop stress of the medial meniscus with respect to intact for anatomic and nonanatomic repairs.

The mean hoop stress within the anteromedial meniscal insertion also significantly decreased for all repairs ($p < 0.03$). Similarly, hoop stresses decreased by at least 60% on average with compression at 0° flexion (Appendix B.3 and B.4). Loosened repairs at 30° and 60° flexion resulted in at least 27% decreases on average in hoop stress with 5 mm anterior repairs (Figure 6.2). Posterior placement of loosened repairs resulted in decreases in hoop stress around 50%. The amount of compressive load did not affect changes to meniscal hoop stresses with respect to intact at any flexion angle.

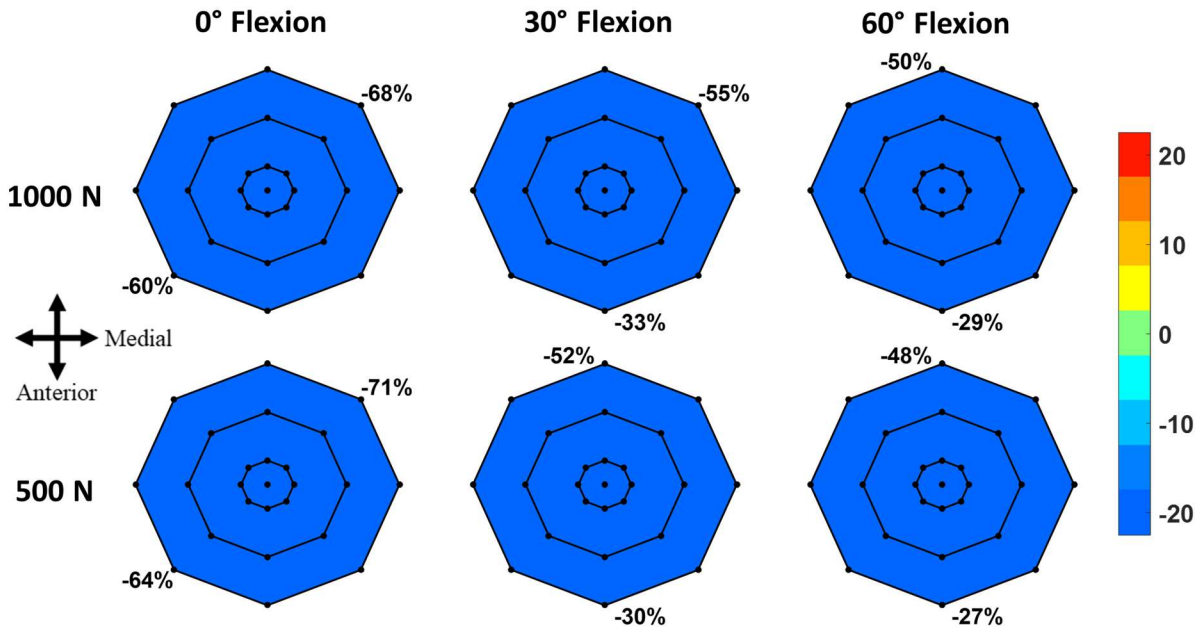

Figure 6.2 – Percent changes to mean hoop stress of the anteromedial meniscal insertion with respect to intact for anatomic and nonanatomic repairs.

6.3.2 Cartilage and Meniscus Contact Areas

The total contact area significantly decreased by at least 23% for all loosened repairs at 0° flexion ($p < 0.03$). At 30° and 60° flexion, decreases in total contact were determined for anatomic and all nonanatomic repairs but were less prominent than at 0° flexion (Figure 6.3). With the 1,000 N compressive load at 30° flexion, all repairs resulted in a significant decrease except the 5 mm anteromedial and the 5 mm medial repairs (Appendix B.5). The 5 mm posterior repair resulted in the greatest significant decrease at 30° flexion of 18% ± 1%. There were no significant changes at 30° flexion with the 500 N compressive load (Appendix B.6). Additionally, there were no significant changes to the total contact area at 60° flexion. Despite this, total contact area at 60° flexion followed a similar trend as with compression at 30° flexion where the 5 mm posterior repair resulted in the greatest decrease and the 5 mm anteromedial repair resulted in the smallest decrease (Figure 6.3).

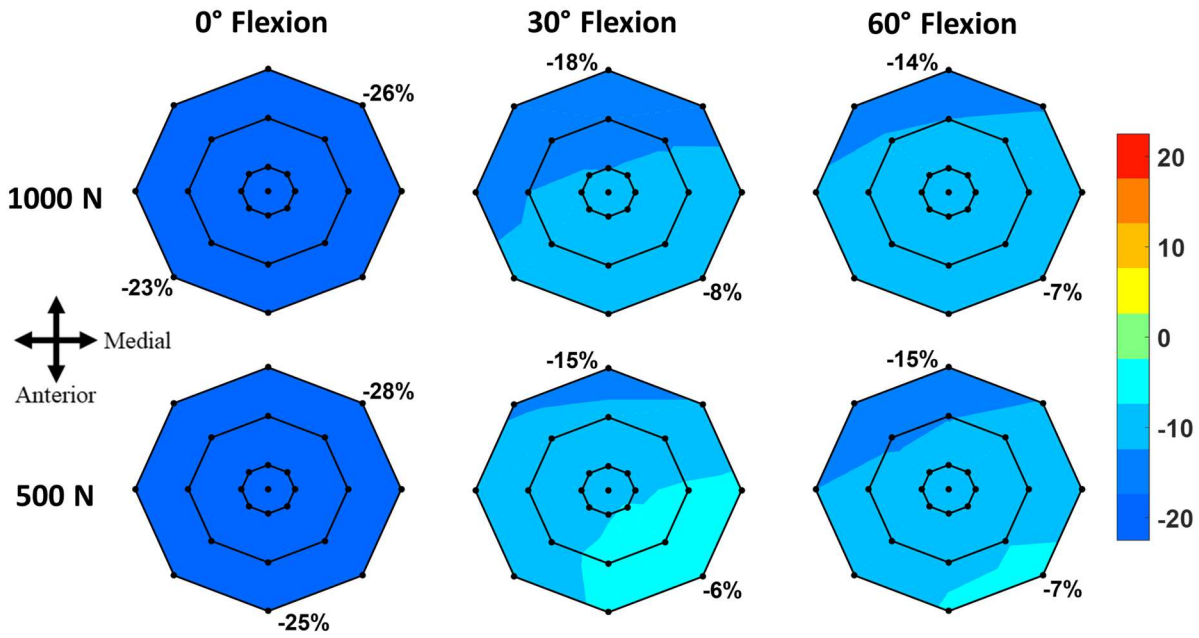

Figure 6.3 – Percent changes of the total contact area on the medial surface of tibial articular cartilage for anatomic and nonanatomic repairs with respect to the intact condition.

Despite the overall decrease in total contact area, the cartilage-cartilage contact area significantly increased for loosened anatomic and all loosened nonanatomic repairs with all loading scenarios except with knee flexion at 30° flexion and a 500 N compressive load (Figure 6.4). The largest increases in cartilage-cartilage contact area with respect to the intact condition occurred at 30° flexion with a 500 N load; however, the variability in the amount of increases resulted in these changes not being significant (Appendix B.7 and B.8). In general, the further posterior repairs resulted in the greatest average increase in cartilage-cartilage contact area. Loosened repairs placed 5 mm anteromedial were able to restore the cartilage-cartilage contact area to intact the best at 60° flexion; however, significant increases of 24% ± 7 % and 29% ± 7% still occurred with 1,000 N and 500 N compressive loads, respectively.

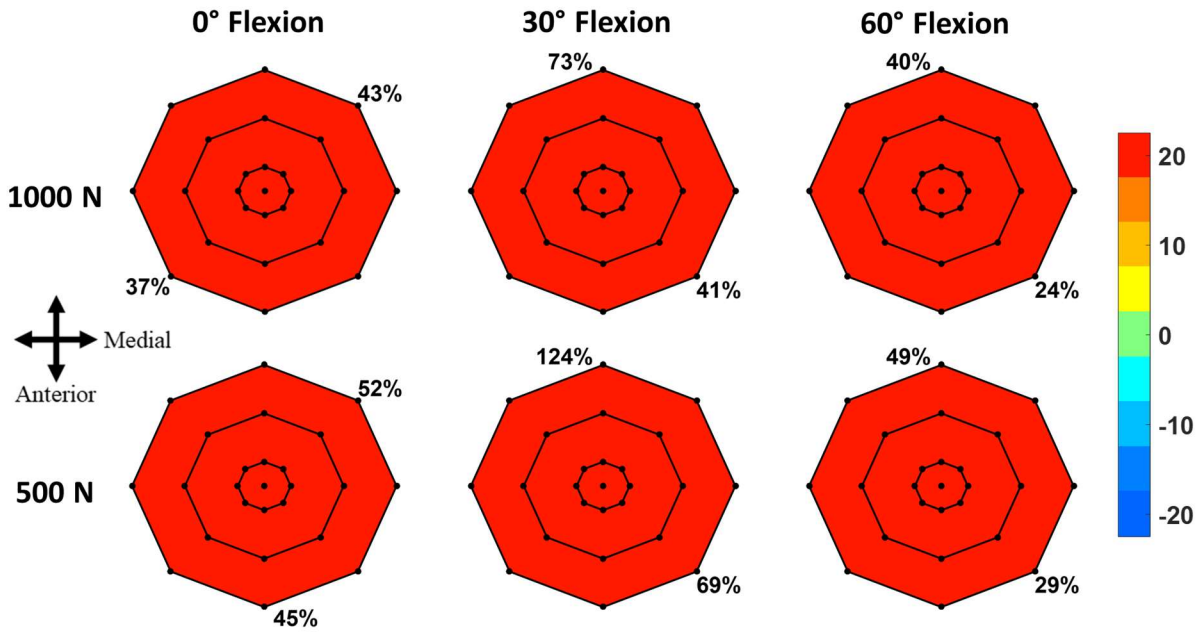

Figure 6.4 – Percent changes of the cartilage-cartilage contact area on the medial surface of tibial articular cartilage for anatomic and nonanatomic repairs with respect to the intact condition.

The total contact area of the medial meniscus with the femoral and tibial articular cartilage significantly decreased for all loosened repairs in all loading scenarios except for the 5 mm anterior repair with a 500 N compressive load and the knee in full extension (Appendix B.9 and B.10). Loosening caused the congruency of the medial meniscus with the articular cartilage surfaces to decrease by around 50% on average for all repairs at 0° flexion and for further posteriorly placed repairs at 30° and 60° flexion (Figure 6.5). Repairs placed further anterior or anteromedial were the best at compensating for loosening; however, they still resulted in significant decreases to meniscal contact area with the cartilage surfaces.

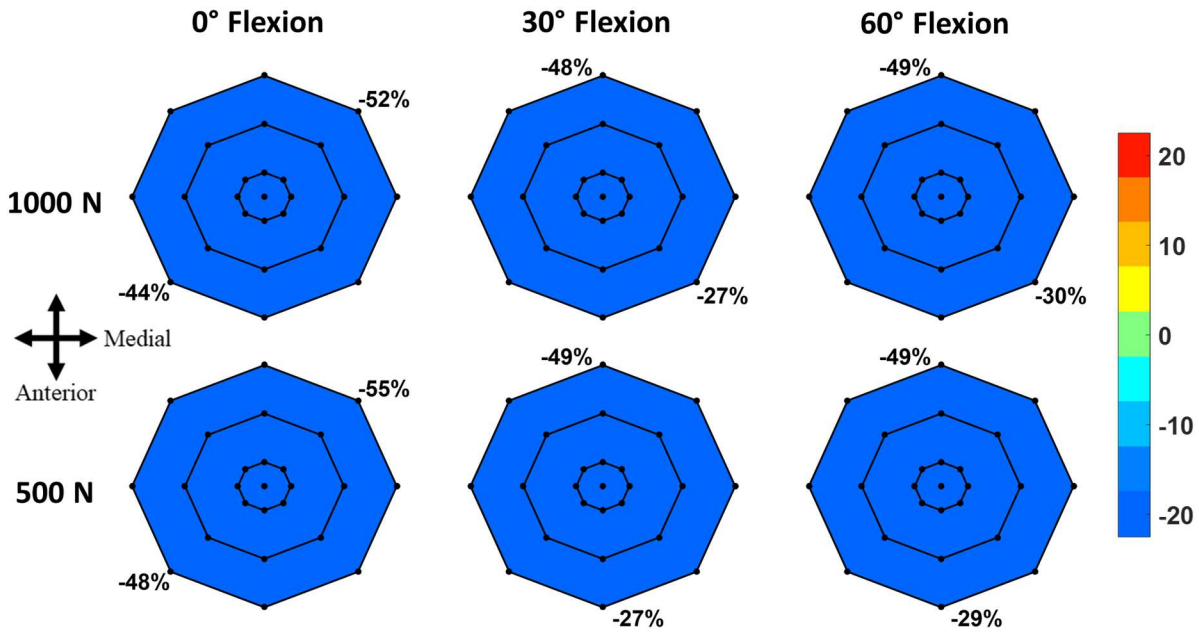

Figure 6.5 – Percent changes to total contact area of the medial meniscus with respect to intact for anatomic and nonanatomic repairs.

6.3.3 Tibial Cartilage Contact Pressure

There were no significant changes to peak contact pressure on the medial surface of the tibial articular cartilage, although all anatomic and nonanatomic repairs resulted in average increases (Appendix B.11 and B.12). The largest average increases to peak contact pressure occurred with knee compression at 30° flexion (Figure 6.6). At 0° and 60° flexion, the average increase of peak contact pressure was around 10% for all repairs.

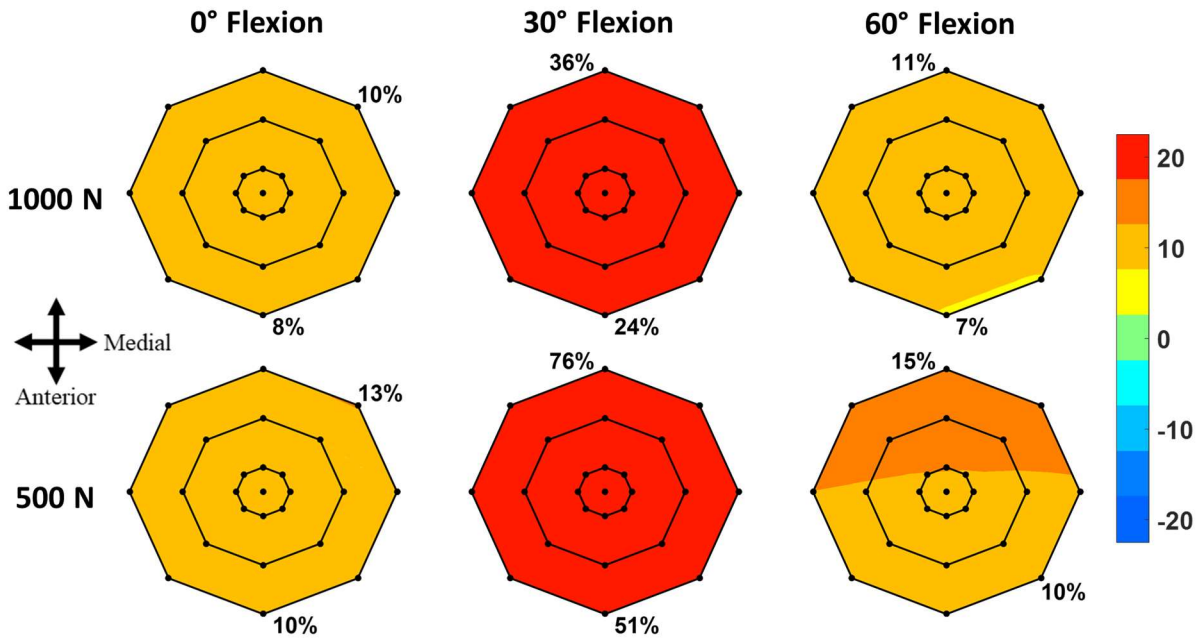

Figure 6.6 – Percent changes to peak contact pressure with respect to intact on medial surface of tibial articular cartilage for anatomic and nonanatomic repairs.

6.3.4 Meniscal Extrusion

Loosened repairs of the posteromedial meniscal root resulted in significant increases to the amount of meniscal extrusion with respect to the intact meniscus (Appendix B.13 and B14). At 0° and 60° flexion, loosened anatomic and all loosened nonanatomic repairs resulted in significant increases ($p < 0.05$). Loosened anatomic repairs resulted in significant increases in extrusion with respect to intact of 0.7 mm ± 0.2 mm, 1.3 mm ± 0.4 mm, and 1.3 mm ± 0.2 mm when the knee was at 0°, 30°, and 60° flexion with a compressive load of 1,000 N, respectively (Figure 6.7). Similarly, loosened anatomic repairs resulted in significant extrusion of 0.6 mm ± 0.2 mm, 1.1 mm ± 0.4 mm, and 1.2 mm ± 0.1 mm when the knee was at 0°, 30°, and 60° flexion with a compressive load of 500 N, respectively (Figure 6.7). The anatomic and repairs placed posteriorly resulted in significant increases at 30° flexion; however, increases resulting from loosened repairs placed 3 mm and 5 mm anterior, anterolateral, and anteromedial were not significant. The most extrusion

occurred with loosened 5 mm posterior repairs at 30 and 60 flexion which was around 2 mm at a 1,000 N compressive load (Figure 6.7). There were no significant changes to meniscal extrusion near the anterior root or the central portion of the medial meniscus.

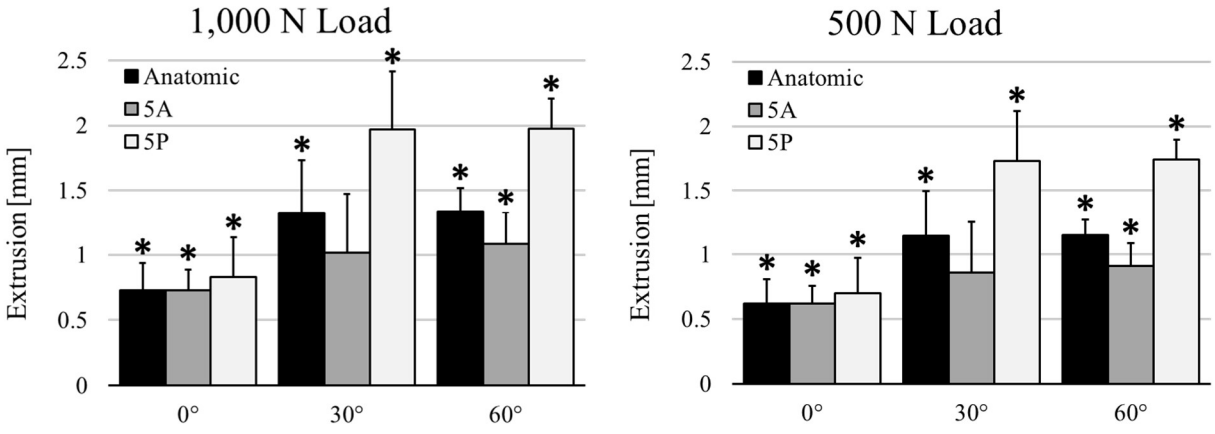

Figure 6.7 – Increases in meniscal extrusion measured near the posterior root of the medial meniscus. * denotes statistical significance of increases greater than zero. 5A = 5 mm anterior repair; 5P = 5 mm posterior repair

6.4 Discussion

The results of this study demonstrate that loosening of meniscal root repairs has a considerable effect on both cartilage and meniscus mechanics. At all flexion angles and all loads assessed, loosened anatomic repairs were unable to restore mechanics to intact. Additionally, nonanatomic repairs were unable to compensate for the changes resulting from repair loosening. Repairs misplaced posteriorly caused a greater change in knee mechanics than anatomic or anterior repairs. Repairs misplaced anteriorly were able to reduce resultant changes and better restore knee mechanics; however, many outcomes still significantly changed with respect to intact.

Meniscal hoop stresses measured for anatomic and all nonanatomic repairs resulted in significant decreases with all loading scenarios. At 0° flexion and with repairs misplaced posteriorly, the load transmission through the meniscus was reduced by around 50%. Repairs

misplaced anteriorly were best at restoring load transmission; however, they still resulted in significant decreases of at least 25%. These results demonstrate that loosening of meniscal root repairs caused the meniscus to be less effective in transmitting compressive loads; therefore, a larger portion of the tibiofemoral load is dispersed directly through the articular cartilage. Röpke et al. demonstrated that cartilage deformed more with cyclic loading when compared to deformation with the meniscus intact.[37] The increase in cartilage deformation with repairs may suggest that load transmission through the menisci decreased and more load was taken up through the articular cartilage. The present study represents mechanics after loosening has already occurred instead of the progressive change that would occur as repairs gradually loosen. However, the results of Röpke et al. help to confirm that meniscal hoop stress decrease with further loosening.

Overall, the total contact area on the medial surface of the tibial plateau decreased with significant changes occurring at full extension and with repairs placed posteriorly. In addition to this, the cartilage-cartilage contact area significantly increased for anatomic and all nonanatomic repairs at most loading conditions. Previous studies in cadavers and finite element knee models demonstrated that total contact area was nearly restored to intact immediately after repairs were created.[5,31,36] The results of the present study suggest that as repairs loosen, the total contact area begins to decrease so that these nearly restorative repairs are no longer restoring the contact. Assessment of repair placement demonstrated that although total contact area was nearly restored, the amount of cartilage-cartilage contact area significantly increased.[43] Therefore, the measurement of total contact area may be misleading because the cartilage-cartilage contact area is compensating for the decrease in contact of the meniscus. In the present study, loosened repairs demonstrated greater increases in cartilage-cartilage contact area than with placement alone.

Despite significant decreases in load transmission through the menisci and increases to cartilage-cartilage contact, the peak contact pressure on the medial surface of the tibial plateau did not significantly change for any loading conditions. For all loosened repairs assessed, the average peak contact pressure increased but the effect was not large enough to detect significance in this study. Since a significant portion of the tibiofemoral load was not transmitted by the menisci into hoop stresses, a greater portion of the compressive load was directed through cartilage-cartilage contact with respect to the intact condition. This load would have been dispersed over the cartilage-cartilage contact area demonstrated to significantly increase for most loosened repairs. The small increase in peak contact pressure may be explained by an increase in load through the cartilage that was not proportional to the significant increase in cartilage-cartilage contact area.

The total contact of the medial meniscus with the tibial and femoral cartilage also significantly decreased for all repairs except the repair placed 5 mm anterior for one loading condition. At 0° flexion and for repairs misplaced posteriorly, the decrease in meniscal congruency was around 50%. These results demonstrate that loosened repairs cause the menisci to be in contact with the articular cartilage half as much as in the intact condition. The total contact of the meniscus with the articular cartilage surfaces is another example within the results of this study that demonstrate the loss of function in the menisci. The decrease in congruency prevents the menisci from being in a proper position to transmit compressive loads away from the articular cartilage and into meniscal hoop stresses. Assessment of repair placement in a previous finite element study demonstrated that meniscal congruency was also a concern with repairs that did not incorporate loosening.[43] Also, comparison of this study to the present study suggests that loosening causes a greater decrease in meniscal congruency than placement alone.[43]

Loosened anatomic repairs resulted in significant extrusion of the posterior root by at least 0.6 mm. When knees were flexed to 30° and 60°, the meniscal extrusion increased to over 1 mm for anatomic repairs. Loosened repairs misplaced posteriorly resulted in meniscal extrusion of around 2 mm. Repair loosening incorporated into the finite element models was taken from a previous ovine cadaveric study simulating typical loads seen in rehabilitation with meniscal root repairs.[42] This cadaver study demonstrated that loosening may occur from as early as rehabilitation and the present study confirmed that this loosening significantly increases the extrusion of the meniscus. Lerer et al. demonstrated that extrusion of the meniscus by at least 3 mm is strongly associated with degeneration and that meniscal extrusion likely precedes degeneration.[33] In the present study, meniscal extrusion did not exceed 3 mm when evaluating misplaced and loosened repairs; however, posterior placement of repairs with loosening from rehabilitation resulted in 2 mm of extrusion. Follow-up clinical studies have demonstrated that extrusion is still present postoperatively and a cadaveric study showed that repairs gradual displace further with continued loading instead of reaching an equilibrium displacement.[27,28,35,42] Therefore, posterior misplacement of repairs and the inability to prevent loosening from occurring in repairs predisposes patients to significant extrusion that may progress beyond 3 mm and precede joint degeneration.

Together, the results of this study help to portray a robust idea of what happens to knee mechanics when meniscal root repairs loosen. During compression, the repaired meniscus is significantly extruded from the joint space. This leads to the menisci being less in contact, or less congruent, with the articular cartilage surfaces. Since the contact with the meniscus decreases, the contact between the tibial and femoral cartilage significantly increases to compensate. This causes a larger portion of the tibiofemoral load to be dispersed through direct contact of the articular

cartilage, resulting in less load being transmitted through the meniscus body and insertions away from the articular cartilage and average increases to the peak contact pressure on the cartilage surface.

A limitation of this study is that it assumes anatomic and all nonanatomic repairs were subjected to a rehabilitative protocol that resulted in the exact same repair loosening for all repairs. The resultant repair loosening may in fact be different clinically depending on the placement of repairs. For example, anterior repairs result in an increase in repair tension from identical compressive load when compared to anatomic.[43] Therefore, if the rehabilitation was the same for both patients, the loosening would likely be greater for the patient with a repair placed anteriorly. Additionally, this study attempts to quantify changes in knee mechanics following repair loosening from rehabilitation which typically begins at 6 weeks and does not account for potential healing that has occurred. Currently, follow-up studies have focused on healing of meniscal root repairs around 1 year postoperatively.[14,38] Therefore, it is unknown how much healing, if any, has occurred by the time rehabilitation has begun when repairs are susceptible to loosening. Additionally, follow-up studies have demonstrated that some patients still have little to no healing that occurs one to two years postoperatively. [14,38] Thus, the results of this study may also help to explain what happens to knee mechanics when healing of the repair does not occur.

6.5 Conclusion

The results of this study demonstrate that loosening of meniscal root repairs significantly hinders meniscus function and alters load distribution throughout the knee. Significant extrusion of the loosened repair lead to significant changes in contact with the meniscus, the ability for the menisci to transmit loads, and the distribution of load on the articular cartilage. Conservative

rehabilitation is recommended for patients to prevent loosening from occurring as the present study has demonstrated that significant changes to knee mechanics that result. Future studies should focus on evaluating the healing process of repairs at earlier time points, such as 6 weeks when rehabilitation typically begins. If little to no healing occurs when patients are beginning to load their repairs, loosening will prevent a successful repair.

REFERENCES

[1] Abraham AC, Haut Donahue TL. From meniscus to bone: a quantitative evaluation of structure and function of the human meniscal attachments. *Acta Biomater*. 2013; 9(5): 6322-6329.

[2] Abraham AC, Moyer JT, Villegas DF, Odegard GM, Haut Donahue TL. Hyperelastic properties of human meniscal attachments. *J Biomech*. 2011; 44(3): 413-418.

[3] Ahn JH, Wang JH, Lim HC, Bae JH, Park JS, Yoo JC, Shyam AK. Double transosseous pull out suture technique for transection of posterior horn of medial meniscus. *Arch Orthop Trauma Surg*. 2009; 129(3): 387-392.

[4] Ahn JH, Wang JH, Yoo JC, Noh HK, Park JH. A pull out suture for transection of the posterior horn of the medial meniscus: using a posterior trans-septal portal. *Knee Surg Sports Traumatol Arthrosc*. 2007; 15(12): 1510-1513.

[5] Allaire R, Muriuki M, Gilbertson L, Harner CD. Biomechanical consequences of a tear of the posterior root of the medial meniscus: similar to total meniscectomy. *J Bone Joint Surg Am*. 2008; 90(9) 1922-1931.

[6] Armstrong CG, Lai WM, Mow VC. An analysis of the unconfined compression of articular cartilage. *J Biomech Eng*. 1984. 106(2): 165-173.

[7] Bennetts CJ, Chokhandre S, Donnola SB, Flask CA, Bonner TF, Colbrunn RW, Erdemir A. Open Knee(s): magnetic resonance imaging for specimen-specific next generation knee models. Paper presented at: *SB3C2015, Summer Biomechanics, Bioengineering and Biotransport Conference*; June 17-20, 2015; Snowbird Resort, Utah.

[8] Bhatia S, LaPrade CM, Ellman MB, LaPrade RF. Meniscal root tears: significance, diagnosis, and treatment. *Am J Sports Med*. 2014; 42(12): 3016-3030.

[9] Blankevoort L, Huiskes R. Ligament-bone interaction in a three-dimensional model of the knee. *J Biomech Eng*. 1991; 113(3): 263-269.

[10] Blankevoort L, Kuiper JH, Huiskes R, Grootenboer HJ. Articular contact in a three-dimensional model of the knee. *J Biomech*. 1991; 24(11): 1019-1031.

[11] Bonner TF, Colbrunn RW, Chokhandre S, Bennetts C, Erdemir A. Open Knee(s): comprehensive tibiofemoral joint testing for specimen-specific next generation knee models Paper presented at: *SB3C2015, Summer Biomechanics, Bioengineering, and Biotransport Conference*; June 17-20, 2015; Snowbird Resort, Utah.

[12] Carey RE, Zheng L, Aiyangar AK, Harner CD, Zhang X. Subject-specific finite element modeling of the tibiofemoral joint based on CT, magnetic resonance imaging and dynamic stereo-radiography data *in vivo*. *J Biomech Eng*. 2014; 136(4): 041004-0410048.

[13] Cerminara AJ, LaPrade CM, Smith SD, Ellman MB, Wijdicks CA, LaPrade RF. Biomechanical evaluation of a transtibial pull-out meniscal root repair: challenging the bungee effect. *Am J Sports Med*. 2014; 42(12): 2988-2995.

[14] Cho JH, Song JG. Second-look arthroscopic assessment and clinical results of modified pull-out suture for posterior root tear of the medial meniscus. *Knee Surg Relat Res*. 2014; 26(2): 106.

[15] de Winter JCF. Using the Student's t-test with extremely small sample sizes. *Pract Assess Res Eval*. 2013; 18(10): 1-12.

[16] Eberhardt AW, Keer LM, Lewis JL, Vithoontien V. An analytical model of joint contact. *J Biomech Eng*. 1990; 112(4): 407-413.
[17] Epperson K, Sawyer AM, Lustig M, Alley M, Uecker M, Virtue P, Lai P, Vasanawala S. Creation of fully sampled MR data repository for compressed sensing of the knee. Paper presented at: *2013 Meeting Proceedings of the Section for Magnetic Resonance Technologists*; April 20-26, 2013; Salt Lake City, Utah.
[18] Erdemir A, Bennetts C, Bonner T, Chokhandre S, Colbrunn R. Open Knee(s): founding data for next generation knee models. Paper presented at: *BMES/FDA Frontiers in Medical Devices Conference: Innovations in Modeling and Simulation*; May 18-20, 2015; Washington, DC.
[19] Erdemir A. Open knee(s): virtual biomechanical representations of the knee joint https://simtk.org/projects/openknee. Updated: April 26, 2017. Accessed: October 21, 2017.
[20] Feucht MJ, Kühle J, Bode G, Mehl J, Schmal H, Südkamp NP, Niemeyer P. Arthroscopic transtibial pullout repair for posterior medial meniscus root tears: A systematic review of clinical, radiographic, and second-look arthroscopic results. *Arthroscopy*. 2015; 31(9): 1808-1816.
[21] Fithian DC, Kelly MA, Mow VC. Material properties and structure-function relationships in the menisci. *Clin Orthop Relat Res*. 1990; 252: 19-31.
[22] Furumatsu T, Kodama Y, Fujii M, Tanaka T, Hino T, Kamatsuki Y, Yamada K, Miyazawa S, Ozaki T. A new aiming guide can create the tibial tunnel at favorable position in transtibial pullout repair for the medial meniscus posterior root tear. *Orthop Traumatol Surg Res*. 2017; 103(3): 367-371.
[23] Guess TM, Razu S, Jahandar H, Stylianou A. Predicted loading on the menisci during gait: the effect of horn laxity. *J Biomech*. 2015; 48(8): 1490-1498.
[24] Hauch KN, Villegas DF, Haut Donahue TL. Geometry, time-dependent and failure properties of human meniscal attachments. *J Biomech*. 2010; 43(3): 463-468.
[25] Haut Donahue TL, Hull ML, Rashid MM, Jacobs CR. A finite element model of the human knee joint for the study of tibio-femoral contact. *J Biomech Eng*. 2002; 124(3): 273-280.
[26] Haut Donahue TL, Hull ML, Rashid MM, Jacobs CR. How the stiffness of meniscal attachments and meniscal material properties affect tibio-femoral contact pressure computed using a validated finite element model of the human knee joint. *J Biomech*. 2003; 36(1): 19-34.
[27] Kim JH Chung JH, Lee DH, Lee YS, Kim JR, Ryu KJ. Arthroscopic suture anchor repair versus pullout suture repair in posterior root tear of the medial meniscus: a prospective comparison study. *Arthroscopy*. 2011; 27(12): 1644-1653.
[28] Kim SB, Ha JK, Lee SW, Kim DW, Shim JC, Kim JG, Lee MY. Medial meniscus root tear refixation: comparison of clinical, radiologic, and arthroscopic findings with medial meniscectomy. *Arthroscopy*. 2011; 27(3): 346-354.
[29] Krych AJ, Johnson NR, Mohan R, Hevesi M, Stuart MJ, Littrell LA, Collins MS. Arthritis progression on serial MRIs following diagnosis of medial meniscal posterior horn root tear. *J Knee Surg*. 2017 [Epub Ahead of Print] PMID: 28950387.
[30] Krych AJ, Reardon PJ, Johnson NR, Mohan R, Peter L, Levy BA, Stuart MJ. Non-operative management of medial meniscus posterior horn root tears is associated with worsening arthritis and poor clinical outcome at 5-year follow-up. *Knee Surg Sports Traumatol Arthrosc*. 2017; 25(2): 383-389.

[31] LaPrade CM, Foad A, Smith SD, Turnbull TL, Dornan GJ, Engebretsen L, Wijdicks CA, LaPrade RF. Biomechanical consequences of a nonanatomic posterior medial meniscal root repair. *Am J Sports Med*. 2015; 43(4): 912-920.
[32] LaPrade CM, LaPrade MD, Turnbull TL, Wijdicks CA, LaPrade RF. Biomechanical evaluation of the transtibial pull-out technique for posterior medial meniscal root repairs using 1 and 2 transtibial bone tunnels. *Am J Sports Med*. 2015; 43(4): 899-904.
[33] Lerer DB, Umans HR, Hu MX, Jones MH. The role of meniscal root pathology and radial meniscal tear in medial meniscal extrusion. *Skeletal Radiol*. 2004; 33(10): 569-574.
[34] Lustig M, Vasanawala S. MRI Datasets for Compressed Sensing. http://mridata.org. Accessed: October 21, 2017.
[35] Moon HK, Koh YG, Kim YC, Park YS, Jo SB, Kwon SK. Prognostic factors of arthroscopic pull-out repair for a posterior root tear of the medial meniscus. *Am J Sports Med*. 2012; 40(5): 1138-1143.
[36] Padalecki JR, Jansson KS, Smith SD, Dornan GJ, Pierce CM, Wijdicks CA, LaPrade RF. Biomechanical consequences of a complete radial tear adjacent to the medial meniscus posterior root attachment site: in situ pull-out repair restores derangement of joint mechanics. *Am J Sports Med*. 2014; 42(3): 699-707.
[37] Röpke EF, Kopf S, Drange S, Becker R, Lohmann CH, Starke C. Biomechanical evaluation of meniscal root repair: a porcine study. *Knee Surg Sports Traumatol Arthrosc*. 2015; 23(1): 45-50.
[38] Seo HS, Lee SC, Jung KA. Second-look arthroscopic findings after repairs of posterior root tears of the medial meniscus. *Am J Sports Med*. 2011; 39(1): 99-107.
[39] Shepherd DE, Seedhom BB. The 'instantaneous' compressive modulus of human articular cartilage in joints of the lower limb. *Rheumatology (Oxford)*. 1999; 38(2) 124-132.
[40] Skaggs DL, Warden WH, Mow VC. Radial tie fibers influence the tensile properties of the bovine medial meniscus. *J Orthop Res*. 1994; 12(2): 176-185.
[41] Stärke C, Kopf S, Lippisch R, Lohmann CH, Becker R. Tensile forces on repaired medial meniscal root tears. *Arthroscopy*. 2013; 29(2): 205-212.
[42] Steineman BD. *Meniscal root tears and repairs* [dissertation]. Chapter 4: Loosening of transtibial pull-out meniscal root repairs due to simulated rehabilitation is unrecoverable: a biomechanical study. Fort Collins: Colorado State University. 2018.
[43] Steineman BD. *Meniscal root tears and repairs* [dissertation]. Chapter 5: Nonanatomic placement of posteromedial meniscal root repairs: a finite element study. Fort Collins: Colorado State University. 2018.
[44] Tissakht M, Ahmed AM. Tensile stress-strain characteristics of the human meniscal material. *J Biomech*. 1995; 28(4): 411-422.
[45] Whipple R, Wirth CR, Mow VC. Mechanical properties of the meniscus. *ASME Advances in Bioengineering*. 1984; 32-33.
[46] Wismans J, Veldpaus F, Janssen J. Huson A, Struben P. A three-dimensional mathematical model of the knee joint. *J Biomech*. 1980; 13(8): 677-685.

CHAPTER 7:

CONCLUSIONS AND FUTURE WORK

In summary, the work presented in the preceding chapters focused on current issues facing meniscal root tears and repairs to improve basic scientific knowledge and clinical practice. Scanning electron microscopy was used to first demonstrate that a significant portion of the anterior cruciate ligament overlapped with the anterolateral meniscal insertion in the coronal and sagittal planes. The morphology of this intricate relationship elucidated the risk of disrupting the meniscal insertion during reconstruction surgeries of the anterior cruciate ligament and needs to be considered. Although this relationship indicates a risk for disruption of meniscal insertions, further studies need to investigate what amount of disruption is acceptable for a clinically successful anterior cruciate ligament reconstruction.

This intricate relationship and the demonstrated potential for clinical disruption of anterior meniscal insertions lead to *in vivo* assessment of joint tissues following untreated anterior root tears. Anterior meniscal root tears that were left untreated in rabbits demonstrated significant degeneration occurring within joint tissue. Although these specific measures of degeneration are still unknown at longer timepoints, this work complements previous studies to conclude that both anterior and posterior root tears are harmful to tissue integrity. Additionally, this work sets the foundation for assessing different repair techniques with future *in vivo* studies.

With knowledge that both anterior and posterior meniscal root tears are detrimental to knee health, the focus of work transitioned to better understanding the current challenges of meniscal root repairs in general to improve their effectiveness. The specific challenges addressed in this work included repair loosening and suture placement. Displacement of meniscal root repairs due

to cyclic loading was shown to not completely recover with rest. Additionally, repair displacement gradually increased with continued cyclic loading instead of reaching an equilibrium. Thus, repairs are susceptible to loosening as early as during rehabilitation, and loosening may continue to increase with continued loading of repairs. Since this experiment only assessed one suture technique, future work should evaluate different techniques to determine if loosening is prevalent for all types of sutures and suture techniques.

The finite element knee models developed as part of this dissertation were used to assess changes in knee mechanics with repair misplacement and changes when unrecoverable loosening is incorporated. Placement of repairs was important for the restoration of cartilage and meniscus mechanics. Repairs misplaced further anterior with respect to anatomic were best at restoring mechanics; however, anterior repairs come with the cost of increasing repair tension and thus increasing risk for suture cut-out or repair failures. When the unrecoverable loosening was incorporated into the finite element models, placement was less impactful than loosening on knee mechanics. Loosened repairs demonstrated significant increases in extrusion and decreases in load transmission through the meniscus no matter if the repairs were placed anatomically or not.

The results of the finite element work provide information to further expand the clinical impact on meniscal root repairs. The biggest concern going forward is repair loosening as it leads to insufficient meniscal function. The repair loosening incorporated into the finite element models did not account for any repair healing; therefore, the progress and quality of healing should be assessed with meniscal root repairs. Progress of healing needs to be evaluated around the typical period of rehabilitation to determine how susceptible these repairs are to the unrecoverable loosening demonstrated. Additionally, a biomechanical analysis of *in vivo* healing would be beneficial to determine if healing prevents or hinders unrecoverable loosening of meniscal root

repairs from occurring. Although loosening appears to be the more urgent concern, placement also needs to be considered when improving meniscal root repairs. The results of the finite element study suggest that anterior repairs are best at restoring knee mechanics with a resultant increase in repair tension; therefore, a retrospective analysis of repair misplaced anteriorly would be valuable to see if patients were more at risk for repair failure or if they had repairs that more successfully promoted healing or reduced extrusion.

APPENDIX A:

CHANGES TO MECHANICS WITH NONANATOMIC PLACEMENT OF MENISCAL ROOT REPAIRS

From the finite element knee models in Chapter 5, the change of outcome variables for all meniscal root repairs are listed for each flexion angle and compressive load evaluated. Results are presented as the mean and standard deviation, and **bold print** represents an outcome that is statistically different from zero using a Benjamini-Hochberg correction with a false discovery rate of 0.05 and number of tests assessed as 25. The 25 tests for each correction relate to the anatomic and the 24 nonanatomic repairs locations evaluated at different loading conditions. A = Anterior; AL = anterolateral; AM = anteromedial; L = lateral; M = medial; P = posterior; PL = posterolateral; PM = posteromedial.

Appendix A.1 – Percent change to the mean hoop stress of the medial meniscus midbody with respect to intact for anatomic and nonanatomic repairs and a 1,000 N compressive load.

0° Flexion		
Anatomic	**-28% ± 6%**	***p* = 0.013**
1 mm A	**-28% ± 7%**	***p* = 0.018**
1 mm AL	**-27% ± 6%**	***p* = 0.016**
1 mm AM	**-29% ± 6%**	***p* = 0.016**
1 mm L	**-27% ± 5%**	***p* = 0.013**
1 mm M	**-29% ± 6%**	***p* = 0.013**
1 mm P	**-28% ± 4%**	***p* = 0.008**
1 mm PL	**-27% ± 5%**	***p* = 0.01**
1 mm PM	**-29% ± 5%**	***p* = 0.009**
3 mm A	**-29% ± 9%**	***p* = 0.027**
3 mm AL	**-27% ± 7%**	***p* = 0.022**
3 mm AM	**-32% ± 8%**	***p* = 0.022**
3 mm L	**-26% ± 5%**	***p* = 0.012**
3 mm M	**-32% ± 6%**	***p* = 0.011**
3 mm P	**-29% ± 3%**	***p* = 0.003**
3 mm PL	**-27% ± 3%**	***p* = 0.005**
3 mm PM	**-31% ± 3%**	***p* = 0.004**
5 mm A	**-31% ± 10%**	***p* = 0.032**
5 mm AL	**-27% ± 8%**	***p* = 0.025**
5 mm AM	**-36% ± 10%**	***p* = 0.024**
5 mm L	**-25% ± 4%**	***p* = 0.01**
5 mm M	**-37% ± 6%**	***p* = 0.009**
5 mm P	**-30% ± 3%**	***p* = 0.003**
5 mm PL	**-26% ± 3%**	***p* = 0.004**
5 mm PM	**-35% ± 2%**	***p* = 0.001**

30° Flexion		
Anatomic	**-16% ± 4%**	***p* = 0.017**
1 mm A	**-15% ± 4%**	***p* = 0.027**
1 mm AL	**-15% ± 4%**	***p* = 0.02**
1 mm AM	**-15% ± 4%**	***p* = 0.028**
1 mm L	**-16% ± 3%**	***p* = 0.013**
1 mm M	**-17% ± 4%**	***p* = 0.022**
1 mm P	**-18% ± 3%**	***p* = 0.011**
1 mm PL	**-17% ± 3%**	***p* = 0.01**
1 mm PM	**-18% ± 4%**	***p* = 0.015**
3 mm A	-12% ± 5%	*p* = 0.057
3 mm AL	**-13% ± 4%**	***p* = 0.028**
3 mm AM	-14% ± 6%	*p* = 0.058
3 mm L	**-16% ± 2%**	***p* = 0.008**
3 mm M	**-18% ± 6%**	***p* = 0.032**
3 mm P	**-23% ± 3%**	***p* = 0.005**
3 mm PL	**-20% ± 2%**	***p* = 0.004**
3 mm PM	**-23% ± 4%**	***p* = 0.011**
5 mm A	-11% ± 7%	*p* = 0.101
5 mm AL	**-12% ± 4%**	***p* = 0.04**
5 mm AM	-15% ± 8%	*p* = 0.094
5 mm L	**-16% ± 2%**	***p* = 0.005**
5 mm M	**-22% ± 8%**	***p* = 0.037**
5 mm P	**-29% ± 3%**	***p* = 0.003**
5 mm PL	**-23% ± 2%**	***p* = 0.002**
5 mm PM	**-29% ± 4%**	***p* = 0.008**

60° Flexion		
Anatomic	-13% ± 5%	*p* = 0.053
1 mm A	-11% ± 6%	*p* = 0.086
1 mm AL	-11% ± 5%	*p* = 0.07
1 mm AM	-12% ± 6%	*p* = 0.08
1 mm L	-12% ± 5%	*p* = 0.048
1 mm M	-13% ± 6%	*p* = 0.058
1 mm P	-14% ± 4%	*p* = 0.029
1 mm PL	-14% ± 4%	*p* = 0.033
1 mm PM	-14% ± 5%	*p* = 0.037
3 mm A	-9% ± 7%	*p* = 0.174
3 mm AL	-10% ± 6%	*p* = 0.108
3 mm AM	-11% ± 8%	*p* = 0.143
3 mm L	-12% ± 4%	*p* = 0.037
3 mm M	-14% ± 7%	*p* = 0.063
3 mm P	**-19% ± 3%**	***p* = 0.007**
3 mm PL	-16% ± 3%	*p* = 0.011
3 mm PM	-18% ± 4%	*p* = 0.017
5 mm A	-8% ± 9%	*p* = 0.252
5 mm AL	-9% ± 6%	*p* = 0.139
5 mm AM	-11% ± 9%	*p* = 0.179
5 mm L	-13% ± 4%	*p* = 0.029
5 mm M	-17% ± 8%	*p* = 0.062
5 mm P	**-25% ± 2%**	***p* = 0.002**
5 mm PL	**-19% ± 2%**	***p* = 0.004**
5 mm PM	**-24% ± 4%**	***p* = 0.007**

Appendix A.2 – Percent change to the mean hoop stress of the medial meniscus midbody with respect to intact for anatomic and nonanatomic repairs and a 500 N compressive load.

0° Flexion		
Anatomic	**-29% ± 8%**	***p* = 0.024**
1 mm A	**-29% ± 9%**	***p* = 0.033**
1 mm AL	**-28% ± 9%**	***p* = 0.03**
1 mm AM	**-30% ± 9%**	***p* = 0.03**
1 mm L	**-28% ± 8%**	***p* = 0.024**
1 mm M	**-30% ± 8%**	***p* = 0.024**
1 mm P	**-28% ± 6%**	***p* = 0.016**
1 mm PL	**-28% ± 7%**	***p* = 0.019**
1 mm PM	**-29% ± 7%**	***p* = 0.018**
3 mm A	**-30% ± 12%**	***p* = 0.047**
3 mm AL	**-28% ± 10%**	***p* = 0.04**
3 mm AM	**-33% ± 12%**	***p* = 0.04**
3 mm L	**-26% ± 7%**	***p* = 0.023**
3 mm M	**-33% ± 9%**	***p* = 0.022**
3 mm P	**-29% ± 4%**	***p* = 0.005**
3 mm PL	**-27% ± 5%**	***p* = 0.01**
3 mm PM	**-31% ± 5%**	***p* = 0.008**
5 mm A	-33% ± 14%	*p* = 0.054
5 mm AL	**-28% ± 11%**	***p* = 0.045**
5 mm AM	**-37% ± 14%**	***p* = 0.042**
5 mm L	**-25% ± 6%**	***p* = 0.02**
5 mm M	**-38% ± 9%**	***p* = 0.018**
5 mm P	**-30% ± 3%**	***p* = 0.003**
5 mm PL	**-26% ± 3%**	***p* = 0.005**
5 mm PM	**-35% ± 3%**	***p* = 0.003**

30° Flexion		
Anatomic	-11% ± 6%	*p* = 0.086
1 mm A	-9% ± 6%	*p* = 0.123
1 mm AL	-10% ± 6%	*p* = 0.106
1 mm AM	-10% ± 7%	*p* = 0.116
1 mm L	-11% ± 6%	*p* = 0.08
1 mm M	-12% ± 7%	*p* = 0.093
1 mm P	-13% ± 6%	*p* = 0.06
1 mm PL	-12% ± 6%	*p* = 0.063
1 mm PM	-13% ± 6%	*p* = 0.07
3 mm A	-7% ± 7%	*p* = 0.222
3 mm AL	-8% ± 6%	*p* = 0.153
3 mm AM	-9% ± %	*p* = 0.184
3 mm L	-11% ± 5%	*p* = 0.066
3 mm M	-13% ± 8%	*p* = 0.1
3 mm P	-18% ± 5%	*p* = 0.029
3 mm PL	-15% ± 5%	*p* = 0.033
3 mm PM	-17% ± 7%	*p* = 0.045
5 mm A	-6% ± 8%	*p* = 0.329
5 mm AL	-7% ± 6%	*p* = 0.205
5 mm AM	-9% ± 10%	*p* = 0.231
5 mm L	-11% ± 5%	*p* = 0.056
5 mm M	-17% ± 9%	*p* = 0.091
5 mm P	-24% ± 5%	*p* = 0.016
5 mm PL	-18% ± 5%	*p* = 0.021
5 mm PM	-24% ± 7%	*p* = 0.027

60° Flexion		
Anatomic	-9% ± 8%	*p* = 0.186
1 mm A	-7% ± 8%	*p* = 0.287
1 mm AL	-7% ± 8%	*p* = 0.246
1 mm AM	-8% ± 9%	*p* = 0.261
1 mm L	-9% ± 7%	*p* = 0.176
1 mm M	-9% ± 8%	*p* = 0.192
1 mm P	-11% ± 7%	*p* = 0.108
1 mm PL	-10% ± 7%	*p* = 0.124
1 mm PM	-10% ± 7%	*p* = 0.132
3 mm A	-5% ± 10%	*p* = 0.5
3 mm AL	-6% ± 8%	*p* = 0.362
3 mm AM	-6% ± 10%	*p* = 0.401
3 mm L	-9% ± 7%	*p* = 0.145
3 mm M	-10% ± 9%	*p* = 0.187
3 mm P	-16% ± 5%	*p* = 0.028
3 mm PL	-13% ± 5%	*p* = 0.048
3 mm PM	-15% ± 6%	*p* = 0.056
5 mm A	-4% ± 11%	*p* = 0.622
5 mm AL	-5% ± 9%	*p* = 0.443
5 mm AM	-7% ± 12%	*p* = 0.434
5 mm L	-9% ± 6%	*p* = 0.114
5 mm M	-13% ± 10%	*p* = 0.154
5 mm P	-22% ± 3%	*p* = 0.006
5 mm PL	-16% ± 4%	*p* = 0.019
5 mm PM	-21% ± 5%	*p* = 0.022

Appendix A.3 – Percent change to the mean hoop stress of the anteromedial meniscal insertion with respect to intact for anatomic and nonanatomic repairs and a 1,000 N compressive load.

0° Flexion		
Anatomic	**-31% ± 7%**	***p* = 0.018**
1 mm A	**-31% ± 9%**	***p* = 0.025**
1 mm AL	**-30% ± 8%**	***p* = 0.022**
1 mm AM	**-32% ± 8%**	***p* = 0.023**
1 mm L	**-30% ± 7%**	***p* = 0.018**
1 mm M	**-32% ± 8%**	***p* = 0.018**
1 mm P	**-31% ± 6%**	***p* = 0.012**
1 mm PL	**-30% ± 6%**	***p* = 0.014**
1 mm PM	**-32% ± 6%**	***p* = 0.014**
3 mm A	**-32% ± 11%**	***p* = 0.036**
3 mm AL	**-30% ± 9%**	***p* = 0.029**
3 mm AM	**-35% ± 11%**	***p* = 0.031**
3 mm L	**-28% ± 6%**	***p* = 0.016**
3 mm M	**-36% ± 8%**	***p* = 0.017**
3 mm P	**-32% ± 4%**	***p* = 0.004**
3 mm PL	**-29% ± 4%**	***p* = 0.007**
3 mm PM	**-34% ± 5%**	***p* = 0.007**
5 mm A	**-35% ± 13%**	***p* = 0.042**
5 mm AL	**-30% ± 10%**	***p* = 0.033**
5 mm AM	**-40% ± 13%**	***p* = 0.034**
5 mm L	**-27% ± 6%**	***p* = 0.014**
5 mm M	**-41% ± 9%**	***p* = 0.015**
5 mm P	**-33% ± 3%**	***p* = 0.002**
5 mm PL	**-29% ± 3%**	***p* = 0.004**
5 mm PM	**-38% ± 3%**	***p* = 0.002**

30° Flexion		
Anatomic	**-18% ± 5%**	***p* = 0.022**
1 mm A	**-16% ± 5%**	***p* = 0.033**
1 mm AL	**-16% ± 5%**	***p* = 0.026**
1 mm AM	**-17% ± 5%**	***p* = 0.034**
1 mm L	**-17% ± 4%**	***p* = 0.018**
1 mm M	**-18% ± 5%**	***p* = 0.027**
1 mm P	**-20% ± 4%**	***p* = 0.015**
1 mm PL	**-19% ± 4%**	***p* = 0.014**
1 mm PM	**-19% ± 5%**	***p* = 0.019**
3 mm A	-13% ± 6%	*p* = 0.066
3 mm AL	**-14% ± 5%**	***p* = 0.035**
3 mm AM	-15% ± 7%	*p* = 0.067
3 mm L	**-17% ± 3%**	***p* = 0.011**
3 mm M	-20% ± 7%	*p* = 0.038
3 mm P	**-25% ± 4%**	***p* = 0.007**
3 mm PL	**-21% ± 3%**	***p* = 0.005**
3 mm PM	**-24% ± 5%**	***p* = 0.015**
5 mm A	-12% ± 8%	*p* = 0.111
5 mm AL	-13% ± 5%	*p* = 0.048
5 mm AM	-16% ± 10%	*p* = 0.104
5 mm L	**-17% ± 3%**	***p* = 0.007**
5 mm M	-24% ± 9%	*p* = 0.044
5 mm P	**-31% ± 3%**	***p* = 0.003**
5 mm PL	**-24% ± 2%**	***p* = 0.003**
5 mm PM	-31% ± 5%	*p* = 0.01

60° Flexion		
Anatomic	-14% ± 5%	*p* = 0.049
1 mm A	-12% ± 6%	*p* = 0.079
1 mm AL	-12% ± 6%	*p* = 0.063
1 mm AM	-13% ± 6%	*p* = 0.075
1 mm L	-13% ± 5%	*p* = 0.042
1 mm M	-14% ± 6%	*p* = 0.055
1 mm P	-16% ± 5%	*p* = 0.027
1 mm PL	-15% ± 4%	*p* = 0.03
1 mm PM	-15% ± 5%	*p* = 0.035
3 mm A	-10% ± 8%	*p* = 0.16
3 mm AL	-10% ± 6%	*p* = 0.095
3 mm AM	-11% ± 8%	*p* = 0.137
3 mm L	-13% ± 4%	*p* = 0.032
3 mm M	-15% ± 7%	*p* = 0.063
3 mm P	**-20% ± 3%**	***p* = 0.007**
3 mm PL	**-17% ± 3%**	***p* = 0.01**
3 mm PM	-20% ± 5%	*p* = 0.018
5 mm A	-9% ± 9%	*p* = 0.236
5 mm AL	-10% ± 6%	*p* = 0.122
5 mm AM	-12% ± 10%	*p* = 0.175
5 mm L	-14% ± 4%	*p* = 0.023
5 mm M	-19% ± 8%	*p* = 0.064
5 mm P	**-26% ± 2%**	***p* = 0.002**
5 mm PL	**-20% ± 2%**	***p* = 0.004**
5 mm PM	**-26% ± 4%**	***p* = 0.008**

Appendix A.4 – Percent change to the mean hoop stress of the anteromedial meniscal insertion with respect to intact for anatomic and nonanatomic repairs and a 500 N compressive load.

0° Flexion		
Anatomic	-31% ± 11%	$p = 0.038$
1 mm A	-32% ± 13%	$p = 0.049$
1 mm AL	-31% ± 12%	$p = 0.045$
1 mm AM	-33% ± 13%	$p = 0.046$
1 mm L	-30% ± 10%	$p = 0.038$
1 mm M	-33% ± 11%	$p = 0.038$
1 mm P	-31% ± 9%	$p = 0.027$
1 mm PL	-30% ± 9%	$p = 0.03$
1 mm PM	-32% ± 10%	$p = 0.03$
3 mm A	-34% ± 16%	$p = 0.067$
3 mm AL	-31% ± 13%	$p = 0.057$
3 mm AM	-36% ± 16%	$p = 0.058$
3 mm L	-29% ± 10%	$p = 0.035$
3 mm M	-36% ± 12%	$p = 0.036$
3 mm P	-32% ± 6%	$p = 0.01$
3 mm PL	-29% ± 7%	$p = 0.016$
3 mm PM	-34% ± 8%	$p = 0.016$
5 mm A	-36% ± 18%	$p = 0.075$
5 mm AL	-31% ± 14%	$p = 0.064$
5 mm AM	-41% ± 19%	$p = 0.062$
5 mm L	-28% ± 9%	$p = 0.032$
5 mm M	-42% ± 13%	$p = 0.031$
5 mm P	-33% ± 3%	$p = 0.002$
5 mm PL	-29% ± 4%	$p = 0.007$
5 mm PM	-38% ± 5%	$p = 0.007$

30° Flexion		
Anatomic	-12% ± 7%	$p = 0.088$
1 mm A	-10% ± 7%	$p = 0.125$
1 mm AL	-10% ± 6%	$p = 0.107$
1 mm AM	-11% ± 7%	$p = 0.119$
1 mm L	-12% ± 6%	$p = 0.08$
1 mm M	-12% ± 7%	$p = 0.095$
1 mm P	-14% ± 6%	$p = 0.06$
1 mm PL	-13% ± 6%	$p = 0.063$
1 mm PM	-14% ± 7%	$p = 0.072$
3 mm A	-8% ± 8%	$p = 0.226$
3 mm AL	-8% ± 6%	$p = 0.154$
3 mm AM	-10% ± 9%	$p = 0.189$
3 mm L	-12% ± 5%	$p = 0.065$
3 mm M	-14% ± 9%	$p = 0.103$
3 mm P	-19% ± 6%	$p = 0.028$
3 mm PL	-16% ± 5%	$p = 0.032$
3 mm PM	-19% ± 7%	$p = 0.046$
5 mm A	-6% ± 9%	$p = 0.333$
5 mm AL	-7% ± 7%	$p = 0.205$
5 mm AM	-10% ± 10%	$p = 0.237$
5 mm L	-12% ± 5%	$p = 0.054$
5 mm M	-18% ± 10%	$p = 0.095$
5 mm P	-26% ± 6%	$p = 0.015$
5 mm PL	-19% ± 5%	$p = 0.019$
5 mm PM	-26% ± 8%	$p = 0.027$

60° Flexion		
Anatomic	-9% ± 8%	$p = 0.173$
1 mm A	-8% ± 9%	$p = 0.269$
1 mm AL	-8% ± 8%	$p = 0.228$
1 mm AM	-8% ± 9%	$p = 0.247$
1 mm L	-9% ± 7%	$p = 0.16$
1 mm M	-10% ± 8%	$p = 0.182$
1 mm P	-12% ± 7%	$p = 0.1$
1 mm PL	-11% ± 7%	$p = 0.113$
1 mm PM	-11% ± 7%	$p = 0.124$
3 mm A	-5% ± 10%	$p = 0.478$
3 mm AL	-6% ± 9%	$p = 0.333$
3 mm AM	-7% ± 11%	$p = 0.388$
3 mm L	-10% ± 7%	$p = 0.127$
3 mm M	-11% ± 9%	$p = 0.182$
3 mm P	-17% ± 5%	$p = 0.026$
3 mm PL	-14% ± 5%	$p = 0.042$
3 mm PM	-16% ± 7%	$p = 0.054$
5 mm A	-4% ± 12%	$p = 0.602$
5 mm AL	-5% ± 9%	$p = 0.408$
5 mm AM	-7% ± 12%	$p = 0.428$
5 mm L	-10% ± 6%	$p = 0.096$
5 mm M	-14% ± 11%	$p = 0.153$
5 mm P	-23% ± 3%	$p = 0.006$
5 mm PL	-17% ± 4%	$p = 0.016$
5 mm PM	-22% ± 6%	$p = 0.023$

Appendix A.5 – Percent change to the mean contact pressure with respect to intact on medial surface of tibial articular cartilage for anatomic and nonanatomic repairs and a 1,000 N compressive load.

0° Flexion		
Anatomic	0% ± 12%	$p = 0.96$
1 mm A	0% ± 12%	$p = 0.969$
1 mm AL	0% ± 12%	$p = 0.975$
1 mm AM	0% ± 13%	$p = 0.957$
1 mm L	0% ± 13%	$p = 0.996$
1 mm M	0% ± 13%	$p = 0.997$
1 mm P	-1% ± 13%	$p = 0.913$
1 mm PL	-1% ± 13%	$p = 0.918$
1 mm PM	0% ± 13%	$p = 0.975$
3 mm A	1% ± 13%	$p = 0.897$
3 mm AL	1% ± 12%	$p = 0.946$
3 mm AM	1% ± 14%	$p = 0.895$
3 mm L	-1% ± 12%	$p = 0.919$
3 mm M	0% ± 14%	$p = 0.975$
3 mm P	-4% ± 11%	$p = 0.624$
3 mm PL	-3% ± 10%	$p = 0.687$
3 mm PM	-2% ± 12%	$p = 0.825$
5 mm A	2% ± 14%	$p = 0.852$
5 mm AL	1% ± 13%	$p = 0.924$
5 mm AM	2% ± 15%	$p = 0.855$
5 mm L	-2% ± 11%	$p = 0.835$
5 mm M	0% ± 15%	$p = 0.988$
5 mm P	-6% ± 9%	$p = 0.336$
5 mm PL	-4% ± 10%	$p = 0.53$
5 mm PM	-5% ± 11%	$p = 0.538$

30° Flexion		
Anatomic	**-11% ± 1%**	$\mathbf{p = 0.002}$
1 mm A	**-9% ± 1%**	$\mathbf{p = 0.007}$
1 mm AL	**-10% ± 2%**	$\mathbf{p = 0.01}$
1 mm AM	**-9% ± 1%**	$\mathbf{p = 0.008}$
1 mm L	**-10% ± 2%**	$\mathbf{p = 0.007}$
1 mm M	**-10% ± 1%**	$\mathbf{p = 0.003}$
1 mm P	**-12% ± 1%**	$\mathbf{p = 0.004}$
1 mm PL	**-12% ± 1%**	$\mathbf{p = 0.004}$
1 mm PM	**-11% ± 1%**	$\mathbf{p = 0.003}$
3 mm A	**-8% ± 1%**	$\mathbf{p = 0.011}$
3 mm AL	**-8% ± 2%**	$\mathbf{p = 0.026}$
3 mm AM	**-8% ± 2%**	$\mathbf{p = 0.019}$
3 mm L	**-10% ± 1%**	$\mathbf{p = 0.002}$
3 mm M	**-11% ± 1%**	$\mathbf{p = 0.005}$
3 mm P	**-15% ± 1%**	$\mathbf{p = 0.003}$
3 mm PL	**-13% ± 1%**	$\mathbf{p < 0.001}$
3 mm PM	**-13% ± 2%**	$\mathbf{p = 0.008}$
5 mm A	**-6% ± 1%**	$\mathbf{p = 0.017}$
5 mm AL	**-7% ± 2%**	$\mathbf{p = 0.033}$
5 mm AM	**-6% ± 2%**	$\mathbf{p = 0.024}$
5 mm L	**-11% ± 1%**	$\mathbf{p = 0.002}$
5 mm M	**-10% ± 4%**	$\mathbf{p = 0.042}$
5 mm P	**-18% ± 1%**	$\mathbf{p < 0.001}$
5 mm PL	**-15% ± 1%**	$\mathbf{p < 0.001}$
5 mm PM	**-17% ± 1%**	$\mathbf{p = 0.001}$

60° Flexion		
Anatomic	-11% ± 4%	$p = 0.043$
1 mm A	-10% ± 4%	$p = 0.035$
1 mm AL	-10% ± 5%	$p = 0.045$
1 mm AM	-10% ± 3%	$p = 0.066$
1 mm L	-11% ± 4%	$p = 0.037$
1 mm M	-10% ± 4%	$p = 0.049$
1 mm P	-11% ± 4%	$p = 0.041$
1 mm PL	-11% ± 5%	$p = 0.048$
1 mm PM	-11% ± 4%	$p = 0.056$
3 mm A	-8% ± 5%	$p = 0.039$
3 mm AL	-9% ± 5%	$p = 0.092$
3 mm AM	-7% ± 4%	$p = 0.084$
3 mm L	-12% ± 5%	$p = 0.075$
3 mm M	-9% ± 4%	$p = 0.052$
3 mm P	-14% ± 5%	$p = 0.046$
3 mm PL	-13% ± 6%	$p = 0.041$
3 mm PM	-13% ± 5%	$p = 0.058$
5 mm A	-6% ± 4%	$p = 0.045$
5 mm AL	-8% ± 6%	$p = 0.129$
5 mm AM	-5% ± 2%	$p = 0.12$
5 mm L	-12% ± 6%	$p = 0.071$
5 mm M	-9% ± 4%	$p = 0.073$
5 mm P	-18% ± 7%	$p = 0.054$
5 mm PL	-15% ± 6%	$p = 0.055$
5 mm PM	-16% ± 6%	$p = 0.055$

Appendix A.6 – Percent change to the mean contact pressure with respect to intact on medial surface of tibial articular cartilage for anatomic and nonanatomic repairs and a 500 N compressive load.

0° Flexion		
Anatomic	2% ± 17%	$p = 0.846$
1 mm A	3% ± 17%	$p = 0.789$
1 mm AL	3% ± 17%	$p = 0.8$
1 mm AM	3% ± 17%	$p = 0.806$
1 mm L	2% ± 16%	$p = 0.834$
1 mm M	2% ± 16%	$p = 0.819$
1 mm P	2% ± 16%	$p = 0.873$
1 mm PL	2% ± 16%	$p = 0.862$
1 mm PM	2% ± 16%	$p = 0.846$
3 mm A	3% ± 17%	$p = 0.755$
3 mm AL	3% ± 16%	$p = 0.796$
3 mm AM	4% ± 16%	$p = 0.744$
3 mm L	1% ± 16%	$p = 0.931$
3 mm M	3% ± 17%	$p = 0.767$
3 mm P	0% ± 14%	$p = 0.97$
3 mm PL	0% ± 16%	$p = 0.985$
3 mm PM	1% ± 16%	$p = 0.903$
5 mm A	5% ± 17%	$p = 0.689$
5 mm AL	3% ± 17%	$p = 0.775$
5 mm AM	6% ± 18%	$p = 0.609$
5 mm L	0% ± 15%	$p = 0.965$
5 mm M	5% ± 17%	$p = 0.675$
5 mm P	-1% ± 13%	$p = 0.869$
5 mm PL	-2% ± 14%	$p = 0.828$
5 mm PM	1% ± 15%	$p = 0.926$

30° Flexion		
Anatomic	**-11% ± 3%**	$\mathbf{p = 0.02}$
1 mm A	**-9% ± 2%**	$\mathbf{p = 0.016}$
1 mm AL	**-10% ± 2%**	$\mathbf{p = 0.012}$
1 mm AM	**-9% ± 2%**	$\mathbf{p = 0.009}$
1 mm L	**-11% ± 2%**	$\mathbf{p = 0.015}$
1 mm M	**-10% ± 2%**	$\mathbf{p = 0.016}$
1 mm P	**-11% ± 2%**	$\mathbf{p = 0.008}$
1 mm PL	**-11% ± 2%**	$\mathbf{p = 0.01}$
1 mm PM	**-11% ± 3%**	$\mathbf{p = 0.019}$
3 mm A	**-7% ± 1%**	$\mathbf{p = 0.009}$
3 mm AL	**-9% ± 2%**	$\mathbf{p = 0.01}$
3 mm AM	**-7% ± 1%**	$\mathbf{p = 0.012}$
3 mm L	**-11% ± 2%**	$\mathbf{p = 0.009}$
3 mm M	**-9% ± 1%**	$\mathbf{p = 0.008}$
3 mm P	**-15% ± 2%**	$\mathbf{p = 0.004}$
3 mm PL	**-13% ± 2%**	$\mathbf{p = 0.009}$
3 mm PM	**-13% ± 2%**	$\mathbf{p = 0.009}$
5 mm A	**-6% ± 0%**	$\mathbf{p < 0.001}$
5 mm AL	**-8% ± 1%**	$\mathbf{p = 0.005}$
5 mm AM	**-5% ± 1%**	$\mathbf{p = 0.012}$
5 mm L	**-12% ± 2%**	$\mathbf{p = 0.011}$
5 mm M	**-9% ± 3%**	$\mathbf{p = 0.032}$
5 mm P	**-18% ± 3%**	$\mathbf{p = 0.009}$
5 mm PL	**-15% ± 3%**	$\mathbf{p = 0.012}$
5 mm PM	**-16% ± 3%**	$\mathbf{p = 0.008}$

60° Flexion		
Anatomic	-10% ± 5%	$p = 0.075$
1 mm A	-8% ± 5%	$p = 0.094$
1 mm AL	-9% ± 5%	$p = 0.079$
1 mm AM	-8% ± 4%	$p = 0.081$
1 mm L	-10% ± 5%	$p = 0.073$
1 mm M	-9% ± 4%	$p = 0.071$
1 mm P	-10% ± 5%	$p = 0.07$
1 mm PL	-11% ± 5%	$p = 0.063$
1 mm PM	-10% ± 4%	$p = 0.065$
3 mm A	-6% ± 6%	$p = 0.195$
3 mm AL	-8% ± 6%	$p = 0.158$
3 mm AM	-6% ± 5%	$p = 0.166$
3 mm L	-11% ± 6%	$p = 0.077$
3 mm M	-7% ± 5%	$p = 0.113$
3 mm P	-15% ± 4%	$p = 0.026$
3 mm PL	-14% ± 6%	$p = 0.056$
3 mm PM	-12% ± 4%	$p = 0.041$
5 mm A	-5% ± 7%	$p = 0.385$
5 mm AL	-7% ± 7%	$p = 0.196$
5 mm AM	-4% ± 4%	$p = 0.213$
5 mm L	-11% ± 7%	$p = 0.108$
5 mm M	-8% ± 4%	$p = 0.07$
5 mm P	-17% ± 5%	$p = 0.028$
5 mm PL	-16% ± 6%	$p = 0.045$
5 mm PM	-16% ± 6%	$p = 0.045$

Appendix A.7 – Percent change to the peak contact pressure with respect to intact on medial surface of tibial articular cartilage for anatomic and nonanatomic repairs and a 1,000 N compressive load.

0° Flexion		
Anatomic	4% ± 2%	$p = 0.064$
1 mm A	4% ± 2%	$p = 0.057$
1 mm AL	4% ± 2%	$p = 0.061$
1 mm AM	4% ± 2%	$p = 0.057$
1 mm L	4% ± 2%	$p = 0.067$
1 mm M	4% ± 2%	$p = 0.062$
1 mm P	5% ± 2%	$p = 0.071$
1 mm PL	4% ± 2%	$p = 0.07$
1 mm PM	4% ± 2%	$p = 0.067$
3 mm A	4% ± 1%	$p = 0.041$
3 mm AL	4% ± 2%	$p = 0.056$
3 mm AM	4% ± 1%	$p = 0.041$
3 mm L	4% ± 2%	$p = 0.072$
3 mm M	5% ± 2%	$p = 0.059$
3 mm P	5% ± 3%	$p = 0.08$
3 mm PL	5% ± 2%	$p = 0.08$
3 mm PM	5% ± 3%	$p = 0.074$
5 mm A	3% ± 1%	$p = 0.027$
5 mm AL	4% ± 1%	$p = 0.052$
5 mm AM	4% ± 1%	$p = 0.027$
5 mm L	4% ± 2%	$p = 0.076$
5 mm M	5% ± 2%	$p = 0.06$
5 mm P	6% ± 3%	$p = 0.085$
5 mm PL	5% ± 3%	$p = 0.086$
5 mm PM	6% ± 3%	$p = 0.078$

30° Flexion		
Anatomic	21% ± 13%	$p = 0.111$
1 mm A	20% ± 13%	$p = 0.116$
1 mm AL	21% ± 13%	$p = 0.118$
1 mm AM	20% ± 13%	$p = 0.11$
1 mm L	21% ± 14%	$p = 0.116$
1 mm M	21% ± 13%	$p = 0.106$
1 mm P	23% ± 14%	$p = 0.107$
1 mm PL	22% ± 14%	$p = 0.112$
1 mm PM	22% ± 13%	$p = 0.105$
3 mm A	18% ± 12%	$p = 0.127$
3 mm AL	19% ± 13%	$p = 0.13$
3 mm AM	18% ± 11%	$p = 0.107$
3 mm L	22% ± 15%	$p = 0.122$
3 mm M	21% ± 12%	$p = 0.091$
3 mm P	26% ± 15%	$p = 0.101$
3 mm PL	24% ± 15%	$p = 0.111$
3 mm PM	24% ± 14%	$p = 0.093$
5 mm A	16% ± 11%	$p = 0.139$
5 mm AL	19% ± 13%	$p = 0.139$
5 mm AM	16% ± 9%	$p = 0.1$
5 mm L	23% ± 15%	$p = 0.125$
5 mm M	21% ± 10%	$p = 0.072$
5 mm P	29% ± 17%	$p = 0.097$
5 mm PL	26% ± 16%	$p = 0.11$
5 mm PM	27% ± 15%	$p = 0.084$

60° Flexion		
Anatomic	6% ± 6%	$p = 0.21$
1 mm A	6% ± 6%	$p = 0.225$
1 mm AL	6% ± 6%	$p = 0.221$
1 mm AM	6% ± 6%	$p = 0.219$
1 mm L	7% ± 6%	$p = 0.211$
1 mm M	6% ± 6%	$p = 0.208$
1 mm P	7% ± 6%	$p = 0.195$
1 mm PL	7% ± 6%	$p = 0.201$
1 mm PM	7% ± 6%	$p = 0.198$
3 mm A	5% ± 6%	$p = 0.253$
3 mm AL	6% ± 6%	$p = 0.239$
3 mm AM	5% ± 6%	$p = 0.236$
3 mm L	7% ± 6%	$p = 0.211$
3 mm M	6% ± 6%	$p = 0.197$
3 mm P	8% ± 6%	$p = 0.169$
3 mm PL	7% ± 6%	$p = 0.185$
3 mm PM	7% ± 6%	$p = 0.171$
5 mm A	5% ± 6%	$p = 0.282$
5 mm AL	6% ± 6%	$p = 0.254$
5 mm AM	5% ± 5%	$p = 0.248$
5 mm L	7% ± 7%	$p = 0.209$
5 mm M	6% ± 5%	$p = 0.179$
5 mm P	9% ± 7%	$p = 0.147$
5 mm PL	8% ± 7%	$p = 0.172$
5 mm PM	8% ± 6%	$p = 0.144$

Appendix A.8 – Percent change to the peak contact pressure with respect to intact on medial surface of tibial articular cartilage for anatomic and nonanatomic repairs and a 500 N compressive load.

0° Flexion		
Anatomic	5% ± 3%	$p = 0.07$
1 mm A	5% ± 2%	$p = 0.06$
1 mm AL	5% ± 2%	$p = 0.065$
1 mm AM	5% ± 2%	$p = 0.061$
1 mm L	5% ± 3%	$p = 0.072$
1 mm M	5% ± 3%	$p = 0.068$
1 mm P	6% ± 3%	$p = 0.078$
1 mm PL	5% ± 3%	$p = 0.077$
1 mm PM	6% ± 3%	$p = 0.075$
3 mm A	5% ± 2%	$p = 0.04$
3 mm AL	5% ± 2%	$p = 0.057$
3 mm AM	5% ± 2%	$p = 0.043$
3 mm L	5% ± 3%	$p = 0.077$
3 mm M	6% ± 3%	$p = 0.065$
3 mm P	6% ± 4%	$p = 0.092$
3 mm PL	6% ± 3%	$p = 0.09$
3 mm PM	6% ± 3%	$p = 0.084$
5 mm A	4% ± 1%	$p = 0.025$
5 mm AL	4% ± 2%	$p = 0.051$
5 mm AM	5% ± 1%	$p = 0.027$
5 mm L	5% ± 3%	$p = 0.082$
5 mm M	6% ± 3%	$p = 0.065$
5 mm P	7% ± 4%	$p = 0.101$
5 mm PL	6% ± 4%	$p = 0.099$
5 mm PM	7% ± 4%	$p = 0.091$

30° Flexion		
Anatomic	44% ± 40%	$p = 0.197$
1 mm A	41% ± 38%	$p = 0.201$
1 mm AL	43% ± 40%	$p = 0.202$
1 mm AM	42% ± 38%	$p = 0.196$
1 mm L	45% ± 41%	$p = 0.201$
1 mm M	44% ± 39%	$p = 0.192$
1 mm P	47% ± 42%	$p = 0.193$
1 mm PL	47% ± 43%	$p = 0.197$
1 mm PM	46% ± 41%	$p = 0.191$
3 mm A	36% ± 35%	$p = 0.211$
3 mm AL	41% ± 39%	$p = 0.213$
3 mm AM	36% ± 33%	$p = 0.194$
3 mm L	46% ± 44%	$p = 0.206$
3 mm M	42% ± 36%	$p = 0.178$
3 mm P	54% ± 47%	$p = 0.188$
3 mm PL	52% ± 47%	$p = 0.197$
3 mm PM	50% ± 43%	$p = 0.18$
5 mm A	32% ± 32%	$p = 0.222$
5 mm AL	39% ± 38%	$p = 0.22$
5 mm AM	31% ± 27%	$p = 0.188$
5 mm L	48% ± 45%	$p = 0.209$
5 mm M	41% ± 33%	$p = 0.158$
5 mm P	61% ± 53%	$p = 0.185$
5 mm PL	56% ± 51%	$p = 0.197$
5 mm PM	56% ± 47%	$p = 0.172$

60° Flexion		
Anatomic	9% ± 8%	$p = 0.212$
1 mm A	8% ± 8%	$p = 0.226$
1 mm AL	8% ± 8%	$p = 0.222$
1 mm AM	8% ± 8%	$p = 0.221$
1 mm L	9% ± 8%	$p = 0.213$
1 mm M	9% ± 8%	$p = 0.21$
1 mm P	9% ± 8%	$p = 0.199$
1 mm PL	9% ± 8%	$p = 0.204$
1 mm PM	9% ± 8%	$p = 0.201$
3 mm A	7% ± 8%	$p = 0.252$
3 mm AL	8% ± 8%	$p = 0.239$
3 mm AM	7% ± 7%	$p = 0.237$
3 mm L	9% ± 9%	$p = 0.213$
3 mm M	8% ± 8%	$p = 0.201$
3 mm P	10% ± 9%	$p = 0.176$
3 mm PL	10% ± 9%	$p = 0.19$
3 mm PM	10% ± 8%	$p = 0.178$
5 mm A	6% ± 8%	$p = 0.276$
5 mm AL	8% ± 8%	$p = 0.249$
5 mm AM	6% ± 7%	$p = 0.248$
5 mm L	9% ± 9%	$p = 0.211$
5 mm M	8% ± 7%	$p = 0.183$
5 mm P	12% ± 9%	$p = 0.153$
5 mm PL	11% ± 9%	$p = 0.178$
5 mm PM	11% ± 8%	$p = 0.15$

Appendix A.9 – Percent change to the total contact area on the medial surface of tibial articular cartilage with respect to intact for anatomic and nonanatomic repairs and a 1,000 N compressive load.

0° Flexion			30° Flexion			60° Flexion		
Anatomic	**-12% ± 3%**	***p* = 0.022**	Anatomic	-4% ± 2%	*p* = 0.085	Anatomic	-3% ± 4%	*p* = 0.407
1 mm A	**-11% ± 3%**	***p* = 0.026**	1 mm A	-4% ± 3%	*p* = 0.118	1 mm A	-2% ± 5%	*p* = 0.453
1 mm AL	**-11% ± 3%**	***p* = 0.025**	1 mm AL	-5% ± 2%	*p* = 0.076	1 mm AL	-3% ± 4%	*p* = 0.381
1 mm AM	**-12% ± 4%**	***p* = 0.031**	1 mm AM	-4% ± 3%	*p* = 0.131	1 mm AM	-2% ± 4%	*p* = 0.443
1 mm L	**-12% ± 3%**	***p* = 0.016**	1 mm L	-5% ± 3%	*p* = 0.068	1 mm L	3% ± 5%	*p* = 0.343
1 mm M	**-12% ± 3%**	***p* = 0.026**	1 mm M	-4% ± 2%	*p* = 0.116	1 mm M	-2% ± 5%	*p* = 0.458
1 mm P	**-12% ± 2%**	***p* = 0.012**	1 mm P	-4% ± 3%	*p* = 0.163	1 mm P	-3% ± 4%	*p* = 0.43
1 mm PL	**-12% ± 2%**	***p* = 0.013**	1 mm PL	-5% ± 3%	*p* = 0.095	1 mm PL	-3% ± 4%	*p* = 0.325
1 mm PM	**-12% ± 3%**	***p* = 0.015**	1 mm PM	-4% ± 3%	*p* = 0.138	1 mm PM	-2% ± 4%	*p* = 0.488
3 mm A	-11% ± 5%	*p* = 0.058	3 mm A	-4% ± 3%	*p* = 0.135	3 mm A	-3% ± 4%	*p* = 0.412
3 mm AL	**-12% ± 4%**	***p* = 0.04**	3 mm AL	-5% ± 3%	*p* = 0.112	3 mm AL	-3% ± 5%	*p* = 0.43
3 mm AM	-12% ± 5%	*p* = 0.048	3 mm AM	-3% ± 2%	*p* = 0.098	3 mm AM	-2% ± 4%	*p* = 0.509
3 mm L	**-12% ± 3%**	***p* = 0.015**	3 mm L	-5% ± 3%	*p* = 0.094	3 mm L	-5% ± 5%	*p* = 0.252
3 mm M	**-12% ± 4%**	***p* = 0.039**	3 mm M	-3% ± 2%	*p* = 0.125	3 mm M	-1% ± 5%	*p* = 0.676
3 mm P	**-13% ± 2%**	***p* = 0.006**	3 mm P	-5% ± 3%	*p* = 0.106	3 mm P	-4% ± 5%	*p* = 0.288
3 mm PL	**-13% ± 1%**	***p* = 0.004**	3 mm PL	-6% ± 3%	*p* = 0.072	3 mm PL	-5% ± 4%	*p* = 0.195
3 mm PM	**-12% ± 3%**	***p* = 0.015**	3 mm PM	-3% ± 3%	*p* = 0.329	3 mm PM	-2% ± 7%	*p* = 0.64
5 mm A	-12% ± 6%	*p* = 0.066	5 mm A	-4% ± 3%	*p* = 0.13	5 mm A	-2% ± 5%	*p* = 0.504
5 mm AL	**-12% ± 4%**	***p* = 0.039**	5 mm AL	-6% ± 3%	*p* = 0.09	5 mm AL	-3% ± 5%	*p* = 0.399
5 mm AM	-12% ± 6%	*p* = 0.082	5 mm AM	-1% ± 3%	*p* = 0.584	5 mm AM	-1% ± 4%	*p* = 0.854
5 mm L	**-12% ± 2%**	***p* = 0.012**	5 mm L	-7% ± 2%	*p* = 0.026	5 mm L	-5% ± 5%	*p* = 0.195
5 mm M	**-13% ± 4%**	***p* = 0.026**	5 mm M	-1% ± 3%	*p* = 0.765	5 mm M	0% ± 5%	*p* = 0.93
5 mm P	**-13% ± 1%**	***p* = 0.002**	5 mm P	-7% ± 2%	*p* = 0.023	5 mm P	-5% ± 6%	*p* = 0.31
5 mm PL	**-13% ± 2%**	***p* = 0.006**	5 mm PL	-7% ± 2%	*p* = 0.025	5 mm PL	-6% ± 5%	*p* = 0.171
5 mm PM	**-14% ± 2%**	***p* = 0.007**	5 mm PM	-4% ± 3%	*p* = 0.184	5 mm PM	-2% ± 7%	*p* = 0.596

Appendix A.10 – Percent change to the total contact area on the medial surface of tibial articular cartilage with respect to intact for anatomic and nonanatomic repairs and a 500 N compressive load.

0° Flexion		
Anatomic	11% ± 4%	$p = 0.048$
1 mm A	12% ± 6%	$p = 0.066$
1 mm AL	12% ± 5%	$p = 0.054$
1 mm AM	12% ± 5%	$p = 0.051$
1 mm L	12% ± 4%	$p = 0.03$
1 mm M	12% ± 5%	$p = 0.049$
1 mm P	12% ± 3%	$p = 0.023$
1 mm PL	12% ± 3%	$p = 0.023$
1 mm PM	12% ± 4%	$p = 0.03$
3 mm A	12% ± 7%	$p = 0.104$
3 mm AL	12% ± 7%	$p = 0.089$
3 mm AM	12% ± 7%	$p = 0.104$
3 mm L	12% ± 4%	$p = 0.029$
3 mm M	12% ± 5%	$p = 0.059$
3 mm P	12% ± 3%	$p = 0.014$
3 mm PL	12% ± 2%	$p = 0.013$
3 mm PM	13% ± 3%	$p = 0.018$
5 mm A	13% ± 8%	$p = 0.112$
5 mm AL	13% ± 7%	$p = 0.084$
5 mm AM	13% ± 9%	$p = 0.112$
5 mm L	13% ± 4%	$p = 0.026$
5 mm M	12% ± 6%	$p = 0.064$
5 mm P	12% ± 2%	$p = 0.011$
5 mm PL	13% ± 2%	$p = 0.006$
5 mm PM	13% ± 2%	$p = 0.009$

30° Flexion		
Anatomic	0% ± 8%	$p = 0.931$
1 mm A	0% ± 7%	$p = 0.915$
1 mm AL	0% ± 8%	$p = 0.995$
1 mm AM	1% ± 8%	$p = 0.866$
1 mm L	0% ± 8%	$p = 0.995$
1 mm M	0% ± 7%	$p = 0.968$
1 mm P	1% ± 8%	$p = 0.926$
1 mm PL	0% ± 8%	$p = 0.974$
1 mm PM	0% ± 8%	$p = 0.997$
3 mm A	1% ± 9%	$p = 0.842$
3 mm AL	-1% ± 8%	$p = 0.832$
3 mm AM	2% ± 9%	$p = 0.7$
3 mm L	-1% ± 8%	$p = 0.853$
3 mm M	2% ± 8%	$p = 0.692$
3 mm P	2% ± 8%	$p = 0.967$
3 mm PL	0% ± 8%	$p = 0.833$
3 mm PM	1% ± 7%	$p = 0.755$
5 mm A	2% ± 8%	$p = 0.753$
5 mm AL	-2% ± 7%	$p = 0.748$
5 mm AM	4% ± 9%	$p = 0.547$
5 mm L	-2% ± 7%	$p = 0.745$
5 mm M	4% ± 8%	$p = 0.482$
5 mm P	-1% ± 8%	$p = 0.868$
5 mm PL	-2% ± 7%	$p = 0.618$
5 mm PM	3% ± 8%	$p = 0.652$

60° Flexion		
Anatomic	-1% ± 5%	$p = 0.752$
1 mm A	-1% ± 6%	$p = 0.852$
1 mm AL	-1% ± 6%	$p = 0.732$
1 mm AM	-1% ± 6%	$p = 0.773$
1 mm L	-2% ± 5%	$p = 0.663$
1 mm M	-1% ± 6%	$p = 0.889$
1 mm P	-1% ± 5%	$p = 0.802$
1 mm PL	-1% ± 5%	$p = 0.706$
1 mm PM	-1% ± 4%	$p = 0.846$
3 mm A	0% ± 7%	$p = 0.927$
3 mm AL	-2% ± 7%	$p = 0.736$
3 mm AM	0% ± 7%	$p = 0.919$
3 mm L	-2% ± 5%	$p = 0.562$
3 mm M	1% ± 6%	$p = 0.746$
3 mm P	-2% ± 5%	$p = 0.566$
3 mm PL	-2% ± 5%	$p = 0.55$
3 mm PM	0% ± 7%	$p = 0.942$
5 mm A	-1% ± 7%	$p = 0.87$
5 mm AL	-2% ± 7%	$p = 0.636$
5 mm AM	2% ± 8%	$p = 0.745$
5 mm L	-3% ± 6%	$p = 0.479$
5 mm M	4% ± 8%	$p = 0.488$
5 mm P	-4% ± 7%	$p = 0.412$
5 mm PL	-4% ± 5%	$p = 0.306$
5 mm PM	-1% ± 9%	$p = 0.845$

Appendix A.11 – Percent change to the cartilage-cartilage contact area on the medial surface of tibial articular cartilage with respect to intact for anatomic and nonanatomic repairs and a 1,000 N compressive load.

0° Flexion		
Anatomic	**15% ± 3%**	***p* = 0.011**
1 mm A	**15% ± 3%**	***p* = 0.014**
1 mm AL	**15% ± 3%**	***p* = 0.013**
1 mm AM	**15% ± 3%**	***p* = 0.017**
1 mm L	**15% ± 2%**	***p* = 0.008**
1 mm M	**15% ± 3%**	***p* = 0.013**
1 mm P	**16% ± 2%**	***p* = 0.005**
1 mm PL	**16% ± 2%**	***p* = 0.006**
1 mm PM	**16% ± 2%**	***p* = 0.007**
3 mm A	**15% ± 5%**	***p* = 0.038**
3 mm AL	**16% ± 4%**	***p* = 0.025**
3 mm AM	**15% ± 5%**	***p* = 0.03**
3 mm L	**16% ± 3%**	***p* = 0.011**
3 mm M	**16% ± 4%**	***p* = 0.02**
3 mm P	**17% ± 1%**	***p* = 0.002**
3 mm PL	**17% ± 2%**	***p* = 0.005**
3 mm PM	**17% ± 1%**	***p* = 0.002**
5 mm A	16% ± 7%	*p* = 0.053
5 mm AL	**16% ± 5%**	***p* = 0.026**
5 mm AM	16% ± 8%	*p* = 0.065
5 mm L	**16% ± 3%**	***p* = 0.009**
5 mm M	**18% ± 3%**	***p* = 0.012**
5 mm P	**19% ± 2%**	***p* = 0.004**
5 mm PL	**18% ± 3%**	***p* = 0.007**
5 mm PM	**19% ± 1%**	***p* < 0.001**

30° Flexion		
Anatomic	**30% ± 9%**	***p* = 0.035**
1 mm A	**27% ± 9%**	***p* = 0.026**
1 mm AL	**29% ± 8%**	***p* = 0.035**
1 mm AM	**27% ± 9%**	***p* = 0.024**
1 mm L	**31% ± 9%**	***p* = 0.029**
1 mm M	**28% ± 8%**	***p* = 0.02**
1 mm P	**33% ± 8%**	***p* = 0.025**
1 mm PL	**33% ± 9%**	***p* = 0.022**
1 mm PM	**31% ± 8%**	***p* = 0.053**
3 mm A	24% ± 10%	*p* = 0.032
3 mm AL	**27% ± 9%**	***p* = 0.049**
3 mm AM	24% ± 9%	*p* = 0.024
3 mm L	**33% ± 9%**	***p* = 0.028**
3 mm M	**27% ± 8%**	***p* = 0.017**
3 mm P	**37% ± 8%**	***p* = 0.016**
3 mm PL	**37% ± 8%**	***p* = 0.013**
3 mm PM	**34% ± 7%**	***p* = 0.084**
5 mm A	21% ± 11%	*p* = 0.042
5 mm AL	27% ± 10%	*p* = 0.095
5 mm AM	19% ± 11%	*p* = 0.027
5 mm L	**36% ± 11%**	***p* = 0.037**
5 mm M	**26% ± 9%**	***p* = 0.016**
5 mm P	**46% ± 10%**	***p* = 0.022**
5 mm PL	**41% ± 11%**	***p* = 0.015**
5 mm PM	**39% ± 8%**	***p* = 0.027**

60° Flexion		
Anatomic	**16% ± 5%**	***p* = 0.03**
1 mm A	**14% ± 4%**	***p* = 0.03**
1 mm AL	**15% ± 5%**	***p* = 0.035**
1 mm AM	**14% ± 4%**	***p* = 0.03**
1 mm L	**16% ± 4%**	***p* = 0.024**
1 mm M	**15% ± 4%**	***p* = 0.025**
1 mm P	**16% ± 5%**	***p* = 0.026**
1 mm PL	**16% ± 5%**	***p* = 0.027**
1 mm PM	**15% ± 5%**	***p* = 0.029**
3 mm A	**14% ± 4%**	***p* = 0.022**
3 mm AL	**15% ± 4%**	***p* = 0.026**
3 mm AM	**12% ± 3%**	***p* = 0.016**
3 mm L	**18% ± 5%**	***p* = 0.021**
3 mm M	**14% ± 3%**	***p* = 0.019**
3 mm P	**19% ± 5%**	***p* = 0.019**
3 mm PL	**20% ± 5%**	***p* = 0.022**
3 mm PM	**17% ± 5%**	***p* = 0.028**
5 mm A	**12% ± 4%**	***p* = 0.03**
5 mm AL	**15% ± 4%**	***p* = 0.02**
5 mm AM	**10% ± 3%**	***p* = 0.036**
5 mm L	**19% ± 5%**	***p* = 0.02**
5 mm M	12% ± 5%	*p* = 0.051
5 mm P	**22% ± 4%**	***p* = 0.014**
5 mm PL	**22% ± 5%**	***p* = 0.015**
5 mm PM	**18% ± 5%**	***p* = 0.027**

Appendix A.12 – Percent change to the cartilage-cartilage contact area on the medial surface of tibial articular cartilage with respect to intact for anatomic and nonanatomic repairs and a 500 N compressive load.

0° Flexion		
Anatomic	**19% ± 2%**	***p* = 0.004**
1 mm A	**20% ± 4%**	***p* = 0.014**
1 mm AL	**19% ± 3%**	***p* = 0.008**
1 mm AM	**20% ± 3%**	***p* = 0.01**
1 mm L	**20% ± 2%**	***p* = 0.004**
1 mm M	**20% ± 2%**	***p* = 0.004**
1 mm P	**20% ± 3%**	***p* = 0.006**
1 mm PL	**20% ± 3%**	***p* = 0.006**
1 mm PM	**21% ± 2%**	***p* = 0.004**
3 mm A	**19% ± 7%**	***p* = 0.043**
3 mm AL	**20% ± 6%**	***p* = 0.031**
3 mm AM	**20% ± 7%**	***p* = 0.035**
3 mm L	**20% ± 1%**	***p* = 0.001**
3 mm M	**21% ± 3%**	***p* = 0.009**
3 mm P	**21% ± 3%**	***p* = 0.008**
3 mm PL	**21% ± 4%**	***p* = 0.01**
3 mm PM	**22% ± 3%**	***p* = 0.007**
5 mm A	20% ± 9%	*p* = 0.06
5 mm AL	**21% ± 7%**	***p* = 0.034**
5 mm AM	21% ± 9%	*p* = 0.055
5 mm L	**21% ± 1%**	***p* = 0.001**
5 mm M	**21% ± 4%**	***p* = 0.014**
5 mm P	**22% ± 7%**	***p* = 0.037**
5 mm PL	**21% ± 5%**	***p* = 0.016**
5 mm PM	**22% ± 5%**	***p* = 0.015**

30° Flexion		
Anatomic	48% ± 23%	*p* = 0.07
1 mm A	46% ± 25%	*p* = 0.084
1 mm AL	47% ± 24%	*p* = 0.077
1 mm AM	46% ± 22%	*p* = 0.069
1 mm L	50% ± 25%	*p* = 0.076
1 mm M	47% ± 24%	*p* = 0.074
1 mm P	51% ± 25%	*p* = 0.071
1 mm PL	52% ± 26%	*p* = 0.074
1 mm PM	50% ± 24%	*p* = 0.068
3 mm A	42% ± 26%	*p* = 0.111
3 mm AL	46% ± 26%	*p* = 0.093
3 mm AM	39% ± 24%	*p* = 0.104
3 mm L	53% ± 26%	*p* = 0.074
3 mm M	44% ± 21%	*p* = 0.069
3 mm P	64% ± 23%	*p* = 0.04
3 mm PL	61% ± 28%	*p* = 0.064
3 mm PM	58% ± 21%	*p* = 0.041
5 mm A	36% ± 23%	*p* = 0.109
5 mm AL	46% ± 28%	*p* = 0.106
5 mm AM	30% ± 16%	*p* = 0.081
5 mm L	57% ± 29%	*p* = 0.077
5 mm M	46% ± 16%	*p* = 0.038
5 mm P	74% ± 27%	*p* = 0.042
5 mm PL	69% ± 28%	*p* = 0.049
5 mm PM	64% ± 19%	*p* = 0.029

60° Flexion		
Anatomic	**18% ± 6%**	***p* = 0.032**
1 mm A	**17% ± 5%**	***p* = 0.03**
1 mm AL	**17% ± 5%**	***p* = 0.029**
1 mm AM	**17% ± 5%**	***p* = 0.026**
1 mm L	**19% ± 6%**	***p* = 0.032**
1 mm M	**17% ± 5%**	***p* = 0.027**
1 mm P	**19% ± 6%**	***p* = 0.035**
1 mm PL	**20% ± 6%**	***p* = 0.031**
1 mm PM	**18% ± 6%**	***p* = 0.034**
3 mm A	**15% ± 2%**	***p* = 0.006**
3 mm AL	**18% ± 4%**	***p* = 0.018**
3 mm AM	**14% ± 3%**	***p* = 0.011**
3 mm L	**20% ± 7%**	***p* = 0.034**
3 mm M	**15% ± 4%**	***p* = 0.019**
3 mm P	**23% ± 6%**	***p* = 0.021**
3 mm PL	**23% ± 7%**	***p* = 0.028**
3 mm PM	**20% ± 5%**	***p* = 0.021**
5 mm A	**13% ± 3%**	***p* = 0.02**
5 mm AL	**18% ± 3%**	***p* = 0.013**
5 mm AM	**10% ± 3%**	***p* = 0.021**
5 mm L	**22% ± 7%**	***p* = 0.03**
5 mm M	**13% ± 6%**	***p* = 0.06**
5 mm P	**27% ± 5%**	***p* = 0.012**
5 mm PL	**26% ± 6%**	***p* = 0.018**
5 mm PM	**23% ± 6%**	***p* = 0.024**

Appendix A.13 – Percent change to the total contact area of the medial meniscus with the femoral and tibial articular cartilage for anatomic and nonanatomic repairs and a 1,000 N compressive load.

0° Flexion		
Anatomic	-20% ± 8%	$p = 0.047$
1 mm A	-20% ± 8%	$p = 0.053$
1 mm AL	-20% ± 8%	$p = 0.054$
1 mm AM	-20% ± 9%	$p = 0.059$
1 mm L	-20% ± 7%	$p = 0.04$
1 mm M	-20% ± 8%	$p = 0.054$
1 mm P	-21% ± 7%	$p = 0.034$
1 mm PL	-20% ± 7%	$p = 0.036$
1 mm PM	-20% ± 7%	$p = 0.038$
3 mm A	-20% ± 7%	$p = 0.09$
3 mm AL	-20% ± 11%	$p = 0.072$
3 mm AM	-20% ± 10%	$p = 0.076$
3 mm L	-20% ± 7%	$p = 0.035$
3 mm M	-21% ± 9%	$p = 0.058$
3 mm P	-23% ± 4%	$p = 0.012$
3 mm PL	-21% ± 4%	$p = 0.013$
3 mm PM	-23% ± 7%	$p = 0.026$
5 mm A	-22% ± 13%	$p = 0.102$
5 mm AL	-21% ± 11%	$p = 0.077$
5 mm AM	-23% ± 14%	$p = 0.107$
5 mm L	-20% ± 6%	$p = 0.028$
5 mm M	-24% ± 9%	$p = 0.046$
5 mm P	-24% ± 4%	$p = 0.007$
5 mm PL	-23% ± 3%	$p = 0.008$
5 mm PM	-26% ± 5%	$p = 0.011$

30° Flexion		
Anatomic	**-20% ± 6%**	**$p = 0.025$**
1 mm A	**-18% ± 5%**	**$p = 0.027$**
1 mm AL	**-19% ± 5%**	**$p = 0.026$**
1 mm AM	**-18% ± 5%**	**$p = 0.022$**
1 mm L	**-21% ± 6%**	**$p = 0.024$**
1 mm M	**-19% ± 5%**	**$p = 0.02$**
1 mm P	**-22% ± 6%**	**$p = 0.022$**
1 mm PL	**-22% ± 6%**	**$p = 0.028$**
1 mm PM	**-21% ± 6%**	**$p = 0.023$**
3 mm A	**-16% ± 4%**	**$p = 0.026$**
3 mm AL	**-18% ± 5%**	**$p = 0.027$**
3 mm AM	**-15% ± 5%**	**$p = 0.03$**
3 mm L	**-22% ± 7%**	**$p = 0.029$**
3 mm M	**-18% ± 4%**	**$p = 0.016$**
3 mm P	**-25% ± 7%**	**$p = 0.025$**
3 mm PL	**-25% ± 7%**	**$p = 0.027$**
3 mm PM	**-22% ± 5%**	**$p = 0.02$**
5 mm A	**-13% ± 5%**	**$p = 0.037$**
5 mm AL	**-17% ± 5%**	**$p = 0.031$**
5 mm AM	**-11% ± 4%**	**$p = 0.039$**
5 mm L	**-24% ± 8%**	**$p = 0.039$**
5 mm M	**-17% ± 2%**	**$p = 0.003$**
5 mm P	**-30% ± 8%**	**$p = 0.025$**
5 mm PL	**-27% ± 8%**	**$p = 0.03$**
5 mm PM	**-26% ± 5%**	**$p = 0.01$**

60° Flexion		
Anatomic	**-21% ± 4%**	**$p = 0.014$**
1 mm A	**-19% ± 4%**	**$p = 0.014$**
1 mm AL	**-20% ± 5%**	**$p = 0.02$**
1 mm AM	**-19% ± 5%**	**$p = 0.018$**
1 mm L	**-22% ± 5%**	**$p = 0.013$**
1 mm M	**-21% ± 4%**	**$p = 0.012$**
1 mm P	**-22% ± 5%**	**$p = 0.016$**
1 mm PL	**-23% ± 5%**	**$p = 0.016$**
1 mm PM	**-21% ± 5%**	**$p = 0.018$**
3 mm A	**-16% ± 3%**	**$p = 0.015$**
3 mm AL	**-18% ± 4%**	**$p = 0.013$**
3 mm AM	**-17% ± 3%**	**$p = 0.009$**
3 mm L	**-23% ± 5%**	**$p = 0.014$**
3 mm M	**-20% ± 3%**	**$p = 0.007$**
3 mm P	**-27% ± 6%**	**$p = 0.016$**
3 mm PL	**-27% ± 7%**	**$p = 0.021$**
3 mm PM	**-28% ± 4%**	**$p = 0.008$**
5 mm A	**-12% ± 3%**	**$p = 0.022$**
5 mm AL	**-17% ± 3%**	**$p = 0.013$**
5 mm AM	**-12% ± 3%**	**$p = 0.025$**
5 mm L	**-25% ± 6%**	**$p = 0.018$**
5 mm M	**-18% ± 3%**	**$p = 0.01$**
5 mm P	**-31% ± 6%**	**$p = 0.011$**
5 mm PL	**-29% ± 7%**	**$p = 0.017$**
5 mm PM	**-28% ± 3%**	**$p = 0.004$**

Appendix A.14 – Percent change to the total contact area of the medial meniscus with the femoral and tibial articular cartilage for anatomic and nonanatomic repairs and a 500 N compressive load.

0° Flexion		
Anatomic	22% ± 9%	$p = 0.056$
1 mm A	23% ± 12%	$p = 0.081$
1 mm AL	22% ± 11%	$p = 0.071$
1 mm AM	23% ± 11%	$p = 0.072$
1 mm L	22% ± 9%	$p = 0.051$
1 mm M	23% ± 10%	$p = 0.057$
1 mm P	23% ± 8%	$p = 0.036$
1 mm PL	23% ± 8%	$p = 0.037$
1 mm PM	23% ± 8%	$p = 0.043$
3 mm A	23% ± 15%	$p = 0.12$
3 mm AL	23% ± 14%	$p = 0.109$
3 mm AM	24% ± 15%	$p = 0.107$
3 mm L	23% ± 9%	$p = 0.052$
3 mm M	24% ± 11%	$p = 0.066$
3 mm P	24% ± 5%	$p = 0.015$
3 mm PL	23% ± 6%	$p = 0.02$
3 mm PM	25% ± 7%	$p = 0.023$
5 mm A	24% ± 17%	$p = 0.129$
5 mm AL	24% ± 15%	$p = 0.114$
5 mm AM	27% ± 17%	$p = 0.117$
5 mm L	23% ± 10%	$p = 0.052$
5 mm M	26% ± 12%	$p = 0.061$
5 mm P	**24% ± 1%**	**$p < 0.001$**
5 mm PL	23% ± 4%	$p = 0.009$
5 mm PM	26% ± 5%	$p = 0.012$

30° Flexion		
Anatomic	**17% ± 4%**	**$p = 0.015$**
1 mm A	**16% ± 3%**	**$p = 0.015$**
1 mm AL	**16% ± 4%**	**$p = 0.016$**
1 mm AM	**16% ± 3%**	**$p = 0.013$**
1 mm L	**17% ± 4%**	**$p = 0.018$**
1 mm M	**17% ± 4%**	**$p = 0.016$**
1 mm P	**19% ± 5%**	**$p = 0.021$**
1 mm PL	**19% ± 5%**	**$p = 0.019$**
1 mm PM	**19% ± 4%**	**$p = 0.016$**
3 mm A	**13% ± 2%**	**$p = 0.007$**
3 mm AL	**16% ± 4%**	**$p = 0.017$**
3 mm AM	**13% ± 0%**	**$p < 0.001$**
3 mm L	**19% ± 6%**	**$p = 0.029$**
3 mm M	**16% ± 3%**	**$p = 0.012$**
3 mm P	**23% ± 8%**	**$p = 0.035$**
3 mm PL	**22% ± 7%**	**$p = 0.0032$**
3 mm PM	**21% ± 6%**	**$p = 0.026$**
5 mm A	**11% ± 1%**	**$p = 0.002$**
5 mm AL	**15% ± 4%**	**$p = 0.019$**
5 mm AM	**9% ± 2%**	**$p = 0.019$**
5 mm L	**21% ± 7%**	**$p = 0.033$**
5 mm M	**15% ± 2%**	**$p = 0.007$**
5 mm P	**28% ± 8%**	**$p = 0.028$**
5 mm PL	**25% ± 9%**	**$p = 0.037$**
5 mm PM	**24% ± 6%**	**$p = 0.02$**

60° Flexion		
Anatomic	**-19% ± 6%**	**$p = 0.026$**
1 mm A	**-18% ± 6%**	**$p = 0.031$**
1 mm AL	**-19% ± 6%**	**$p = 0.027$**
1 mm AM	**-19% ± 6%**	**$p = 0.029$**
1 mm L	**-20% ± 6%**	**$p = 0.025$**
1 mm M	**-19% ± 5%**	**$p = 0.022$**
1 mm P	**-22% ± 7%**	**$p = 0.029$**
1 mm PL	**-22% ± 6%**	**$p = 0.025$**
1 mm PM	**-20% ± 6%**	**$p = 0.027$**
3 mm A	**-15% ± 3%**	**$p = 0.013$**
3 mm AL	**-18% ± 4%**	**$p = 0.017$**
3 mm AM	**-15% ± 2%**	**$p = 0.008$**
3 mm L	**-22% ± 6%**	**$p = 0.026$**
3 mm M	**-18% ± 4%**	**$p = 0.019$**
3 mm P	**-26% ± 7%**	**$p = 0.026$**
3 mm PL	**-25% ± 7%**	**$p = 0.027$**
3 mm PM	**-23% ± 5%**	**$p = 0.018$**
5 mm A	**-12% ± 3%**	**$p = 0.025$**
5 mm AL	**-17% ± 3%**	**$p = 0.012$**
5 mm AM	**-11% ± 2%**	**$p = 0.01$**
5 mm L	**-23% ± 6%**	**$p = 0.024$**
5 mm M	**-15% ± 3%**	**$p = 0.015$**
5 mm P	**-31% ± 6%**	**$p = 0.014$**
5 mm PL	**-28% ± 8%**	**$p = 0.026$**
5 mm PM	**-27% ± 3%**	**$p = 0.005$**

Appendix A.15 – Meniscal extrusion measured at the posterior root of the medial meniscus with respect to intact for anatomic and nonanatomic repairs and a 1,000 N compressive load.

0° Flexion		
Anatomic	0.33 ± 0.10 mm	$p = 0.03$
1 mm A	0.32 ± 0.09 mm	$p = 0.023$
1 mm AL	0.32 ± 0.09 mm	$p = 0.026$
1 mm AM	0.33 ± 0.09 mm	$p = 0.024$
1 mm L	0.32 ± 0.10 mm	$p = 0.031$
1 mm M	0.34 ± 0.10 mm	$p = 0.029$
1 mm P	0.33 ± 0.11 mm	$p = 0.037$
1 mm PL	0.32 ± 0.11 mm	$p = 0.036$
1 mm PM	0.34 ± 0.11 mm	$p = 0.034$
3 mm A	0.32 ± 0.07 mm	$p = 0.015$
3 mm AL	0.30 ± 0.08 mm	$p = 0.02$
3 mm AM	0.35 ± 0.08 mm	$p = 0.016$
3 mm L	0.31 ± 0.10 mm	$p = 0.035$
3 mm M	0.37 ± 0.11 mm	$p = 0.029$
3 mm P	0.36 ± 0.15 mm	$p = 0.052$
3 mm PL	0.33 ± 0.13 mm	$p = 0.048$
3 mm PM	0.38 ± 0.14 mm	$p = 0.045$
5 mm A	0.34 ± 0.05 mm	$p = 0.008$
5 mm AL	0.30 ± 0.07 mm	$p = 0.017$
5 mm AM	0.39 ± 0.08 mm	$p = 0.013$
5 mm L	0.30 ± 0.11 mm	$p = 0.038$
5 mm M	0.43 ± 0.14 mm	$p = 0.032$
5 mm P	0.40 ± 0.18 mm	$p = 0.064$
5 mm PL	0.34 ± 0.15 mm	$p = 0.059$
5 mm PM	0.44 ± 0.18 mm	$p = 0.054$

30° Flexion		
Anatomic	0.58 ± 0.35 mm	$p = 0.134$
1 mm A	0.50 ± 0.36 mm	$p = 0.121$
1 mm AL	0.53 ± 0.35 mm	$p = 0.128$
1 mm AM	0.53 ± 0.36 mm	$p = 0.1$
1 mm L	0.58 ± 0.34 mm	$p = 0.107$
1 mm M	0.58 ± 0.36 mm	$p = 0.079$
1 mm P	0.66 ± 0.34 mm	$p = 0.084$
1 mm PL	0.63 ± 0.34 mm	$p = 0.086$
1 mm PM	0.64 ± 0.35 mm	$p = 0.217$
3 mm A	0.39 ± 0.38 mm	$p = 0.158$
3 mm AL	0.45 ± 0.36 mm	$p = 0.199$
3 mm AM	0.44 ± 0.40 mm	$p = 0.095$
3 mm L	0.59 ± 0.34 mm	$p = 0.114$
3 mm M	0.61 ± 0.39 mm	$p = 0.047$
3 mm P	0.87 ± 0.34 mm	$p = 0.059$
3 mm PL	0.76 ± 0.33 mm	$p = 0.058$
3 mm PM	0.81 ± 0.36 mm	$p = 0.309$
5 mm A	0.32 ± 0.42 mm	$p = 0.19$
5 mm AL	0.41 ± 0.37 mm	$p = 0.279$
5 mm AM	0.40 ± 0.48 mm	$p = 0.09$
5 mm L	0.62 ± 0.34 mm	$p = 0.118$
5 mm M	0.70 ± 0.46 mm	$p = 0.03$
5 mm P	1.12 ± 0.34 mm	$p = 0.046$
5 mm PL	0.89 ± 0.34 mm	$p = 0.037$
5 mm PM	1.06 ± 0.36 mm	$p = 0.103$

60° Flexion		
Anatomic	**0.58 ± 0.15 mm**	$\mathbf{p = 0.022}$
1 mm A	**0.52 ± 0.16 mm**	$\mathbf{p = 0.031}$
1 mm AL	**0.54 ± 0.16 mm**	$\mathbf{p = 0.027}$
1 mm AM	**0.53 ± 0.16 mm**	$\mathbf{p = 0.03}$
1 mm L	**0.59 ± 0.15 mm**	$\mathbf{p = 0.022}$
1 mm M	**0.58 ± 0.16 mm**	$\mathbf{p = 0.023}$
1 mm P	**0.66 ± 0.14 mm**	$\mathbf{p = 0.015}$
1 mm PL	**0.64 ± 0.15 mm**	$\mathbf{p = 0.017}$
1 mm PM	**0.64 ± 0.15 mm**	$\mathbf{p = 0.017}$
3 mm A	0.43 ± 0.19 mm	$p = 0.062$
3 mm AL	0.49 ± 0.17 mm	$p = 0.04$
3 mm AM	0.45 ± 0.21 mm	$p = 0.067$
3 mm L	**0.61 ± 0.17 mm**	$\mathbf{p = 0.023}$
3 mm M	**0.60 ± 0.20 mm**	$\mathbf{p = 0.034}$
3 mm P	**0.86 ± 0.15 mm**	$\mathbf{p = 0.01}$
3 mm PL	**0.76 ± 0.16 mm**	$\mathbf{p = 0.015}$
3 mm PM	**0.80 ± 0.14 mm**	$\mathbf{p = 0.01}$
5 mm A	0.38 ± 0.23 mm	$p = 0.105$
5 mm AL	0.47 ± 0.20 mm	$p = 0.052$
5 mm AM	0.42 ± 0.30 mm	$p = 0.134$
5 mm L	**0.65 ± 0.18 mm**	$\mathbf{p = 0.026}$
5 mm M	0.67 ± 0.27 mm	$p = 0.051$
5 mm P	**1.10 ± 0.19 mm**	$\mathbf{p = 0.009}$
5 mm PL	**0.89 ± 0.20 mm**	$\mathbf{p = 0.016}$
5 mm PM	**1.04 ± 0.13 mm**	$\mathbf{p = 0.005}$

Appendix A.16 – Meniscal extrusion measured at the posterior root of the medial meniscus with respect to intact for anatomic and nonanatomic repairs and a 500 N compressive load.

0° Flexion		
Anatomic	0.25 ± 0.08 mm	$p = 0.032$
1 mm A	0.25 ± 0.07 mm	$p = 0.024$
1 mm AL	0.24 ± 0.07 mm	$p = 0.028$
1 mm AM	0.26 ± 0.07 mm	$p = 0.026$
1 mm L	0.25 ± 0.08 mm	$p = 0.034$
1 mm M	0.26 ± 0.08 mm	$p = 0.031$
1 mm P	0.26 ± 0.09 mm	$p = 0.042$
1 mm PL	0.25 ± 0.09 mm	$p = 0.04$
1 mm PM	0.26 ± 0.09 mm	$p = 0.038$
3 mm A	0.25 ± 0.05 mm	$p = 0.012$
3 mm AL	0.24 ± 0.06 mm	$p = 0.02$
3 mm AM	0.27 ± 0.06 mm	$p = 0.015$
3 mm L	0.24 ± 0.08 mm	$p = 0.037$
3 mm M	0.29 ± 0.09 mm	$p = 0.031$
3 mm P	0.28 ± 0.13 mm	$p = 0.061$
3 mm PL	0.25 ± 0.11 mm	$p = 0.055$
3 mm PM	0.30 ± 0.12 mm	$p = 0.051$
5 mm A	0.26 ± 0.04 mm	$p = 0.006$
5 mm AL	0.23 ± 0.05 mm	$p = 0.016$
5 mm AM	0.31 ± 0.05 mm	$p = 0.01$
5 mm L	0.23 ± 0.08 mm	$p = 0.042$
5 mm M	0.34 ± 0.11 mm	$p = 0.034$
5 mm P	0.31 ± 0.16 mm	$p = 0.077$
5 mm PL	0.26 ± 0.13 mm	$p = 0.068$
5 mm PM	0.34 ± 0.16 mm	$p = 0.065$

30° Flexion		
Anatomic	0.42 ± 0.30 mm	$p = 0.14$
1 mm A	0.35 ± 0.31 mm	$p = 0.192$
1 mm AL	0.37 ± 0.30 mm	$p = 0.169$
1 mm AM	0.37 ± 0.32 mm	$p = 0.181$
1 mm L	0.42 ± 0.30 mm	$p = 0.134$
1 mm M	0.42 ± 0.31 mm	$p = 0.145$
1 mm P	0.50 ± 0.30 mm	$p = 0.101$
1 mm PL	0.47 ± 0.30 mm	$p = 0.109$
1 mm PM	0.48 ± 0.30 mm	$p = 0.113$
3 mm A	0.25 ± 0.33 mm	$p = 0.328$
3 mm AL	0.31 ± 0.31 mm	$p = 0.229$
3 mm AM	0.29 ± 0.35 mm	$p = 0.293$
3 mm L	0.44 ± 0.30 mm	$p = 0.125$
3 mm M	0.44 ± 0.34 mm	$p = 0.155$
3 mm P	0.69 ± 0.29 mm	$p = 0.054$
3 mm PL	0.59 ± 0.29 mm	$p = 0.072$
3 mm PM	0.63 ± 0.31 mm	$p = 0.071$
5 mm A	0.24 ± 0.27 mm	$p = 0.268$
5 mm AL	0.27 ± 0.32 mm	$p = 0.282$
5 mm AM	0.28 ± 0.36 mm	$p = 0.315$
5 mm L	0.46 ± 0.30 mm	$p = 0.116$
5 mm M	0.51 ± 0.40 mm	$p = 0.156$
5 mm P	0.92 ± 0.29 mm	$p = 0.032$
5 mm PL	0.71 ± 0.29 mm	$p = 0.052$
5 mm PM	0.85 ± 0.31 mm	$p = 0.042$

60° Flexion		
Anatomic	**0.43 ± 0.11 mm**	$\mathbf{p = 0.021}$
1 mm A	0.37 ± 0.12 mm	$p = 0.035$
1 mm AL	**0.39 ± 0.11 mm**	$\mathbf{p = 0.027}$
1 mm AM	0.38 ± 0.13 mm	$p = 0.034$
1 mm L	**0.44 ± 0.11 mm**	$\mathbf{p = 0.019}$
1 mm M	**0.43 ± 0.12 mm**	$\mathbf{p = 0.025}$
1 mm P	**0.50 ± 0.10 mm**	$\mathbf{p = 0.013}$
1 mm PL	**0.48 ± 0.10 mm**	$\mathbf{p = 0.014}$
1 mm PM	**0.48 ± 0.11 mm**	$\mathbf{p = 0.016}$
3 mm A	0.28 ± 0.15 mm	$p = 0.086$
3 mm AL	0.35 ± 0.13 mm	$p = 0.043$
3 mm AM	0.30 ± 0.18 mm	$p = 0.098$
3 mm L	**0.46 ± 0.12 mm**	$\mathbf{p = 0.02}$
3 mm M	0.44 ± 0.16 mm	$p = 0.043$
3 mm P	**0.68 ± 0.10 mm**	$\mathbf{p = 0.007}$
3 mm PL	**0.60 ± 0.11 mm**	$\mathbf{p = 0.011}$
3 mm PM	**0.62 ± 0.10 mm**	$\mathbf{p = 0.009}$
5 mm A	0.24 ± 0.19 mm	$p = 0.163$
5 mm AL	0.33 ± 0.15 mm	$p = 0.063$
5 mm AM	0.27 ± 0.25 mm	$p = 0.21$
5 mm L	**0.50 ± 0.13 mm**	$\mathbf{p = 0.023}$
5 mm M	0.49 ± 0.24 mm	$p = 0.068$
5 mm P	**0.90 ± 0.12 mm**	$\mathbf{p = 0.006}$
5 mm PL	**0.72 ± 0.14 mm**	$\mathbf{p = 0.012}$
5 mm PM	**0.83 ± 0.10 mm**	$\mathbf{p = 0.004}$

Appendix A.17 – Percent change in nonanatomic repair tension with respect to anatomic repair and a 1,000 N compressive load.

0° Flexion		
1 mm A	0% ± 2%	$p = 0.799$
1 mm AL	0% ± 1%	$p = 0.74$
1 mm AM	0% ± 2%	$p = 0.842$
1 mm L	0% ± 1%	$p = 0.966$
1 mm M	0% ± 1%	$p = 0.98$
1 mm P	0% ± 2%	$p = 0.831$
1 mm PL	0% ± 2%	$p = 0.859$
1 mm PM	0% ± 1%	$p = 0.765$
3 mm A	-1% ± 7%	$p = 0.802$
3 mm AL	-1% ± 3%	$p = 0.772$
3 mm AM	-1% ± 8%	$p = 0.838$
3 mm L	0% ± 2%	$p = 0.924$
3 mm M	0% ± 3%	$p = 0.972$
3 mm P	1% ± 7%	$p = 0.869$
3 mm PL	1% ± 6%	$p = 0.863$
3 mm PM	1% ± 4%	$p = 0.813$
5 mm A	-2% ± 12%	$p = 0.808$
5 mm AL	-1% ± 5%	$p = 0.8$
5 mm AM	-2% ± 14%	$p = 0.837$
5 mm L	0% ± 2%	$p = 0.879$
5 mm M	0% ± 5%	$p = 0.912$
5 mm P	1% ± 11%	$p = 0.932$
5 mm PL	1% ± 8%	$p = 0.879$
5 mm PM	0% ± 7%	$p = 0.916$

30° Flexion		
1 mm A	2% ± 1%	$p = 0.134$
1 mm AL	0% ± 0%	$p = 0.121$
1 mm AM	3% ± 1%	$p = 0.128$
1 mm L	-1% ± 0%	$p = 0.1$
1 mm M	2% ± 1%	$p = 0.107$
1 mm P	-2% ± 1%	$p = 0.079$
1 mm PL	-2% ± 1%	$p = 0.084$
1 mm PM	0% ± 0%	$p = 0.086$
3 mm A	6% ± 3%	$p = 0.217$
3 mm AL	1% ± 1%	$p = 0.158$
3 mm AM	8% ± 4%	$p = 0.199$
3 mm L	-3% ± 1%	$p = 0.095$
3 mm M	6% ± 2%	$p = 0.114$
3 mm P	-6% ± 3%	$p = 0.047$
3 mm PL	-6% ± 3%	$p = 0.059$
3 mm PM	-1% ± 1%	$p = 0.058$
5 mm A	10% ± 5%	$p = 0.309$
5 mm AL	2% ± 2%	$p = 0.19$
5 mm AM	16% ± 6%	$p = 0.279$
5 mm L	-5% ± 2%	$p = 0.09$
5 mm M	11% ± 4%	$p = 0.118$
5 mm P	-11% ± 5%	$p = 0.03$
5 mm PL	-10% ± 5%	$p = 0.046$
5 mm PM	-3% ± 1%	$p = 0.037$

60° Flexion		
1 mm A	2% ± 2%	$p = 0.226$
1 mm AL	0% ± 1%	$p = 0.814$
1 mm AM	3% ± 2%	$p = 0.122$
1 mm L	-2% ± 0%	$p = 0.031$
1 mm M	2% ± 1%	$p = 0.027$
1 mm P	-2% ± 2%	$p = 0.237$
1 mm PL	-2% ± 2%	$p = 0.133$
1 mm PM	0% ± 1%	$p = 0.862$
3 mm A	6% ± 6%	$p = 0.212$
3 mm AL	1% ± 3%	$p = 0.747$
3 mm AM	9% ± 6%	$p = 0.113$
3 mm L	-4% ± 1%	$p = 0.038$
3 mm M	7% ± 2%	$p = 0.025$
3 mm P	-6% ± 5%	$p = 0.221$
3 mm PL	-6% ± 4%	$p = 0.136$
3 mm PM	0% ± 3%	$p = 0.884$
5 mm A	10% ± 9%	$p = 0.172$
5 mm AL	1% ± 3%	$p = 0.604$
5 mm AM	17% ± 10%	$p = 0.099$
5 mm L	-6% ± 2%	$p = 0.039$
5 mm M	13% ± 4%	$p = 0.029$
5 mm P	-10% ± 9%	$p = 0.184$
5 mm PL	-10% ± 7%	$p = 0.136$
5 mm PM	-1% ± 4%	$p = 0.733$

Appendix A.18 – Percent change in nonanatomic repair tension with respect to anatomic repair and a 500 N compressive load.

0° Flexion		
1 mm A	-1% ± 3%	$p = 0.715$
1 mm AL	0% ± 2%	$p = 0.676$
1 mm AM	-1% ± 3%	$p = 0.747$
1 mm L	0% ± 1%	$p = 0.835$
1 mm M	0% ± 1%	$p = 0.856$
1 mm P	1% ± 3%	$p = 0.726$
1 mm PL	1% ± 3%	$p = 0.744$
1 mm PM	0% ± 2%	$p = 0.681$
3 mm A	-2% ± 9%	$p = 0.719$
3 mm AL	-1% ± 4%	$p = 0.691$
3 mm AM	2% ± 10%	$p = 0.746$
3 mm L	0% ± 2%	$p = 0.792$
3 mm M	0% ± 3%	$p = 0.849$
3 mm P	2% ± 9%	$p = 0.747$
3 mm PL	2% ± 7%	$p = 0.745$
3 mm PM	1% ± 5%	$p = 0.715$
5 mm A	-3% ± 15%	$p = 0.734$
5 mm AL	-2% ± 7%	$p = 0.723$
5 mm AM	-3% ± 17%	$p = 0.755$
5 mm L	1% ± 3%	$p = 0.76$
5 mm M	-1% ± 6%	$p = 0.804$
5 mm P	3% ± 15%	$p = 0.79$
5 mm PL	2% ± 11%	$p = 0.751$
5 mm PM	2% ± 9%	$p = 0.79$

30° Flexion		
1 mm A	2% ± 1%	$p = 0.096$
1 mm AL	0% ± 0%	$p = 0.322$
1 mm AM	3% ± 1%	$p = 0.062$
1 mm L	-1% ± 0%	$p = 0.039$
1 mm M	2% ± 1%	$p = 0.034$
1 mm P	-2% ± 1%	$p = 0.092$
1 mm PL	-2% ± 1%	$p = 0.068$
1 mm PM	0% ± 0%	$p = 0.317$
3 mm A	6% ± 3%	$p = 0.099$
3 mm AL	1% ± 1%	$p = 0.31$
3 mm AM	8% ± 4%	$p = 0.059$
3 mm L	-4% ± 1%	$p = 0.044$
3 mm M	6% ± 2%	$p = 0.032$
3 mm P	-6% ± 3%	$p = 0.073$
3 mm PL	-6% ± 3%	$p = 0.07$
3 mm PM	-1% ± 1%	$p = 0.177$
5 mm A	10% ± 6%	$p = 0.095$
5 mm AL	2% ± 2%	$p = 0.255$
5 mm AM	16% ± 7%	$p = 0.052$
5 mm L	-5% ± 2%	$p = 0.048$
5 mm M	12% ± 4%	$p = 0.037$
5 mm P	-11% ± 5%	$p = 0.059$
5 mm PL	-10% ± 5%	$p = 0.068$
5 mm PM	-3% ± 1%	$p = 0.069$

60° Flexion		
1 mm A	2% ± 2%	$p = 0.225$
1 mm AL	0% ± 1%	$p = 0.735$
1 mm AM	3% ± 2%	$p = 0.131$
1 mm L	2% ± 1%	$p = 0.046$
1 mm M	2% ± 1%	$p = 0.042$
1 mm P	-2% ± 2%	$p = 0.222$
1 mm PL	-3% ± 2%	$p = 0.138$
1 mm PM	0% ± 1%	$p = 0.778$
3 mm A	6% ± 6%	$p = 0.224$
3 mm AL	1% ± 3%	$p = 0.741$
3 mm AM	10% ± 6%	$p = 0.121$
3 mm L	-4% ± 2%	$p = 0.052$
3 mm M	7% ± 2%	$p = 0.036$
3 mm P	-6% ± 6%	$p = 0.208$
3 mm PL	-7% ± 5%	$p = 0.139$
3 mm PM	-1% ± 3%	$p = 0.771$
5 mm A	10% ± 10%	$p = 0.205$
5 mm AL	1% ± 4%	$p = 0.727$
5 mm AM	18% ± 11%	$p = 0.107$
5 mm L	-6% ± 3%	$p = 0.052$
5 mm M	14% ± 5%	$p = 0.037$
5 mm P	-11% ± 10%	$p = 0.188$
5 mm PL	-11% ± 8%	$p = 0.138$
5 mm PM	-1% ± 5%	$p = 0.662$

APPENDIX B:

CHANGES TO MECHANICS WITH LOOSENED MENISCAL ROOT REPAIRS

From the finite element knee models in Chapter 6, the change of outcome variables for all meniscal root repairs are listed for each flexion angle and compressive load evaluated. Results are presented as the mean and standard deviation, and **bold print** represents an outcome that is statistically different from zero using a Benjamini-Hochberg correction with a false discovery rate of 0.05 and number of tests assessed as 25. The 25 tests for each correction relate to the anatomic and the 24 nonanatomic repairs locations evaluated at different loading conditions. A = Anterior; AL = anterolateral; AM = anteromedial; L = lateral; M = medial; P = posterior; PL = posterolateral; PM = posteromedial.

Appendix B.1 – Percent change to the mean hoop stress of the medial meniscus midbody with respect to intact for loosened anatomic and loosened nonanatomic repairs and a 1,000 N compressive load.

0° Flexion		
Anatomic	**-56% ± 8%**	***p* = 0.008**
1 mm A	**-56% ± 9%**	***p* = 0.009**
1 mm AL	**-55% ± 9%**	***p* = 0.009**
1 mm AM	**-56% ± 9%**	***p* = 0.008**
1 mm L	**-55% ± 9%**	***p* = 0.008**
1 mm M	**-57% ± 8%**	***p* = 0.007**
1 mm P	**-56% ± 8%**	***p* = 0.006**
1 mm PL	**-56% ± 8%**	***p* = 0.007**
1 mm PM	**-57% ± 8%**	***p* = 0.006**
3 mm A	**-56% ± 10%**	***p* = 0.011**
3 mm AL	**-55% ± 10%**	***p* = 0.011**
3 mm AM	**-58% ± 10%**	***p* = 0.009**
3 mm L	**-55% ± 9%**	***p* = 0.008**
3 mm M	**-59% ± 8%**	***p* = 0.006**
3 mm P	**-58% ± 6%**	***p* = 0.004**
3 mm PL	**-56% ± 7%**	***p* = 0.006**
3 mm PM	**-59% ± 6%**	***p* = 0.004**
5 mm A	**-57% ± 11%**	***p* = 0.012**
5 mm AL	**-55% ± 10%**	***p* = 0.012**
5 mm AM	**-60% ± 10%**	***p* = 0.009**
5 mm L	**-54% ± 8%**	***p* = 0.008**
5 mm M	**-62% ± 7%**	***p* = 0.004**
5 mm P	**-60% ± 5%**	***p* = 0.002**
5 mm PL	**-56% ± 6%**	***p* = 0.004**
5 mm PM	**-62% ± 5%**	***p* = 0.002**

30° Flexion		
Anatomic	**-37% ± 2%**	***p* < 0.001**
1 mm A	**-35% ± 2%**	***p* = 0.001**
1 mm AL	**-36% ± 2%**	***p* < 0.001**
1 mm AM	**-36% ± 3%**	***p* = 0.002**
1 mm L	**-37% ± 1%**	***p* < 0.001**
1 mm M	**-38% ± 3%**	***p* = 0.002**
1 mm P	**-40% ± 2%**	***p* < 0.001**
1 mm PL	**-39% ± 1%**	***p* < 0.001**
1 mm PM	**-39% ± 2%**	***p* = 0.001**
3 mm A	**-33% ± 3%**	***p* = 0.003**
3 mm AL	**-33% ± 2%**	***p* < 0.001**
3 mm AM	**-35% ± 4%**	***p* = 0.005**
3 mm L	**-37% ± 1%**	***p* < 0.001**
3 mm M	**-40% ± 4%**	***p* = 0.004**
3 mm P	**-45% ± 2%**	***p* < 0.001**
3 mm PL	**-41% ± 1%**	***p* < 0.001**
3 mm PM	**-45% ± 3%**	***p* = 0.001**
5 mm A	**-31% ± 4%**	***p* = 0.007**
5 mm AL	**-32% ± 2%**	***p* = 0.001**
5 mm AM	**-35% ± 6%**	***p* = 0.011**
5 mm L	**-37% ± 0%**	***p* < 0.001**
5 mm M	**-43% ± 6%**	***p* = 0.007**
5 mm P	**-51% ± 2%**	***p* < 0.001**
5 mm PL	**-44% ± 2%**	***p* < 0.001**
5 mm PM	**-52% ± 3%**	***p* = 0.001**

60° Flexion		
Anatomic	**-33% ± 1%**	***p* < 0.001**
1 mm A	**-31% ± 1%**	***p* < 0.001**
1 mm AL	**-32% ± 1%**	***p* < 0.001**
1 mm AM	**-32% ± 2%**	***p* < 0.001**
1 mm L	**-33% ± 0%**	***p* < 0.001**
1 mm M	**-34% ± 1%**	***p* < 0.001**
1 mm P	**-35% ± 0%**	***p* < 0.001**
1 mm PL	**-35% ± 0%**	***p* < 0.001**
1 mm PM	**-35% ± 1%**	***p* < 0.001**
3 mm A	**-29% ± 3%**	***p* = 0.003**
3 mm AL	**-30% ± 1%**	***p* < 0.001**
3 mm AM	**-30% ± 4%**	***p* = 0.005**
3 mm L	**-33% ± 1%**	***p* < 0.001**
3 mm M	**-35% ± 3%**	***p* = 0.002**
3 mm P	**-41% ± 1%**	***p* < 0.001**
3 mm PL	**-37% ± 3%**	***p* < 0.001**
3 mm PM	**-40% ± 0%**	***p* < 0.001**
5 mm A	**-28% ± 4%**	***p* = 0.007**
5 mm AL	**-29% ± 1%**	***p* < 0.001**
5 mm AM	**-30% ± 6%**	***p* = 0.012**
5 mm L	**-33% ± 1%**	***p* < 0.001**
5 mm M	**-38% ± 5%**	***p* = 0.005**
5 mm P	**-47% ± 3%**	***p* = 0.002**
5 mm PL	**-40% ± 3%**	***p* = 0.002**
5 mm PM	**-46% ± 0%**	***p* < 0.001**

Appendix B.2 – Percent change to the mean hoop stress of the medial meniscus midbody with respect to intact for loosened anatomic and loosened nonanatomic repairs and a 500 N compressive load.

0° Flexion		
Anatomic	**-59% ± 10%**	***p* = 0.01**
1 mm A	**-59% ± 11%**	***p* = 0.012**
1 mm AL	**-59% ± 11%**	***p* = 0.012**
1 mm AM	**-60% ± 11%**	***p* = 0.011**
1 mm L	**-59% ± 10%**	***p* = 0.01**
1 mm M	**-60% ± 10%**	***p* = 0.01**
1 mm P	**-60% ± 9%**	***p* = 0.008**
1 mm PL	**-59% ± 10%**	***p* = 0.009**
1 mm PM	**-60% ± 10%**	***p* = 0.009**
3 mm A	**-59% ± 13%**	***p* = 0.015**
3 mm AL	**-58% ± 12%**	***p* = 0.014**
3 mm AM	**-61% ± 12%**	***p* = 0.012**
3 mm L	**-58% ± 10%**	***p* = 0.011**
3 mm M	**-62% ± 10%**	***p* = 0.008**
3 mm P	**-61% ± 8%**	***p* = 0.005**
3 mm PL	**-59% ± 9%**	***p* = 0.007**
3 mm PM	**-62% ± 8%**	***p* = 0.005**
5 mm A	**-60% ± 13%**	***p* = 0.016**
5 mm AL	**-58% ± 13%**	***p* = 0.015**
5 mm AM	**-63% ± 12%**	***p* = 0.012**
5 mm L	**58% ± 10%**	***p* = 0.01**
5 mm M	**-65% ± 9%**	***p* = 0.006**
5 mm P	**-63% ± 6%**	***p* = 0.003**
5 mm PL	**-60% ± 8%**	***p* = 0.006**
5 mm PM	**-65% ± 6%**	***p* = 0.003**

30° Flexion		
Anatomic	**-34% ± 4%**	***p* = 0.004**
1 mm A	**-32% ± 4%**	***p* = 0.005**
1 mm AL	**-33% ± 3%**	***p* = 0.004**
1 mm AM	**-33% ± 4%**	***p* = 0.005**
1 mm L	**-34% ± 3%**	***p* = 0.003**
1 mm M	**-35% ± 4%**	***p* = 0.005**
1 mm P	**-37% ± 4%**	***p* = 0.003**
1 mm PL	**-36% ± 3%**	***p* = 0.003**
1 mm PM	**-36% ± 4%**	***p* = 0.004**
3 mm A	**-29% ± 4%**	***p* = 0.007**
3 mm AL	**-30% ± 3%**	***p* = 0.004**
3 mm AM	**-31% ± 6%**	***p* = 0.01**
3 mm L	**-34% ± 3%**	***p* = 0.002**
3 mm M	**-36% ± 6%**	***p* = 0.008**
3 mm P	**-42% ± 3%**	***p* = 0.002**
3 mm PL	**-39% ± 3%**	***p* = 0.002**
3 mm PM	**-41% ± 5%**	***p* = 0.004**
5 mm A	**-28% ± 5%**	***p* = 0.012**
5 mm AL	**-29% ± 3%**	***p* = 0.004**
5 mm AM	**-31% ± 7%**	***p* = 0.018**
5 mm L	**-34% ± 2%**	***p* = 0.002**
5 mm M	**-39% ± 8%**	***p* = 0.013**
5 mm P	**-49% ± 3%**	***p* = 0.002**
5 mm PL	**-42% ± 3%**	***p* = 0.002**
5 mm PM	**-48% ± 5%**	***p* = 0.003**

60° Flexion		
Anatomic	**-32% ± 1%**	***p* < 0.001**
1 mm A	**-30% ± 2%**	***p* = 0.002**
1 mm AL	**-30% ± 2%**	***p* < 0.001**
1 mm AM	**-30% ± 2%**	***p* = 0.002**
1 mm L	**-31% ± 1%**	***p* < 0.001**
1 mm M	**-32% ± 2%**	***p* = 0.002**
1 mm P	**-34% ± 1%**	***p* < 0.001**
1 mm PL	**-33% ± 1%**	***p* < 0.001**
1 mm PM	**-33% ± 1%**	***p* < 0.001**
3 mm A	**-27% ± 3%**	***p* = 0.005**
3 mm AL	**-28% ± 2%**	***p* = 0.001**
3 mm AM	**-28% ± 4%**	***p* = 0.008**
3 mm L	**-32% ± 0%**	***p* < 0.001**
3 mm M	**-33% ± 4%**	***p* = 0.004**
3 mm P	**-39% ± 1%**	***p* < 0.001**
3 mm PL	**-36% ± 1%**	***p* < 0.001**
3 mm PM	**-38% ± 1%**	***p* < 0.001**
5 mm A	**-25% ± 5%**	***p* = 0.011**
5 mm AL	**-27% ± 2%**	***p* = 0.002**
5 mm AM	**-28% ± 6%**	***p* = 0.018**
5 mm L	**-32% ± 1%**	***p* < 0.001**
5 mm M	**-35% ± 5%**	***p* = 0.008**
5 mm P	**-45% ± 3%**	***p* = 0.001**
5 mm PL	**-39% ± 3%**	***p* = 0.002**
5 mm PM	**-45% ± 1%**	***p* < 0.001**

Appendix B.3 – Percent change to the mean hoop stress of the anteromedial meniscal insertion with respect to intact for loosened anatomic and loosened nonanatomic repairs and a 1,000 N compressive load.

0° Flexion		
Anatomic	**-62% ± 12%**	***p* = 0.012**
1 mm A	**-62% ± 13%**	***p* = 0.014**
1 mm AL	**-61% ± 13%**	***p* = 0.014**
1 mm AM	**-62% ± 13%**	***p* = 0.013**
1 mm L	**-61% ± 12%**	***p* = 0.013**
1 mm M	**-63% ± 12%**	***p* = 0.012**
1 mm P	**-62% ± 11%**	***p* = 0.011**
1 mm PL	**-62% ± 11%**	***p* = 0.011**
1 mm PM	**-63% ± 11%**	***p* = 0.011**
3 mm A	**-62% ± 14%**	***p* = 0.017**
3 mm AL	**-61% ± 14%**	***p* = 0.016**
3 mm AM	**-64% ± 14%**	***p* = 0.015**
3 mm L	**-60% ± 12%**	***p* = 0.013**
3 mm M	**-65% ± 12%**	***p* = 0.01**
3 mm P	**-64% ± 9%**	***p* = 0.007**
3 mm PL	**-62% ± 10%**	***p* = 0.009**
3 mm PM	**-65% ± 10%**	***p* = 0.007**
5 mm A	**-63% ± 15%**	***p* = 0.019**
5 mm AL	**-60% ± 14%**	***p* = 0.018**
5 mm AM	**-66% ± 14%**	***p* = 0.015**
5 mm L	**-60% ± 12%**	***p* = 0.012**
5 mm M	**-68% ± 11%**	***p* = 0.008**
5 mm P	**-66% ± 8%**	***p* = 0.005**
5 mm PL	**-62% ± 9%**	***p* = 0.007**
5 mm PM	**-68% ± 8%**	***p* = 0.004**

30° Flexion		
Anatomic	**-40% ± 3%**	***p* = 0.002**
1 mm A	**-38% ± 3%**	***p* = 0.002**
1 mm AL	**-38% ± 3%**	***p* = 0.002**
1 mm AM	**-39% ± 4%**	***p* = 0.003**
1 mm L	**-40% ± 2%**	***p* = 0.001**
1 mm M	**-41% ± 4%**	***p* = 0.003**
1 mm P	**-43% ± 3%**	***p* = 0.001**
1 mm PL	**-41% ± 2%**	***p* = 0.001**
1 mm PM	**-42% ± 3%**	***p* = 0.002**
3 mm A	**-35% ± 4%**	***p* = 0.005**
3 mm AL	**-36% ± 3%**	***p* = 0.002**
3 mm AM	**-37% ± 5%**	***p* = 0.007**
3 mm L	**-39% ± 1%**	***p* < 0.001**
3 mm M	**-43% ± 5%**	***p* = 0.005**
3 mm P	**-48% ± 2%**	***p* < 0.001**
3 mm PL	**-44% ± 1%**	***p* < 0.001**
3 mm PM	**-48% ± 4%**	***p* = 0.002**
5 mm A	**-33% ± 6%**	***p* = 0.009**
5 mm AL	**-34% ± 3%**	***p* = 0.002**
5 mm AM	**-37% ± 8%**	***p* = 0.014**
5 mm L	**-40% ± 1%**	***p* < 0.001**
5 mm M	**-46% ± 8%**	***p* = 0.009**
5 mm P	**-55% ± 2%**	***p* < 0.001**
5 mm PL	**-48% ± 1%**	***p* < 0.001**
5 mm PM	**-55% ± 4%**	***p* = 0.002**

60° Flexion		
Anatomic	**-35% ± 1%**	***p* < 0.001**
1 mm A	**-34% ± 1%**	***p* < 0.001**
1 mm AL	**-34% ± 1%**	***p* < 0.001**
1 mm AM	**-34% ± 2%**	***p* < 0.001**
1 mm L	**-35% ± 0%**	***p* < 0.001**
1 mm M	**-36% ± 1%**	***p* < 0.001**
1 mm P	**-38% ± 0%**	***p* < 0.001**
1 mm PL	**-37% ± 0%**	***p* < 0.001**
1 mm PM	**-37% ± 1%**	***p* < 0.001**
3 mm A	**-31% ± 3%**	***p* = 0.003**
3 mm AL	**-32% ± 1%**	***p* < 0.001**
3 mm AM	**-32% ± 4%**	***p* = 0.005**
3 mm L	**-35% ± 1%**	***p* < 0.001**
3 mm M	**-37% ± 3%**	***p* = 0.002**
3 mm P	**-43% ± 1%**	***p* < 0.001**
3 mm PL	**-40% ± 2%**	***p* < 0.001**
3 mm PM	**-42% ± 1%**	***p* < 0.001**
5 mm A	**-29% ± 4%**	***p* = 0.006**
5 mm AL	**-31% ± 2%**	***p* < 0.001**
5 mm AM	**-32% ± 6%**	***p* = 0.011**
5 mm L	**-36% ± 1%**	***p* < 0.001**
5 mm M	**-40% ± 5%**	***p* = 0.005**
5 mm P	**-50% ± 3%**	***p* = 0.001**
5 mm PL	**-43% ± 3%**	***p* = 0.002**
5 mm PM	**-49% ± 0%**	***p* < 0.001**

Appendix B.4 – Percent change to the mean hoop stress of the anteromedial meniscal insertion with respect to intact for loosened anatomic and loosened nonanatomic repairs and a 500 N compressive load.

0° Flexion		
Anatomic	**-65% ± 16%**	***p* = 0.02**
1 mm A	**-65% ± 17%**	***p* = 0.022**
1 mm AL	**-65% ± 17%**	***p* = 0.022**
1 mm AM	**-66% ± 17%**	***p* = 0.021**
1 mm L	**-65% ± 16%**	***p* = 0.02**
1 mm M	**-66% ± 16%**	***p* = 0.019**
1 mm P	**-66% ± 15%**	***p* = 0.017**
1 mm PL	**-65% ± 15%**	***p* = 0.018**
1 mm PM	**-66% ± 15%**	***p* = 0.017**
3 mm A	**-66% ± 19%**	***p* = 0.026**
3 mm AL	**-64% ± 18%**	***p* = 0.025**
3 mm AM	**-67% ± 18%**	***p* = 0.023**
3 mm L	**-64% ± 16%**	***p* = 0.02**
3 mm M	**-68% ± 16%**	***p* = 0.017**
3 mm P	**-67% ± 13%**	***p* = 0.012**
3 mm PL	**-65% ± 14%**	***p* = 0.015**
3 mm PM	**-68% ± 13%**	***p* = 0.013**
5 mm A	**-67% ± 20%**	***p* = 0.028**
5 mm AL	**-64% ± 18%**	***p* = 0.026**
5 mm AM	**-70% ± 19%**	***p* = 0.023**
5 mm L	**-64% ± 16%**	***p* = 0.02**
5 mm M	**-71% ± 15%**	***p* = 0.014**
5 mm P	**-69% ± 11%**	***p* = 0.008**
5 mm PL	**-66% ± 13%**	***p* = 0.012**
5 mm PM	**-71% ± 11%**	***p* = 0.008**

30° Flexion		
Anatomic	**-37% ± 4%**	***p* = 0.004**
1 mm A	**-34% ± 4%**	***p* = 0.005**
1 mm AL	**-35% ± 4%**	***p* = 0.004**
1 mm AM	**-35% ± 5%**	***p* = 0.006**
1 mm L	**-36% ± 4%**	***p* = 0.003**
1 mm M	**-37% ± 5%**	***p* = 0.006**
1 mm P	**-39% ± 4%**	***p* = 0.003**
1 mm PL	**-38% ± 4%**	***p* = 0.003**
1 mm PM	**-39% ± 4%**	***p* = 0.004**
3 mm A	**-31% ± 5%**	***p* = 0.009**
3 mm AL	**-32% ± 4%**	***p* = 0.004**
3 mm AM	**-33% ± 6%**	***p* = 0.012**
3 mm L	**-36% ± 3%**	***p* = 0.002**
3 mm M	**-39% ± 7%**	***p* = 0.009**
3 mm P	**-45% ± 4%**	***p* = 0.002**
3 mm PL	**-41% ± 3%**	***p* = 0.002**
3 mm PM	**-44% ± 5%**	***p* = 0.005**
5 mm A	**-30% ± 6%**	***p* = 0.014**
5 mm AL	**-31% ± 4%**	***p* = 0.005**
5 mm AM	**-33% ± 8%**	***p* = 0.02**
5 mm L	**-36% ± 2%**	***p* = 0.001**
5 mm M	**-42% ± 9%**	***p* = 0.014**
5 mm P	**-52% ± 3%**	***p* = 0.001**
5 mm PL	**-44% ± 2%**	***p* = 0.001**
5 mm PM	**-51% ± 6%**	***p* = 0.004**

60° Flexion		
Anatomic	**-34% ± 2%**	***p* < 0.001**
1 mm A	**-31% ± 2%**	***p* = 0.002**
1 mm AL	**-32% ± 2%**	***p* < 0.001**
1 mm AM	**-32% ± 3%**	***p* = 0.002**
1 mm L	**-33% ± 1%**	***p* < 0.001**
1 mm M	**-34% ± 2%**	***p* = 0.001**
1 mm P	**-36% ± 1%**	***p* < 0.001**
1 mm PL	**-35% ± 1%**	***p* < 0.001**
1 mm PM	**-35% ± 1%**	***p* < 0.001**
3 mm A	**-29% ± 3%**	***p* = 0.005**
3 mm AL	**-30% ± 2%**	***p* = 0.001**
3 mm AM	**-30% ± 5%**	***p* = 0.008**
3 mm L	**-34% ± 0%**	***p* < 0.001**
3 mm M	**-35% ± 4%**	***p* = 0.004**
3 mm P	**-42% ± 1%**	***p* < 0.001**
3 mm PL	**-38% ± 1%**	***p* < 0.001**
3 mm PM	**-40% ± 1%**	***p* < 0.001**
5 mm A	**-27% ± 5%**	***p* = 0.01**
5 mm AL	**-29% ± 2%**	***p* = 0.002**
5 mm AM	**-29% ± 7%**	***p* = 0.017**
5 mm L	**-34% ± 1%**	***p* < 0.001**
5 mm M	**-38% ± 6%**	***p* = 0.008**
5 mm P	**-48% ± 3%**	***p* = 0.001**
5 mm PL	**-42% ± 3%**	***p* = 0.002**
5 mm PM	**-47% ± 1%**	***p* < 0.001**

Appendix B.5 – Percent change to the total contact area on the medial surface of tibial articular cartilage with respect to intact for loosened anatomic and loosened nonanatomic repairs and a 1,000 N compressive load.

0° Flexion			30° Flexion			60° Flexion		
Anatomic	**-23% ± 5%**	***p* = 0.015**	Anatomic	-12% ± 2%	*p* = 0.094	Anatomic	-10% ± 5%	*p* = 0.073
1 mm A	**-23% ± 5%**	***p* = 0.017**	1 mm A	-11% ± 2%	*p* = 0.096	1 mm A	-9% ± 5%	*p* = 0.085
1 mm AL	**-23% ± 5%**	***p* = 0.016**	1 mm AL	-12% ± 2%	*p* = 0.097	1 mm AL	-10% ± 4%	*p* = 0.052
1 mm AM	**-23% ± 5%**	***p* = 0.017**	1 mm AM	-11% ± 2%	*p* = 0.093	1 mm AM	-9% ± 5%	*p* = 0.096
1 mm L	**-23% ± 5%**	***p* = 0.014**	1 mm L	-12% ± 2%	*p* = 0.097	1 mm L	-10% ± 4%	*p* = 0.053
1 mm M	**-23% ± 5%**	***p* = 0.014**	1 mm M	-11% ± 2%	*p* = 0.09	1 mm M	-9% ± 6%	*p* = 0.101
1 mm P	**-24% ± 5%**	***p* = 0.013**	1 mm P	-13% ± 2%	*p* = 0.092	1 mm P	-10% ± 5%	*p* = 0.061
1 mm PL	**-24% ± 5%**	***p* = 0.014**	1 mm PL	-12% ± 2%	*p* = 0.094	1 mm PL	-11% ± 5%	*p* = 0.056
1 mm PM	**-24% ± 5%**	***p* = 0.013**	1 mm PM	-12% ± 2%	*p* = 0.09	1 mm PM	-10% ± 5%	*p* = 0.081
3 mm A	**-23% ± 6%**	***p* = 0.021**	3 mm A	-10% ± 2%	*p* = 0.1	3 mm A	-9% ± 5%	*p* = 0.088
3 mm AL	**-23% ± 5%**	***p* = 0.015**	3 mm AL	-12% ± 2%	*p* = 0.104	3 mm AL	-10% ± 5%	*p* = 0.068
3 mm AM	**-24% ± 5%**	***p* = 0.017**	3 mm AM	-10% ± 2%	*p* = 0.089	3 mm AM	-8% ± 5%	*p* = 0.097
3 mm L	**-24% ± 5%**	***p* = 0.014**	3 mm L	-13% ± 1%	*p* = 0.101	3 mm L	-11% ± 4%	*p* = 0.04
3 mm M	**-24% ± 5%**	***p* = 0.012**	3 mm M	-11% ± 3%	*p* = 0.081	3 mm M	-9% ± 6%	*p* = 0.125
3 mm P	**-24% ± 4%**	***p* = 0.009**	3 mm P	-14% ± 2%	*p* = 0.089	3 mm P	-13% ± 4%	*p* = 0.028
3 mm PL	**-24% ± 4%**	***p* = 0.009**	3 mm PL	-14% ± 1%	*p* = 0.096	3 mm PL	-12% ± 5%	*p* = 0.044
3 mm PM	**-24% ± 4%**	***p* = 0.008**	3 mm PM	-13% ± 3%	*p* = 0.084	3 mm PM	-11% ± 4%	*p* = 0.053
5 mm A	**-24% ± 6%**	***p* = 0.02**	5 mm A	-10% ± 2%	*p* = 0.104	5 mm A	-8% ± 5%	*p* = 0.104
5 mm AL	**-24% ± 5%**	***p* = 0.017**	5 mm AL	-12% ± 3%	*p* = 0.109	5 mm AL	-10% ± 5%	*p* = 0.064
5 mm AM	**-24% ± 6%**	***p* = 0.019**	5 mm AM	-8% ± 4%	*p* = 0.083	5 mm AM	-7% ± 6%	*p* = 0.176
5 mm L	**-24% ± 4%**	***p* = 0.011**	5 mm L	-14% ± 1%	*p* = 0.104	5 mm L	-12% ± 4%	*p* = 0.029
5 mm M	**-25% ± 4%**	***p* = 0.007**	5 mm M	-10% ± 4%	*p* = 0.07	5 mm M	-8% ± 7%	*p* = 0.164
5 mm P	**-25% ± 3%**	***p* = 0.005**	5 mm P	-18% ± 1%	*p* = 0.089	5 mm P	-14% ± 4%	*p* = 0.027
5 mm PL	**-24% ± 4%**	***p* = 0.008**	5 mm PL	-15% ± 1%	*p* = 0.096	5 mm PL	-13% ± 4%	*p* = 0.034
5 mm PM	**-26% ± 2%**	***p* = 0.003**	5 mm PM	-15% ± 3%	*p* = 0.079	5 mm PM	-13% ± 5%	*p* = 0.043

Appendix B.6 – Percent change to the total contact area on the medial surface of tibial articular cartilage with respect to intact for loosened anatomic and loosened nonanatomic repairs and a 500 N compressive load.

0° Flexion		
Anatomic	**-26% ± 6%**	***p* = 0.016**
1 mm A	**-26% ± 6%**	***p* = 0.02**
1 mm AL	**-25% ± 6%**	***p* = 0.019**
1 mm AM	**-26% ± 6%**	***p* = 0.018**
1 mm L	**-26% ± 6%**	***p* = 0.017**
1 mm M	**-26% ± 6%**	***p* = 0.019**
1 mm P	**-26% ± 6%**	***p* = 0.015**
1 mm PL	**-26% ± 6%**	***p* = 0.015**
1 mm PM	**-26% ± 6%**	***p* = 0.016**
3 mm A	**-25% ± 7%**	***p* = 0.027**
3 mm AL	**-25% ± 7%**	***p* = 0.023**
3 mm AM	**-25% ± 7%**	***p* = 0.025**
3 mm L	**-26% ± 6%**	***p* = 0.015**
3 mm M	**-26% ± 6%**	***p* = 0.016**
3 mm P	**-26% ± 4%**	***p* = 0.007**
3 mm PL	**-26% ± 5%**	***p* = 0.011**
3 mm PM	**-27% ± 5%**	***p* = 0.01**
5 mm A	**-25% ± 8%**	***p* = 0.028**
5 mm AL	**-26% ± 7%**	***p* = 0.021**
5 mm AM	**-26% ± 7%**	***p* = 0.025**
5 mm L	**-26% ± 5%**	***p* = 0.013**
5 mm M	**-27% ± 5%**	***p* = 0.011**
5 mm P	**-27% ± 3%**	***p* = 0.004**
5 mm PL	**-26% ± 4%**	***p* = 0.009**
5 mm PM	**-28% ± 3%**	***p* = 0.004**

30° Flexion		
Anatomic	-8% ± 5%	$p = 0.097$
1 mm A	-8% ± 6%	$p = 0.147$
1 mm AL	-8% ± 6%	$p = 0.129$
1 mm AM	-7% ± 6%	$p = 0.151$
1 mm L	-9% ± 5%	$p = 0.097$
1 mm M	-8% ± 6%	$p = 0.129$
1 mm P	-10% ± 6%	$p = 0.099$
1 mm PL	-9% ± 5%	$p = 0.072$
1 mm PM	-9% ± 6%	$p = 0.123$
3 mm A	-7% ± 7%	$p = 0.211$
3 mm AL	-8% ± 6%	$p = 0.125$
3 mm AM	-6% ± 8%	$p = 0.306$
3 mm L	-9% ± 5%	$p = 0.084$
3 mm M	-7% ± 6%	$p = 0.203$
3 mm P	-11% ± 5%	$p = 0.072$
3 mm PL	-11% ± 5%	$p = 0.055$
3 mm PM	-11% ± 6%	$p = 0.082$
5 mm A	-7% ± 6%	$p = 0.178$
5 mm AL	-9% ± 7%	$p = 0.14$
5 mm AM	-6% ± 8%	$p = 0.305$
5 mm L	-10% ± 4%	$p = 0.052$
5 mm M	-6% ± 8%	$p = 0.323$
5 mm P	-15% ± 5%	$p = 0.029$
5 mm PL	-13% ± 4%	$p = 0.033$
5 mm PM	-12% ± 8%	$p = 0.116$

60° Flexion		
Anatomic	-10% ± 6%	$p = 0.084$
1 mm A	-9% ± 6%	$p = 0.132$
1 mm AL	-10% ± 6%	$p = 0.107$
1 mm AM	-9% ± 7%	$p = 0.15$
1 mm L	-11% ± 6%	$p = 0.081$
1 mm M	-9% ± 6%	$p = 0.114$
1 mm P	-11% ± 6%	$p = 0.083$
1 mm PL	-11% ± 6%	$p = 0.081$
1 mm PM	-11% ± 5%	$p = 0.73$
3 mm A	-8% ± 6%	$p = 0.164$
3 mm AL	-9% ± 6%	$p = 0.117$
3 mm AM	-8% ± 7%	$p = 0.208$
3 mm L	-11% ± 6%	$p = 0.078$
3 mm M	-9% ± 7%	$p = 0.175$
3 mm P	-13% ± 5%	$p = 0.056$
3 mm PL	-13% ± 5%	$p = 0.046$
3 mm PM	-11% ± 7%	$p = 0.119$
5 mm A	-7% ± 6%	$p = 0.187$
5 mm AL	-9% ± 6%	$p = 0.113$
5 mm AM	-7% ± 7%	$p = 0.202$
5 mm L	-13% ± 5%	$p = 0.052$
5 mm M	-8% ± 8%	$p = 0.238$
5 mm P	-15% ± 4%	$p = 0.021$
5 mm PL	-15% ± 5%	$p = 0.037$
5 mm PM	-12% ± 7%	$p = 0.086$

Appendix B.7 – Percent change to the cartilage-cartilage contact area on the medial surface of tibial articular cartilage with respect to intact for loosened anatomic and loosened nonanatomic repairs and a 1,000 N compressive load.

0° Flexion		
Anatomic	**37% ± 6%**	***p* = 0.008**
1 mm A	**37% ± 7%**	***p* = 0.012**
1 mm AL	**37% ± 7%**	***p* = 0.01**
1 mm AM	**37% ± 7%**	***p* = 0.01**
1 mm L	**37% ± 6%**	***p* = 0.008**
1 mm M	**37% ± 6%**	***p* = 0.008**
1 mm P	**38% ± 6%**	***p* = 0.007**
1 mm PL	**38% ± 6%**	***p* = 0.008**
1 mm PM	**38% ± 6%**	***p* = 0.007**
3 mm A	**37% ± 8%**	***p* = 0.016**
3 mm AL	**37% ± 6%**	***p* = 0.01**
3 mm AM	**37% ± 7%**	***p* = 0.012**
3 mm L	**38% ± 6%**	***p* = 0.008**
3 mm M	**39% ± 5%**	***p* = 0.007**
3 mm P	**39% ± 4%**	***p* = 0.004**
3 mm PL	**39% ± 5%**	***p* = 0.005**
3 mm PM	**39% ± 4%**	***p* = 0.004**
5 mm A	**37% ± 9%**	***p* = 0.018**
5 mm AL	**37% ± 7%**	***p* = 0.012**
5 mm AM	**38% ± 8%**	***p* = 0.015**
5 mm L	**38% ± 5%**	***p* = 0.006**
5 mm M	**41% ± 4%**	***p* = 0.003**
5 mm P	**42% ± 3%**	***p* = 0.002**
5 mm PL	**39% ± 4%**	***p* = 0.004**
5 mm PM	**43% ± 2%**	***p* < 0.001**

30° Flexion		
Anatomic	**53% ± 14%**	***p* = 0.023**
1 mm A	**51% ± 13%**	***p* = 0.022**
1 mm AL	**52% ± 13%**	***p* = 0.022**
1 mm AM	**51% ± 13%**	***p* = 0.022**
1 mm L	**54% ± 14%**	***p* = 0.023**
1 mm M	**52% ± 13%**	***p* = 0.021**
1 mm P	**57% ± 14%**	***p* = 0.019**
1 mm PL	**56% ± 13%**	***p* = 0.018**
1 mm PM	**55% ± 14%**	***p* = 0.02**
3 mm A	**46% ± 13%**	***p* = 0.026**
3 mm AL	**50% ± 14%**	***p* = 0.025**
3 mm AM	**47% ± 12%**	***p* = 0.02**
3 mm L	**55% ± 14%**	***p* = 0.021**
3 mm M	**52% ± 14%**	***p* = 0.024**
3 mm P	**63% ± 13%**	***p* = 0.014**
3 mm PL	**13% ± 60%**	***p* = 0.016**
3 mm PM	**59% ± 13%**	***p* = 0.017**
5 mm A	**43% ± 13%**	***p* = 0.031**
5 mm AL	**49% ± 15%**	***p* = 0.03**
5 mm AM	**41% ± 13%**	***p* = 0.03**
5 mm L	**58% ± 15%**	***p* = 0.021**
5 mm M	**51% ± 14%**	***p* = 0.023**
5 mm P	**73% ± 14%**	***p* = 0.011**
5 mm PL	**65% ± 15%**	***p* = 0.017**
5 mm PM	**67% ± 13%**	***p* = 0.013**

60° Flexion		
Anatomic	**29% ± 5%**	***p* = 0.012**
1 mm A	**28% ± 6%**	***p* = 0.015**
1 mm AL	**29% ± 6%**	***p* = 0.013**
1 mm AM	**27% ± 6%**	***p* = 0.015**
1 mm L	**30% ± 5%**	***p* = 0.011**
1 mm M	**28% ± 6%**	***p* = 0.014**
1 mm P	**30% ± 5%**	***p* = 0.01**
1 mm PL	**31% ± 6%**	***p* = 0.013**
1 mm PM	**29% ± 6%**	***p* = 0.012**
3 mm A	**26% ± 6%**	***p* = 0.017**
3 mm AL	**28% ± 6%**	***p* = 0.017**
3 mm AM	**26% ± 6%**	***p* = 0.016**
3 mm L	**32% ± 6%**	***p* = 0.01**
3 mm M	**28% ± 7%**	***p* = 0.018**
3 mm P	**35% ± 5%**	***p* = 0.007**
3 mm PL	**34% ± 6%**	***p* = 0.009**
3 mm PM	**32% ± 5%**	***p* = 0.008**
5 mm A	**25% ± 6%**	***p* = 0.018**
5 mm AL	**28% ± 6%**	***p* = 0.014**
5 mm AM	**24% ± 7%**	***p* = 0.029**
5 mm L	**33% ± 5%**	***p* = 0.008**
5 mm M	**28% ± 9%**	***p* = 0.031**
5 mm P	**40% ± 7%**	***p* = 0.009**
5 mm PL	**36% ± 6%**	***p* = 0.008**
5 mm PM	**38% ± 7%**	***p* = 0.012**

Appendix B.8 – Percent change to the cartilage-cartilage contact area on the medial surface of tibial articular cartilage with respect to intact for loosened anatomic and loosened nonanatomic repairs and a 500 N compressive load.

0° Flexion		
Anatomic	**47% ± 2%**	***p* < 0.001**
1 mm A	**46% ± 3%**	***p* = 0.002**
1 mm AL	**46% ± 2%**	***p* = 0.001**
1 mm AM	**46% ± 3%**	***p* = 0.001**
1 mm L	**46% ± 2%**	***p* < 0.001**
1 mm M	**46% ± 3%**	***p* = 0.001**
1 mm P	**47% ± 1%**	***p* < 0.001**
1 mm PL	**47% ± 1%**	***p* < 0.001**
1 mm PM	**47% ± 2%**	***p* < 0.001**
3 mm A	**45% ± 5%**	***p* = 0.004**
3 mm AL	**45% ± 4%**	***p* = 0.003**
3 mm AM	**46% ± 5%**	***p* = 0.004**
3 mm L	**46% ± 1%**	***p* < 0.001**
3 mm M	**47% ± 2%**	***p* < 0.001**
3 mm P	**48% ± 3%**	***p* = 0.001**
3 mm PL	**47% ± 0%**	***p* < 0.001**
3 mm PM	**49% ± 1%**	***p* < 0.001**
5 mm A	**45% ± 6%**	***p* = 0.007**
5 mm AL	**46% ± 4%**	***p* = 0.003**
5 mm AM	**46% ± 5%**	***p* = 0.004**
5 mm L	**47% ± 0%**	***p* < 0.001**
5 mm M	**49% ± 3%**	***p* < 0.001**
5 mm P	**51% ± 5%**	***p* = 0.004**
5 mm PL	**48% ± 2%**	***p* < 0.001**
5 mm PM	**52% ± 5%**	***p* = 0.003**

30° Flexion		
Anatomic	91% ± 34%	$p = 0.044$
1 mm A	86% ± 34%	$p = 0.049$
1 mm AL	89% ± 36%	$p = 0.052$
1 mm AM	86% ± 33%	$p = 0.047$
1 mm L	92% ± 35%	$p = 0.046$
1 mm M	90% ± 35%	$p = 0.047$
1 mm P	96% ± 37%	$p = 0.047$
1 mm PL	96% ± 39%	$p = 0.05$
1 mm PM	94% ± 35%	$p = 0.043$
3 mm A	76% ± 27%	$p = 0.041$
3 mm AL	85% ± 35%	$p = 0.054$
3 mm AM	75% ± 23%	$p = 0.031$
3 mm L	95% ± 38%	$p = 0.051$
3 mm M	86% ± 29%	$p = 0.035$
3 mm P	109% ± 40%	$p = 0.042$
3 mm PL	103% ± 40%	$p = 0.047$
3 mm PM	104% ± 35%	$p = 0.036$
5 mm A	71% ± 27%	$p = 0.046$
5 mm AL	85% ± 37%	$p = 0.057$
5 mm AM	69% ± 23%	$p = 0.036$
5 mm L	96% ± 41%	$p = 0.056$
5 mm M	85% ± 23%	$p = 0.023$
5 mm P	124% ± 44%	$p = 0.04$
5 mm PL	115% ± 43%	$p = 0.043$
5 mm PM	114% ± 37%	$p = 0.033$

60° Flexion		
Anatomic	**37% ± 7%**	***p* = 0.013**
1 mm A	**34% ± 7%**	***p* = 0.013**
1 mm AL	**35% ± 7%**	***p* = 0.012**
1 mm AM	**34% ± 7%**	***p* = 0.016**
1 mm L	**37% ± 7%**	***p* = 0.013**
1 mm M	**35% ± 7%**	***p* = 0.012**
1 mm P	**38% ± 7%**	***p* = 0.012**
1 mm PL	**38% ± 7%**	***p* = 0.012**
1 mm PM	**38% ± 6%**	***p* = 0.01**
3 mm A	**31% ± 8%**	***p* = 0.02**
3 mm AL	**35% ± 7%**	***p* = 0.013**
3 mm AM	**31% ± 8%**	***p* = 0.021**
3 mm L	**38% ± 8%**	***p* = 0.015**
3 mm M	**34% ± 7%**	***p* = 0.015**
3 mm P	**42% ± 7%**	***p* = 0.01**
3 mm PL	**42% ± 7%**	***p* = 0.009**
3 mm PM	**39% ± 7%**	***p* = 0.011**
5 mm A	**30% ± 7%**	***p* = 0.019**
5 mm AL	**34% ± 7%**	***p* = 0.014**
5 mm AM	**29% ± 7%**	***p* = 0.02**
5 mm L	**41% ± 7%**	***p* = 0.009**
5 mm M	**33% ± 9%**	***p* = 0.025**
5 mm P	**49% ± 7%**	***p* = 0.007**
5 mm PL	**45% ± 8%**	***p* = 0.01**
5 mm PM	**44% ± 8%**	***p* = 0.012**

Appendix B.9 – Percent change to the total contact area of the medial meniscus with the femoral and tibial articular cartilage for loosened anatomic and loosened nonanatomic repairs and a 1,000 N compressive load.

0° Flexion		
Anatomic	**-45% ± 15%**	***p* = 0.035**
1 mm A	**-45% ± 16%**	***p* = 0.038**
1 mm AL	**-45% ± 15%**	***p* = 0.037**
1 mm AM	**-45% ± 16%**	***p* = 0.037**
1 mm L	**-45% ± 15%**	***p* = 0.034**
1 mm M	**-46% ± 16%**	***p* = 0.038**
1 mm P	**-46% ± 15%**	***p* = 0.033**
1 mm PL	**-46% ± 15%**	***p* = 0.035**
1 mm PM	**-46% ± 15%**	***p* = 0.034**
3 mm A	**-45% ± 16%**	***p* = 0.043**
3 mm AL	**-45% ± 16%**	***p* = 0.038**
3 mm AM	**-45% ± 16%**	***p* = 0.041**
3 mm L	**-45% ± 15%**	***p* = 0.034**
3 mm M	**-47% ± 16%**	***p* = 0.035**
3 mm P	**-48% ± 13%**	***p* = 0.023**
3 mm PL	**-47% ± 14%**	***p* = 0.029**
3 mm PM	**-48% ± 14%**	***p* = 0.025**
5 mm A	**-45% ± 18%**	***p* = 0.047**
5 mm AL	**-44% ± 16%**	***p* = 0.04**
5 mm AM	**-47% ± 18%**	***p* = 0.045**
5 mm L	**-45% ± 14%**	***p* = 0.031**
5 mm M	**-50% ± 14%**	***p* = 0.027**
5 mm P	**-51% ± 11%**	***p* = 0.014**
5 mm PL	**-48% ± 12%**	***p* = 0.021**
5 mm PM	**-52% ± 11%**	***p* = 0.014**

30° Flexion		
Anatomic	**-35% ± 7%**	***p* = 0.014**
1 mm A	**-34% ± 8%**	***p* = 0.017**
1 mm AL	**-34% ± 8%**	***p* = 0.017**
1 mm AM	**-34% ± 7%**	***p* = 0.015**
1 mm L	**-36% ± 7%**	***p* = 0.014**
1 mm M	**-35% ± 7%**	***p* = 0.012**
1 mm P	**-37% ± 7%**	***p* = 0.011**
1 mm PL	**-37% ± 7%**	***p* = 0.014**
1 mm PM	**-37% ± 6%**	***p* = 0.01**
3 mm A	**-30% ± 7%**	***p* = 0.016**
3 mm AL	**-33% ± 8%**	***p* = 0.019**
3 mm AM	**-31% ± 5%**	***p* = 0.009**
3 mm L	**-36% ± 8%**	***p* = 0.017**
3 mm M	**-35% ± 5%**	***p* = 0.006**
3 mm P	**-42% ± 8%**	***p* = 0.013**
3 mm PL	**-39% ± 8%**	***p* = 0.014**
3 mm PM	**-39% ± 5%**	***p* = 0.006**
5 mm A	**-28% ± 5%**	***p* = 0.012**
5 mm AL	**-32% ± 8%**	***p* = 0.02**
5 mm AM	**-27% ± 3%**	***p* = 0.003**
5 mm L	**-37% ± 9%**	***p* = 0.019**
5 mm M	**-34% ± 2%**	***p* = 0.001**
5 mm P	**-48% ± 9%**	***p* = 0.011**
5 mm PL	**-42% ± 10%**	***p* = 0.017**
5 mm PM	**-46% ± 6%**	***p* = 0.005**

60° Flexion		
Anatomic	**-36% ± 5%**	***p* = 0.007**
1 mm A	**-35% ± 5%**	***p* = 0.008**
1 mm AL	**-36% ± 6%**	***p* = 0.011**
1 mm AM	**-35% ± 5%**	***p* = 0.008**
1 mm L	**-37% ± 6%**	***p* = 0.01**
1 mm M	**-36% ± 5%**	***p* = 0.005**
1 mm P	**-39% ± 6%**	***p* = 0.009**
1 mm PL	**-38% ± 7%**	***p* = 0.01**
1 mm PM	**-38% ± 5%**	***p* = 0.006**
3 mm A	**-32% ± 5%**	***p* = 0.008**
3 mm AL	**-35% ± 7%**	***p* = 0.014**
3 mm AM	**-32% ± 4%**	***p* = 0.006**
3 mm L	**-39% ± 7%**	***p* = 0.011**
3 mm M	**-36% ± 4%**	***p* = 0.004**
3 mm P	**-44% ± 8%**	***p* = 0.01**
3 mm PL	**-42% ± 7%**	***p* = 0.01**
3 mm PM	**-41% ± 6%**	***p* = 0.007**
5 mm A	**-30% ± 4%**	***p* = 0.006**
5 mm AL	**-34% ± 6%**	***p* = 0.011**
5 mm AM	**-30% ± 3%**	***p* = 0.003**
5 mm L	**-40% ± 7%**	***p* = 0.011**
5 mm M	**-36% ± 2%**	***p* < 0.001**
5 mm P	**-49% ± 8%**	***p* = 0.01**
5 mm PL	**-45% ± 8%**	***p* = 0.011**
5 mm PM	**-47% ± 5%**	***p* = 0.004**

Appendix B.10 – Percent change to the total contact area of the medial meniscus with the femoral and tibial articular cartilage for loosened anatomic and loosened nonanatomic repairs and a 500 N compressive load.

0° Flexion		
Anatomic	**-49% ± 16%**	***p* = 0.034**
1 mm A	**-49% ± 17%**	***p* = 0.039**
1 mm AL	**-49% ± 17%**	***p* = 0.037**
1 mm AM	**-49% ± 17%**	***p* = 0.037**
1 mm L	**-49% ± 16%**	***p* = 0.035**
1 mm M	**-49% ± 17%**	***p* = 0.036**
1 mm P	**-49% ± 15%**	***p* = 0.032**
1 mm PL	**-49% ± 16%**	***p* = 0.033**
1 mm PM	**-49% ± 16%**	***p* = 0.032**
3 mm A	**-48% ± 19%**	***p* = 0.046**
3 mm AL	**-48% ± 18%**	***p* = 0.043**
3 mm AM	**-49% ± 18%**	***p* = 0.044**
3 mm L	**-48% ± 16%**	***p* = 0.034**
3 mm M	**-50% ± 17%**	***p* = 0.034**
3 mm P	**-51% ± 12%**	***p* = 0.017**
3 mm PL	**-49% ± 14%**	***p* = 0.026**
3 mm PM	**-51% ± 14%**	***p* = 0.023**
5 mm A	-49% ± 20%	*p* = 0.051
5 mm AL	**-48% ± 18%**	***p* = 0.044**
5 mm AM	**-50% ± 19%**	***p* = 0.047**
5 mm L	**-48% ± 15%**	***p* = 0.031**
5 mm M	**-52% ± 16%**	***p* = 0.029**
5 mm P	**-53% ± 10%**	***p* = 0.011**
5 mm PL	**-51% ± 13%**	***p* = 0.021**
5 mm PM	**-55% ± 11%**	***p* = 0.014**

30° Flexion		
Anatomic	**-35% ± 7%**	***p* = 0.013**
1 mm A	**-33% ± 6%**	***p* = 0.009**
1 mm AL	**-33% ± 6%**	***p* = 0.011**
1 mm AM	**-33% ± 5%**	***p* = 0.009**
1 mm L	**-35% ± 7%**	***p* = 0.012**
1 mm M	**-34% ± 6%**	***p* = 0.01**
1 mm P	**-37% ± 6%**	***p* = 0.01**
1 mm PL	**-36% ± 7%**	***p* = 0.012**
1 mm PM	**-36% ± 6%**	***p* = 0.008**
3 mm A	**-29% ± 4%**	***p* = 0.006**
3 mm AL	**-31% ± 6%**	***p* = 0.012**
3 mm AM	**-29% ± 4%**	***p* = 0.005**
3 mm L	**-36% ± 8%**	***p* = 0.015**
3 mm M	**-33% ± 4%**	***p* = 0.004**
3 mm P	**-41% ± 8%**	***p* = 0.012**
3 mm PL	**-39% ± 8%**	***p* = 0.014**
3 mm PM	**-40% ± 6%**	***p* = 0.008**
5 mm A	**-27% ± 3%**	***p* = 0.005**
5 mm AL	**-31% ± 5%**	***p* = 0.008**
5 mm AM	**-27% ± 2%**	***p* = 0.001**
5 mm L	**-36% ± 9%**	***p* = 0.018**
5 mm M	**-33% ± 2%**	***p* < 0.001**
5 mm P	**-49% ± 10%**	***p* = 0.013**
5 mm PL	**-43% ± 10%**	***p* = 0.016**
5 mm PM	**-45% ± 5%**	***p* = 0.004**

60° Flexion		
Anatomic	**-37% ± 6%**	***p* = 0.009**
1 mm A	**-34% ± 5%**	***p* = 0.007**
1 mm AL	**-35% ± 5%**	***p* = 0.008**
1 mm AM	**-35% ± 5%**	***p* = 0.006**
1 mm L	**-37% ± 6%**	***p* = 0.01**
1 mm M	**-36% ± 6%**	***p* = 0.008**
1 mm P	**-39% ± 7%**	***p* = 0.01**
1 mm PL	**-39% ± 7%**	***p* = 0.011**
1 mm PM	**-38% ± 7%**	***p* = 0.01**
3 mm A	**-31% ± 4%**	***p* = 0.006**
3 mm AL	**-34% ± 5%**	***p* = 0.008**
3 mm AM	**-31% ± 3%**	***p* = 0.004**
3 mm L	**-38% ± 7%**	***p* = 0.012**
3 mm M	**-35% ± 4%**	***p* = 0.004**
3 mm P	**-44% ± 8%**	***p* = 0.009**
3 mm PL	**-43% ± 9%**	***p* = 0.013**
3 mm PM	**-41% ± 6%**	***p* = 0.006**
5 mm A	**-29% ± 3%**	***p* = 0.004**
5 mm AL	**-33% ± 5%**	***p* = 0.008**
5 mm AM	**-30% ± 3%**	***p* = 0.002**
5 mm L	**-40% ± 7%**	***p* = 0.011**
5 mm M	**-35% ± 3%**	***p* = 0.003**
5 mm P	**-49% ± 10%**	***p* = 0.013**
5 mm PL	**-46% ± 9%**	***p* = 0.012**
5 mm PM	**-46% ± 6%**	***p* = 0.005**

Appendix B.11 – Percent change to the peak contact pressure with respect to intact on medial surface of tibial articular cartilage for loosened anatomic and loosened nonanatomic repairs and a 1,000 N compressive load.

0° Flexion		
Anatomic	8% ± 3%	$p = 0.048$
1 mm A	8% ± 3%	$p = 0.045$
1 mm AL	8% ± 3%	$p = 0.046$
1 mm AM	8% ± 3%	$p = 0.046$
1 mm L	8% ± 3%	$p = 0.049$
1 mm M	9% ± 3%	$p = 0.048$
1 mm P	9% ± 4%	$p = 0.051$
1 mm PL	9% ± 3%	$p = 0.051$
1 mm PM	9% ± 4%	$p = 0.051$
3 mm A	8% ± 3%	$p = 0.04$
3 mm AL	8% ± 3%	$p = 0.043$
3 mm AM	8% ± 3%	$p = 0.042$
3 mm L	8% ± 3%	$p = 0.049$
3 mm M	9% ± 3%	$p = 0.049$
3 mm P	9% ± 4%	$p = 0.057$
3 mm PL	9% ± 4%	$p = 0.054$
3 mm PM	9% ± 4%	$p = 0.056$
5 mm A	8% ± 3%	$p = 0.035$
5 mm AL	8% ± 3%	$p = 0.041$
5 mm AM	8% ± 3%	$p = 0.038$
5 mm L	8% ± 3%	$p = 0.05$
5 mm M	9% ± 4%	$p = 0.052$
5 mm P	10% ± 4%	$p = 0.061$
5 mm PL	9% ± 4%	$p = 0.058$
5 mm PM	10% ± 4%	$p = 0.06$

30° Flexion		
Anatomic	29% ± 16%	$p = 0.094$
1 mm A	28% ± 16%	$p = 0.096$
1 mm AL	28% ± 16%	$p = 0.097$
1 mm AM	28% ± 16%	$p = 0.093$
1 mm L	29% ± 17%	$p = 0.097$
1 mm M	29% ± 16%	$p = 0.09$
1 mm P	30% ± 17%	$p = 0.092$
1 mm PL	30% ± 17%	$p = 0.094$
1 mm PM	30% ± 17%	$p = 0.09$
3 mm A	26% ± 15%	$p = 0.1$
3 mm AL	27% ± 16%	$p = 0.104$
3 mm AM	26% ± 14%	$p = 0.089$
3 mm L	29% ± 17%	$p = 0.101$
3 mm M	29% ± 15%	$p = 0.081$
3 mm P	33% ± 18%	$p = 0.089$
3 mm PL	32% ± 18%	$p = 0.096$
3 mm PM	32% ± 17%	$p = 0.084$
5 mm A	24% ± 14%	$p = 0.104$
5 mm AL	26% ± 16%	$p = 0.109$
5 mm AM	24% ± 13%	$p = 0.083$
5 mm L	30% ± 18%	$p = 0.104$
5 mm M	29% ± 14%	$p = 0.07$
5 mm P	36% ± 20%	$p = 0.089$
5 mm PL	33% ± 19%	$p = 0.096$
5 mm PM	35% ± 18%	$p = 0.079$

60° Flexion		
Anatomic	9% ± 6%	$p = 0.138$
1 mm A	9% ± 6%	$p = 0.146$
1 mm AL	9% ± 6%	$p = 0.145$
1 mm AM	9% ± 6%	$p = 0.143$
1 mm L	9% ± 7%	$p = 0.14$
1 mm M	9% ± 6%	$p = 0.136$
1 mm P	9% ± 7%	$p = 0.13$
1 mm PL	9% ± 7%	$p = 0.134$
1 mm PM	9% ± 6%	$p = 0.131$
3 mm A	8% ± 6%	$p = 0.161$
3 mm AL	8% ± 7%	$p = 0.155$
3 mm AM	8% ± 6%	$p = 0.15$
3 mm L	9% ± 7%	$p = 0.141$
3 mm M	9% ± 6%	$p = 0.129$
3 mm P	10% ± 7%	$p = 0.115$
3 mm PL	10% ± 7%	$p = 0.126$
3 mm PM	10% ± 6%	$p = 0.115$
5 mm A	7% ± 6%	$p = 0.173$
5 mm AL	8% ± 7%	$p = 0.163$
5 mm AM	7% ± 6%	$p = 0.155$
5 mm L	9% ± 7%	$p = 0.141$
5 mm M	9% ± 6%	$p = 0.118$
5 mm P	11% ± 7%	$p = 0.1$
5 mm PL	10% ± 7%	$p = 0.118$
5 mm PM	11% ± 6%	$p = 0.097$

Appendix B.12 – Percent change to the peak contact pressure with respect to intact on medial surface of tibial articular cartilage for loosened anatomic and loosened nonanatomic repairs and a 500 N compressive load.

0° Flexion		
Anatomic	11% ± 5%	$p = 0.057$
1 mm A	11% ± 4%	$p = 0.054$
1 mm AL	11% ± 5%	$p = 0.055$
1 mm AM	11% ± 5%	$p = 0.055$
1 mm L	11% ± 5%	$p = 0.057$
1 mm M	11% ± 5%	$p = 0.057$
1 mm P	11% ± 5%	$p = 0.06$
1 mm PL	11% ± 5%	$p = 0.059$
1 mm PM	11% ± 5%	$p = 0.059$
3 mm A	10% ± 4%	$p = 0.048$
3 mm AL	10% ± 4%	$p = 0.052$
3 mm AM	11% ± 4%	$p = 0.05$
3 mm L	11% ± 5%	$p = 0.058$
3 mm M	11% ± 5%	$p = 0.058$
3 mm P	12% ± 6%	$p = 0.066$
3 mm PL	11% ± 5%	$p = 0.064$
3 mm PM	12% ± 5%	$p = 0.064$
5 mm A	10% ± 4%	$p = 0.044$
5 mm AL	10% ± 4%	$p = 0.05$
5 mm AM	11% ± 4%	$p = 0.046$
5 mm L	11% ± 5%	$p = 0.059$
5 mm M	12% ± 5%	$p = 0.059$
5 mm P	12% ± 6%	$p = 0.071$
5 mm PL	12% ± 6%	$p = 0.067$
5 mm PM	13% ± 6%	$p = 0.069$

30° Flexion		
Anatomic	62% ± 53%	$p = 0.183$
1 mm A	59% ± 51%	$p = 0.185$
1 mm AL	61% ± 53%	$p = 0.186$
1 mm AM	59% ± 51%	$p = 0.182$
1 mm L	62% ± 54%	$p = 0.186$
1 mm M	61% ± 52%	$p = 0.18$
1 mm P	64% ± 55%	$p = 0.182$
1 mm PL	64% ± 55%	$p = 0.184$
1 mm PM	63% ± 54%	$p = 0.18$
3 mm A	54% ± 48%	$p = 0.189$
3 mm AL	58% ± 52%	$p = 0.192$
3 mm AM	55% ± 46%	$p = 0.178$
3 mm L	63% ± 56%	$p = 0.19$
3 mm M	60% ± 50%	$p = 0.171$
3 mm P	70% ± 60%	$p = 0.18$
3 mm PL	68% ± 59%	$p = 0.185$
3 mm PM	68% ± 57%	$p = 0.174$
5 mm A	51% ± 45%	$p = 0.192$
5 mm AL	57% ± 51%	$p = 0.196$
5 mm AM	50% ± 42%	$p = 0.173$
5 mm L	64% ± 58%	$p = 0.192$
5 mm M	60% ± 47%	$p = 0.16$
5 mm P	76% ± 65%	$p = 0.179$
5 mm PL	72% ± 63%	$p = 0.186$
5 mm PM	73% ± 60%	$p = 0.17$

60° Flexion		
Anatomic	12% ± 9%	$p = 0.143$
1 mm A	12% ± 9%	$p = 0.15$
1 mm AL	12% ± 9%	$p = 0.149$
1 mm AM	12% ± 9%	$p = 0.147$
1 mm L	12% ± 9%	$p = 0.144$
1 mm M	12% ± 9%	$p = 0.14$
1 mm P	13% ± 9%	$p = 0.135$
1 mm PL	12% ± 9%	$p = 0.138$
1 mm PM	12% ± 9%	$p = 0.135$
3 mm A	11% ± 9%	$p = 0.164$
3 mm AL	11% ± 9%	$p = 0.159$
3 mm AM	11% ± 8%	$p = 0.154$
3 mm L	12% ± 9%	$p = 0.145$
3 mm M	12% ± 8%	$p = 0.134$
3 mm P	14% ± 9%	$p = 0.119$
3 mm PL	13% ± 9%	$p = 0.13$
3 mm PM	13% ± 9%	$p = 0.119$
5 mm A	10% ± 8%	$p = 0.175$
5 mm AL	11% ± 9%	$p = 0.165$
5 mm AM	10% ± 8%	$p = 0.159$
5 mm L	12% ± 9%	$p = 0.145$
5 mm M	12% ± 8%	$p = 0.123$
5 mm P	15% ± 9%	$p = 0.104$
5 mm PL	14% ± 9%	$p = 0.122$
5 mm PM	15% ± 9%	$p = 0.101$

Appendix B.13 – Meniscal extrusion measured at the posterior root of the medial meniscus with respect to intact for loosened anatomic and loosened nonanatomic repairs and a 1,000 N compressive load.

0° Flexion		
Anatomic	**0.73 ± 0.21 mm**	***p* = 0.026**
1 mm A	**0.72 ± 0.19 mm**	***p* = 0.023**
1 mm AL	**0.72 ± 0.19 mm**	***p* = 0.024**
1 mm AM	**0.73 ± 0.20 mm**	***p* = 0.023**
1 mm L	**0.72 ± 0.21 mm**	***p* = 0.026**
1 mm M	**0.74 ± 0.21 mm**	***p* = 0.026**
1 mm P	**0.74 ± 0.22 mm**	***p* = 0.029**
1 mm PL	**0.73 ± 0.22 mm**	***p* = 0.028**
1 mm PM	**0.75 ± 0.22 mm**	***p* = 0.028**
3 mm A	**0.72 ± 0.17 mm**	***p* = 0.018**
3 mm AL	**0.71 ± 0.18 mm**	***p* = 0.021**
3 mm AM	**0.74 ± 0.18 mm**	***p* = 0.02**
3 mm L	**0.71 ± 0.21 mm**	***p* = 0.027**
3 mm M	**0.77 ± 0.22 mm**	***p* = 0.026**
3 mm P	**0.78 ± 0.26 mm**	***p* = 0.035**
3 mm PL	**0.74 ± 0.24 mm**	***p* = 0.032**
3 mm PM	**0.79 ± 0.26 mm**	***p* = 0.033**
5 mm A	**0.73 ± 0.15 mm**	***p* = 0.015**
5 mm AL	**0.70 ± 0.17 mm**	***p* = 0.019**
5 mm AM	**0.78 ± 0.18 mm**	***p* = 0.017**
5 mm L	**0.71 ± 0.21 mm**	***p* = 0.028**
5 mm M	**0.83 ± 0.25 mm**	***p* = 0.028**
5 mm P	**0.83 ± 0.30 mm**	***p* = 0.041**
5 mm PL	**0.76 ± 0.26 mm**	***p* = 0.037**
5 mm PM	**0.86 ± 0.30 mm**	***p* = 0.039**

30° Flexion		
Anatomic	**1.32 ± 0.41 mm**	***p* = 0.03**
1 mm A	**1.23 ± 0.41 mm**	***p* = 0.035**
1 mm AL	**1.26 ± 0.41 mm**	***p* = 0.034**
1 mm AM	**1.26 ± 0.41 mm**	***p* = 0.034**
1 mm L	**1.32 ± 0.41 mm**	***p* = 0.03**
1 mm M	**1.33 ± 0.41 mm**	***p* = 0.03**
1 mm P	**1.43 ± 0.41 mm**	***p* = 0.026**
1 mm PL	**1.39 ± 0.41 mm**	***p* = 0.028**
1 mm PM	**1.40 ± 0.41 mm**	***p* = 0.027**
3 mm A	1.10 ± 0.43 mm	*p* = 0.047
3 mm AL	1.17 ± 0.42 mm	*p* = 0.04
3 mm AM	1.15 ± 0.44 mm	*p* = 0.045
3 mm L	**1.34 ± 0.42 mm**	***p* = 0.031**
3 mm M	**1.37 ± 0.43 mm**	***p* = 0.032**
3 mm P	**1.67 ± 0.42 mm**	***p* = 0.021**
3 mm PL	**1.54 ± 0.42 mm**	***p* = 0.024**
3 mm PM	**1.61 ± 0.41 mm**	***p* = 0.021**
5 mm A	1.02 ± 0.45 mm	*p* = 0.06
5 mm AL	1.13 ± 0.43 mm	*p* = 0.046
5 mm AM	1.10 ± 0.5 mm	*p* = 0.061
5 mm L	**1.36 ± 0.43 mm**	***p* = 0.032**
5 mm M	**1.46 ± 0.48 mm**	***p* = 0.035**
5 mm P	**1.97 ± 0.45 mm**	***p* = 0.017**
5 mm PL	**1.68 ± 0.45 mm**	***p* = 0.023**
5 mm PM	**1.91 ± 0.42 mm**	***p* = 0.016**

60° Flexion		
Anatomic	**1.34 ± 0.18 mm**	***p* = 0.006**
1 mm A	**1.26 ± 0.18 mm**	***p* = 0.007**
1 mm AL	**1.28 ± 0.19 mm**	***p* = 0.007**
1 mm AM	**1.28 ± 0.18 mm**	***p* = 0.006**
1 mm L	**1.34 ± 0.20 mm**	***p* = 0.007**
1 mm M	**1.34 ± 0.17 mm**	***p* = 0.005**
1 mm P	**1.43 ± 0.18 mm**	***p* = 0.005**
1 mm PL	**1.40 ± 0.19 mm**	***p* = 0.006**
1 mm PM	**1.41 ± 0.17 mm**	***p* = 0.005**
3 mm A	**1.14 ± 0.21 mm**	***p* = 0.011**
3 mm AL	**1.22 ± 0.21 mm**	***p* = 0.01**
3 mm AM	**1.18 ± 0.21 mm**	***p* = 0.01**
3 mm L	**1.36 ± 0.23 mm**	***p* = 0.01**
3 mm M	**1.37 ± 0.18 mm**	***p* = 0.006**
3 mm P	**1.68 ± 0.19 mm**	***p* = 0.005**
3 mm PL	**1.55 ± 0.22 mm**	***p* = 0.007**
3 mm PM	**1.61 ± 0.15 mm**	***p* = 0.003**
5 mm A	**1.08 ± 0.24 mm**	***p* = 0.016**
5 mm AL	**1.19 ± 0.24 mm**	***p* = 0.013**
5 mm AM	**1.13 ± 0.28 mm**	***p* = 0.02**
5 mm L	**1.39 ± 0.25 mm**	***p* = 0.011**
5 mm M	**1.45 ± 0.24 mm**	***p* = 0.009**
5 mm P	**1.98 ± 0.23 mm**	***p* = 0.004**
5 mm PL	**1.69 ± 0.26 mm**	***p* = 0.008**
5 mm PM	**1.92 ± 0.12 mm**	***p* = 0.001**

Appendix B.14 – Meniscal extrusion measured at the posterior root of the medial meniscus with respect to intact for loosened anatomic and loosened nonanatomic repairs and a 500 N compressive load.

0° Flexion		
Anatomic	**0.62 ± 0.18 mm**	***p* = 0.028**
1 mm A	**0.61 ± 0.17 mm**	***p* = 0.025**
1 mm AL	**0.61 ± 0.17 mm**	***p* = 0.026**
1 mm AM	**0.62 ± 0.18 mm**	***p* = 0.026**
1 mm L	**0.61 ± 0.18 mm**	***p* = 0.029**
1 mm M	**0.63 ± 0.19 mm**	***p* = 0.028**
1 mm P	**0.63 ± 0.20 mm**	***p* = 0.032**
1 mm PL	**0.62 ± 0.19 mm**	***p* = 0.031**
1 mm PM	**0.63 ± 0.20 mm**	***p* = 0.031**
3 mm A	**0.61 ± 0.15 mm**	***p* = 0.02**
3 mm AL	**0.60 ± 0.16 mm**	***p* = 0.023**
3 mm AM	**0.63 ± 0.16 mm**	***p* = 0.022**
3 mm L	**0.61 ± 0.18 mm**	***p* = 0.029**
3 mm M	**0.65 ± 0.20 mm**	***p* = 0.029**
3 mm P	**0.66 ± 0.23 mm**	***p* = 0.039**
3 mm PL	**0.63 ± 0.21 mm**	***p* = 0.036**
3 mm PM	**0.67 ± 0.23 mm**	***p* = 0.037**
5 mm A	**0.62 ± 0.14 mm**	***p* = 0.016**
5 mm AL	**0.60 ± 0.15 mm**	***p* = 0.021**
5 mm AM	**0.66 ± 0.16 mm**	***p* = 0.019**
5 mm L	**0.61 ± 0.19 mm**	***p* = 0.03**
5 mm M	**0.70 ± 0.22 mm**	***p* = 0.031**
5 mm P	**0.70 ± 0.27 mm**	***p* = 0.047**
5 mm PL	**0.65 ± 0.23 mm**	***p* = 0.041**
5 mm PM	**0.72 ± 0.27 mm**	***p* = 0.044**

30° Flexion		
Anatomic	**1.14 ± 0.35 mm**	***p* = 0.031**
1 mm A	**1.06 ± 0.36 mm**	***p* = 0.036**
1 mm AL	**1.09 ± 0.36 mm**	***p* = 0.034**
1 mm AM	**1.08 ± 0.36 mm**	***p* = 0.035**
1 mm L	**1.15 ± 0.36 mm**	***p* = 0.031**
1 mm M	**1.15 ± 0.36 mm**	***p* = 0.031**
1 mm P	**1.24 ± 0.35 mm**	***p* = 0.026**
1 mm PL	**1.21 ± 0.35 mm**	***p* = 0.027**
1 mm PM	**1.21 ± 0.35 mm**	***p* = 0.027**
3 mm A	0.93 ± 0.37 mm	*p* = 0.049
3 mm AL	1.01 ± 0.36 mm	*p* = 0.041
3 mm AM	0.98 ± 0.38 mm	*p* = 0.047
3 mm L	**1.16 ± 0.36 mm**	***p* = 0.031**
3 mm M	**1.17 ± 0.37 mm**	***p* = 0.032**
3 mm P	**1.46 ± 0.36 mm**	***p* = 0.02**
3 mm PL	**1.35 ± 0.37 mm**	***p* = 0.024**
3 mm PM	**1.40 ± 0.36 mm**	***p* = 0.021**
5 mm A	0.86 ± 0.40 mm	*p* = 0.064
5 mm AL	0.96 ± 0.38 mm	*p* = 0.048
5 mm AM	0.93 ± 0.43 mm	*p* = 0.065
5 mm L	**1.19 ± 0.38 mm**	***p* = 0.032**
5 mm M	**1.24 ± 0.42 mm**	***p* = 0.036**
5 mm P	**1.73 ± 0.39 mm**	***p* = 0.016**
5 mm PL	**1.48 ± 0.39 mm**	***p* = 0.022**
5 mm PM	**1.66 ± 0.37 mm**	***p* = 0.016**

60° Flexion		
Anatomic	**1.15 ± 0.12 mm**	***p* = 0.009**
1 mm A	**1.08 ± 0.12 mm**	***p* = 0.007**
1 mm AL	**1.10 ± 0.13 mm**	***p* = 0.008**
1 mm AM	**1.09 ± 0.11 mm**	***p* = 0.006**
1 mm L	**1.16 ± 0.13 mm**	***p* = 0.01**
1 mm M	**1.15 ± 0.11 mm**	***p* = 0.008**
1 mm P	**1.24 ± 0.12 mm**	***p* = 0.01**
1 mm PL	**1.21 ± 0.13 mm**	***p* = 0.011**
1 mm PM	**1.22 ± 0.11 mm**	***p* = 0.01**
3 mm A	**0.97 ± 0.14 mm**	***p* = 0.006**
3 mm AL	**1.04 ± 0.15 mm**	***p* = 0.008**
3 mm AM	**1.00 ± 0.15 mm**	***p* = 0.004**
3 mm L	**1.18 ± 0.16 mm**	***p* = 0.012**
3 mm M	**1.17 ± 0.13 mm**	***p* = 0.004**
3 mm P	**1.46 ± 0.13 mm**	***p* = 0.009**
3 mm PL	**1.35 ± 0.16 mm**	***p* = 0.013**
3 mm PM	**1.39 ± 0.09 mm**	***p* = 0.006**
5 mm A	**0.91 ± 0.18 mm**	***p* = 0.004**
5 mm AL	**1.01 ± 0.17 mm**	***p* = 0.008**
5 mm AM	**0.95 ± 0.23 mm**	***p* = 0.002**
5 mm L	**1.21 ± 0.18 mm**	***p* = 0.011**
5 mm M	**1.24 ± 0.21 mm**	***p* = 0.003**
5 mm P	**1.74 ± 0.15 mm**	***p* = 0.013**
5 mm PL	**1.49 ± 0.19 mm**	***p* = 0.012**
5 mm PM	**1.67 ± 0.05 mm**	***p* = 0.005**